INVESTIGATION OF HNO-INDUCED MODIFICATIONS IN VARIOUS SYSTEMS

by

Gizem Keceli

A dissertation submitted to Johns Hopkins University in conformity with the requirements for the degree of Doctor of Philosophy

Baltimore, Maryland

May, 2014

Abstract

Nitroxyl (HNO), a potential heart failure therapeutic, is known to post-translationally modify cysteine residues. Among reactive nitrogen oxide species, the modification of cysteine residues to sulfinamides [$RS(O)NH_2$] is unique to HNO. Because this modification can alter protein structure and function, we have examined the reactivity of sulfinamides in several systems, including small organic molecules, peptides, and a protein. At physiological pH and temperature, relevant reactions of sulfinamides involve reduction to free thiols in the presence of excess thiol and hydrolysis to form sulfinic acids [RS(O)OH]. In addition to utilizing ESI-MS and other spectroscopic methods to investigate sulfinamide reduction, we have applied ^{15}N-edited ^{1}H-NMR techniques to sulfinamide detection and used this method to explore sulfinamide hydrolysis.

Since HNO-derived modifications may depend on local environment, we have also investigated the reactivity of HNO with cysteine derivatives and C-terminal cysteine-containing peptides. Apart from the lack of sulfinamide formation, these studies have revealed the presence of new products, a sulfohydroxamic acid derivative [$RS(O)_2NHOH$] and a thiosulfonate [$RS(O)_2SR$], presumably produced under our experimental conditions via the intermediacy of a cyclic structure that is hydrolyzed to give a sulfenic acid (RSOH).

Apart from its role in thiol oxidation, HNO has been reported to have nitrosative properties, for example with tryptophan resulting in *N*-nitrosotryptophan formation. We have examined the reactivity of HNO with tryptophan and small peptides containing either tryptophan or both a tryptophan and a cysteine residue.

HNO has been shown to enhance cardiac sarcoplasmic reticulum Ca^{2+} cycling independent of the β-adrenergic pathway. In a collaborative project, the effects of HNO on the cardiac proteins, phospholamban (PLN) and sarco(endo)plasmic reticulum Ca^{2+}-ATPase (SERCA2a) were investigated.

Advisor: Professor John P. Toscano

Readers: Professor Mark M. Greenberg

Professor Craig A. Townsend

Acknowledgments

First and foremost, I would like to thank my advisor, Professor John P. Toscano, for providing me the research opportunity in his laboratory and also for all his help throughout my studies. I sincerely appreciate and respect his strive for excellence, and also would like to express my gratitude for his patience, tolerance, optimism, and understanding over the years. It has always been a great pleasure to work with him.

I would also like to acknowledge Professor Mark M. Greenberg and Professor Craig A. Townsend for serving on my thesis committee and reading my dissertation.

I am very grateful to our collaborator, Professor Nazareno Paolocci (Johns Hopkins Medical Institutions), who has been like a co-advisor to me since I joined Toscano group. So I would like to thank him for all his help and guidance over the years.

I thank to our collaborators Professor James E. Mahaney (Edward Via Virginia School of Osteopathic Medicine) and the late Professor Jeffrey P. Froehlich (Johns Hopkins Medical Institutions) on the phospholamban project, and Professor Michael P. Yassa on the caffeine project. I really appreciate the support of Professor Naod Kebede (Edinboro University) in synthesis and Professor Tamara L. Hendrickson (Wayne State University) in biochemistry protocols and peptide synthesis. I would also like to recognize Dr. Jason W. Labonte for conducting the computational studies and Daniel Borota for his work in the caffeine project. The facility managers, Dr. I. Phillip Mortimer and Dr. Cathy D. Moore, have been extremely helpful throughout my studies and I would like to thank them for teaching me MS and NMR experiments, respectively.

I appreciate the support and input of all the past and present members of the Toscano group. In chronological order, I thank Dr. Christopher M. Pavlos (for his previous work on phospholamban), Dr. Andrew D. Cohen (for showing me around the office), and Dr. Yonglin Liu. I owe special thanks to my labmates with whom we have gone through all the ups and downs of graduate school, Dr. Anthony S. Evans, Dr. Art D. Sutton, and Dr. Daryl A. Guthrie, as well as the new members of our lab, Christopher Bianco, Tyler Chavez, Hyunah Cho, and Saghar Nourian for all the useful conversations and their friendship.

Also I would like to thank all my friends for their support and encouragement, and acknowledge everyone who has helped me one way or the other over the years. Lastly, thanks to my parents, and my brother in Turkey for always supporting me in all my decisions.

Table of Contents

List of Tables

List of Figures

List of Schemes

Chapter 1 – Introduction

1.1 Nitroxyl (HNO)

HNO is the protonated, one-electron reduced form of nitric oxide (NO). Its nomenclature is often ambiguous and includes nitroxyl, nitrosyl hydride, hydrogen oxonitrate, and azanone.[1, 2]

Recent discoveries of important pharmacological properties have drawn significant attention to the biochemistry of HNO. Among these are the therapeutic potential of HNO in heart failure, chronic alcoholism, cancer, and as a preconditioning agent in the treatment of myocardial ischemia-reperfusion.[3-5] Also recent reviews highlight the potential uses of HNO in the treatments of other cardiovascular conditions such as angina, atherosclerosis, and acute hypertensive crisis.[3, 4] Moreover, studies indicate that the physiological properties of HNO are different from those of NO.[4, 6-8]

Although HNO has been known since late 19th century, its pK_a has been re-evaluated and determined with confidence only approximately a decade ago.[9, 10] The electronic ground state of HNO is singlet, whereas that of the deprotonated form, NO^-, is triplet.[11-13] Due to the spin forbidden nature of the protonation/deprotonation of NO^-/HNO, the equilibrium is slow, complicating the process.[12] Experimental and theoretical studies have shown the pK_a ($^1HNO/^3NO^-$) to be ca. 11.4,[9, 10] indicating that HNO is the predominant species under physiological conditions.

Despite several proposed pathways, endogeneous production of HNO has yet to be determined.[4-6] These potential pathways include the decomposition of *S*-nitrosothiols, oxidation of L-arginine by nitric oxide synthase (NOS) in the absence of cofactor, and

oxidation of *N*-hydroxy-L-arginine or hydroxylamine.[14-23] Thus, the potential role of HNO in signaling is currently unknown. However, as mentioned in recent reviews, the impact of HNO is considered to be potent, very selective.[4, 6]

Another important feature of HNO is its rapid dimerization reaction ($k = 8 \times 10^6\ M^{-1}s^{-1}$). In this process, one HNO molecule reacts as a nucleophile and another acts as an electrophile to produce hyponitrous acid, which then undergoes spontaneous dehydration to generate nitrous oxide (N_2O) and water (Scheme 1-1).[1, 24, 25] Consequently, storage of HNO is not possible and it is normally generated *in situ* by the decomposition of donor compounds.

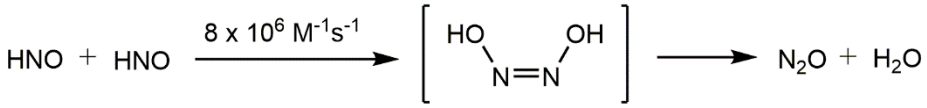

Scheme 1-1. Dimerization of HNO.

The most common HNO donor is Angeli's salt ($Na_2N_2O_3$; AS),[26, 27] which has a half-life of approximately 2.4 min at physiological pH and temperature, and decomposes to produce HNO and nitrite (NO_2^-) (Scheme 1-2). Throughout this work, we have employed AS, as well as other HNO donors, including 2-bromo-*N*-hydroxy-benzenesulfonamide (2-BrPA),[28] *N*-hydroxy-2-(methylsulfonyl)benzenesulfonamide (2-MSPA),[28] and 5-(*N*-hydroxylamine)-5-(acetyl-*O*-methoxyoxime)-*N,N*-dimethylbarbituric acid (HABA).[29]

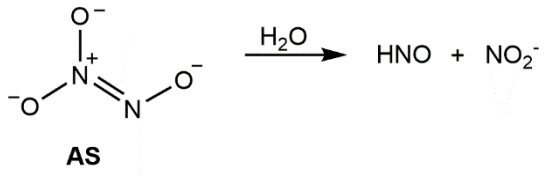

Scheme 1-2. Decomposition of Angeli's salt (AS).

1.2 Effects of HNO on Ca^{2+} Cycling

One of the unique pharmacological properties of HNO is its effects on the cardiovascular system.[6, 30] Cardiac excitation-contraction (EC) coupling is described as the process of converting the electrical excitation of the myocyte into the contraction of the heart (Figure 1-1).[31] The second messenger, Ca^{2+}, plays a crucial role in this process.[31] Contraction is initiated by the entrance of a small amount of Ca^{2+} to the cardiomyocyte through L-type Ca^{2+} channels.[31] Triggered by this Ca^{2+} entry, Ca^{2+} is released from the sarco(endo)plasmic reticulum (SR) to the cytosol via specialized Ca^{2+}-gated channels, ryanodine receptors (RyR2).[31] The increase in the free intracellular Ca^{2+} concentration allows the binding of Ca^{2+} to myofilament proteins, which switches on the contractile machinery.[31] The dissociation of Ca^{2+} from the myofilament proteins and consequently relaxation is achieved by the removal of the cytosolic Ca^{2+}.[31] Approximately 70% of the cytosolic Ca^{2+} is transported into the SR by the sarco(endo)plasmic reticulum Ca^{2+}-ATPase (SERCA2a).[31] The activity of SERCA2a is regulated by a small protein, phospholamban (PLN).[32] The inhibitory effect of PLN on SERCA2a can be relieved by phosphorylation of PLN via β-adrenergic pathway, which involves the activation of cyclic adenosine monophosphate (cAMP)-dependent protein kinase A (PKA) upon β-adrenergic stimulation.[32] Moreover, many components of the EC machinery have cysteine residues,

which can be modified by reactive nitrogen or oxygen species (RNS or ROS) and act as redox switches.[6, 33]

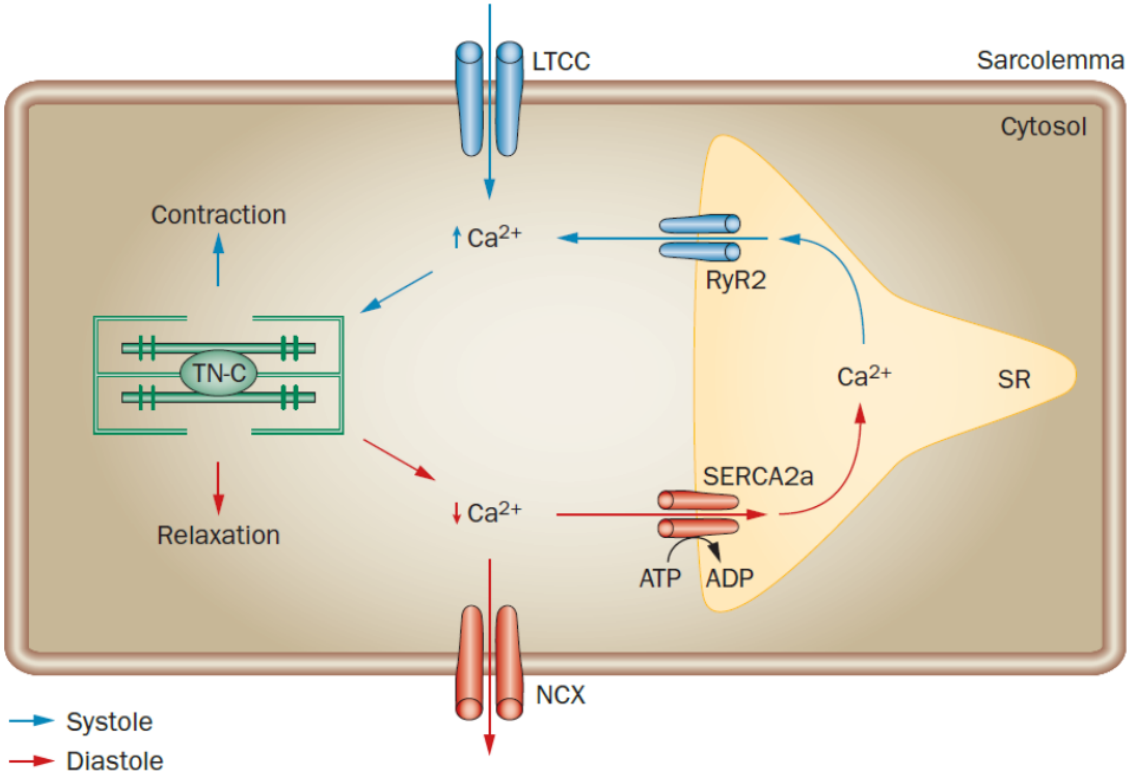

Figure 1-1. Excitation-contraction coupling. Adapted from Kho, C.; Lee, A.; Hajjar, R. J. (2012) Altered sarcoplasmic reticulum calcium cycling – targets for heart failure therapy, *Nat. Rev. Cardiol. 9*, 717-733.

Impaired contractility and slowed relaxation are commonly observed features of congestive heart failure.[34, 35] The downregulation of β-adrenergic system has also been reported.[6, 36] Recent studies by Paolocci and coworkers have shown that HNO augments contractility and accelerates relaxation in both normal and failing hearts.[4, 6-8] Their findings suggest that HNO improves myocyte Ca^{2+} cycling independent of the β-adrenergic pathway.[6, 37] Importantly, the observed effects are not reproduced by NO donors.[6]

As shown in Figure 1-2, HNO has been shown to interact directly and modify several proteins in the system. HNO-induced stimulation of skeletal and cardiac Ca^{2+}-

release channels (RyR1 and RyR2) has been reported in isolated rodent myocytes and in receptors reconstituted in lipid bilayers.[37, 38] Also, in a collaborative project, we have shown that HNO modifies PLN and affects the activity of the Ca^{2+}-ATPase in a PLN-dependent manner (Chapter 6). Although the physiological relevance has not been investigated, a direct modification of SERCA2a by HNO has also been reported.[39]

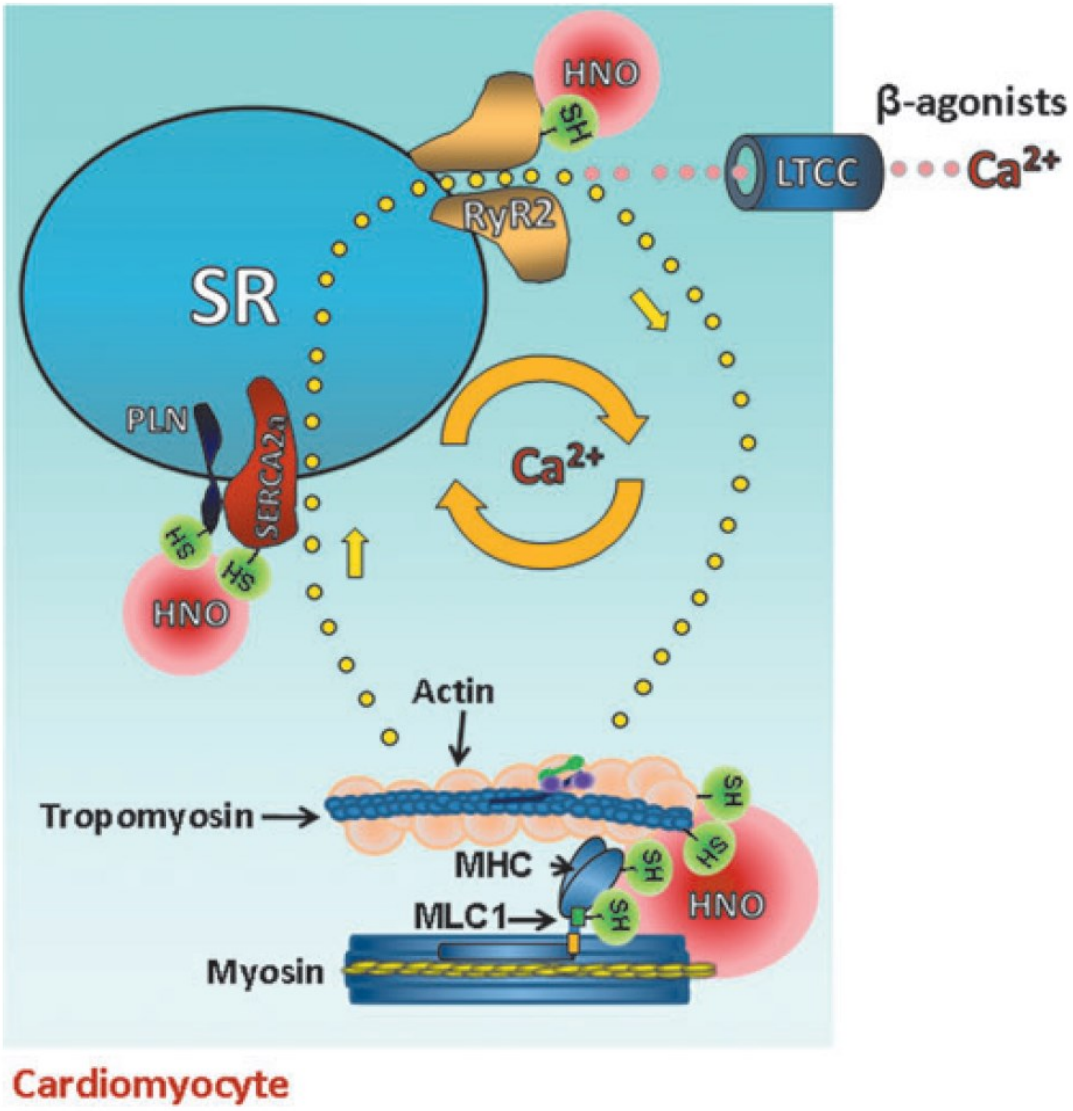

Figure 1-2. Effects of HNO cardiomyocyte Ca^{2+} cycling. Tocchetti, C. G., Stanley, B. A., Murray, C. I., Sivakumaran, V., Donzelli, S., Mancardi, D., Pagliaro, P., Gao, W. D., van Eyk, J., Kass, D. A., Wink, D. A., and Paolocci, N. (2011) Playing with cardiac "redox switches": The "HNO way" to modulate cardiac function, *Antioxid. Redox Signaling 14*, 1687-1698.

The effects of HNO on cardiac contractility have also been demonstrated by recent investigations conducted with the contractile machinery.[40] These studies have indicated that HNO increases myofilament Ca^{2+} responsiveness and consequently enhances force generation by modifying the cardiac myofilament proteins, actin and tropomyosin, to form a heterodimer.[40] In all cases, the HNO-derived effects were found to be readily reversible with thiol reducing agents.[40]

1.3 Reactivity of HNO

HNO is a reactive intermediate which undergoes various reactions with itself, thiols, nitrogen oxides, metals, oxygen, amines, and indoles.[2, 5, 11, 27, 41-43] Although HNO can act both as an electrophile and a nucleophile, recent reviews highlight the electrophilic nature of HNO towards soft bases such as thiols and phosphines.[27, 41, 44] Moreover, it is reported to be less reactive towards hard bases such as oxygen-containing nucleophiles.[41]

A distinct feature of HNO from other nitrogen oxides is its high thiophilicity.[41] The reaction of HNO with thiols results in the formation of an initial *N*-hydroxysulfenamide (RSNHOH) intermediate. This unstable species further reacts with either excess thiol to form a disulfide or rearranges to form a sulfinamide ($RS(O)NH_2$) (Scheme 1-3).[45, 46] The reactivity of HNO with C-terminal cysteines is discussed in Chapter 4.

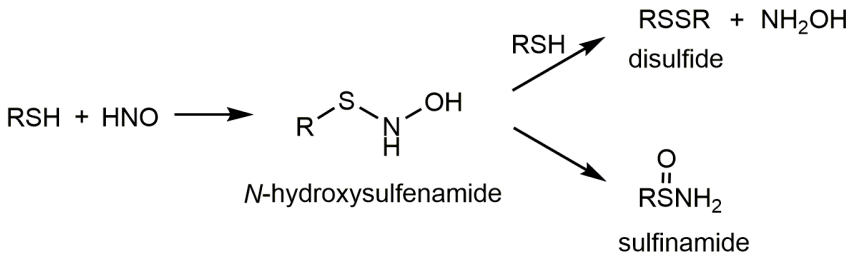

Scheme 1-3. The reaction of HNO with thiols

Indeed, the majority of HNO-induced biological effects are attributed to the reactivity of HNO with thiols.[6, 41] For example, studies suggest that the alcohol deterrent, cyanamide, interacts with the active site cysteine residues of aldehyde dehydrogenase via the intermediacy of HNO.[47] Similarly, HNO has been shown to affect glycolysis via modification of the thiol residues of the glycolytic enzyme, GAPDH, potentially interfering with the major energy pathway for most solid tumors.[5, 48-50] Consistent with these investigations, recent reports indicate the inhibition of cancer proliferation in breast cancer and neuroblastoma in mouse tissue and culture following HNO treatment.[5, 51, 52]

The rate constants for the reaction of HNO with several biomolecules have been experimentally determined by competition studies (Table 1-1).[53] These findings support that the major biological targets of HNO involve thiols, thiol-containing proteins, and metalloenzymes.[53] The second-order rate constant for the reaction of HNO with glutathione was determined to be 8×10^6 $M^{-1}s^{-1}$.[53] Moreover, some thiol-containing proteins such as the cysteine protease, papain, are estimated to have higher rate constants ($k_{papain} = 2 \times 10^7$ $M^{-1}s^{-1}$).[54]

The selectivity of HNO towards certain protein thiols has also been observed in cellular systems.[48, 54] Investigations have shown that HNO can specifically react with GAPDH without being trapped by cellular GSH in yeast.[48] Similarly, intracellular GSH levels were found to be unchanged upon inhibition of aldehyde dehydrogenase by HNO (generated from cyanamide) in cultured hepatocytes.[47, 48, 55, 56] Likewise, another cysteine protease, cathepsin B, is inhibited by HNO in macrophages containing cellular glutathione and endogeneously produced NO. Although the exact mechanisms for the observed

selectivity are yet to be determined, these reports emphasize further the potency of HNO as a thiol-modifying agent.[54]

Table 1-1. Rate constants of HNO with biomolecules.[53]

Biomolecule	***k*** **($M^{-1}s^{-1}$)**
Ferricytochrome c	4×10^4
Oxygen	3×10^3
Cu/Zn Superoxide Dismutase	1×10^6
Mn Superoxide Dismutase	7×10^5
Glutathione	2×10^6
N-Acetyl-L-Cysteine	5×10^5
Catalase	3×10^5
Metmyoglobin	8×10^5
Oxymyoglobin	1×10^7
Horseradish Peroxidase	2×10^6
Tempol	8×10^4

As mentioned above, HNO has also been shown to react with metalloporphyrins and metalloenzymes such as iron heme proteins.[2, 41, 57, 58] Initial studies have revealed the quenching of HNO by both methemoglobin and metmyoglobin.[45, 59] Recent findings indicate that HNO can react with either ferric or ferrous forms of the enzymes (Scheme 1-4).[2, 41] Farmer and coworkers have characterized an HNO adduct of myoglobin (Mb), formed by trapping of HNO by deoxy Mb or reduction of ferrous-NO complex.[60] Later studies with isolated metalloporphyrins have suggested that the strong influence of protein environment on the stability of Mb-HNO adduct.[2] Nevertheless, several metalloporphyrin nitrosyl complexes are obtained from the reaction of Fe(III), Co(III), or Mn(III) porphyrins

with HNO.[2] Similar to NO, HNO is also known to react with dioxygen complexes of ferrous heme proteins (Scheme 1-4).[41]

Scheme 1-4. Reaction of HNO with (a) ferrous, (b) ferric, and (c) dioxygen complex of ferrous myoglobin (Mb).

Studies indicate that although HNO and NO cannot be distinguished by iron porphyrins due to the reductive nitrosylation reaction, both Mn and Co porphyrins can be employed to differentiate between the two nitrogen oxides.[2] Based on these findings, Co(III) and Mn(III) porphyrins react with HNO, but not with NO, whereas Co(II) and Mn(II) porphyrins react with only NO.[2]

As shown in Table 1-1, HNO reacts with O_2 to form a currently uncharacterized HNO-O_2 adduct.[61, 62] Due to its spin forbidden nature, this reaction is slow ($k = 3 \times 10^3$ $M^{-1}s^{-1}$).[53] Unlike the analogous reaction of NO^- with O_2, which proceeds rapidly to form peroxynitrite ($ONOO^-$), the HNO-O_2 adduct has been suggested to be distinct from $ONOO^-$.[61, 62]

Recent reports also point to the nitrosation of indoles by HNO in the presence of oxygen.[42, 63] Although the mechanistic details have yet to be confirmed, treatment of the indolic compounds, melatonin, *N*-acetyl-L-tryptophan, and indole-3-acetic acid, with HNO generated from AS under aerobic conditions results in the formation of *N*-nitrosoindoles.[42] Moreover, the product profiles obtained following exposure to HNO and $ONOO^-$ have been demonstrated to be different.[42]

The nitrosative properties of HNO, produced from AS, have also been observed following *in vivo* studies.[42] Using reductive denitrosation to generate NO and a chemiluminescence method for NO detection, the amount of *N*-nitroso species have been determined in various tissues.[42] These reports indicate that the quantity of *N*-nitroso species are significantly higher in the heart tissue upon treatment with AS.[42] Experiments with the NO donor, DEA/NO, resulted in lower amounts of *N*-nitroso species in heart tissue compared with AS, although similar amounts were obtained in blood upon treatment with AS or DEA/NO.[42] These findings also confirm that the biological chemistry of HNO and NO are different, and the environment may affect their nitrosative properties.[42]

1.4 Introduction to This Work

As mentioned previously, thiols play a crucial role in HNO biology. To better understand the impact of HNO in biological systems, the fundamental reactivity of HNO and HNO-derived modifications require further investigation. Although disulfides are well-studied in the literature, there are very few reports on sulfinamides. Since sulfinamide formation is one of the major HNO-induced modifications, we have explored the reactivity of HNO-derived sulfinamides in small organic molecules, peptides, and proteins. The reduction of sulfinamides to free thiols at physiological pH and temperature is discussed in Chapter 2.

Although mass spectrometry has been shown to be a valuable tool for the detection of sulfinamides,[46, 64] alternate detection methods are also needed to investigate the reactivity of sulfinamides. The application of ^{15}N-edited ^{1}H NMR techniques to sulfinamide detection and the study of hydrolysis of HNO-derived sulfinamides using this NMR method are discussed in Chapter 3.

Investigation of HNO-derived modifications has revealed the presence of different end-products following exposure of C-terminal cysteines to HNO. The reactivity of C-terminal cysteines with HNO and the intermediacy of a sulfenic acid is explained in Chapter 4.

As mentioned in the previous section, recent reports point to the presence of an HNO-derived *N*-nitrosotryptophan formation.[42, 63] The reactivity of HNO with tryptophan and small peptides containing either tryptophan or both a tryptophan and a cysteine residue is discussed in Chapter 5.

To gain more insight into the impact of HNO on the cardiovascular system, the effects of HNO on phospholamban (PLN) and its interaction with the sarco(endo)plasmic reticulum Ca^{2+}-ATPase (SERCA2a) have been explored in a collaborative project. Additionally, brief investigations involving the reactivity of other nitrogen oxides with PLN and SERCA2a have been carried out. These studies are reported in Chapter 6.

Miscellaneous studies conducted to understand the reactivity of HNO, as well as other nitrogen oxides in various systems, and the reactivity of the corresponding modifications are described in Chapter 7.

Lastly, in a collaborative project, we have assisted the investigation of the effects of post-training caffeine administration on memory consolidation. This double-blind study, including a memory test and an HPLC assay to analyze the caffeine and paraxanthine levels in saliva, is reported in Chapter 8.

1.5 References

1. Fukuto, J. M., and Carrington, S. J. (2011) HNO signaling mechanisms, *Antioxid. Redox Signaling 14*, 1649-1657.
2. Doctorevich, F., Bikiel, D., Pellegrino, J., Suarez, S. A., Larsen, A., and Marti, M. A. (2011) Nitroxyl (azanone) trapping by metalloporphyrins, *Coordin. Chem. Rev. 255*, 2764-2784.
3. Irvine, J. C., Ritchie, R. H., Favaloro, J. L., Andrews, K. L., Widdop, R. E., and Kemp-Harper, B. K. (2008) Nitroxyl (HNO): the Cinderella of the nitric oxide story, *Trends Pharmacol. Sci. 29*, 601-608.
4. Paolocci, N., Jackson, M. I., Lopez, B. E., Miranda, K. M., Tocchetti, C. G., Wink, D. A., Hobbs, A. J., and Fukuto, J. M. (2007) The pharmacology of nitroxyl (HNO) and its therapeutic potential: Not just the janus face of NO, *Pharmacol. Ther. 113*, 442-458.
5. Flores-Santana, W., Salmon, D. J., Donzelli, S., Switzer, C. H., Basudhar, D., Ridnour, L., Cheng, R., Glynn, S. A., Paolocci, N., Fukuto, J. M., Miranda, K. M., and Wink, D. A. (2011) The specificity of nitroxyl chemistry is unique among nitrogen oxides in biological systems, *Antioxid. Redox Signaling 14*, 1659-1674.
6. Tocchetti, C. G., Stanley, B. A., Murray, C. I., Sivakumaran, V., Donzelli, S., Mancardi, D., Pagliaro, P., Gao, W. D., van Eyk, J., Kass, D. A., Wink, D. A., and Paolocci, N. (2011) Playing with cardiac "redox switches": The "HNO way" to modulate cardiac function, *Antioxid. Redox Signaling 14*, 1687-1698.
7. Paolocci, N., Katori, T., Champion, H. C., St John, M. E., Miranda, K. M., Fukuto, J. M., Wink, D. A., and Kass, D. A. (2003) Positive inotropic and lusitropic effects

of HNO/NO^- in failing hearts: Independence from beta-adrenergic signaling, *Proc. Natl. Acad. Sci. U. S. A. 100*, 5537-5542.

8. Paolocci, N., Saavedra, W. F., Miranda, K. M., Martignani, C., Isoda, T., Hare, J. M., Espey, M. G., Fukuto, J. M., Feelisch, M., Wink, D. A., and Kass, D. A. (2001) Nitroxyl anion exerts redox-sensitive positive cardiac inotropy in vivo by calcitonin gene-related peptide signaling, *Proc. Natl. Acad. Sci. U. S. A. 98*, 10463-10468.

9. Shafirovich, V., and Lymar, S. V. (2002) Nitroxyl and its anion in aqueous solutions: Spin states, protic equilibria, and reactivities toward oxygen and nitric oxide, *Proc. Natl. Acad. Sci. U. S. A. 99*, 7340-7345.

10. Bartberger, M. D., Liu, W., Ford, E., Miranda, K. M., Switzer, C. H., Fukuto, J. M., Farmer, P. J., Wink, D. A., and Houk, K. N. (2002) The reduction potential of nitric oxide (NO) and its importance to NO biochemistry, *Proc. Natl. Acad. Sci. U. S. A. 99*, 10958-10963.

11. Bartberger, M. D., Fukuto, J. M., and Houk, K. N. (2001) On the acidity and reactivity of HNO in aqueous solution and biological systems, *Proc. Natl. Acad. Sci. U. S. A. 98*, 2194-2198.

12. Janaway, G. A., and Brauman, J. I. (2000) Direct observation of spin forbidden proton-transfer reactions: $^3NO^- + HA \rightarrow {}^1HNO + A^-$, *Journal of Physical Chemistry A 104*, 1795-1798.

13. Fukuto, J. M., Switzer, C. H., Miranda, K. M., and Wink, D. A. (2005) Nitroxyl (HNO): Chemistry, biochemistry, and pharmacology, *Annu. Rev. Pharmacol. Toxicol. 45*, 335-355.

14. Fukuto, J. M., Stuehr, D. J., Feldman, P. L., Bova, M. P., and Wong, P. (1993.) Peracid oxidation of an *N*-hydroxyguanidine compound: a chemical model for the oxidation of N^{w}-hydroxyl-L-arginine by nitric oxide synthase, *J. Med. Chem. 36*, 2666-2670.

15. Fukuto, J. M., Wallace, G. C., Hszieh, R., and Chaudhuri, G. (1992) Chemical oxidation of *N*-hydroxyguanidine compounds. Release of nitric oxide, nitroxyl and possible relationship to the mechanism of biological nitric oxide generation, *Biochem. Pharmacol. 43*, 607-613.

16. Adak, S., Wang, Q., and Stuehr, D. J. (2000) Arginine conversion to nitroxide by tetrahydrobiopterin-free neuronal nitric-oxide synthase. Implications for mechanism, *J. Biol. Chem. 275*, 33554-33561.

17. Pufahl, R. A., Wishnok, J. S., and Marletta, M. A. (1995) Hydrogen peroxide-supported oxidation of Ng-hydroxy-L-arginine by nitric oxide synthase, *Biochemistry 34*, 1930-1941.

18. Rusche, K. M., Spiering, M. M., and Marletta, M. A. (1998) Reactions catalyzed by tetrahydrobiopterin-free nitric oxide synthase, *Biochemistry 37*, 15503-15512.

19. Schmidt, H. H. H. W., Hofmann, H., Schindler, U., Shutenko, Z. S., Cunningham, D. D., and Feelisch, M. (1996) No NO from NO synthase, *Proc. Natl. Acad. Sci. U. S. A. 93*, 14492-14497.

20. Donzelli, S., Espey, M. G., Flores-Santana, W., Switzer, C. H., Yeh, G. C., Huang, J., Stuehr, D. J., King, S. B., Miranda, K. M., and Wink, D. A. (2008) Generation of nitroxyl by heme protein-mediated peroxidation of hydroxylamine but not *N*-hydroxy-L-arginine, *Free Radical Biol. Med. 45*, 578-584.

21. Filipovic, M. R., Stanic, D., Raicevic, S., Spasic, M., and Niketic, V. (2007) Consequences of MnSOD interactions with nitric oxide: nitric oxide dismutation and the generation of peroxynitrite and hydrogen peroxide, *Free Radic. Res. 41*, 62-72.

22. Arnelle, D. R., and Stamler, J. S. (1995) NO^+, NO, and NO^- donation by *S*-nitrosothiols: implications for regulation of physiological functions by *S*-nitrosylation and acceleration of disulfide formation, *Arch. Biochem. Biophys. 318*, 279-285.

23. Hogg, N., Singh, R. J., and Kalyanaraman, B. (1996) The role of glutathione in the transport and catabolism of nitric oxide, *FEBS Lett. 382*, 223-228.

24. Hoffmann, R., Gleiter, R., and Mallory, F. B. (1970) Non-least-motion potential surfaces. The dimerization of methylenes and nitroso compounds, *J. Am. Chem. Soc. 92*, 1460-1466.

25. Bazylinski, D. A., and Hollocher, T. C. (1985) Evidence from the reaction between trioxodinitrate (II) and ^{15}NO that trioxodinitrate(II) decomposes into nitrosyl hydride and nitrite in neutral aqueous solution, *Inorg. Chem. 24*, 4285-4288.

26. Hughes, M. N., and Cammack, R. (1999) Synthesis, chemistry, and applications of nitroxyl ion releasers sodium trioxodinitrate or Angeli's salt and Piloty's acid, *Methods Enzymol. 301*, 279-287.

27. Fukuto, J. M., Bartberger, M. D., Dutton, A. S., Paolocci, N., Wink, D. A., and Houk, K. N. (2005) The physiological chemistry and biological activity of nitroxyl (HNO): The neglected, misunderstood, and enigmatic nitrogen oxide, *Chem. Res. Toxicol. 18*, 790-801.

28. Toscano, J. P., Brookfield, F. A., Cohen, A. D., Courtney, S. M., Frost, L. M., and Kalish, V. J. (2011) *N*-hydroxylsulfonamide derivatives as new physiologically useful nitroxyl donors, (Johns Hopkins University, USA). U.S. Patent 8,030,356.

29. Guthrie, D. A., Kim, N. Y., Siegler, M. A., Moore, C. D., and Toscano, J. P. (2012) Development of *N*-substituted hydroxylamines as efficient nitroxyl (HNO) donors, *J. Am. Chem. Soc. 134*, 1962-1965.

30. Kemp-Harper, B. K. (2011) Nitroxyl (HNO): A novel redox signaling molecule, *Antioxid. Redox Signaling 14*, 1609-1613.

31. Bers, D. M. (2002) Cardiac excitation-contraction coupling, *Nature 415*, 198-205.

32. MacLennan, D. H., and Kranias, E. G. (2003) Phospholamban: A crucial regulator of cardiac contractility, *Nature Rev. Mol. Cell Biol. 4*, 566-577.

33. Wouters, M. A., Fan, S. W., and Haworth, N. L. (2010) Disulfides as redox switches: from molecular mechanisms to functional significance, *Antioxid. Redox Signaling 12*, 53-91.

34. Houser, S. R., and Margulies, K. B. (2003) Is depressed myocyte contractility centrally involved in heart failure?, *Circ. Res. 92*, 350-358.

35. Hasenfuss, G., and Teerlink, J. R. (2011) Cardiac inotropes: Current agents and future directions, *Eur. Heart J. 32*, 1838-1845.

36. Dorn, G. W. (2010) Adrenergic signaling polymorphisms and their impact on cardiovascular disease, *Physiol. Rev. 90*, 1013-1062.

37. Tocchetti, C. G., Wang, W., Froehlich, J. P., Huke, S., Aon, M. A., Wilson, G. M., Di Benedetto, G., O'Rourke, B., Gao, W. D., Wink, D. A., Toscano, J. P., Zaccolo, M., Bers, D. M., Valdivia, H. H., Cheng, H., Kass, D. A., and Paolocci, N. (2007)

Nitroxyl improves cellular heart function by directly enhancing cardiac sarcoplasmic reticulum Ca^{2+} cycling, *Circ. Res. 100*, 96-104.

38. Cheong, E., Tumbev, V., Abramson, J., Salama, G., and Stoyanovsky, D. A. (2005) Nitroxyl triggers Ca^{2+} release from skeletal and cardiac sarcoplasmic reticulum by oxidizing ryanodine receptors, *Cell Calcium 37*, 87-96.

39. Lancel, S., Zhang, J., Evangelista, A., Trucillo, M. P., Tong, X. Y., Siwik, D. A., Cohen, R. A., and Colucci, W. S. (2009) Nitroxyl activates SERCA in cardiac myocytes via glutathiolation of cysteine 674, *Circ. Res. 104*, 720-723.

40. Gao, W. D., Murray, C. I., Tian, Y., Zhong, X., DuMond, J. F., Shen, X., Stanley, B. A., Foster, D. B., Wink, D. A., King, S. B., Van Eyk, J. E., and Paolocci, N. (2012) Nitroxyl-mediated disulfide bond formation between cardiac myofilament cysteines enhances contractile function, *Circ. Res. 111*, 1002-1011.

41. Fukuto, J. M., Cisneros, C. J., and Kinkade, R. L. (2013) A comparison of the chemistry associated with the biological signaling and actions of nitroxyl (HNO) and nitric oxide (NO), *J. Inorg. Biochem. 118*, 201-208.

42. Peyrot, F., Fernandez, B. O., Bryan, N. S., Feelisch, M., and Ducrocq, C. (2006) *N*-Nitroso products from the reduction of indoles with Angeli's salt, *Chem. Res. Toxicol. 19*, 58-67.

43. Zhang, Y. (2013) Computational investigations of HNO in biology, *J. Inorg. Biochem. 118*, 191-200.

44. Reisz, J. A., Klorig, E. B., Wright, M. W., and King, S. B. (2009) Reductive phosphine-mediated ligation of nitroxyl (HNO), *Org. Lett. 11*, 2719-2721.

45. Doyle, M. P., Mahapatro, S. N., Broene, R. D., and Guy, J. K. (1988) Oxidation and reduction of hemoproteins by trioxodinitrate(II). The role of nitrosyl hydride and nitrite, *J. Am. Chem. Soc. 110*, 593-599.

46. Wong, P. S. Y., Hyun, J., Fukuto, J. M., Shirota, F. N., DeMaster, E. G., Shoeman, D. W., and Nagasawa, H. T. (1998) Reaction between *S*-nitrosothiols and thiols: Generation of nitroxyl (HNO) and subsequent chemistry, *Biochemistry 37*, 5362-5371.

47. Demaster, E. G., Redfern, B., and Nagasawa, H. T. (1998) Mechanisms of inhibition of aldehyde dehydrogenase by nitroxyl, the active metabolite of the alcohol deterrent agent cyanamide, *Biochem. Pharmacol. 55*, 2007-2015.

48. Lopez, B. E., Rodriguez, C. E., Pribadi, M., Cook, N. M., Shinyashiki, M., and Fukuto, J. M. (2005) Inhibition of yeast glycolysis by nitroxyl (HNO): A mechanism of HNO toxicity and implications to HNO biology, *Arch. Biochem. Biophys. 442*, 140-148.

49. Lopez, B. E., Wink, D. A., and Fukuto, J. M. (2007) The inhibition of glyceraldehyde-3-phosphate dehydrogenase by nitroxyl (HNO), *Arch. Biochem. Biophys. 465*, 430-436.

50. Shen, B., and English, A. M. (2005) Mass spectrometric analysis of nitroxyl-mediated protein modification: Comparison of products formed with free and protein-based cysteines, *Biochemistry 44*, 14030-14044.

51. Norris, A. J., Sartippour, M. R., Lu, M., Park, T., Rao, J. Y., Jackson, M. I., Fukuto, J. M., and Brooks, M. N. (2008) Nitroxyl inhibits breast tumor growth and angiogenesis, *Int. J. Cancer 122*, 1905-1910.

52. Stoyanovsky, D. A., Schor, N. F., Nylander, K. D., and Salama, G. (2004) Effects of pH on the cytotoxicity of sodium trioxodinitrate (Angeli's salt), *J. Med. Chem. 47*, 210-217.

53. Miranda, K. M., Paolocci, N., Katori, T., Thomas, D. D., Ford, E., Bartberger, M. D., Espey, M. G., Feelisch, M., Fukuto, J. M., and Wink, D. A. (2003) A biochemical rationale for the discrete behavior of nitroxyl and nitric oxide in the cardiovascular system, *Proc. Natl. Acad. Sci. U. S. A. 100*, 9196-9201.

54. Vaananen Antti, J., Selmenpera, P., Hukkanen, M., Miranda, K. M., Harjula, A., Rauhala, P., and Kankuri, E. (2008) Persistent susceptibility of cathepsin B to irreversible inhibition by nitroxyl (HNO) in the presence of endogenous nitric oxide, *Free Radical Biol. Med. 45*, 749-755.

55. Hammond, A. H., and Fry, J. R. (1999) Effect of cyanamide on toxicity and glutathione depletion in rat hepatocyte cultures: differences between two dichloropropanol isomers, *Chem.-Biol. Interactions 122*, 107-115.

56. Lee, M. J. C., Nagasawa, H. T., Elberling, J. A., and DeMaster, E. G. (1992) Prodrugs of nitroxyl as inhibitors of aldehyde dehydrogenase, *J. Med. Chem. 35*, 3648-3652.

57. Kumar, M. R., Fukuto, J. M., Miranda, K. M., and Farmer, P. J. (2010) Reactions of HNO with heme proteins: New routes to HNO-heme complexes and insight into physiological effects, *Inorg. Chem. 49*, 6283-6292.

58. Farmer, P. J., and Sulc, F. (2005) Coordination chemistry of the HNO ligand with hemes and synthetic coordination complexes, *J. Inorg. Biochem. 99*, 166-184.

59. Bazylinski, D. A., and Hollocher, T. C. (1985) Metmyoglobin and methemoglobin as efficient traps for nitrosyl hydride (nitroxyl) in neutral aqueous solution, *J. Am. Chem. Soc. 107*, 7982-7986.

60. Sulc, F., Immoos, C. E., Pervitsky, D., and Farmer, P. J. (2004) Efficient trapping of HNO by deoxymyoglobin, *J. Am. Chem. Soc. 126*, 1096-1101.

61. Miranda, K. M., Espey, M. G., Yamada, K., Krishna, M., Ludwick, N., Kim, S., Jourd'heuil, D., Grisham, M. B., Feelisch, M., Fukuto, J. M., and Wink, D. A. (2001) Unique oxidative mechanisms for the reactive nitrogen oxide species, nitroxyl anion, *J. Biol. Chem. 276*, 1720-1727.

62. Miranda, K. M., Yamada, K., Espey, M. G., Thomas, D. D., DeGraff, W., Mitchell, J. B., Krishna, M., Colton, C. A., and Wink, D. A. (2002) Further evidence for distinct reactive intermediates from nitroxyl and peroxynitrite: effects of buffer composition on the chemistry of Angeli's salt and synthetic peroxynitrite, *Arch. Biochem. Biophys. 401*, 134-144.

63. Suzuki, T., Mower, H. F., Friesen, M. D., Gilibert, I., Sawa, T., and Ohshima, H. (2004) Nitration and nitrosation of *N*-acetyl-L-tryptophan and tryptophan residues in proteins by various reactive nitrogen species, *Free Radical Biol. Med. 37*, 671-681.

64. Hoffman, M. D., Walsh, G. M., Rogalski, J. C., and Kast, J. (2009) Identification of nitroxyl-induced modifications in human platelet proteins using a novel mass spectrometric detection method, *Mol. Cell. Proteomics 8*, 887-903.

Chapter 2 – Reactivity of HNO-Derived Sulfinamides

2.1 Introduction

Thiol residues are prone to several post-translational modifications under oxidative conditions. These include the formation of disulfide bonds, sulfinamides, and sulfenic, sulfinic and sulfonic acids.[1, 2] Nitroxyl (HNO), the protonated one-electron reduced form of nitric oxide (NO), has been shown to be a potential therapeutic agent for heart failure.[3, 4] Moreover, recent reviews highlight the potential uses of HNO in the treatments of alcoholism, vascular dysfunction, and cancer.[5, 6] One of the most significant features of HNO is its reactivity towards thiols.[7, 8] This reactivity can result in the formation of a disulfide or a sulfinamide depending on the concentration of thiol (Scheme 2-1). In the presence of excess thiol, the end products are disulfide and hydroxylamine, whereas at low thiol concentration the product is sulfinamide.

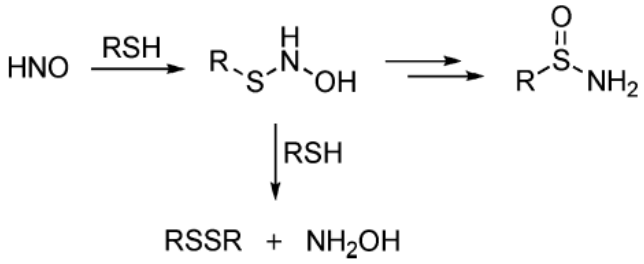

Scheme 2-1. The reaction of HNO with thiols

Previous studies have shown that protein cysteine residues are targets of HNO.[9, 10] HNO-induced disulfide and/or sulfinamide modifications are observed in papain,[11] glyceraldehyde-3-phosphate dehydrogenase (GAPDH),[12, 13] cathepsin B,[14] yeast

transcription factor Ace1,[15] ryanodine receptors (RyR),[16] *N*-methyl-D-aspartate (NMDA) receptor,[17] bovine serum albumin (BSA),[18] aldehyde dehydrogenase (AlDH)[19] and phospholamban (PLB).[20] Traditionally, disulfide formation is considered to be reversible, whereas sulfinamide modification has been considered to be irreversible in peptides and proteins.[8, 9, 11-15, 19, 20] To date, there have been no reports of sulfinamide reduction under physiologically relevant conditions. Also, recent studies with *t*-butanesulfinamide indicate that it is unreactive towards dithiothreitol (DTT).[20] Moreover, we are aware of only one example of the reduction of a sulfinic acid in a biological system, which occurs by an ATP-dependent process.[21-23]

Although not investigated thoroughly, the possible reduction of sulfinamides by thiols has been suggested by some recent studies. For example, free thiols have recently been observed upon treatment of peptide sulfinamides with DTT at elevated temperatures.[24] Similarly, the reaction of *N*-phenylbenzenesulfinamide and thiophenol in ethanol produces aniline and diphenyl disulfide, via a direct thiolysis mechanism involving the initial protonation of the sulfinyl group followed by a series of nucleophilic displacement reactions, the first of which gives thiosulfinate and elimination of the amine (Scheme 2-2).[25] The thiosulfinate is then reduced ultimately to the thiol upon reaction with excess thiophenol.[26]

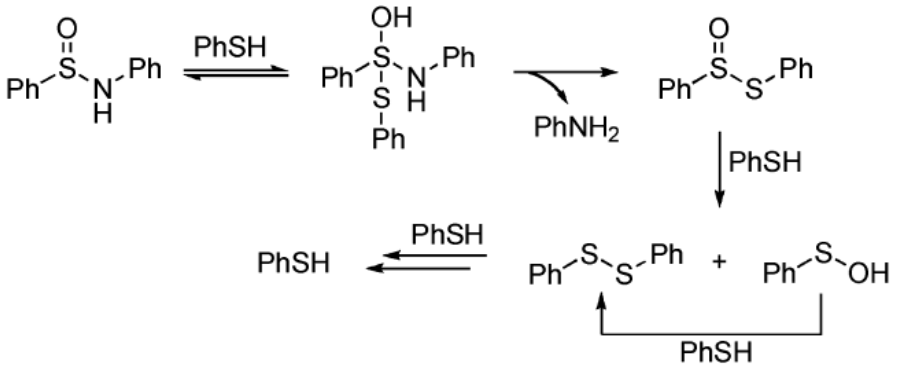

Scheme 2-2. Direct thiolysis mechanism of *N*-phenylbenzenesulfinamide

A well-known process affecting proteins at physiological pH and temperature is the succinimide-mediated deamidation reaction. In this non-enzymatic reaction, the side chain amide linkage in an asparagine residue is hydrolyzed to form a carboxylic acid.[27-29] The mechanism is thought to involve an intramolecular cyclization in which the α-amino group of the carboxyl-side amino acid residue attacks the side chain carbonyl carbon of an asparaginyl residue forming a succinimide intermediate.[27-29] This cyclic intermediate is then hydrolyzed to give the carboxylic acid, either in the L-normal or L-iso peptide (Scheme 2-3). Consistent with the involvement of the cyclic succinimide intermediate, significant substituent effects on the C-terminal side of the asparagine residue have been observed.[27] In addition, the effect of solvent dielectric constant on this reaction has been examined and indicates that the rate of deamidation is significantly reduced in solvents of low dielectric strength.[30]

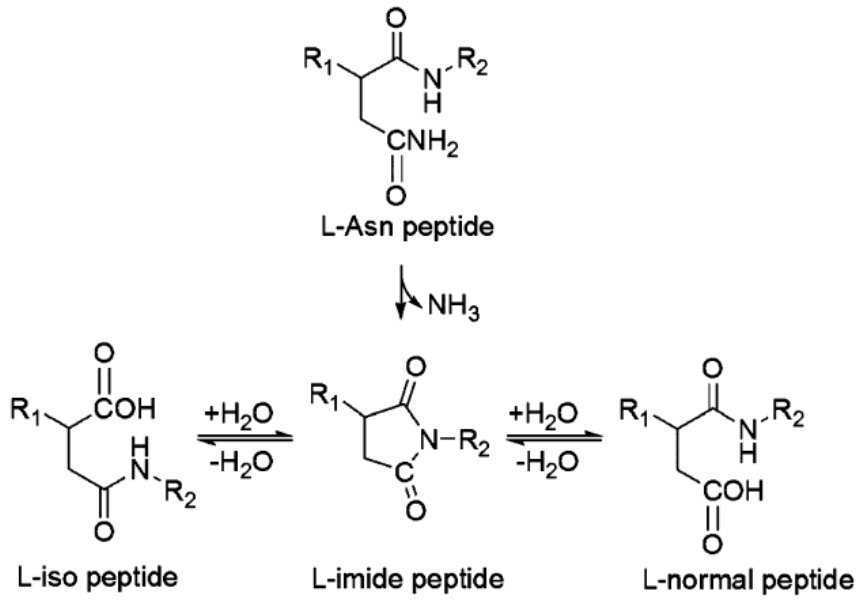

Scheme 2-3. Succinimide-mediated deamidation mechanism

A sulfinamide ($RS(O)NH_2$) to sulfinic acid (RS(O)OH) conversion has recently been proposed to occur via a mechanism analogous to the succinimide-mediated deamidation reaction, mainly under gel electrophoresis conditions.[24] The mechanism involves the formation of a five-membered succinimide-like intermediate **1** (Scheme 2-4) with subsequent hydrolysis to yield the corresponding sulfinic acid-containing peptide. Considering the greater nucleophilicity of thiols over water, we hypothesized that the reduction of sulfinamides might be facilitated in peptides via a similar mechanism. To test this hypothesis, we have studied the reactivity of sulfinamides in a small organic molecule, peptides, and a protein. In addition, we have also examined the impact of solvent dielectric constant on this reactivity.

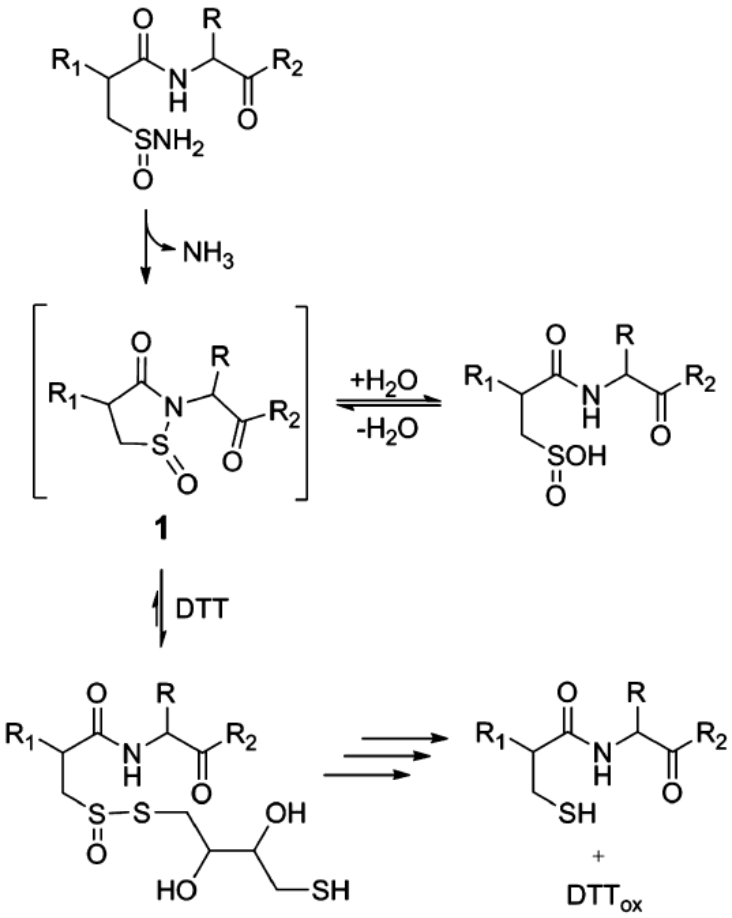

Scheme 2-4. Mechanism of sulfinamide reduction via a cyclic intermediate

2.2 Results

2.2.1 Formation of Peptide Sulfinamides by Reaction with HNO

We initially investigated the reaction of HNO with the cysteine-containing peptides VYPCGA and VYPCLA to determine the product distribution and to optimize conditions for sulfinamide formation. Both sulfinamide and disulfide modifications are observed upon treatment with HNO, as has been reported in the literature.[7, 8] At the concentrations employed, ESI-MS was responsive to the relative concentration of the sulfinamide. As the ratio of HNO-donor to peptide was increased, we observe an increase in the relative amount

of sulfinamide along with a corresponding decrease in observed thiol (Figure 2-1a, c). As expected, higher yields of disulfide are observed at lower HNO-donor to peptide ratios (Figure 2-1b, d). For 0.1 mM peptide, sulfinamide formation was most efficient with 0.3 - 1 mM AS. A similar trend is observed upon incubation of GSH with an HNO-donor in ammonium bicarbonate buffer, also consistent with previous HPLC studies.[31] (Due to the low molecular weight of GSH, desalting was inefficient and experiments were conducted in ammonium bicarbonate, an MS-compatible buffer.) The higher sulfinamide yield observed with VYPCLA (97%) versus VYPCGA (66%) is presumably due to the presence of the adjacent Leu residue, which inhibits the formation of peptide disulfide due to steric hindrance (Figure 2-1b, d).[32-34]

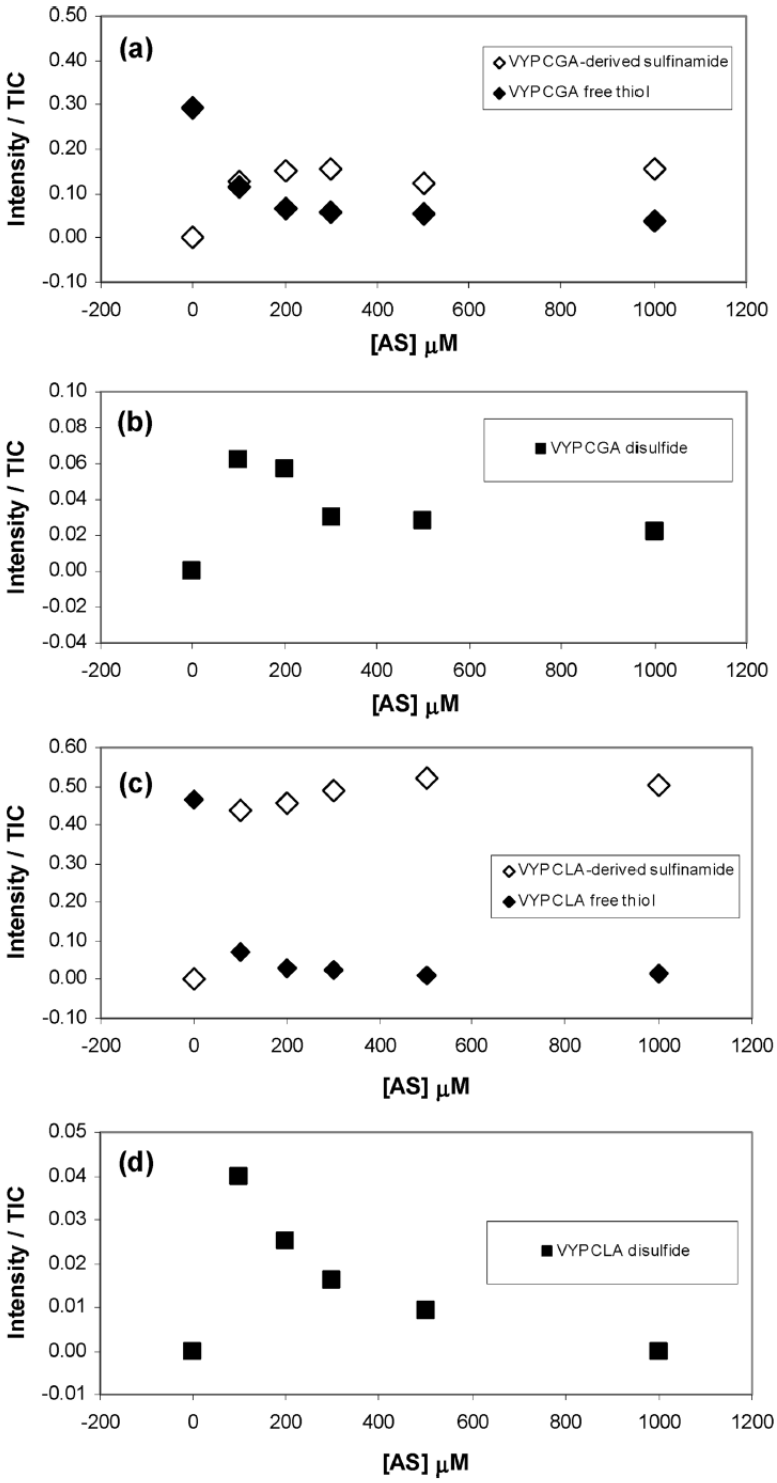

Figure 2-1. Formation of peptide-derived sulfinamides and disulfides in phosphate buffer. The ratios of sulfinamide, disulfide, and thiol ion abundance to total ion count were analyzed for (a, b) VYPCGA (0.1 mM) and (c, d) VYPCLA (0.1 mM) following incubation with 0-1000 μM AS in 10 mM phosphate buffer with 50 μM DTPA (pH 7.4) at 37 °C for 30 minutes (SEM ±5%, n≥3).

2.2.2 Sulfinamide Reduction

To determine the extent of sulfinamide reduction back to the free thiol at physiological pH and temperature, the VYPCGA-derived sulfinamide (CG-S(O)NH_2) was incubated with 50 mM DTT in phosphate buffer for a total of 26 h and aliquots were analyzed after 0, 1, 6 and 26 h. As observed by ESI-MS (Figure 2-2a), the ratio of CG-S(O)NH_2 to the corresponding thiol-containing peptide (VYPCGA, CG-SH) decreases significantly after 26 h incubation. Note that the disulfide-modified peptide, which can be observed in the absence of reducing agents, was not detected in the initial sample due its immediate reduction by DTT. Thus, we attribute the increase in free thiol observed following incubation to reduction of the sulfinamide. As can be seen in Figure 2-2a, no other significant changes are observed in the ESI-MS data. After 1, 6 and 26 h incubation at 37 °C, 7, 30, 69% sulfinamide reduction was observed, respectively, with a corresponding increase in thiol (18, 34 and 66%, respectively). As shown in Table 2-1, the ESI-MS-derived increase in thiol agrees very well with that determined by a standard DTNB assay.[35] Upon 64 h incubation at 37 °C, the sulfinamide reduction was found to be 86%. In the absence of DTT, no increase in free thiol was observed upon incubation of CG-S(O)NH_2 at 37 °C.

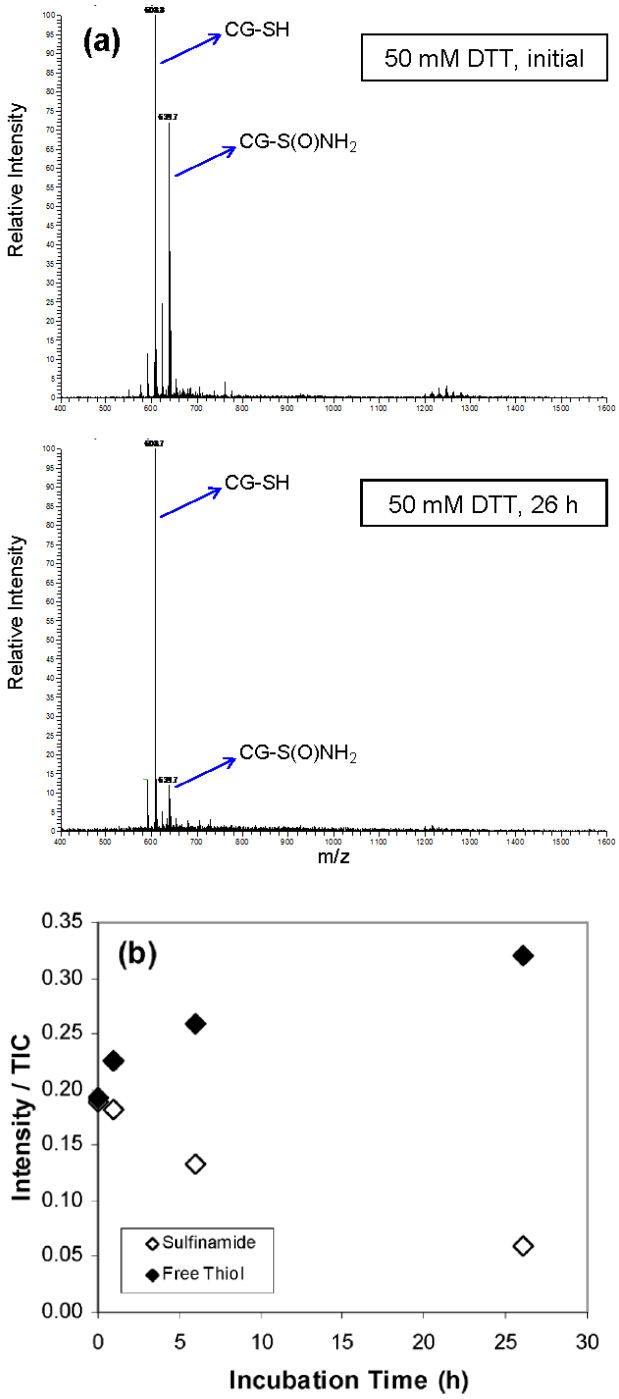

Figure 2-2. Reduction of the VYPCGA-derived sulfinamide (CG-S(O)NH_2). VYPCGA (0.1 mM) was treated with 0.3 mM AS to produce the corresponding sulfinamide. The sample was incubated in phosphate buffer at 37 °C in the presence of 50 mM DTT. (a) Representative ESI-MS spectra showing the reduction of CG-S(O)NH_2 to the free thiol (CG-SH). No disulfide was observed in the initial sample due to its immediate reduction by DTT. (b) The ratios of CG-S(O)NH_2 (◊) and CG-SH (♦) ion abundance to total ion count observed by ESI-MS during the reduction of CG-S(O)NH_2 in the presence of 50 mM DTT (SEM ±5%, n≥3).

Table 2-1. Percent Increase in VYPCGA Free Thiol Upon DTT Treatment of VYPCGA-derived Sulfinamide

Time (h)[a]	ESI-MS[b]	DTNB[c]
1	18	22
6	34	36
26	66	64

[a]Incubation time in phosphate buffer at 37 °C in the presence of 50 mM DTT.
[b]The ratio of free thiol (CG-SH) ion abundance to total ion count was measured for each incubation time. The percent increase reported was determined by normalization with respect to the initial (t = 0) sample (SEM ±5%, n≥3).
[c]The percent increase reported was determined by a standard DTNB assay normalized with respect to the initial (t = 0) sample (SEM ±5%, n≥3).

Similar results were obtained with 50 mM BME, indicating that the reduction is not specific to DTT and should take place in the presence of thiol-based reducing agents in general (Figure 2-3 and Supporting Information). Also, upon increasing BME concentration from 50 to 320 mM, the observed reaction was nearly complete after 26 h.

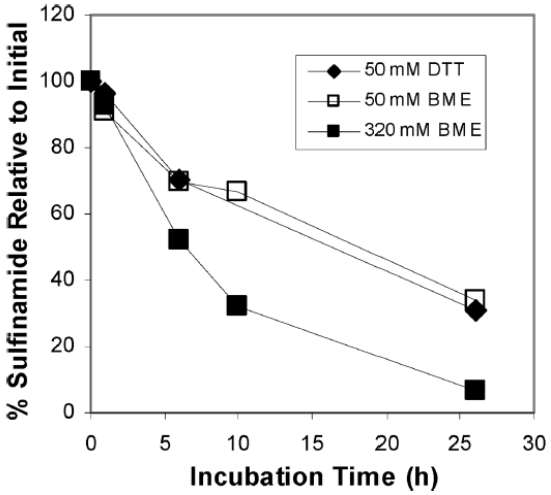

Figure 2-3. Reduction of the VYPCGA-derived sulfinamide (CG-S(O)NH_2) in the presence of various reducing agents. VYPCGA (0.1 mM) was treated with 1 mM AS to form the corresponding sulfinamide. The samples were incubated with 50 mM DTT (◆), 50 mM BME (□), or 320 mM BME (■) in phosphate buffer at 37 °C. The ratio of CG-S(O)NH_2 ion abundance to total ion count was determined for each incubation time. The percent CG-S(O)NH_2 was determined by normalizing the ion abundance ratios with respect to that detected in the initial peptide sample (SEM ±5%, n≥3).

The rate of the protein deamidation reaction is known to be dependent on the nature of the amino acid located at the C-terminal side of the Asn residue. To determine if a similar effect is observed in the reduction of peptide sulfinamides, we utilized the VYPCLA-derived sulfinamide (CL-S(O)NH_2), which contains an adjacent Leu rather than Gly. Again, as observed by ESI-MS (Figure 2-4), a significant amount of CL-S(O)NH_2 was reduced to the corresponding thiol-containing peptide (VYPCLA, CL-SH) in the presence of DTT. Compared with CG-S(O)NH_2, a small decrease in the extent of reduction upon 26 h incubation with DTT in phosphate buffer was observed (Figure 2-5). CG-S(O)NH_2 and CL-S(O)NH_2 were reduced by approximately 70 and 60% after 26 h, respectively, suggesting that sulfinamide reduction is not as sensitive to peptide sequence as the deamidation reaction. The reactivities of VYPCGA-derived and GSH-derived sulfinamides were found to be comparable in ammonium bicarbonate buffer (Figure 2-5).

The difference in CG-S(O)NH_2 reduction observed in phosphate (70%) versus bicarbonate (47%) may indicate the importance of buffer conditions, as has been observed in previous deamidation studies.[36]

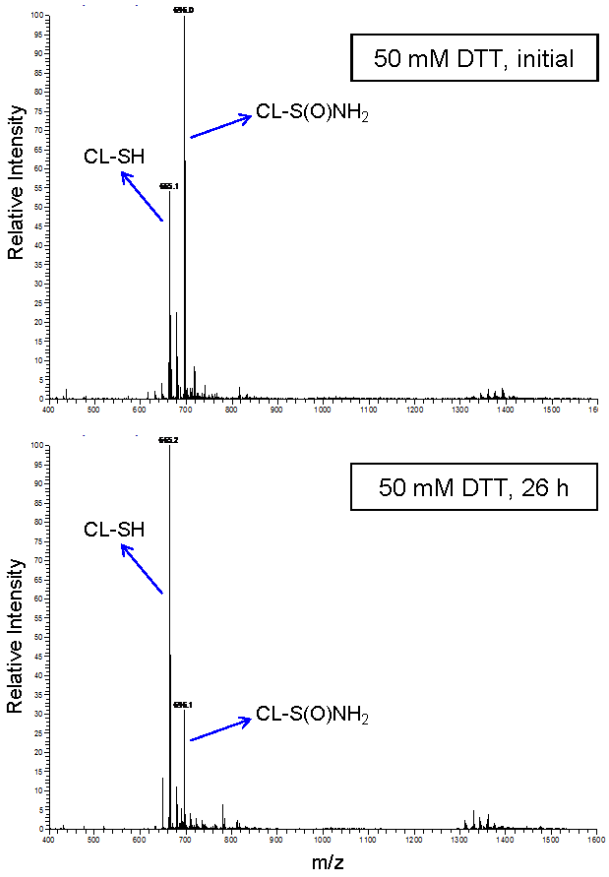

Figure 2-4. Representative ESI-MS spectra showing the reduction of VYPCLA-derived sulfinamide (CL-S(O)NH_2) to the free thiol (CL-SH). VYPCLA (0.1 mM) was treated with 0.3 mM AS to form the corresponding sulfinamide. The sample was incubated in phosphate buffer at 37 °C in the presence of 50 mM DTT for 26 h. No disulfide was observed in the initial sample due to its immediate reduction by DTT.

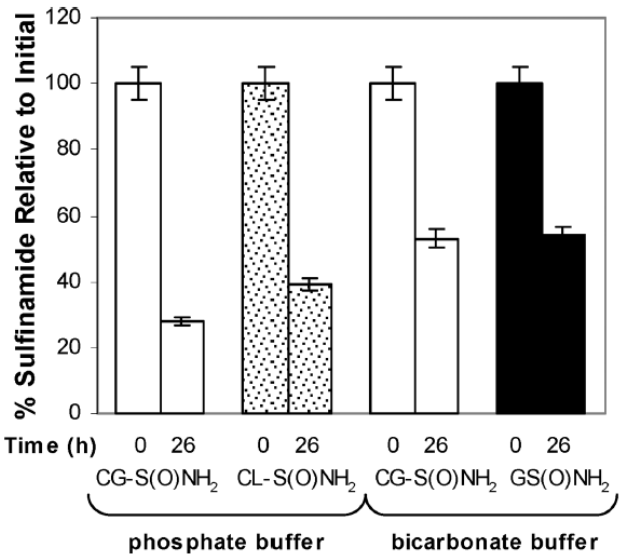

Figure 2-5. Reduction of the VYPCGA-derived (CG-S(O)NH_2), VYPCLA-derived (CL-S(O)NH_2), and glutathione-derived (GS(O)NH_2) sulfinamides in phosphate or bicarbonate buffer. The samples were incubated with 50 mM DTT in sodium phosphate or ammonium bicarbonate buffer (as indicated) at 37 °C for 26 h. The ratio of sulfinamide ion abundance to total ion count was determined in each case. The percent sulfinamide was determined by normalizing the ion abundance ratios with respect to that detected in each initial peptide sample (SEM ±5%, n≥3).

2.2.3 Sulfinamide Reduction in Peptides versus a Small Organic Molecule as a Function of Solvent Dielectric Constant

To test the hypothesis that sulfinamide reduction is facilitated in the peptides, we conducted experiments with a small organic molecule, which cannot form a "succinimide-like" intermediate **1** (Scheme 2-4). For this purpose, we employed 2-phenylethanesulfinamide (PE-S(O)NH_2) and compared its reactivity to that of sulfinamides generated by HNO in the VYPCGA and VYPCLA peptides (CG-S(O)NH_2 and CL-S(O)NH_2, respectively). Also, to probe the reactivity of sulfinamides in hydrophobic environments, we examined the effect of solvent dielectric on these reductions in buffer,

ACN/buffer 50:50 (v/v), and dioxane/buffer 50:50 (v/v), which have dielectric constants of approximately 74, 55, and 34, respectively.[30, 37, 38]

As shown in Figure 2-6a, DTT reduction of PE-S(O)NH_2 is much more facile in buffer versus either ACN/buffer or dioxane/buffer, demonstrating that the direct thiolysis reaction rate is substantially inhibited in lower dielectric environments. Relative to this PE-S(O)NH_2 result, the reduction of both CG-S(O)NH_2 and CL-S(O)NH_2 is more efficient in ACN/buffer and dioxane/buffer (Figure 2-6b-c). A similar behavior was also observed when the experiments were conducted at 55 ^oC in ACN/buffer (Supporting Information). These results indicate that the reduction of peptide sulfinamides involves a second mechanism, implicating the proposed cyclic intermediate **1** (Scheme 2-4) in addition to the direct thiolysis reaction. Moreover, in dioxane/buffer, it appears that the reduction of CG-S(O)NH_2 is more efficient than that of CL-S(O)NH_2. This result suggests a substituent effect (Gly versus Leu) on this reaction that becomes more apparent in dioxane/buffer and may be further indication of the participation of a cyclic intermediate as has been observed with asparagine deamidation.[27]

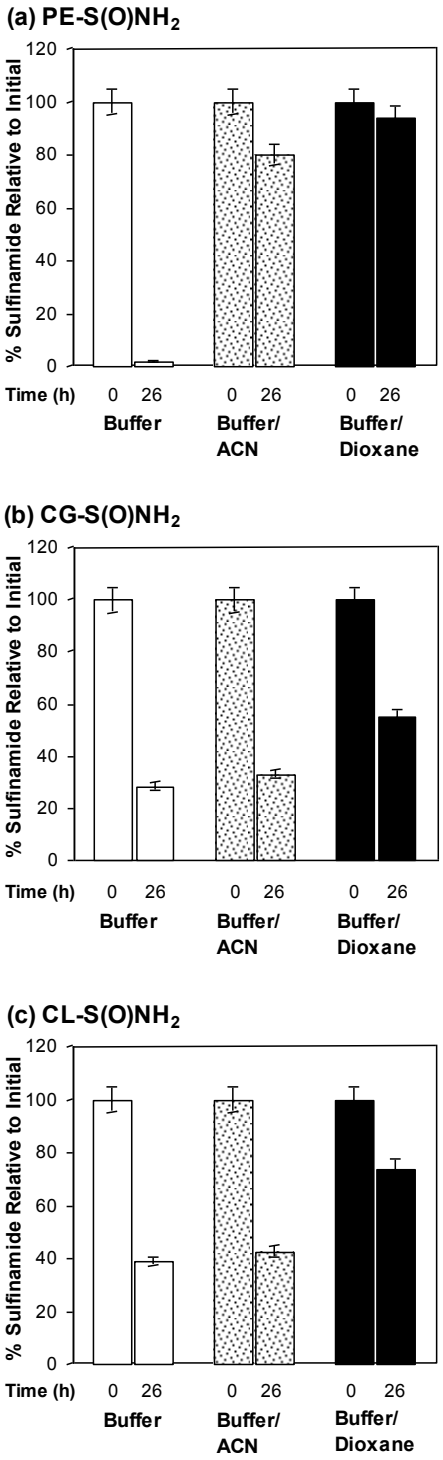

Figure 2-6. Reduction of (a) 2-phenylethanesulfinamide (PE-S(O)NH_2), (b) the VYPCGA-derived sulfinamide (CG-S(O)NH_2), and (c) the VYPCLA-derived sulfinamide (CL-S(O)NH_2) as a function of solvent dielectric constant. The samples were incubated with 50 mM DTT in buffer, ACN/buffer or dioxane/buffer at 37 °C for 26 h. The relative amounts of PE-S(O)NH_2 were quantified by HPLC (SEM ±5%, n≥3). CG-S(O)NH_2 and CL-S(O)NH_2 were analyzed by ESI-MS by examining the ratios of CG-S(O)NH_2 and CL-

$S(O)NH_2$ ion abundance to total ion count in each case. The percent sulfinamide was determined by normalizing each ion abundance ratio with respect to that detected in the initial peptide sample (SEM ±5%, n≥3).

2.2.4 Deamidation of Asn-Containing Peptides

The mass difference between a sulfinamide and its corresponding sulfinic acid is 1 Da. To confirm that sulfinamides and sulfinic acids can be distinguished by ESI-MS, initial experiments were performed with the previously studied peptides, VYPNGA and VYPNLA, which are known to undergo deamidation.[27, 28, 30, 39] Upon incubation of these peptides at 100 °C for 1 h, VYPDGA, the corresponding deamidation product of VYPNGA, was detected in significant amounts, whereas no VYPDLA was observed (Supporting Information). VYPDLA, however, was detected following extended incubation at 100 °C for 10 h. These results correlate well with the reported half-lives of 0.15 and 4.9 h for VYPNGA and VYPNLA, respectively.[27] Thus, a 1 Da shift (i.e., the mass difference between an amide and a carboxylic acid) can be observed with our ESI-MS system, making it a viable technique for the analysis of the sulfinamide to sulfinic acid reaction.

2.2.5 Conversion of Sulfinamides to Sulfinic Acids

The time frame for sulfinic acid formation was investigated by incubating CG-$S(O)NH_2$ in phosphate buffer at 37 °C. As observed by ESI-MS (Figures 2-7 and 2-8), slow conversion of CG-$S(O)NH_2$ to the corresponding VYPCGA-derived sulfinic acid (CG-S(O)OH) occurs in the absence of reducing agents. No reaction was observed when the incubations were done at -20 °C. Interestingly, the reaction was found to be even slower

in ammonium bicarbonate buffer at pH 7.4, again indicating the potential importance of buffer conditions.[36]

To confirm the relative rates of sulfinamide reduction (to form thiol) versus hydrolysis (to form sulfinic acid), analogous experiments were conducted in the presence of DTT. Under these conditions, no sulfinic acid is observed, suggesting that there is a competition between the two reactions. Similar results were obtained upon conducting HPLC experiments with PE-S(O)NH_2 in the presence or absence of DTT. These results demonstrate that sulfinamide reduction by thiols is faster than sulfinamide hydrolysis, as expected.

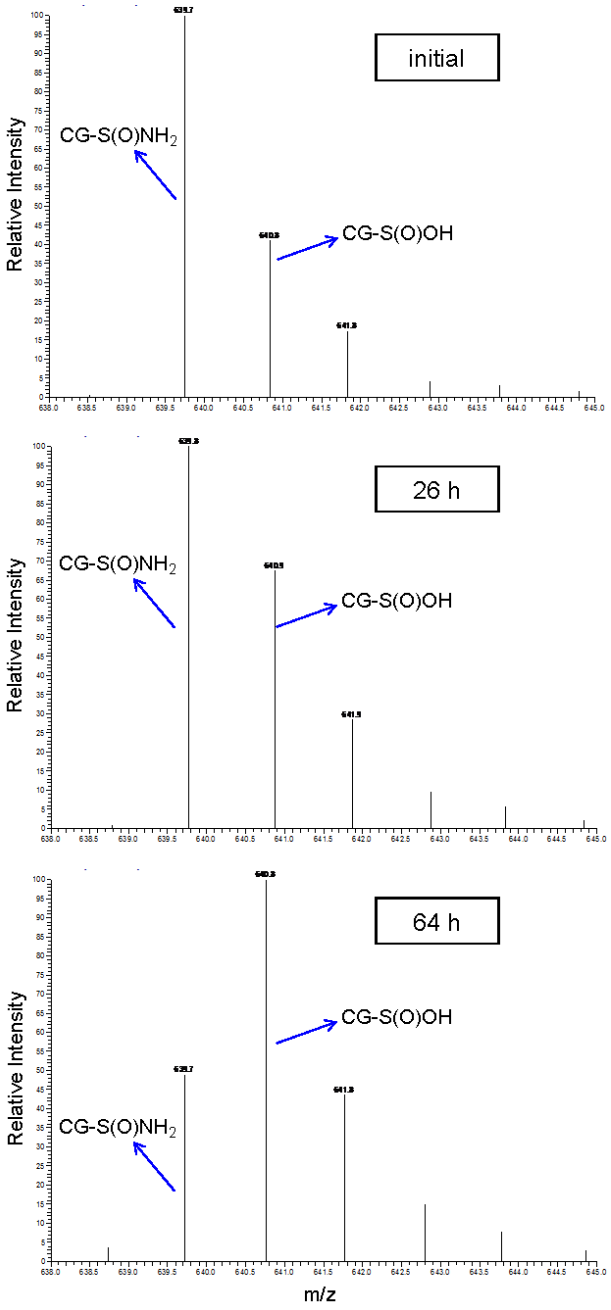

Figure 2-7. Representative ESI-MS spectra showing the formation of the VYPCGA-derived sulfinic acid (CG-S(O)OH) from the VYPCGA-derived sulfinamide (CG-S(O)NH_2). VYPCGA (0.1 mM) was treated with 0.3 mM AS to form the corresponding sulfinamide. The sample was incubated in phosphate buffer at 37 °C in the absence of reducing agents. During data analysis, the intensity of the CG-S(O)NH_2 M+1 isotope was subtracted to determine the actual intensity of the CG-S(O)OH peak.

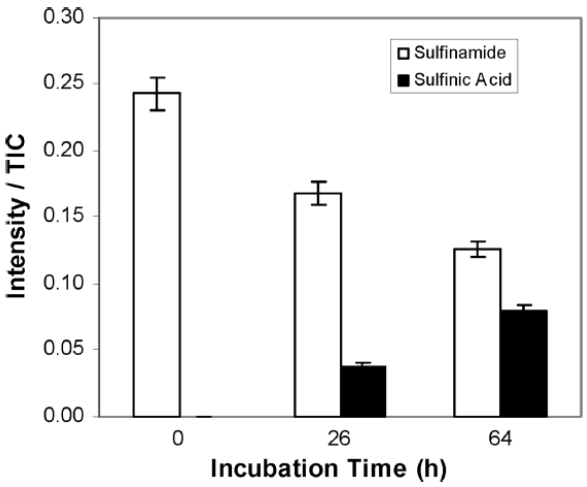

Figure 2-8. Hydrolysis of the VYPCGA-derived sulfinamide (CG-S(O)NH_2) to the VYPCGA-derived sulfinic acid (CG-S(O)OH). VYPCGA (0.1 mM) was treated with 0.3 mM AS to form the corresponding sulfinamide and the samples were incubated in phosphate buffer at 37 °C. CG-S(O)NH_2 and CG-S(O)OH were analyzed by ESI-MS by examining the ratios of CG-S(O)NH_2 (□) and CG-S(O)OH (■) ion abundance to total ion count (SEM ±5%, n≥3).

2.2.6 Detection of Ammonia

The release of ammonia as a byproduct in the reduction of 2-phenylethanesulfinamide was confirmed by a fluorometric assay.[40] When this sulfinamide is incubated in the presence of DTT, increasing concentrations of ammonia are detected corresponding to 53% and 100% reduction after 6 and 26 h, respectively (Figure 2-9a); no ammonia is detected in the initial sample. These results are consistent with the reduction results obtained for 2-phenylethanesulfinamide by HPLC (54% after 6 h; 98% after 26 h). Moreover, Figure 2-9b shows that a small quantity of ammonia (corresponding to 27% sulfinamide hydrolysis after 26 h) is detected in the absence of DTT, which again corresponds well to the amount of 2-phenylethanesulfinic acid formed in buffer as detected by HPLC (23% after 26 h).

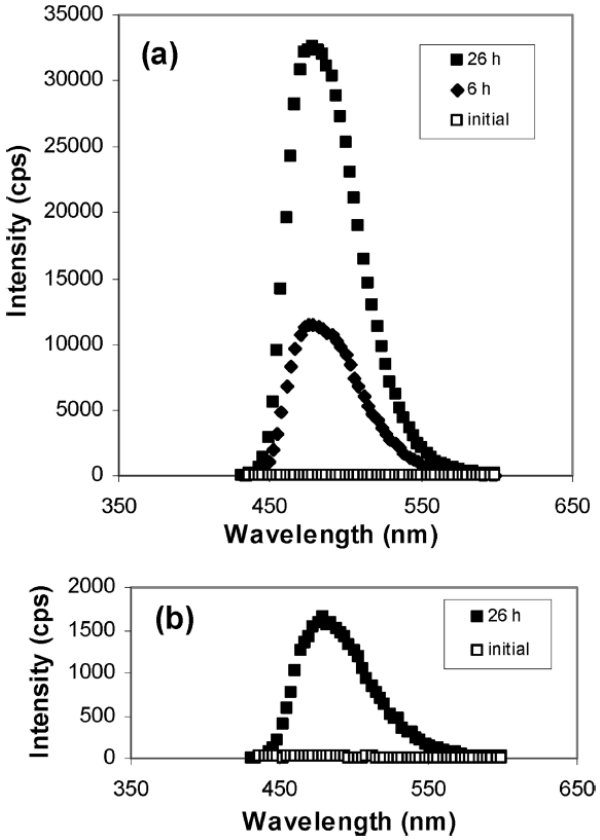

Figure 2-9. Formation of ammonia detected by OPA fluorescence assay. A 2.5 mM solution of 2-phenylethanesulfinamide (PE-S(O)NH_2) was incubated at 37 °C for 26 h (a) in the presence or (b) in the absence of 50 mM DTT and the amount of ammonia was detected in the initial (□), 6 h-incubated (◆) and 26 h-incubated (■) samples.

2.2.7 Reduction of Sulfinamide Modification in Papain

HNO targets several enzymes with active site thiol residues resulting in the loss of enzyme activity.[8, 11-14] The cysteine protease, papain, which in its active form has a single free thiol,[41, 42] is known to be inhibited by HNO. The mechanism of inhibition has been proposed to be due to the formation of a sulfinamide.[11] In addition, it has been observed that incubation of AS-treated papain with DTT for 1 h results in a small recovery in enzyme activity.[11] To determine whether a sulfinamide modification in a protein can be reverted back to the free thiol, we investigated the reactivity of this modification in AS-treated

papain. As seen in Figure 2-10, the inhibition of papain activity can be partially reversed upon incubation with thiol reducing agents over 10 h. Moreover, 26 and 105 h incubation with GSH led to 18% and 44% activity recovery, respectively. Longer incubations were not possible with DTT or BME due to the significant loss of papain activity observed in the control samples.

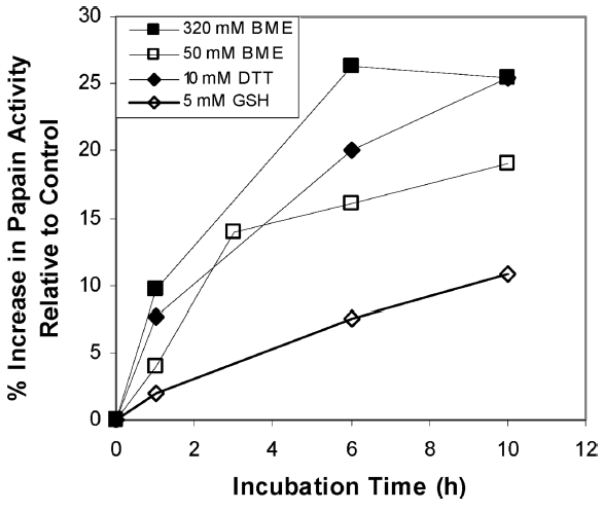

Figure 2-10. Reduction of the HNO-derived sulfinamide in papain. Previously activated papain (0.2 mg/ml) was treated with 100 μM AS. The samples were incubated with 5 mM GSH (◊), 10 mM DTT (◆), 50 mM BME (□), or 320 mM BME (■) in phosphate buffer at 37 °C. Data is expressed as the percentage of the activity of the control samples (SEM ±5%, n≥3). No increase in papain activity was observed in the absence of reducing agents.

To rule out the presence of an HNO-induced disulfide and its subsequent reduction, we investigated the time frame for the reduction of disulfide-modified papain. Non-activated papain was used for these experiments, since its single, active site cysteine is known to exist in a mixed disulfide form rather than the free sulfhydryl form.[43] As expected, non-activated papain had no significant activity. Upon incubation with 50 or 320 mM BME at physiological pH and temperature, the enzyme was activated in less than 10 min (Supporting Information). These results support the hypothesis that the gain of

activity observed after much longer incubation times with AS-treated papain in the presence of reducing agents is due to the reduction of a sulfinamide.

2.3 Discussion

Sulfinamide formation is observed upon the reaction of HNO with thiols. Many examples of sulfinamide-modified proteins have been reported, with several of them being enzymes containing critical cysteine residues.[11-14, 44] Thiol modification has been shown to have dramatic effects on the activities of these enzymes. Although the reduction of this sulfinamide modification has not been studied under physiologically relevant conditions, it has generally been assumed to be stable.[8, 11-14, 20, 44] Our results, employing short peptides as model systems, indicate that the HNO-induced thiol to sulfinamide modification can be reduced in the presence of excess thiol, albeit quite slowly. At physiological pH and temperature, about one third of the sulfinamide-modified peptide is reduced back to free thiol after 6 h. This reduction does not seem to be strongly dependent on the peptide sequence in buffer, but a substituent effect is observed in lower dielectric constant solvents.

Direct thiolysis (Scheme 2-2) and a mechanism analogous to the succinimide-mediated deamidation mechanism (Scheme 2-4) are two plausible pathways. The major difference between the two mechanisms is the involvement of a cyclic intermediate **1**, the formation of which is facilitated by a peptide structure. Intermediate **1** has been proposed in the hydrolysis of peptide sulfinamides to produce the corresponding sulfinic acids.[24] We have observed that under physiological conditions only a small amount of our peptide sulfinamides are converted to the corresponding sulfinic acids after 26 h. Due to the relatively longer half-life of sulfinic acid formation, the reduction of sulfinic acids to thiols

is not considered to be a probable pathway.[45, 46] This is supported by the fact that no significant sulfinic acid formation is observed in the presence of DTT.

Previously we have reported that *t*-butanesulfinamide is unreactive with DTT at room temperature over 12 h.[20] Since *t*-butanesulfinamide is extremely sterically hindered, we tested the reactivity of a more relevant small organic molecule sulfinamide, 2-phenylethanesulfinamide (PE-S(O)NH_2). Upon 26 h incubation in thiol-containing buffer at 37 °C, >90% reduction is observed, demonstrating that direct thiolysis (Scheme 2-2) is a viable mechanism at physiological pH and temperature. It should also be noted that sulfinic acid formation is not detected upon incubating 2-phenylethanesulfinamide in the presence of DTT, indicating that direct thiolysis of this sulfinamide is more efficient than the corresponding hydrolysis reaction.

To learn more about the reactivity of sulfinamides, we have also investigated the effect of solvent dielectric by employing different co-solvents. Our results with PE-S(O)NH_2 indicate that the direct thiolysis reaction is significantly inhibited as the solvent dielectric constant decreases. Moreover, we have shown that in lower dielectric environments peptide sulfinamides are more reactive towards reduction by DTT compared with PE-S(O)NH_2. A possible explanation for the observed difference in reactivity is that in the case of the peptide sulfinamides there is a contribution from cyclic intermediate **1**, which becomes more significant upon inhibition of the direct thiolysis pathway. This explanation is further supported by the observed sequence dependence (analogous to that for the asparagine deamidation reaction[27]) that is manifested only under low dielectric constant conditions. Based on the overall results, it can also be inferred that the impact of solvent dielectric is larger on the direct thiolysis mechanism (Scheme 2-2) compared to the

mechanism involving cyclic intermediate **1** (Scheme 2-4), although both mechanisms are affected. Our results are consistent with a recent computational study, where the energetics and feasibilities of several asparagine deamidation pathways were compared.[47] These computational results indicate that direct hydrolysis is a competitive reaction with the imide-mediated deamidation reaction even in the absence of acid or base catalysis.[47]

Considering that the half-life of proteins varies from less than 3 min to more than 20 h in vivo,[48-51] the time scales presented here are relevant to cellular proteins (e.g., GAPDH, $t_{1/2}$=38.1 h).[52] Moreover, our results in lower solvent dielectric media indicate that sulfinamide reduction can take place in hydrophobic as well as hydrophilic regions of proteins. This may also be particularly relevant to HNO-targeted proteins containing cysteines in their hydrophobic domains such as the regulatory protein of the sarcoplasmic reticulum Ca^{2+} pump, phospholamban.[20] Since the irreversible inhibition of proteins with critical thiol residues has been hypothesized to have detrimental effects on lysosomal protein degradation, cell cycle, and energy metabolism at the glycolytic level,[11, 14, 53] the reduction of a sulfinamide modification is relevant to the use of HNO as a therapeutic agent. It should be noted that the peptides used in the present study do not have well-defined secondary structure and that the presence of higher order structures may very likely affect reaction rates.

Papain is a well-studied cysteine protease containing three disulfide bonds and a single active site cysteine residue,[41, 42] which is prone to inhibition presumably due to HNO-induced sulfinamide formation.[11] In a previous study, AS-treated papain was incubated with DTT for a short period of time (1 h) and some recovery in the activity was observed.[11] Since sulfinamide reduction was previously thought to be unlikely, this

recovery was attributed to the reduction of a possible disulfide modification. We have observed that the time frame for the reduction of disulfides (<10 min) and sulfinamides (several hours) are significantly different. Although we have not yet directly characterized the modification, based on the results reported here, we suggest that the HNO-derived sulfinamide in papain can be reduced back to free thiol in the presence of reducing agents, indicating the feasibility of this reaction in a protein environment.

2.4 Conclusions

We have demonstrated that HNO-derived sulfinamides can be reverted back to free thiols under physiologically relevant conditions. In the presence of reducing agents, this reaction is feasible in small organic molecules, peptides, and proteins. Although both peptide and small organic molecule sulfinamides are susceptible to hydrolysis, this reaction is slower than reduction by thiols. Our results suggest that the mechanism of peptide sulfinamide reduction involves a contribution from a cyclic intermediate, whose relative impact becomes more significant in environments of lower dielectric constant. Considering the broad spectrum of pharmacological effects attributed to HNO,[5, 6, 53] these findings are relevant to the study of HNO-induced modifications in biological systems.

2.5 Experimental Methods

Reagents. Glutathione (GSH), papain, N_{α}-Benzoyl-L-arginine 4-nitroanilide hydrochloride (L-BAPNA), 5,5'-dithiobis(2-nitrobenzoic acid) (DTNB), *o*-phthalaldehyde (OPA), β-mercaptoethanol (BME) and DTT were of the highest purity available and purchased from Sigma (St. Louis, MO). 2-Phenylethanethiol and 2-(bromoethyl)benzene were purchased from Acros. HPLC grade acetonitrile (ACN) was purchased from Thermo Fisher Scientific (Rockford, IL). The HNO-donors, Angeli's salt ($Na_2N_2O_3$, AS) and 2-

bromo-*N*-hydroxybenzenesulfonamide (2-BrPA), were synthesized as previously described.[54, 55] Milli Q water was used for all purifications and experiments.

Peptide Synthesis and Purification. Synthetic peptides VYPCGA, VYPCLA, VYPNGA and VYPNLA were synthesized on a Symphony Quartet peptide synthesizer (Protein Technologies Inc., Tucson, AZ) following Fmoc solid-phase peptide synthesis methods.[56] The crude product was dissolved in 0.1% trifluoroacetic acid (TFA) and purified by HPLC (Waters HPLC equipped with Delta 600 pump system and dual wavelength absorbance detector) on an Apollo C_{18} reverse-phase column using a linear gradient of 5-75% ACN with 0.1% TFA over 50 min at room temperature. Peptide fractions were identified by electrospray ionization mass spectrometry (ESI-MS). Pure fractions were pooled and lyophilized, and the purified product was quantified based on the absorbance at 280 nm (ε_{280}= 1490 M^{-1} cm^{-1}).[57] In all cases, the peptides were stored at -20 °C in lyophilized form until use.

Synthesis of 2-Phenylethanesulfinamide. The synthesis was carried out based on known methods for the synthesis of sulfinamides.[58] Briefly, bis(2-phenylethyl) disulfide was generated from (2-bromoethyl)benzene using thiourea, MnO_2 and Na_2CO_3 as described in the literature.[59] The disulfide was reacted with 1.5 equivalents of *N*-bromosuccinimide (NBS) in methanol to form the corresponding methyl sulfinate. After stirring the reaction at room temperature for 3 h, the mixture was diluted with CH_2Cl_2, washed with saturated $NaHSO_3$ solution, and extracted with a saturated solution of $NaHCO_3$. 2-Phenylethanesulfinamide was formed by reacting methyl 2-phenylethylsulfinate with 2 equivalents of butyllithium and 2 equivalents of bis(trimethylsilyl)amine in tetrahydrofuran at -78 °C. (Caution: Butyllithium is water-

reactive, extremely flammable, and pyrophoric.) The reaction was then stirred at room temperature for 2 h and quenched by adding a saturated solution of NH_4Cl. The mixture was extracted with ethyl acetate (EtOAc), dried with $MgSO_4$, and the solvent was evaporated under vacuum. The resulting sulfinamide was purified on a silica column by employing a hexane/EtOAc solvent system. The solvent was evaporated under vacuum to obtain a white solid: ^1H NMR ($CDCl_3$) δ 7.27 (m, 5H), 4.10 (s, 2H), 3.06 (m, 4H); ^{13}C NMR ($CDCl_3$) δ 138.8, 128.8, 128.5, 126.8, 58.7, 29.0; FAB-MS (3-NBA): *m/z* calcd 170.06396 [M+H], found 170.06470. The structure of 2-phenylethanesulfinamide was also confirmed by X-ray crystallography (Supporting Information).

Formation of Peptide Sulfinamides by Reaction with HNO. Peptides were dissolved in 10 mM sodium phosphate buffer with 50 μM of the metal chelator, diethylenetriamine pentaacetic acid (DTPA), at pH 7.4 (or in 10 mM ammonium bicarbonate buffer with 50 μM DTPA at pH 7.4 where indicated) to have a final concentration of 100 μM and used immediately. Stock solutions of AS were prepared in 0.01 M NaOH, kept in ice, and used within 15 min of preparation. Stock solutions of 2-BrPA were prepared in ACN and used within 15 min of preparation. The peptides were incubated with various concentrations of AS or 2-BrPA (as indicated) at 37 °C for 30 min in a block heater. The samples were flash-frozen and lyophilized overnight. The lyophilized samples were stored at -20 °C and used within a day.

In the case of ammonium bicarbonate buffer, the peptides were dissolved to have a final concentration of 250 μM and incubated with 5 mM 2-BrPA as described above. The samples were used immediately without prior lyophilization. Under the conditions of our experiments, ammonium bicarbonate buffer remained stable over a period of 69 h, as

indicated by a pH increase of only 0.7 units over this time period. For all experiments, the volume of 0.01 M NaOH or ACN introduced was less than 1% of the total sample volume.

Peptide Incubations in Buffer. Stock solutions of DTT (1 M) were freshly prepared in water and used within 15 min of preparation. BME was used directly. The sulfinamide-containing peptides were redissolved in water to have a final peptide concentration of 0.8 mM and buffer concentration of 82 mM sodium phosphate with 410 μM DTPA at pH 7.4. The samples were aliquoted and incubated in the presence or absence of reducing agents at 37 °C as indicated. Individual aliquots were removed from the samples for analysis at certain time intervals. The peptides were purified and desalted with C_{18} PepClean spin columns, and then diluted into 70% ACN with 0.1% TFA for immediate ESI-MS analysis.

Peptide Incubations in ACN/Buffer or Dioxane/Buffer. Stock solutions of the reducing agents were prepared as described above. The sulfinamide-containing peptides were redissolved in ACN/water 50:50 (v/v) or dioxane/water 50:50 (v/v) to have a final peptide concentration of 0.8 mM and buffer concentration of 82 mM sodium phosphate with 410 μM DTPA. The samples were incubated in the presence of reducing agents at 37 or 55 °C. Individual aliquots were removed from the samples for analysis at certain time intervals. The solvent was then removed under vacuum at room temperature in a Savant Speedvac apparatus. The residue was dissolved in water and prepared for ESI-MS analysis as described above. As a control, in all cases, a side-by-side experiment was conducted in sodium phosphate buffer and the sample was exposed to the same sample preparation steps as the sample in ACN/buffer or dioxane/buffer.

Incubation of Asn-Containing Peptides. VYPNGA and VYPNLA were dissolved in 50 mM phosphate buffer at pH 7.4. The samples were incubated at 100 °C and aliquots were taken for analysis at certain time intervals. They were prepared for ESI-MS analysis as described above.

Incubation of 2-Phenylethanesulfinamide and HPLC Analysis. Stock solutions of the reducing agents were prepared as described above. 2-Phenylethanesulfinamide was dissolved in 82 mM sodium phosphate buffer with 410 μM DTPA at pH 7.4 to have a final sulfinamide concentration of 2.5 mM. The samples were incubated in the presence or absence of reducing agents at 37 °C. Individual aliquots were removed from the samples for analysis at certain time intervals and cooled in ice for 5 min. They were then immediately analyzed by HPLC. All the analyses were performed on an Apollo C_{18} reverse-phase column connected to the HPLC system described above. A linear gradient of 35-80% ACN with 0.1% TFA over 35 min was employed at room temperature. The compounds were followed at 220 nm and peaks were assigned based on co-injection with authentic samples.

For experiments performed in organic co-solvents, 2-phenylethanesulfinamide was dissolved in ACN/pH 7.4 phosphate buffer 50:50 (v/v) or dioxane/pH 7.4 phosphate buffer 50:50 (v/v) to have a final sulfinamide concentration of 2.5 mM and buffer concentration of 82 mM sodium phosphate with 410 μM DTPA. The samples were incubated in the presence or absence of reducing agents at 37 or 55 °C and analyzed as described above.

Mass Spectrometric Analyses. ESI-MS analysis was carried out on a Thermo Finnigan LCQ Deca Ion Trap Mass Spectrometer fitted with an electrospray ionization source, operating in the positive ion mode with an accuracy of ca. 0.1 m/z. In all

experiments, the samples were introduced to the instrument at a rate of 10 μL/min using a syringe pump via a silica capillary line. The heated capillary temperature was 250 °C and the spray voltage was 5 kV.

DTNB Assay for Quantitation of Free Thiol. Stock solutions of DTT were prepared as described above. The sulfinamide-containing peptides were redissolved in water to have a final peptide concentration of 0.8 mM and buffer concentration of 82 mM sodium phosphate with 410 μM DTPA at pH 7.4. The samples were incubated in the presence of reducing agents at 37 °C. Individual aliquots were removed from the samples for analysis at certain time intervals. The peptides were desalted with C_{18} PepClean spin columns to remove excess DTT. The solvent was then removed under vacuum at room temperature and the residue was redissolved in 10 mM phosphate buffer with 50 μM DTPA at pH 8. The free sulfhydryl content was immediately determined by DTNB titration.[35] In all cases, a peptide sample incubated without AS and exposed to the same sample preparation procedure was employed as a control. The results were corrected for the amount of free thiol in the initial sample and normalized with respect to the indicated control sample.

Detection of Ammonia. 2-Phenylethanesulfinamide was dissolved in 82 mM sodium phosphate buffer with 410 μM DTPA at pH 7.4 to have a final sulfinamide concentration of 2.5 mM. The samples were incubated in the presence or absence of DTT at 37 °C. Individual aliquots were removed from the samples for analysis at certain time intervals and the concentration of ammonia was analyzed by a fluorometric assay using OPA.[40] $(NH_4)_2SO_4$ solutions were used as calibration standards. For the standard solutions and incubations carried out in the absence of DTT, the reducing agent was added at the

time of the fluorometric assay (which requires DTT). The fluorometric analyses were conducted on a Spex Fluorolog equipped with a 450 W Xe lamp.

Activation of Papain. A 0.5 mg/ml papain solution was prepared by dissolving the lyophilized enzyme in 82 mM sodium phosphate buffer with 410 μM DTPA at pH 7.4. The papain sample was activated by treating it with 2 mM DTT for 1.5 h at room temperature to reconvert its single free cysteine to the sulfhydryl form. The activated enzyme was stored at -20 °C. Before analysis, it was thawed and desalted with Zeba spin desalting columns to remove excess DTT. The papain solution was then diluted to 0.2 mg/ml with sodium phosphate buffer. To overcome batch to batch variation in the actual activity of the reduced papain preparation, all activity results are expressed as a percentage of the indicated control.

Incubation of Papain Solutions and Activity Assay. A solution of 0.2 mg/ml activated papain in 82 mM sodium phosphate buffer with 410 μM DTPA at pH 7.4 was divided into two and the aliquots were incubated with 0 or 100 μM AS at 37 °C for 30 min. Reducing agents were then added to both solutions to have the required concentration, as indicated. The samples were incubated at 37 °C and aliquots were taken from each sample at certain time intervals, and immediately analyzed by a 20 min kinetic assay using L-BAPNA as the substrate.[11] In all cases, the sample incubated without AS served as the control sample to correct for the decrease in papain activity due to long incubations. In some experiments, non-activated papain, whose single active site cysteine is in a mixed disulfide form,[43] was utilized instead of the activated papain as indicated. All the spectrophotometric analyses were conducted on a Hewlett-Packard 8453 Diode Array Spectrophotometer.

Analysis of the Data. All analyses were carried out in triplicate. Although the absolute amounts of the relevant thiol-containing species cannot be determined from any one of the reported ESI-MS experiments, the changes in the relative amounts of sulfinamide, sulfinic acid, thiol, and disulfide can be determined by calculating the percentage of each species in the total ion count (TIC). Such analyses, where ratios of ion abundances are compared in different experiments, have been commonly employed as label-free quantification methods in proteomics.[60] In addition, for comparison, absolute yields of thiol were determined by DTNB assay and were in good agreement with the ESI-MS determined relative yields. In all cases, error (SEM) was found to be ±5%.

2.6 References

1. Leonard, S. E., and Carroll, K. S. (2011) Chemical omics' approaches for understanding protein cysteine oxidation in biology, *Curr. Opin. Chem. Biol. 15*, 88-102.
2. Reddie, K. G., and Carroll, K. S. (2008) Expanding the functional diversity of proteins through cysteine oxidation, *Curr. Opin. Chem. Biol. 12*, 746-754.
3. Paolocci, N., Katori, T., Champion, H. C., St John, M. E., Miranda, K. M., Fukuto, J. M., Wink, D. A., and Kass, D. A. (2003) Positive inotropic and lusitropic effects of HNO/NO^- in failing hearts: Independence from beta-adrenergic signaling, *Proc. Natl. Acad. Sci. U. S. A. 100*, 5537-5542.
4. Paolocci, N., Saavedra, W. F., Miranda, K. M., Martignani, C., Isoda, T., Hare, J. M., Espey, M. G., Fukuto, J. M., Feelisch, M., Wink, D. A., and Kass, D. A. (2001) Nitroxyl anion exerts redox-sensitive positive cardiac inotropy in vivo by calcitonin gene-related peptide signaling, *Proc. Natl. Acad. Sci. U. S. A. 98*, 10463-10468.

5. Kemp-Harper, B. K. (2011) Nitroxyl (HNO): A novel redox signaling molecule, *Antioxid. Redox Signaling 14*, 1609-1613.

6. Flores-Santana, W., Salmon, D. J., Donzelli, S., Switzer, C. H., Basudhar, D., Ridnour, L., Cheng, R., Glynn, S. A., Paolocci, N., Fukuto, J. M., Miranda, K. M., and Wink, D. A. (2011) The specificity of nitroxyl chemistry is unique among nitrogen oxides in biological systems, *Antioxid. Redox Signaling 14*, 1659-1674.

7. Doyle, M. P., Mahapatro, S. N., Broene, R. D., and Guy, J. K. (1988) Oxidation and reduction of hemoproteins by trioxodinitrate(II). The role of nitrosyl hydride and nitrite, *J. Am. Chem. Soc. 110*, 593-599.

8. Wong, P. S. Y., Hyun, J., Fukuto, J. M., Shirota, F. N., DeMaster, E. G., Shoeman, D. W., and Nagasawa, H. T. (1998) Reaction between *S*-nitrosothiols and thiols: Generation of nitroxyl (HNO) and subsequent chemistry, *Biochemistry 37*, 5362-5371.

9. Fukuto, J. M., and Carrington, S. J. (2011) HNO signaling mechanisms, *Antioxid. Redox Signaling 14*, 1649-1657.

10. Tocchetti, C. G., Stanley, B. A., Murray, C. I., Sivakumaran, V., Donzelli, S., Mancardi, D., Pagliaro, P., Gao, W. D., van Eyk, J., Kass, D. A., Wink, D. A., and Paolocci, N. (2011) Playing with cardiac "redox switches": The "HNO way" to modulate cardiac function, *Antioxid. Redox Signaling 14*, 1687-1698.

11. Vaananen Antti, J., Kankuri, E., and Rauhala, P. (2005) Nitric oxide-related species-induced protein oxidation: reversible, irreversible, and protective effects on enzyme function of papain, *Free Radical Biol. Med. 38*, 1102-1111.

12. Lopez, B. E., Rodriguez, C. E., Pribadi, M., Cook, N. M., Shinyashiki, M., and Fukuto, J. M. (2005) Inhibition of yeast glycolysis by nitroxyl (HNO): A mechanism of HNO toxicity and implications to HNO biology, *Arch. Biochem. Biophys. 442*, 140-148.

13. Lopez, B. E., Wink, D. A., and Fukuto, J. M. (2007) The inhibition of glyceraldehyde-3-phosphate dehydrogenase by nitroxyl (HNO), *Arch. Biochem. Biophys. 465*, 430-436.

14. Vaananen Antti, J., Salmenpera, P., Hukkanen, M., Rauhala, P., and Kankuri, E. (2006) Cathepsin B is a differentiation-resistant target for nitroxyl (HNO) in THP-1 monocyte/macrophages, *Free Radical Biol. Med. 41*, 120-131.

15. Cook, N. M., Shinyashiki, M., Jackson, M. I., Leal, F. A., and Fukuto, J. M. (2003) Nitroxyl-mediated disruption of thiol proteins: inhibition of the yeast transcription factor Ace1, *Arch. Biochem. Biophys. 410*, 89-95.

16. Cheong, E., Tumbev, V., Abramson, J., Salama, G., and Stoyanovsky, D. A. (2005) Nitroxyl triggers Ca^{2+} release from skeletal and cardiac sarcoplasmic reticulum by oxidizing ryanodine receptors, *Cell Calcium 37*, 87-96.

17. Kim, W.-K., Choi, Y.-B., Rayudu, P. V., Das, P., Asaad, W., Arnelle, D. R., Stamler, J. S., and Lipton, S. A. (1999) Attenuation of NMDA receptor activity and neurotoxicity by nitroxyl anion, NO^-, *Neuron 24*, 461-469.

18. Shen, B., and English, A. M. (2005) Mass spectrometric analysis of nitroxyl-mediated protein modification: Comparison of products formed with free and protein-based cysteines, *Biochemistry 44*, 14030-14044.

19. Demaster, E. G., Redfern, B., and Nagasawa, H. T. (1998) Mechanisms of inhibition of aldehyde dehydrogenase by nitroxyl, the active metabolite of the alcohol deterrent agent cyanamide, *Biochem. Pharmacol. 55*, 2007-2015.

20. Froehlich, J. P., Mahaney, J. E., Keceli, G., Pavlos, C. M., Goldstein, R., Redwood, A. J., Sumbilla, C., Lee, D. I., Tocchetti, C. G., Kass, D. A., Paolocci, N., and Toscano, J. P. (2008) Phospholamban thiols play a central role in activation of the cardiac muscle sarcoplasmic reticulum calcium pump by nitroxyl, *Biochemistry 47*, 13150-13152.

21. Rhee, S. G., Chae, H. Z., and Kim, K. (2005) Peroxiredoxins: A historical overview and speculative preview of novel mechanisms and emerging concepts in cell signaling, *Free Radical Biol. Med. 38*, 1543-1552.

22. Joensson, T. J., Murray, M. S., Johnson, L. C., Poole, L. B., and Lowther, W. T. (2005) Structural basis for the retroreduction of inactivated peroxiredoxins by human sulfiredoxin, *Biochemistry 44*, 8634-8642.

23. Joensson, T. J., Murray, M. S., Johnson, L. C., and Lowther, W. T. (2008) Reduction of cysteine sulfinic acid in peroxiredoxin by sulfiredoxin proceeds directly through a sulfinic phosphoryl ester intermediate, *J. Biol. Chem. 283*, 23846-23851.

24. Hoffman, M. D., Walsh, G. M., Rogalski, J. C., and Kast, J. (2009) Identification of nitroxyl-induced modifications in human platelet proteins using a novel mass spectrometric detection method, *Mol. Cell. Proteomics 8*, 887-903.

25. Clarke, V., and Cole, E. R. (1994) Sulfenamides and sulfinamides. X. Oxidation of thiols by aryl sulfinamides, *Phosphorus, Sulfur Silicon Relat. Elem. 91*, 45-52.

26. Kice, J. L., and Large, G. B. (1968) Mechanisms of reactions of thiolsulfinates (sulfenic anhydrides). II. The thiolsulfinate-mercaptan reaction, *J. Org. Chem. 33*, 1940-1944.

27. Geiger, T., and Clarke, S. (1987) Deamidation, isomerization, and racemization at asparaginyl and aspartyl residues in peptides. Succinimide-linked reactions that contribute to protein degradation, *J. Biol. Chem. 262*, 785-794.

28. Stephenson, R. C., and Clarke, S. (1989) Succinimide formation from aspartyl and asparaginyl peptides as a model for the spontaneous degradation of proteins, *J. Biol. Chem. 264*, 6164-6170.

29. Kossiakoff, A. A. (1988) Tertiary structure is a principal determinant to protein deamidation, *Science 240*, 191-194.

30. Brennan, T. V., and Clarke, S. (1993) Spontaneous degradation of polypeptides at aspartyl and asparaginyl residues: Effects of the solvent dielectric, *Prot. Sci. 2*, 331-338.

31. Donzelli, S., Espey, M. G., Thomas, D. D., Mancardi, D., Tocchetti, C. G., Ridnour, L. A., Paolocci, N., King, S. B., Miranda, K. M., Lazzarino, G., Fukuto, J. M., and Wink, D. A. (2006) Discriminating formation of HNO from other reactive nitrogen oxide species, *Free Radic Biol Med 40*, 1056-1066.

32. Sherman, M. P., Grither, W. R., and McCulla, R. D. (2010) Computational investigation of the reaction mechanisms of nitroxyl and thiols, *J. Org. Chem. 75*, 4014-4024.

33. Muskal, S. M., Holbrook, S. R., and Kim, S. H. (1990) Prediction of the disulfide-bonding state of cysteine in proteins, *Protein Eng 3*, 667-672.

34. Fiser, A., Cserzo, M., Tudos, E., and Simon, I. (1992) Different sequence environments of cysteines and half cystines in proteins. Application to predict disulfide forming residues, *FEBS Lett. 302*, 117-120.

35. Ellman, G. E. (1959) Tissue Sulfhydryl Groups, *Arch. Biochem. Biophys. 82*, 70-77.

36. Patel, K., and Borchardt, R. T. (1990) Chemical Pathways of Peptide Degradation. II. Kinetics of Damidation of an Asparaginyl Residue in a Model Hexapeptide, *Pharm. Res. 7*, 703-711.

37. Gagliardi, L. G., Castells, C. B., Rafols, C., Roses, M., and Bosch, E. (2007) Static dielectric constants of acetonitrile/water mixtures at different temperatures and Debye-Huckel A and a_0B parameters for activity coefficients, *J. Chem. Eng. Data 52*, 1103-1107.

38. Critchfield, F. E., Gibson, J. A., and Hall, J. L. (1953) Dielectric constants for the dioxane-water system from 20 to 35 ^{o}C, *J. Am. Chem. Soc. 75*, 1991-1992.

39. Patel, K., and Borchardt, R. T. (1990) Chemical pathways of peptide degradation. III. Effect of primary sequence on the pathways of deamidation of asparaginyl residues in hexapeptides, *Pharm. Res. 7*, 787-793.

40. Sugawara, K., and Oyama, F. (1981) Fluorogenic reaction and specific microdetermination of ammonia, *J. Biochem. 89*, 771-774.

41. Drenth, J., Jansonius, J. N., Koekoek, R., Swen, H. M., and Wolthers, B. G. (1968) Structure of Papain, *Nature 218*, 929-932.

42. Mitchell, R. E. J., Chaiken, I. M., and Smith, E. L. (1970) Complete amino acid sequence of papain. Additions and corrections, *J. Biol. Chem. 245*, 3485-3492.

43. Sluyterman, L. A. A. (1967) The activation reaction of papain, *Biochim. Biophys. Acta, Enzymol. 139*, 430-438.

44. Shoeman, D. W., Shirota, F. N., DeMaster, E. G., and Nagasawa, H. T. (2000) Reaction of nitroxyl, an aldehyde dehydrogenase inhibitor, with *N*-acetyl-L-cysteine, *Alcohol 20*, 55-59.

45. Hoyle, J. (1990) The Oxidation and Reduction of Sulphinic Acids and Their Derivatives, In *The Chemistry of Sulphinic Acids, Esters and Their Derivatives* (Patai, S., Ed.), pp 453-474, John Wiley & Sons, New York.

46. Marvel, C. S., and Johnson, R. S. (1948) 1-Dodecanesulfinic Acid, *J. Org. Chem. 13*, 822-829.

47. Catak, S., Monard, G., Aviyente, V., and Ruiz-Lopez, M. F. (2009) Deamidation of ssparagine residues: Direct hydrolysis versus succinimide-mediated deamidation mechanisms, *J. Phys. Chem. A 113*, 1111-1120.

48. Boggaram, V., Zuber, M. X., and Waterman, M. R. (1984) Turnover of Newly Synthesized Cytochromes P-450_{scc} and P-$450_{11\beta}$ and Adrenodoxin in Bovine Adrenocortical Cells in Monolayer Culture: Effect of Adrenocorticotropin, *Arch. Biochem. Biophys. 231*, 518-523.

49. Rogers, S., and Rechsteiner, M. (1985) In *Intracellular Protein Catabolism* (Khairallah, E., Bond, J., and Bird, J. W., Eds.), p 405, Liss, New York.

50. Bachmair, A., Finley, D., and Varshavsky, A. (1986) In vivo half-life of a protein is a function of its amino-terminal residue, *Science 234*, 179-186.

51. Li, R., Soosairajah, J., Harari, D., Citri, A., Price, J., Ng, H. L., Morton, C. J., Parker, M. W., Yarden, Y., and Bernard, O. (2006) Hsp90 Increases LIM Kinase Activity by Promoting Its Homo-Dimerization, *FASEB J.*, E417-E425.

52. Franch, H. A., Sooparb, S., and Du, J. (2001) A Mechanism Regulating Proteolysis of Specific Proteins during Renal Tubular Cell Growth, *J. Biol. Chem. 276*, 19126-19131.

53. Choe, C. U., Lewerenz, J., Gerloff, C., Magnus, T., and Donzelli, S. (2011) Nitroxyl in the central nervous system, *Antioxid. Redox Signaling 14*, 1699-1711.

54. Hughes, M. N., and Cammack, R. (1999) Synthesis, chemistry, and applications of nitroxyl ion releasers sodium trioxodinitrate or Angeli's salt and Piloty's acid, *Methods Enzymol. 301*, 279-287.

55. Toscano, J. P., Brookfield, F. A., Cohen, A. D., Courtney, S. M., Frost, L. M., and Kalish, V. J. (2011) *N*-hydroxylsulfonamide derivatives as new physiologically useful nitroxyl donors In *US Patent*, 8,030,356.

56. Chan, W. C., White, P. D., and Editors (2000) *Fmoc Solid Phase Peptide Synthesis: A Practical Approach*.

57. Edelhoch, H. (1967) Spectroscopic determination of tryptophan and tyrosine in proteins, *Biochemistry 6*, 1948-1954.

58. Ruano, J. L. G., Aleman, J., Fajardo, C., and Parra, A. (2005) A new general method for the preparation of *N*-sulfonyloxaziridines, *Org. Lett. 7*, 5493-5496.

59. Firouzabadi, H., Iranpoor, N., and Abbasi, M. (2010) A one-pot, efficient, and odorless synthesis of symmetrical disulfides using organic halides and thiourea in

the presence of manganese dioxide and wet polyethylene glycol (PEG-200), *Tetrahedron Lett. 51*, 508-509.

60. Wong, J. W. H., and Cagney, G. (2010) An Overview of Label-Free Quantitation Methods in Proteomics by Mass Spectrometry, In *Proteome Bioinformatics* (Hubbard, S. J., and Jones, A. R., Eds.), pp 273-283, Humana Press, New York.

2.7 Supporting Information

X-Ray Crystallography of 2-phenylethanesulfinamide. All reflection intensities were measured using a KM4/Xcalibur (detector: Sapphire3) with enhance graphite-monochromated Mo *K*α radiation (λ = 0.71073 Å) under the program CrysAlisPro (Version 1.171.35.11 Oxford Diffraction Ltd., 2011). The program CrysAlisPro (Version 1.171.35.11, Oxford Diffraction Ltd., 2011) was used to refine the cell dimensions. Data reduction was done using the program CrysAlisPro (Version 1.171.35.11, Oxford Diffraction Ltd., 2011). The structure was solved with the program SHELXS-97 (Sheldrick, 2008) and was refined on F^2 with SHELXL-97 (Sheldrick, 2008). Analytical numeric absorption corrections based on a multifaceted crystal model were applied using CrysAlisPro (Version 1.171.35.11, Oxford Diffraction Ltd., 2011). The temperature of the data collection was controlled using the system Cryojet (manufactured by Oxford Instruments). The H atoms (except for the H atoms attached to N1) were placed at calculated positions using the instructions AFIX 23 or AFIX 43 with isotropic displacement parameters having values 1.2 times *U*eq of the attached C atoms. The positions of the H atoms attached to N1 were found from Fourier difference maps. The N–H distances were restrained to 0.88(3). Data were collected at 110 (2) K after the crystal had been flash-cooled from room temperature. The structure is ordered.

Results:

Fw = 169.24, colorless block, 0.41 × 0.30 × 0.13 mm^3, monoclinic, $P2_1/c$ (no. 14), a = 13.9432(7), b = 5.24461(18), c = 11.9405(5) Å, β = 105.094(5)°, V = 843.04(6) $Å^3$, Z = 4, D_x = 1.333 g cm^{-3}, μ = 0.324 mm^{-1}, abs. corr. range: 0.904–0.969. 5149 Reflections were

measured up to a resolution of $(\sin \theta/\lambda)_{max} = 0.62$ Å^{-1}. 1708 Reflections were unique (R_{int} = 0.0260), of which 1505 were observed [$I > 2\sigma(I)$]. 106 Parameters were refined using 2 restraints. $R1/wR2$ [$I > 2\sigma(I)$]: 0.0311/0.0837. $R1/wR2$ [all refl.]: 0.0360/0.0866. S = 1.067. Residual electron density found between −0.27 and 0.32 e Å^{-3}.

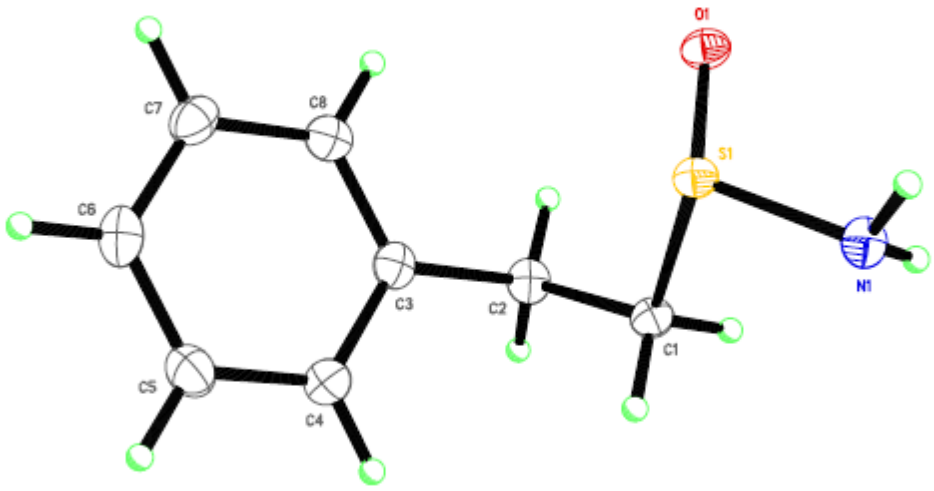

Figure 2-11. X-ray crystal structure of 2-phenylethanesulfinamide.

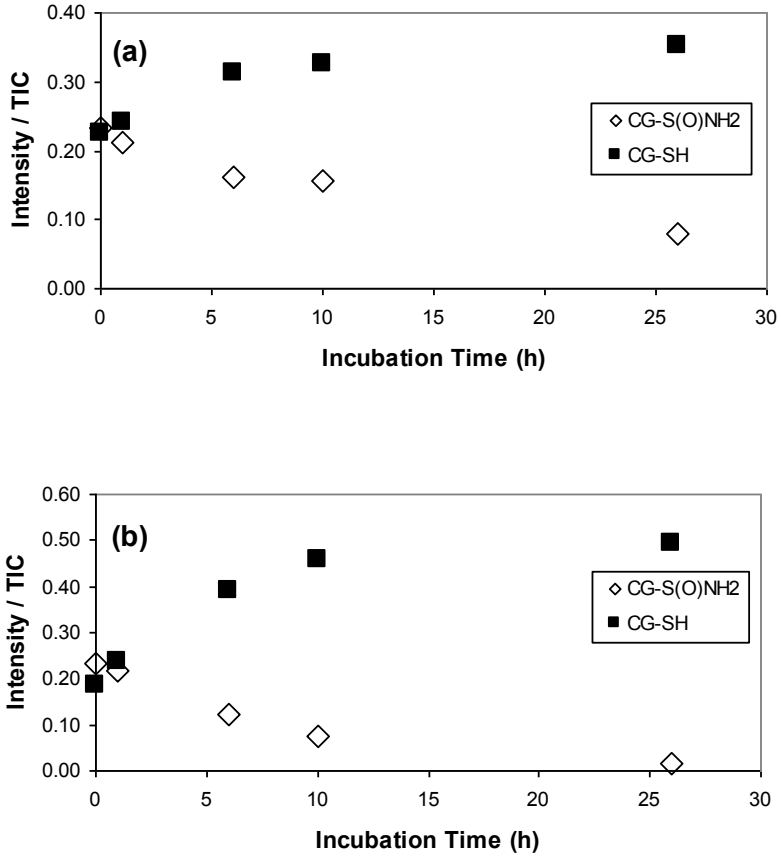

Figure 2-12. Reduction of the VYPCGA-derived sulfinamide (CG-S(O)NH_2). The samples were incubated with (a) 50 mM and (b) 320 mM BME in sodium phosphate buffer at 37 °C for 26 h. The relative ratios of sulfinamide and thiol were determined by normalizing the peak intensities with respect to the total ion count (SEM ±5%, n≥3).

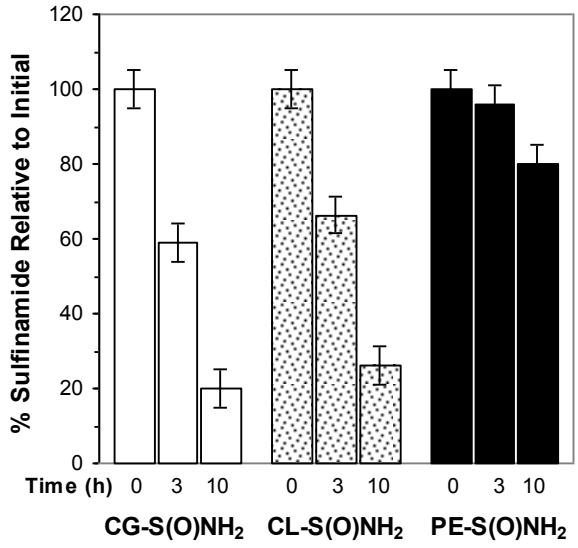

Figure 2-13. Sulfinamide reduction in peptides versus a small organic molecule in ACN/Buffer at 55 ºC. VYPCGA (0.1 mM) and VYPCLA (0.1 mM) were treated with 1 mM AS to form the corresponding sulfinamides, CG-S(O)NH_2 and CL-S(O)NH_2, respectively. The synthesis of 2-phenylethanesulfinamide (PE-S(O)NH_2) was carried out as described in the experimental section. The samples were incubated with 50 mM DTT. The amount of sulfinamide was normalized with respect to that detected in the initial sample (SEM ±5%, n≥3).

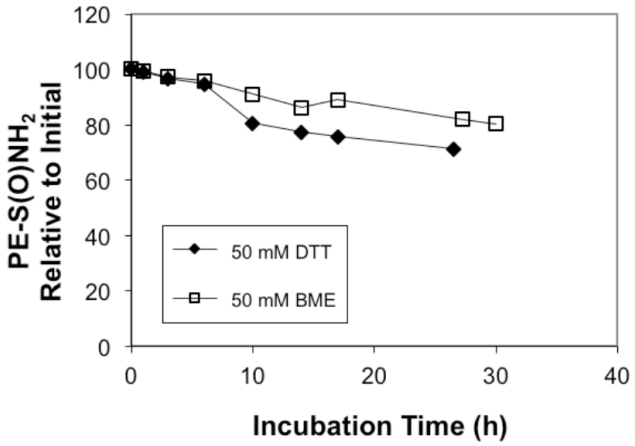

Figure 2-14. Effects of DTT and BME on 2-phenylethanesulfinamide in ACN/pH 7.4 phosphate buffer 50:50 (v/v) at 55 °C. Synthetic 2-phenylethane-sulfinamide (2.5 mM) was incubated in the presence of 50 mM DTT (◆) or BME (□). The samples were analyzed by HPLC (SEM ±5%, n≥3).

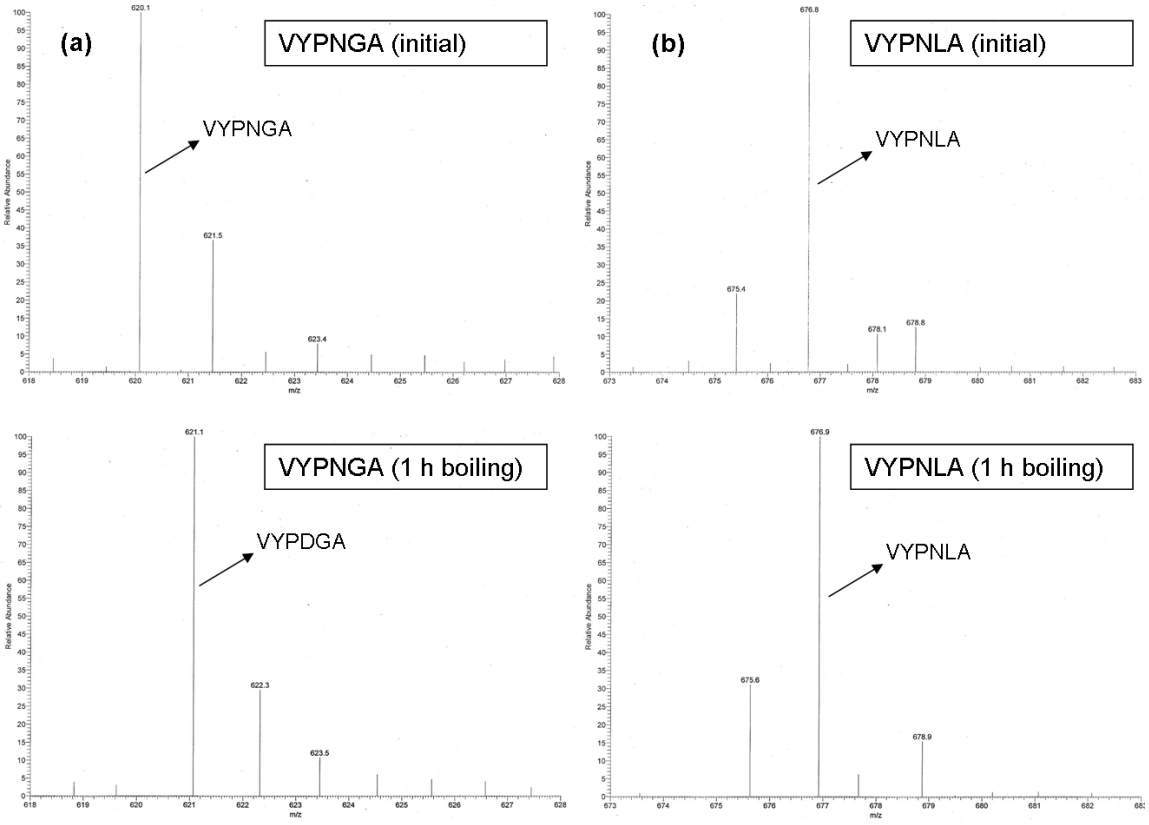

Figure 2-15. (a) Representative ESI-MS spectra showing the deamidation of VYPNGA peptide upon 1 h boiling in buffer. (b) No change was observed upon boiling VYPNLA peptide for 1 h.

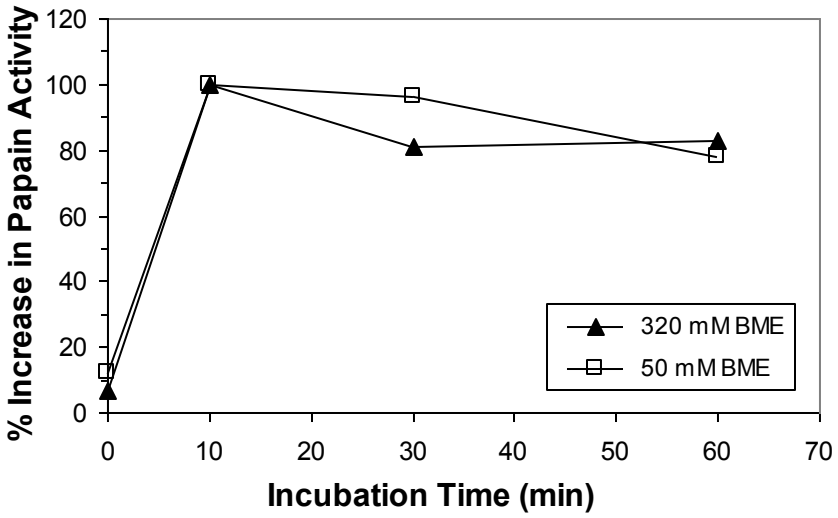

Figure 2-16. Disulfide reduction in papain. Non-activated papain (0.2 mg/ml) was incubated with 50 or 320 mM BME in phosphate buffer at 37 °C. Data is normalized with respect to the maximum activity obtained (SEM ±5%, n≥3).

Chapter 3 – NMR Detection and Study of the Hydrolysis of HNO-Derived Sulfinamides

3.1 Introduction

Cysteine residues are known to be targets of reactive nitrogen oxide species (RNOS).[1-3] Nitroxyl (HNO), the protonated, one-electron reduced form of NO, has been shown to have potential uses in the treatments of heart failure, alcoholism, vascular dysfunction, and cancer.[2, 4-6] HNO is very reactive with thiols, forming sulfinamides or disulfides depending on the concentration of thiol (Scheme 1).[7, 8] Sulfinamide formation dominates at low thiol concentrations, whereas disulfide and hydroxylamine become the major end products in the presence of excess thiol.

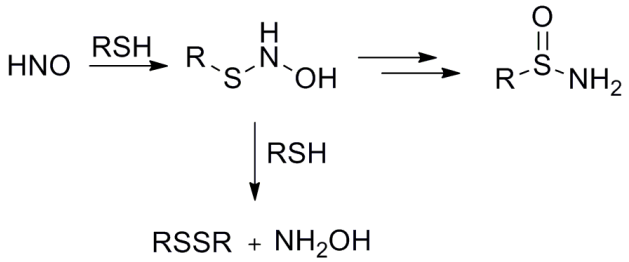

Scheme 3-1. The reaction of HNO with thiols

HNO-induced effects have been detected on several cysteine-containing proteins.[9-23] In many of these proteins the observed effects are attributed to the formation of a sulfinamide. Apart from these HNO studies, administration of sulfonamide antibiotics and arylamines has been shown to result in formation of *N*-substituted sulfinamides in proteins.[24, 25] To understand the pharmacological effects of HNO more completely, the

reactivity of sulfinamides under biologically relevant conditions requires further investigation.

At physiological pH and temperature, the major reactions of sulfinamides involve the reduction to free thiols in the presence of excess thiol and hydrolysis to form sulfinic acids.[26, 27] There are very few studies on the hydrolysis of sulfinamides, the majority of which have been carried out under aqueous, acidic conditions.[28-30] The mechanism is thought to involve a sulfurane intermediate (Scheme 2).[30] Studies conducted with several *N*-substituted alkyl sulfinamides indicate that aliphatic secondary sulfinamides are relatively stable at basic pH, but hydrolysis can proceed readily at pH 3.[17, 28] Also, tertiary sulfinamides have been found to be more reactive than secondary sulfinamides.[28] Although the hydrolysis of HNO-derived sulfinamides has been observed,[17, 26, 27] the reaction has not been studied in detail under physiological conditions. In recent studies, sulfinic acid modifications of thiols were seen upon exposure of HNO-treated samples to proteomic analysis or upon storage.[17, 26] Moreover, we recently reported the slow conversion of primary sulfinamides to sulfinic acids under physiological conditions as observed by ESI-MS.[27]

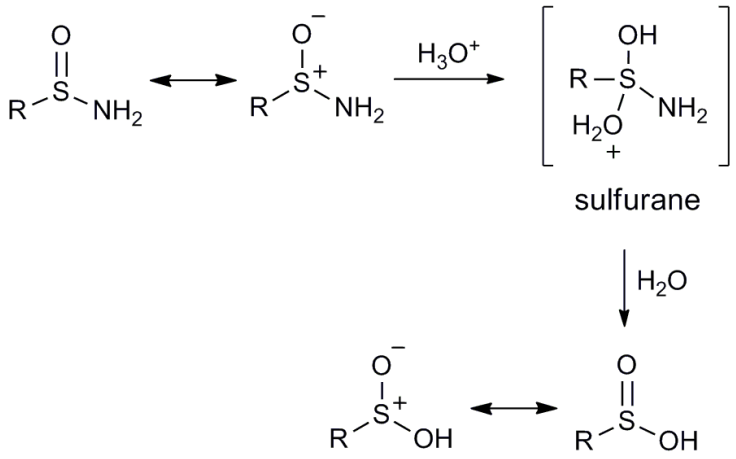

Scheme 3-2. Hydrolysis of sulfinamides

Isotope-edited ^{1}H NMR techniques are generally used for investigating interactions in macromolecular complexes such as ligand-protein, protein-protein, or protein-nucleic acid interactions.[31-33] In this method, one or more components of the complex are labeled with NMR active isotopes and the selective detection of protons bonded to the isotope-labeled atom is achieved.[31] Sulfamate groups on glycosaminoglycans and a DNA-peptide adduct were recently characterized using an analogous NMR method.[34, 35] Herein, we are pleased to report the application of ^{15}N-edited NMR spectroscopy to detect and study the hydrolysis of sulfinamides in several small organic molecules, peptides, and the cysteine protease, papain.

3.2 Results and Discussion

Since protein structure and function can be altered significantly due to post-translational modifications of cysteine residues, the biological effects of HNO are often attributed to its reactivity with thiols.[6, 27, 36-38] Sulfinamides are one of the major thiol

modifications observed upon exposure to HNO.[7, 8] Although thiols are known to react with other RNOS, sulfinamide formation is considered to be unique to HNO.[39] Despite being a well-established modification, very few studies on the reactivity of HNO-derived sulfinamides have been reported.

To detect and study the reactivity of sulfinamides in a facile manner, we have applied ^{15}N-edited NMR techniques, which are commonly used to study ligand-protein interactions.[31-33] These techniques are based on distinguishing between protons bonded to isotope-labeled and unlabeled nuclei.[31-33] Although direct ^{15}N NMR detection is a well-known technique, unfortunately it suffers from low sensitivity.[40-42] To determine the potential applicability of direct ^{15}N NMR spectroscopy to the study of sulfinamides, we explored its detection limit by employing ^{15}N-labeled urea. These preliminary studies have shown that although 1 M ^{15}N-labeled urea can be observed in less than 30 min, the addition of relaxation agents[42] and an extended number of scans are needed to observe 10-100 mM ^{15}N-labeled urea. These results suggest that ^{15}N NMR spectroscopy would not be convenient for the detection of HNO-derived sulfinamides, which are expected to be formed in much lower concentrations. Apart from retaining the sensitivity of ^{1}H NMR, the major advantage of ^{15}N-edited NMR procedures is the ability to provide simpler and more easily interpretable spectra, which becomes especially important for the detection of protein modifications.

3.2.1 Detection of Synthetic and HNO-Derived Small Organic Molecule Sulfinamides by ^{1}H NMR

We initially investigated the conditions necessary to detect sulfinamides by ^{1}H NMR in order to identify characteristic chemical shifts for the sulfinamide functional group. For this purpose, commercially available *t*-butanesulfinamide was employed. Although we attempted NMR analysis directly in buffer using water suppression techniques, the sulfinamide NH signal resonates too closely with the water signal, precluding its detection. Among the NMR solvents employed ($CDCl_3$, ACN-d_3, DMSO-d_6, THF-d_8), DMSO-d_6 provided the best results in terms of sample solubility and the clean observation of sulfinamide chemical shifts (5.1-6.3 ppm) (Figure 3-1). Also, the lack of exchangeable protons in DMSO-d_6 avoided the possible exchange between the sulfinamide NH's and deuterated solvent, allowing for better detection and accurate quantification. Similar results were obtained with synthetic 2-phenylethanesulfinamide, confirming the characteristic chemical shift region for the sulfinamide functional group and the general applicability of the method to other sulfinamides (Figure 3-1). Therefore, we carried out all reactions in phosphate buffer and then transferred the samples into DMSO-d_6 (via lyophilization) for NMR analyses.

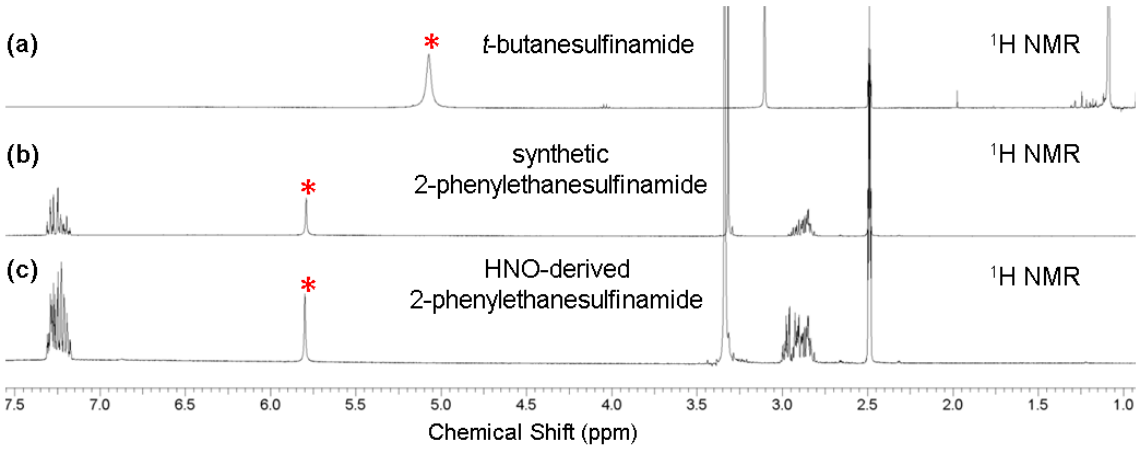

Figure 3-1. ^{1}H NMR spectra of (a) *t*-butanesulfinamide, (b) synthetic, and (c) HNO-derived 2-phenylethanesulfinamide collected in DMSO-d_6 at 30 ^{o}C. The HNO-derived sulfinamide was formed by treating 2-phenylethanethiol (0.1 mM) with AS (1 mM) in 10 mM phosphate buffer with 50 μM DTPA (pH 7.4) at 37 °C for 30 minutes. An asterisk (*) indicates the sulfinamide NH signals.

To determine if the above conditions can be applied to HNO-derived sulfinamides, we treated 2-phenylethanethiol with AS in buffer to form the corresponding 2-phenylethanesulfinamide. Similar to our previous ESI-MS results,[27] using a thiol to HNO donor ratio of 1:5 or 1:10 provided sufficient amount of 2-phenylethanesulfinamide. HPLC and ESI-MS analysis confirmed that the reaction of 2-phenylethanethiol with HNO produces the corresponding sulfinamide with a small amount of disulfide (Supporting Information). The ^{1}H NMR analysis was carried out following lyophilization of the sulfinamide from buffer and re-dissolving it in DMSO-d_6. As expected, the characteristic sulfinamide NH signal was observed at the same chemical shift for the synthetic and HNO-derived 2-phenylethanesulfinamides (5.8 ppm) (Figure 3-1b,c).

Since hydroxylamine is obtained as a byproduct in the case of HNO-induced disulfide formation (Scheme 3-1), we carried out control experiments with hydroxylamine exposed to the same sample preparation procedures or directly dissolved in the NMR

solvent. These results did not show any peaks in the chemical shift region assigned to the sulfinamide NH's (data not shown).

3.2.2 ^{15}N-Edited ^{1}H 1D NMR to Detect ^{15}N-Labeled Small Organic Molecule Sulfinamides

As mentioned previously, the use of isotope-edited methods simplifies the NMR spectra of complex samples by allowing selective detection of protons bonded to the isotope-labeled atom. The labeling of sulfinamides with ^{15}N was achieved by incubating thiols with ^{15}N-AS, which decomposes to produce ^{15}N-labeled HNO (H^{15}NO) and unlabeled NO_2^-. As seen in Figure 3a, treatment of β-mercaptoethanol (BME) with H^{15}NO resulted in the formation of the corresponding ^{15}N-labeled sulfinamide (BME-S(O)$^{15}NH_2$) with a ^{1}H-^{15}N coupling constant (J_{NH}) of 76 Hz. Upon application of an isotope filter to select for ^{15}N, only the sulfinamide ^{15}NH signal is observed in the decoupled ^{15}N-edited spectrum (Figure 3-2b).

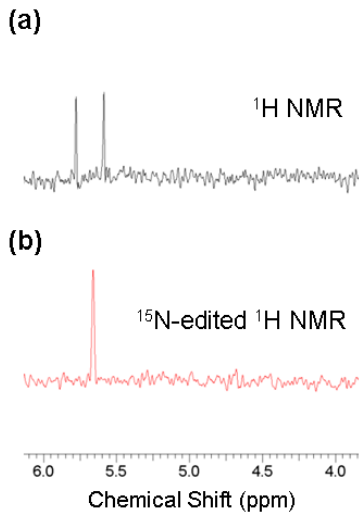

Figure 3-2. Selected region of ^{1}H NMR spectrum showing (a) sulfinamide ^{15}NH signals following the treatment of β-mercaptoethanol (0.1 mM) with ^{15}N-AS (1 mM) in 10 mM phosphate buffer with 50 μM DTPA (pH 7.4) at 37 °C for 30 min and (b) the corresponding region of the ^{15}N-edited ^{1}H 1D-NMR decoupled spectrum acquired using the HSQC pulse sequence for selection. The spectra were collected in DMSO-d_6 at 30 °C.

3.2.3 Detection of HNO-Derived Sulfinamides in Peptides

Given the results described above, the hexapeptide, VYPCLA, was employed to test our detection method on a more complex system. In our previous work, the sulfinamide yield of this peptide was determined to be greater than 90% upon incubation with ten times excess AS.[27] As seen in Figure 3-3a-e, the sulfinamide NH peaks (5.8-6.3 ppm) are observed only after HNO treatment of the thiol-containing peptide. Control experiments conducted with the unmodified peptide or following treatment with DEA/NO, did not result in any sulfinamide NH signals (Figure 3-3a and e).

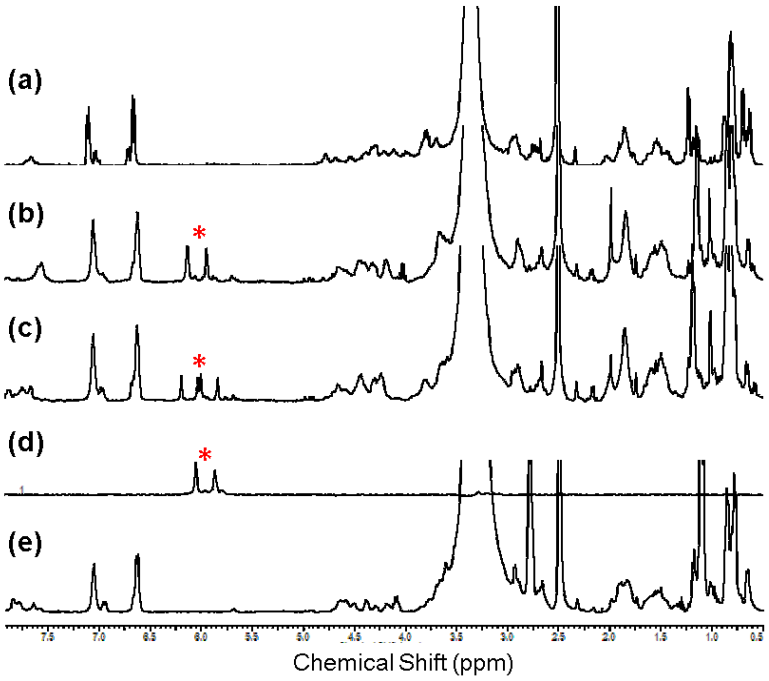

Figure 3-3. NMR spectra observed for VYPCLA (0.1 mM) (a) untreated or treated with (b) 1 mM AS, (c,d) 1 mM ^{15}N-AS, and (e) 0.5 mM DEA/NO in 10 mM phosphate buffer with 50 μM DTPA (pH 7.4) at 37 ºC for 30 min. Spectra (a-c) and (e) are ^{1}H NMR spectra and (d) is an ^{15}N-edited ^{1}H 1D-NMR spectrum which uses the HSQC pulse sequence for selection. The spectra were collected in DMSO-d_6 at 30 ºC. An asterisk (*) indicates the sulfinamide NH and ^{15}NH signals.

Unlike the signals for small organic molecule sulfinamides, two different signals are observed for the VYPCLA-generated sulfinamide (Figure 3-3b-d). This result can be explained based on the known chirality of the sulfur atom in sulfinamides.[43, 44] Upon sulfinamide formation, the stereochemistry at sulfur can be either R or S. In a small organic molecule sulfinamide, where the sulfur is the only chiral center, the resulting compound is racemic, and therefore, shows only one NMR signal. However, in the case of an L-peptide, the resulting sample is composed of two diastereomers (more specifically epimers) with the L-peptide containing either an R or S sulfinamide, consistent with the observed two NMR signals.

We have also conducted 2D-ROESY and COSY experiments on the HNO-derived VYPCLA sulfinamide. These data indicate the presence of two distinct sulfinamide species with a single NH_2 signal at 5.97 and 6.07 ppm (Figure 4). Moreover, the 5.97 ppm peak shows ROE cross peaks with the cysteine β- and α-H's, whereas the downfield species shows ROE cross peaks only with the cysteine β-H's (Figure 3-4). These results are consistent with the presence of two diastereomers. Comparison of the cysteine β-H's also reveals a 0.2 ppm downfield shift between the unmodified and sulfinamide modified-VYPCLA, further confirming that the HNO-derived modification is on the cysteine residue (Supporting Information).

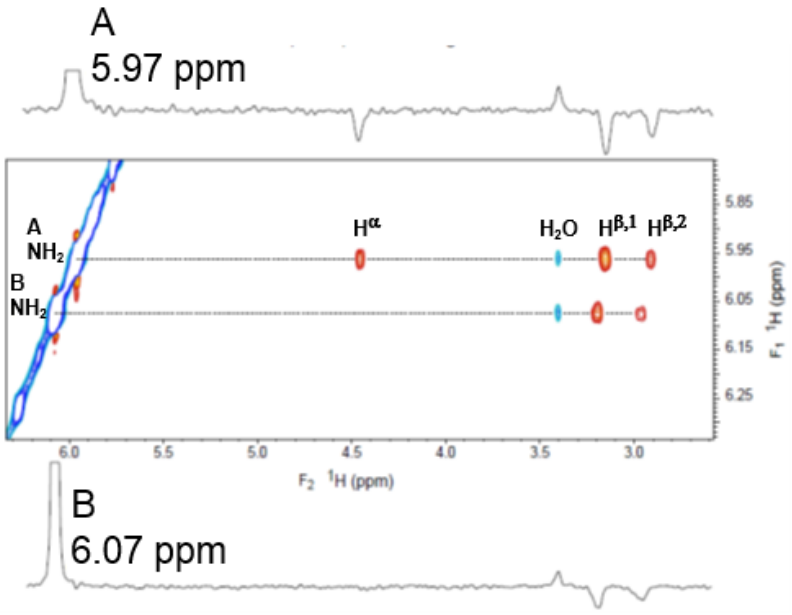

Figure 3-4. Selected region of 2D-ROESY spectrum showing ROE cross peaks involving sulfinamide NH_2 signals of VYPCLA (0.1 mM) treated with 1 mM AS in 10 mM phosphate buffer with 50 µM DTPA (pH 7.4) at 37 ºC for 30 min. The spectra were collected in DMSO-d_6. (A) and (B) indicate the 5.97 and 6.07 ppm signals, respectively.

The presence of two peaks could potentially be due to restricted rotation of the sulfinamide group causing the -NH's to be magnetically non-equivalent. However, the discrepancy between small organic molecule and peptide sulfinamides, as well as the low rotational barrier (~8.5 kcal/mole) suggested for the S-N bond, which would correspond to approximately -92 ºC, make restricted rotation unlikely.[45] Nevertheless, to eliminate this possibility, we performed NMR experiments, in which the same NMR sample was analyzed at temperatures from 30 to 70 ºC (Supporting Information). These data show that two sulfinamide peaks can be observed even at 70 ºC, indicating that the two peaks are not due to restricted rotation around the S-N bond.

As seen in Figure 3-5, results similar to those observed with VYPCLA are obtained upon treatment of glutathione with $H^{15}NO$ to produce the glutathione sulfinamide. Moreover, for both peptides, unequal amounts of the two diastereomers were obtained indicating that one diasteromer has lower energy and potentially the reaction is under kinetic control under these conditions. The ^{1}H-^{15}N coupling was determined to be 76 Hz, as observed for all the peptide sulfinamides detected.

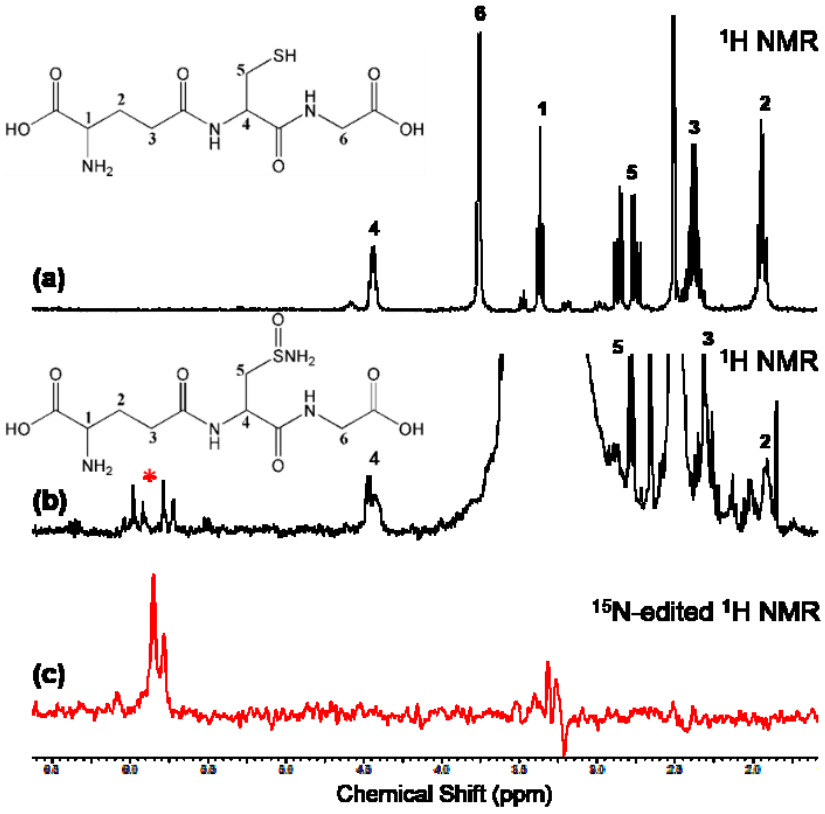

Figure 3-5. ^{1}H NMR spectrum of (a) unmodified GSH or (b) the glutathione sulfinamide formed by treating GSH (0.2 mM) with 1 mM ^{15}N-AS in 2 mM phosphate buffer with 12.5 µM DTPA (pH 6) at 37 ºC for 30 min. (c) ^{15}N-edited ^{1}H 1D-NMR spectrum of the glutathione sulfinamide acquired using the HSQC pulse sequence for selection. The samples were analyzed in DMSO-d_6 at 55 ºC. An asterisk (*) indicates the sulfinamide ^{15}NH signals.

3.2.4 Detection of an HNO-Derived Sulfinamide in Papain

The 23.4 kDa cysteine protease, papain, is one of the several enzymes known to be inhibited by HNO.[21] It has significant similarities with important mammalian proteases such as cathepsins and calpains.[46] The active site of papain contains a catalytic triad, which involves Cys25, His159 and Asn175.[47] In its active form, Cys25 exists as a thiolate and constitutes the only free thiol in the papain structure.[47, 48] The catalytic mechanism of papain involves nucleophilic attack of the Cys25 thiolate to form an acylenzyme

intermediate followed by a deacylation step.[47, 49] The roles of His159 include participation in a thiolate/imidazolium ion pair to maintain the thiolate anion and also participation as a general acid catalyst during acylation and as a general base catalyst during deacylation.[47, 48]

Although the formation of a sulfinamide has been proposed for papain after HNO treatment, to the best of our knowledge, it has not been observed directly. Therefore, we applied the ^{15}N-edited ^{1}H 1D NMR method to characterize the HNO-derived modification of papain. Figure 3-6 demonstrates that although the sulfinamide -NH signal could not be unambiguosly detected by ^{1}H NMR spectroscopy due to the interference of other signals and an inherently weak signal, it can be observed clearly in the ^{15}N-edited NMR spectrum (at 5.8 ppm), demonstrating that this technique is a convenient method to study HNO-derived sulfinamides in proteins.

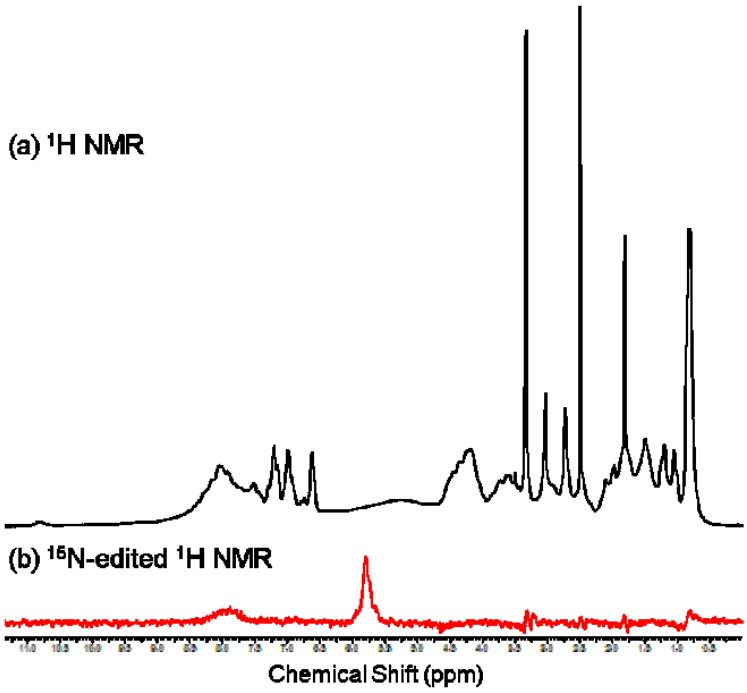

Figure 3-6. (a) ^{1}H NMR spectrum of sulfinamide modified-papain formed by treating papain (0.2 mM) with 1 mM ^{15}N-AS in 10 mM phosphate buffer with 50 µM DTPA (pH 7.4) at 37 ºC for 30 min. (b) ^{15}N-edited ^{1}H NMR spectrum of sulfinamide modified-papain acquired using the HSQC pulse sequence for selection. The spectra were collected in DMSO-d_6 at 30 ºC. The relatively small, broad peak observed at approximately 7.9 ppm in Figure 6b corresponds to the natural abundance ^{15}NH of backbone NH's.

Note that only one sulfinamide signal is detected, potentially due to the large peak width (>90 Hz) associated with this protein sulfinamide. However, the preferential formation of one diastereomer in papain active site is certainly possible. Indeed, steepest descent minimizations performed with the Rosetta modeling suite suggests that the R sulfinamide papain variant is slightly more stable than the S sulfinamide variant (-308.05±0.08 Rosetta energy units vs. -307.1±0.2 REU, respectively).

The formation of the sulfinamide modification in papain was also confirmed by ESI-MS (Supporting Information). Moreover, the inhibition of activated papain by AS under the conditions described above was confirmed by papain activity assays. As has

been observed previously,[21] no significant papain activity could be detected after AS treatment, consistent with sulfinamide formation (Supporting Information).

3.2.5 Reduction of Peptide Sulfinamides

Previously we had used ESI-MS to demonstrate that approximately 60% of the VYPCLA sulfinamide can be reverted back to free thiol upon 26 h-incubation with excess thiol at physiological pH and temperature. To determine if the ^{15}N-edited ^{1}H NMR method can be applied to study sulfinamide reactivity, we repeated the above experiment by incubating VYPCLA sulfinamide with BME and employing ^{15}N-labeled benzamide as the internal standard during NMR analysis. The NMR data, which indicates 57% sulfinamide reduction, is in very good agreement with the previous ESI-MS results (Supporting Information).

3.2.6 Hydrolysis of Peptide Sulfinamides

Sulfinamides are known to undergo hydrolysis to form sulfinic acids, especially under acidic conditions.[17, 26, 28-30] We have previously observed the slow conversion of primary sulfinamides to their corresponding sulfinic acids[27] and determined that have now explored this reactivity using the ^{15}N-edited ^{1}H NMR method.

The extent of sulfinamide hydrolysis was investigated by incubating the HNO-derived VYPCLA sulfinamide under physiological conditions and analyzing aliquots at different time intervals. Following 28 h incubation, a 13% decrease in the sulfinamide peak was observed with respect to initial (Figure 3-7), confirming that slow hydrolysis of sulfinamides takes place under physiological conditions.[26-28] Moreover, these findings are consistent with our previous ESI-MS results obtained for a similar hexapeptide (VYPCGA).[27] Upon one week incubation under similar conditions, very slow sulfinamide

hydrolysis (50%) was observed (data not shown). Almost complete hydrolysis (94%) was achieved upon boiling the sample for 5 days (Supporting Information). The hydrolysis of glutathione sulfinamide was found to be 28% after 28 h incubation at physiological pH and temperature, indicating this peptide is more prone to hydrolysis compared with the VYPCLA sulfinamide. Moreover, similar results were obtained when glutathione sulfinamide was formed using *N*-hydroxy-2-(methylsulfonyl)benzenesulfonamide (2-MSPA) as HNO donor, which does not produce NO_2^- as a byproduct, suggesting this reaction is independent of the presence of NO_2^-.

Figure 3-7. Representative ^{15}N-edited ^{1}H NMR spectra showing the hydrolysis of HNO-derived VYPCLA sulfinamide. VYPCLA (0.1 mM) was treated with 1 mM ^{15}N-AS in 10 mM phosphate buffer with 50 µM DTPA (pH 7.4) at 37 ºC for 30 min to form the corresponding sulfinamide. The sample was incubated in buffer at 37 ºC for 28 h resulting in 13% decrease in sulfinamide peak with respect to initial. ^{15}N-labeled benzamide was added as an internal standard before NMR analysis. ^{15}N-edited ^{1}H NMR spectra were acquired using the HSQC pulse sequence for selection. The spectra were collected in DMSO-d_6 at 30 ºC.

We have explored the effect of pH on the hydrolysis of primary sulfinamides by incubating peptide sulfinamides at pH 5-9. Upon 26 h incubation of the VYPCLA sulfinamide, we observed 33, 16, 13 and 14% sulfinamide hydrolysis at pH 5, 6, 7.4 and 9, respectively. Similarly, 46 and 24% hydrolysis is detected upon incubation of the glutathione sulfinamide at pH 5 and 7.4 for 26 h, respectively. These results indicate that sulfinamide hydrolysis is more facile at acidic pH values, presumably due to protonation of the sulfinamide (Scheme 3-2). Potentiometric titration studies of the primary sulfinamide, *t*-butanesulfinamide, indicate that its pK_a is ~3.9 (Supporting Information), consistent with the above results and the reported value of 3-3.5 for secondary sulfinamides.[50]

3.2.7 Hydrolysis of Sulfinamide-Modified Papain and Comparison with Its Model Peptide

Tertiary structure and local environment are known to have significant effects on reactivity.[51-53] To determine the extent of sulfinamide hydrolysis in a protein environment, we investigated the reactivity of this modification in ^{15}N-AS-treated papain. Interestingly, 54% of the sulfinamide was hydrolyzed after 28 h incubation under physiological conditions (Figure 3-8), which points to the reaction being significantly faster in the papain active site compared to the peptides tested (i.e., VYPCLA (13%) and GSH (28%)). Moreover, activity studies conducted with AS-treated papain has shown no significant change in papain activity after 28 h incubation, supporting the formation of a sulfinic acid (data not shown).

The active site thiol is contained in the sequence GSCWA (residues 23-27) of papain.[54] Since variations in the peptide sequence might cause changes in reactivity, a

model peptide (AGSCWA) of the papain active site was synthesized. Upon analyzing the extent of hydrolysis in this $H^{15}NO$-treated hexapeptide, no significant sulfinamide hydrolysis was observed after 28 h (Figure 3-8). These results indicate that the hydrolysis reaction is significantly enhanced by the papain environment rather than as a result of the specific peptide sequence.

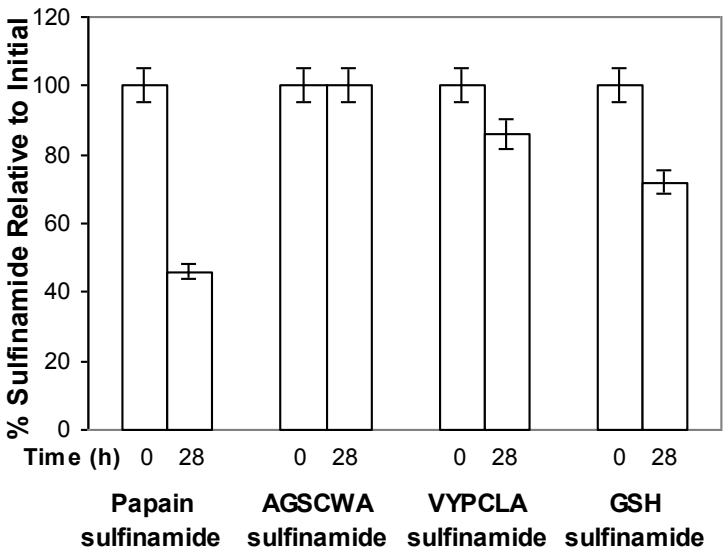

Figure 3-8. Hydrolysis of HNO-derived sulfinamides in papain, AGSCWA, VYPCLA, and glutathione (GSH). Papain (0.2 mM), AGSCWA (0.1 mM), VYPCLA (0.1 mM) and GSH (0.2 mM) were treated with 1 mM ^{15}N-AS in 10 mM phosphate buffer with 50 μM DTPA (pH 7.4) at 37 ºC for 30 min to form the corresponding sulfinamides. The samples were incubated in buffer at 37 ºC for 28 h. The amounts of sulfinamide were normalized with respect to that detected in the initial peptide samples (SEM ±5%, n=3).

We used Rosetta to assist in formulating a hypothesis for the mechanism of sulfinamide hydrolysis within the papain active site environment. The crystal structure of papain (PDB ID 9PAP), which contains a sulfonate modification on Cys25, was used as a template for generating PDB files for the wild type (WT), R sulfinamide, S sulfinamide, and sulfinate (hydrolysis product) papain variants. The WT papain structure and the three

variants were minimized and the resulting structures were examined. In the case of all three variants, the oxygen atom bound to sulfur is placed in the oxyanion hole (Gln19) for the standard papain reaction (Figure 3-9). This is similar to the orientation of the sulfonate oxygen in the 9PAP structure.

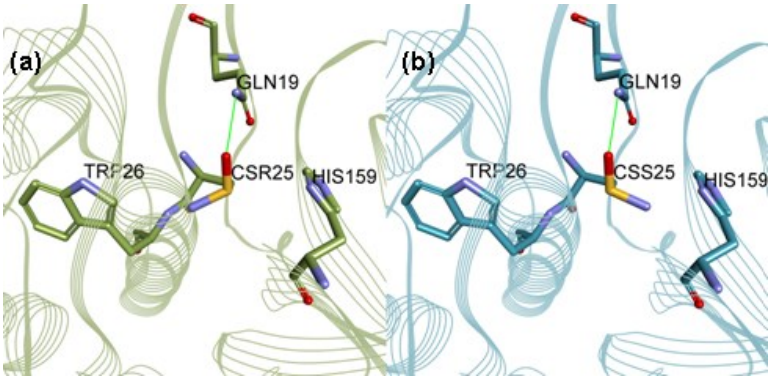

Figure 3-9. Active site of sulfinamide-modified papain involving (a) R and (b) S sulfinamide. Models were generated using Rosetta software.

The first step in sulfinamide hydrolysis is generally thought to be protonation of the sulfinamide oxygen. In the S sulfinamide structure (Figure 3-9b), the sulfinamide NH_2 can hydrogen bond with His159; in the R sulfinamide structure (Figure 3-9a), the NH_2 sits at the positively polarized end of an α helix and hydrogen bonds with the backbone of Trp26. Only in the R sulfinamide structure is the catalytic His159 poised to function as a general base for deprotonation of water, just as it does in the standard papain reaction. In our hydrolysis product model, $N\delta_1$ of His159 is within hydrogen bonding distance of the second oxygen bound to sulfur. It is also worth noting that the Rosetta score for the product (-311.7±4 REU) is lower than either the R or S sulfinamide (-308.05±0.08 and -307.1±0.2 REU, respectively). Thus, we propose the following mechanism, shown in Scheme 3-3.

The sulfinamide is activated by the partial positive character of the enzymatic oxyanion hole and the positive dipole of the α helix and the backbone amide of Trp26. As in the papain enzymatic reaction, His159 deprotonates a water molecule for nucleophilic attack. After formation of the sulfurane, solvent-assisted proton transfer occurs, followed by loss of free ammonia to give the sulfinic acid.

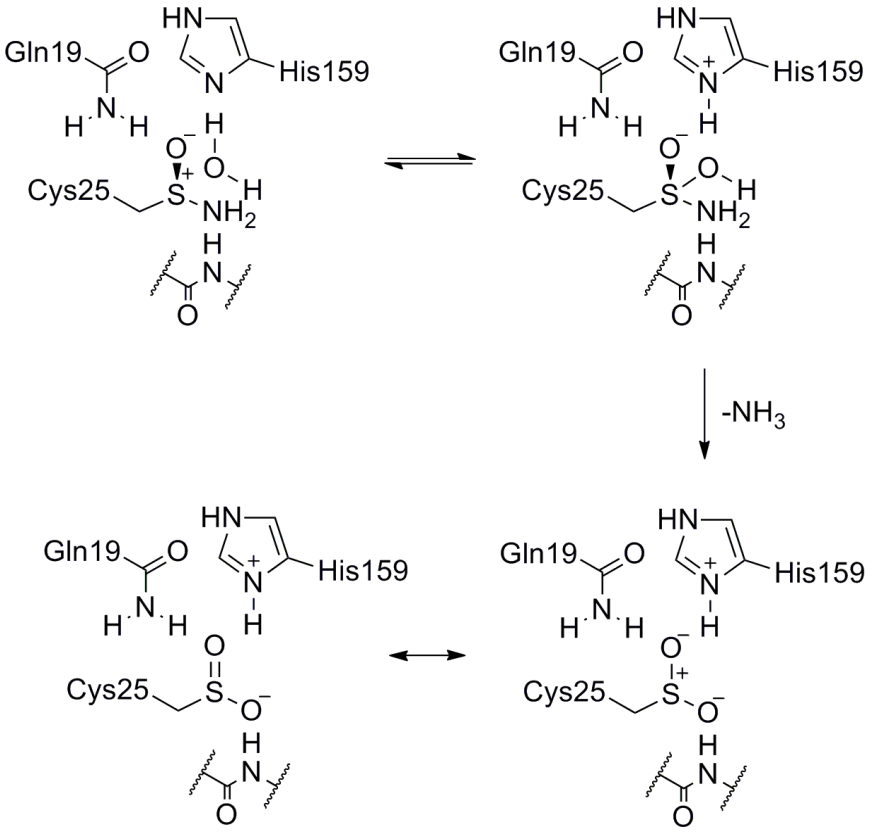

Scheme 3-3. Hydrolysis of sulfinamide in papain

3.3 Conclusions

Using the ^{15}N-edited NMR method we have been able to detect primary sulfinamides in organic molecules, peptides, and proteins. Moreover, analysis of the peptide sulfinamides indicates the generation of peptide diastereomers upon sulfinamide formation. The capability to distinguish between stereoisomers makes this a beneficial method for sulfinamide detection. Furthermore, this technique could also be used for the detection of *N*-substituted sulfinamides provided that there is a proton bonded to the labeled nucleus.

We have extended our previous work[27] on sulfinamide reactivity to investigate further sulfinamide hydrolysis at physiological pH and temperature. Our results with peptide sulfinamides are consistent with our initial findings, indicating that despite being a slow reaction, hydrolysis is viable under physiological conditions. Although the number of cases examined to date is limited, the hydrolysis of peptide sulfinamides seems to be affected minimally by peptide sequence (e.g. AGSCWA vs. VYPCLA vs. GSH), but substantially more by protein environment (e.g. papain); further investigations are required. In addition, the hydrolysis reaction is facilitated at lower pH values similar to that observed for secondary sulfinamides and consistent with the generally accepted mechanism.[17, 26, 28-30] Recent studies point to the potential signaling role of sulfinic acid formation in controlling protein function.[55-57] Moreover, the reduction of sulfinic acids to thiols by an ATP-dependent process is well-established for the peroxiredoxin system.[58-60] The hydrolysis of HNO-derived sulfinamides to sulfinic acids might represent another pathway to sulfinic acid formation in proteins.

Papain, whose activity depends on a catalytic triad of Cys25, His159 and Asn175, is one of the most studied cysteine proteases.[47] Our NMR experiments demonstrate sulfinamide formation upon HNO treatment, which correlates well with previous predictions that the observed inhibition of papain is due to the modification of its single free cysteine residue by HNO.[21] Further analysis has shown that sulfinamide hydrolysis is significantly more efficient in the papain active site compared to small organic molecules[27] and related peptide systems. These findings are also supported by computational studies, which indicate that hydrolysis can be enhanced in papain active site due to activation of the sulfinamide and facilitation of nucleophilic attack.

3.4 Experimental Methods

Reagents. Glutathione (GSH), papain, N_α-Benzoyl-L-arginine 4-nitroanilide hydrochloride (L-BAPNA), β-mercaptoethanol (BME), *t*-butanesulfinamide (racemic), *N*-ethylmaleimide (NEM), and dithiothreitol (DTT) were of the highest purity available and purchased from Sigma (St. Louis, MO). 2-Phenylethanethiol and 2-(bromoethyl)benzene were purchased from Acros. HPLC grade acetonitrile (ACN) was purchased from Thermo Fisher Scientific (Rockford, IL). Dimethyl sulfoxide-d_6 (DMSO-d_6), ^{15}N-labeled hydroxylamine hydrochloride and ^{15}N-labeled benzamide were purchased from Cambridge Isotope Laboratories (Andover, MA). The syntheses of 2-phenylethanesulfinamide, the HNO-donor, Angeli's salt ($Na_2N_2O_3$, AS), and the NO-donor (DEA/NO) were carried out as previously described.[27, 61-63] The ^{15}N-labeled HNO-donor, *N*-hydroxy-2-(methylsulfonyl)benzenesulfonamide[64] (^{15}N-2-MSPA), was a generous gift from Cardioxyl Pharmaceuticals. Milli Q water was used for all purifications and experiments.

Peptide Synthesis and Purification. Synthetic peptides VYPCLA and AGSCWA were synthesized on a Symphony Quartet peptide synthesizer (Protein Technologies Inc., Tucson, AZ) following Fmoc solid-phase peptide synthesis methods.[65] The crude product was dissolved in 0.1% trifluoroacetic acid (TFA) and purified by HPLC (Waters HPLC equipped with Delta 600 pump system and dual wavelength absorbance detector) on an Apollo C_{18} reverse-phase column using a linear gradient of 5-75% ACN with 0.1% TFA over 50 min at room temperature. Peptide fractions were identified by electrospray ionization mass spectrometry (ESI-MS). Pure fractions were pooled and lyophilized, and the purified product was quantified based on the absorbance at 280 nm (ε_{280}= 1490 M^{-1} cm^{-1}).[66] In all cases, peptides were stored at -80 °C in lyophilized form until use.

Synthesis of ^{15}N-labeled Angeli's salt (^{15}N-AS). Synthesis of ^{15}N-labeled AS, which produces ^{15}N-labeled HNO ($H^{15}NO$) and unlabeled nitrite (NO_2^-), was carried out based on a literature procedure by reacting $^{15}NH_2OH$ and isoamyl nitrate in basic methanol.[67] The purity of ^{15}N-AS was confirmed by comparison of the extinction coefficient at 248 nm in 0.01 M NaOH with the literature value (ε_{248} = 8300 $M^{-1}cm^{-1}$).[62]

Formation of Sulfinamides by Reaction with HNO. Organic thiols or thiol-containing peptides were dissolved in 10 mM sodium phosphate buffer with 50 μM of the metal chelator, diethylenetriamine pentaacetic acid (DTPA), at pH 7.4 to have a final concentration of 0.1 or 0.2 mM and used immediately. Stock solutions of AS or ^{15}N-AS were prepared in 0.01 M NaOH, kept on ice, and used within 15 min of preparation. Stock solutions of ^{15}N-labeled 2-MSPA were prepared in ACN and used within 15 min of preparation. The organic molecules or peptides were incubated with 1 mM AS or ^{15}N-AS at 37 °C for 30 min in a block heater. The samples were then aliquoted, flash-frozen and

lyophilized. Following lyophilization, the samples were re-dissolved in DMSO-d_6 for immediate NMR analysis.

For experiments conducted at varied pH's, glutathione sulfinamide was formed by incubating GSH with 1 mM ^{15}N-2-MSPA (rather than with AS) at 37 ^{o}C for 30 min in pH 7.4 phosphate buffer due to higher sulfinamide yield obtained. The samples were prepared for NMR analysis as described above.

Incubations with DEA/NO. The VYPCLA peptide was dissolved in 10 mM sodium phosphate buffer with 50 μM DTPA, at pH 7.4 to have a final concentration of 0.1 mM and used immediately. Stock solutions of DEA/NO were prepared in 0.01 M NaOH, kept on ice and used within 15 min of preparation. The peptide was incubated with 0.5 mM DEA/NO at 37 °C for 30 min in a block heater. (Note that DEA/NO was administered at half the concentration of HNO-donors used to account for two equivalents of NO production from one equivalent of DEA/NO.) The samples were then prepared as described above for NMR analysis.

Preparation of NMR Samples for Synthetic Sulfinamides. Commercially available *t*-butanesulfinamide and synthetic 2-phenylethanesulfinamide were dissolved in DMSO-d_6 to have a final concentration of 100 and 10 mM. The samples were analyzed by NMR without any further treatment.

HPLC Analyses of 2-Phenylethanesulfinamide. All the analyses were performed on an Apollo C_{18} reverse-phase column connected to the HPLC system described above. A linear gradient of 35-80% ACN with 0.1% TFA over 35 min was employed at room temperature. The compounds were followed at 220 nm and peaks were assigned based on co-injection with authentic samples.

Activation of Papain. A 0.2 mM papain solution was prepared by dissolving the lyophilized enzyme in 10 mM sodium phosphate buffer with 50 μM DTPA at pH 7.4. The papain sample was activated by treatment with 1 mM DTT for 30 min at room temperature to reconvert its single free cysteine to the sulfhydryl form. The activated enzyme was then desalted with Zeba spin desalting columns to remove excess DTT.

Generation of Sulfinamide-Modified Papain. The activated papain in 10 mM sodium phosphate buffer with 50 μM DTPA at pH 7.4 was immediately incubated with 1 mM ^{15}N-AS at 37 ºC for 30 min to form the ^{15}N-labeled sulfinamide as described above.

Papain Activity Assay. An aliquot from the 0.2 mM papain (with or without prior AS treatment) in 10 mM sodium phosphate buffer with 50 μM DTPA at pH 7.4 was diluted into buffer to have a final papain concentration of 8.5 μM. The activity of papain was analyzed by a 20 min spectrophotometric assay using L-BAPNA as the substrate.[21]

ESI-MS Analyses of Papain. An aliquot from the 0.2 mM papain (with or without prior AS treatment) in 10 mM sodium phosphate buffer with 50 μM DTPA at pH 7.4 was lyophilized and purified by HPLC on a Viva C_4 reverse-phase analytical column using a linear gradient of 5-95% ACN with 0.1% TFA over 80 min at room temperature.[68] The samples were then analyzed on a Thermo Finnigan LCQ Deca Ion Trap Mass Spectrometer fitted with an electrospray ionization source, operating in the positive ion mode. In all experiments, the samples were introduced to the instrument at a rate of 10 μL/min using a syringe pump via a silica capillary line. The heated capillary temperature was 250 °C and the spray voltage was 5 kV. Data analysis and deconvolution were carried out using Bioworks 3.2 software.

As a control, an aliquot from the papain sample was incubated with 2 mM NEM (with or without prior AS treatment) in buffer at 37 ºC for 1.5 h. The samples were purified and analyzed by ESI-MS as described above.

Incubations of Peptides and Proteins in Buffer. Aliquots of the sulfinamide-containing samples (in 10 mM sodium phosphate buffer with 50 μM DTPA, at pH 7.4) were incubated at 37 ºC. Individual aliquots were removed from the samples for analysis at certain time intervals, flash-frozen, lyophilized, and prepared for immediate NMR analysis as described above. In all cases, 1 mM ^{15}N-labeled benzamide was added to the NMR sample as an internal standard. In some cases, VYPCLA sulfinamide was incubated in the presence of 50 mM BME (as indicated) and the samples were prepared as described above for NMR analysis.

Incubations of Peptides at Varied pH. Aliquots of the sulfinamide-containing samples (in 10 mM sodium phosphate buffer with 212 μM DTPA, at pH 7.4) were adjusted to the desired pH by adding 10% H_3PO_4 or 1 M NaOH while stirring. The samples were incubated at 37 ºC. Individual aliquots were removed from the samples for analysis at certain time intervals, re-adjusted to pH 7.4, flash-frozen, lyophilized, and prepared for immediate NMR analysis as described above. In all cases, 1 mM ^{15}N-labeled benzamide was added to the NMR sample as an internal standard.

Potentiometric Determination of *t*-Butanesulfinamide pK_a. The potentiometric titration was adapted from a literature procedure.[69] Briefly, commercially available *t*-butanesulfinamide was dissolved in 0.05 M KCl to have a concentration of 2 mM. The solution was titrated with either 20 mM NaOH or 20 mM HCl prepared in 0.05 M KCl at

room temperature. The changes in pH were determined using a general purpose combination pH probe with a built-in temperature sensor connected to a pH meter.

NMR Analyses. All ^{1}H-NMR and ^{15}N-edited ^{1}H 1D-NMR analyses were carried out on a Bruker Avance 400 MHz FT-NMR spectrometer at 303 K. In some cases, spectra were collected at temperatures from 303 K to 343 K (as indicated). ^{15}N-edited ^{1}H 1D-NMR spectra were acquired using the HSQC pulse sequence for selection. 2D-ROESY and COSY spectra of the VYPCLA sulfinamide were obtained on a Bruker Avance 600 MHz FT-NMR spectrometer. All chemical shifts are reported in parts per million (ppm) relative to residual DMSO (2.49 ppm for ^{1}H).

Active Site Modeling. The computational studies were conducted by Dr. Jason W. Labonte. Briefly, a Python (v2.7) script was written using the PyRosetta v3.4.0 r53345 libraries.[70] Atom type parameters were added to the Rosetta database for the sp^3-hybridized NH_2 group of sulfinamide. Rosetta residue type parameter files were added for cysteine sulfinate and each cysteine sulfinamide stereoisomer. Ideal bond lengths and angles were taken from PDB ID 1ACD and several references.[71, 72] The Dunbrack rotamer library[73] was used to select rotamers for each standard amino acid residue side chain. Ten cycles of side-chain packing followed by steepest descent minimization were performed for each protein variant examined using the standard "score12" scoring function. Structures generated by Rosetta were output as pdb files and viewed in DS Visualizer.[74]

3.5 References

1. Chung, H. S., Wang, S.-B., Venkatraman, V., Murray, C. I., and Van Eyk, J. E. (2013) Cysteine oxidative posttranslational modifications: emerging regulation in the cardiovascular system, *Circ. Res. 112*, 382-392.
2. Flores-Santana, W., Salmon, D. J., Donzelli, S., Switzer, C. H., Basudhar, D., Ridnour, L., Cheng, R., Glynn, S. A., Paolocci, N., Fukuto, J. M., Miranda, K. M., and Wink, D. A. (2011) The specificity of nitroxyl chemistry is unique among nitrogen oxides in biological systems, *Antioxid. Redox Signaling 14*, 1659-1674.
3. Ridnour, L. A., Thomas, D. D., Mancardi, D., Espey, M. G., Miranda, K. M., Paolocci, N., Feelisch, M., Fukuto, J., and Wink, D. A. (2004) The chemistry of nitrosative stress induced by nitric oxide and reactive nitrogen oxide species. Putting perspective on stressful biological situations, *Biol. Chem. 385*, 1-10.
4. Paolocci, N., Katori, T., Champion, H. C., St John, M. E., Miranda, K. M., Fukuto, J. M., Wink, D. A., and Kass, D. A. (2003) Positive inotropic and lusitropic effects of HNO/NO^- in failing hearts: Independence from beta-adrenergic signaling, *Proc. Natl. Acad. Sci. U. S. A. 100*, 5537-5542.
5. Paolocci, N., Saavedra, W. F., Miranda, K. M., Martignani, C., Isoda, T., Hare, J. M., Espey, M. G., Fukuto, J. M., Feelisch, M., Wink, D. A., and Kass, D. A. (2001) Nitroxyl anion exerts redox-sensitive positive cardiac inotropy in vivo by calcitonin gene-related peptide signaling, *Proc. Natl. Acad. Sci. U. S. A. 98*, 10463-10468.
6. Kemp-Harper, B. K. (2011) Nitroxyl (HNO): A novel redox signaling molecule, *Antioxid. Redox Signaling 14*, 1609-1613.

7. Doyle, M. P., Mahapatro, S. N., Broene, R. D., and Guy, J. K. (1988) Oxidation and reduction of hemoproteins by trioxodinitrate(II). The role of nitrosyl hydride and nitrite, *J. Am. Chem. Soc. 110*, 593-599.

8. Wong, P. S. Y., Hyun, J., Fukuto, J. M., Shirota, F. N., DeMaster, E. G., Shoeman, D. W., and Nagasawa, H. T. (1998) Reaction between *S*-nitrosothiols and thiols: Generation of nitroxyl (HNO) and subsequent chemistry, *Biochemistry 37*, 5362-5371.

9. Cheong, E., Tumbev, V., Abramson, J., Salama, G., and Stoyanovsky, D. A. (2005) Nitroxyl triggers Ca^{2+} release from skeletal and cardiac sarcoplasmic reticulum by oxidizing ryanodine receptors, *Cell Calcium 37*, 87-96.

10. Cook, N. M., Shinyashiki, M., Jackson, M. I., Leal, F. A., and Fukuto, J. M. (2003) Nitroxyl-mediated disruption of thiol proteins: inhibition of the yeast transcription factor Ace1, *Arch. Biochem. Biophys. 410*, 89-95.

11. Demaster, E. G., Redfern, B., and Nagasawa, H. T. (1998) Mechanisms of inhibition of aldehyde dehydrogenase by nitroxyl, the active metabolite of the alcohol deterrent agent cyanamide, *Biochem. Pharmacol. 55*, 2007-2015.

12. Froehlich, J. P., Mahaney, J. E., Keceli, G., Pavlos, C. M., Goldstein, R., Redwood, A. J., Sumbilla, C., Lee, D. I., Tocchetti, C. G., Kass, D. A., Paolocci, N., and Toscano, J. P. (2008) Phospholamban thiols play a central role in activation of the cardiac muscle sarcoplasmic reticulum calcium pump by nitroxyl, *Biochemistry 47*, 13150-13152.

13. Gao, W. D., Murray, C. I., Tian, Y., Zhong, X., DuMond, J. F., Shen, X., Stanley, B. A., Foster, D. B., Wink, D. A., King, S. B., Van Eyk, J. E., and Paolocci, N.

(2012) Nitroxyl-mediated disulfide bond formation between cardiac myofilament cysteines enhances contractile function, *Circ. Res. 111*, 1002-1011.

14. Kim, W.-K., Choi, Y.-B., Rayudu, P. V., Das, P., Asaad, W., Arnelle, D. R., Stamler, J. S., and Lipton, S. A. (1999) Attenuation of NMDA receptor activity and neurotoxicity by nitroxyl anion, NO^-, *Neuron 24*, 461-469.

15. Landino, L. M., Koumas, M. T., Mason, C. E., and Alston, J. A. (2007) Modification of tubulin cysteines by nitric oxide and nitroxyl donors alters tubulin polymerization activity, *Chem. Res. Toxicol. 20*, 1693-1700.

16. Lopez, B. E., Wink, D. A., and Fukuto, J. M. (2007) The inhibition of glyceraldehyde-3-phosphate dehydrogenase by nitroxyl (HNO), *Arch. Biochem. Biophys. 465*, 430-436.

17. Mitroka, S., Shoman, M. E., DuMond, J. F., Bellavia, L., Aly, O. M., Abdel-Aziz, M., Kim-Shapiro, D. B., and King, S. B. (2013) Direct and nitroxyl (HNO)-mediated reactions of acyloxy nitroso compounds with the thiol-containing proteins glyceraldehyde 3-phosphate dehydrogenase and alkyl hydroperoxide reductase subunit C, *J. Med. Chem.*, in press.

18. Salie, M. J., Oram, D. S., Kuipers, D. P., Scripture, J. P., Chenge, J., MacDonald, G. J., and Louters, L. L. (2012) Nitroxyl (HNO) acutely activates the glucose uptake activity of GLUT1, *Biochimie 94*, 864-869.

19. Shen, B., and English, A. M. (2005) Mass spectrometric analysis of nitroxyl-mediated protein modification: Comparison of products formed with free and protein-based cysteines, *Biochemistry 44*, 14030-14044.

20. Tocchetti, C. G., Wang, W., Froehlich, J. P., Huke, S., Aon, M. A., Wilson, G. M., Di Benedetto, G., O'Rourke, B., Gao, W. D., Wink, D. A., Toscano, J. P., Zaccolo, M., Bers, D. M., Valdivia, H. H., Cheng, H., Kass, D. A., and Paolocci, N. (2007) Nitroxyl improves cellular heart function by directly enhancing cardiac sarcoplasmic reticulum Ca^{2+} cycling, *Circ. Res. 100*, 96-104.

21. Vaananen Antti, J., Kankuri, E., and Rauhala, P. (2005) Nitric oxide-related species-induced protein oxidation: reversible, irreversible, and protective effects on enzyme function of papain, *Free Radical Biol. Med. 38*, 1102-1111.

22. Vaananen Antti, J., Salmenpera, P., Hukkanen, M., Rauhala, P., and Kankuri, E. (2006) Cathepsin B is a differentiation-resistant target for nitroxyl (HNO) in THP-1 monocyte/macrophages, *Free Radical Biol. Med. 41*, 120-131.

23. Lopez, B. E., Rodriguez, C. E., Pribadi, M., Cook, N. M., Shinyashiki, M., and Fukuto, J. M. (2005) Inhibition of yeast glycolysis by nitroxyl (HNO): A mechanism of HNO toxicity and implications to HNO biology, *Arch. Biochem. Biophys. 442*, 140-148.

24. Liu, L., Wagner, C. R., and Hanna, P. E. (2009) Isoform-selective Inactivation of human arylamine N-acetyltransferases by reactive metabolites of carcinogenic arylamines, *Chem. Res. Toxicol. 22*, 1962-1974.

25. Callan, H. E., Jenkins, R. E., Maggs, J. L., Lavergne, S. N., Clarke, S. E., Naisbitt, D. J., and Park, B. K. (2009) Multiple adduction reactions of nitroso sulfamethoxazole with cysteinyl residues of peptides and proteins: Implications for hapten formation, *Chem. Res. Toxicol. 22*, 937-948.

26. Hoffman, M. D., Walsh, G. M., Rogalski, J. C., and Kast, J. (2009) Identification of nitroxyl-induced modifications in human platelet proteins using a novel mass spectrometric detection method, *Mol. Cell. Proteomics 8*, 887-903.

27. Keceli, G., and Toscano, J. P. (2012) Reactivity of nitroxyl-derived sulfinamides, *Biochemistry 51*, 4206-4216.

28. Piggott, A. M., and Karuso, P. (2007) Hydrolysis rates of alkyl and aryl sulfinamides: evidence of general acid catalysis, *Tetrahedron Lett. FIELD Full Journal Title:Tetrahedron Letters 48*, 7452-7455.

29. Asefi, H., and Tillett, J. G. (1979) Nucleophilic substitution at sulfur. Part 2. The acid-catalyzed hydrolysis of arenesulfinamides, *J. Chem. Soc., Perkin Trans. 2*, 1579-1582.

30. Okuyama, T., Lee, J. P., and Ohnishi, K. (1994) Evidence for hypervalent intermediates in acid hydrolysis of sulfinamide. ^{18}O exchange and a break in pH-rate profile, *J. Am. Chem. Soc. 116*, 6480-6481.

31. Breeze, A. L. (2000) Isotope-filtered NMR methods for the study of biomolecular structure and interactions, *Prog. NMR Spectrosc. 36*, 323-372.

32. Tsang, P., and Rance, M. (1996) Some practical aspects of double-resonance techniques in solution-state NMR studies of high-molecular-weight systems, *J. Magn. Reson., Ser. B 111*, 135-148.

33. Stockman, B. J., and Markley, J. L. (1991) NMR analysis of ligand binding, *Curr. Opin. Struct. Biol. 2*, 52-56.

34. Huang, H., Wang, H., Voehler, M. W., Kozekova, A., Rizzo, C. J., McCullough, A. K., Lloyd, R. S., and Stone, M. P. (2011) g-hydroxy-1,N^2-propano-2'-

deoxyguanosine DNA adduct conjugates the N-terminal amine of the KWKK peptide via a carbinolamine linkage, *Chem. Res. Toxicol. 24*, 1123-1133.

35. Langeslay, D. J., Beni, S., and Larive, C. K. (2011) Detection of the ^{1}H and ^{15}N NMR resonances of sulfamate groups in aqueous solution: a new tool for heparin and heparan sulfate characterization, *Anal. Chem. 83*, 8006-8010.

36. Choe, C. U., Lewerenz, J., Gerloff, C., Magnus, T., and Donzelli, S. (2011) Nitroxyl in the central nervous system, *Antioxid. Redox Signaling 14*, 1699-1711.

37. Fukuto, J. M., and Carrington, S. J. (2011) HNO signaling mechanisms, *Antioxid. Redox Signaling 14*, 1649-1657.

38. Sivakumaran, V., Stanley, B. A., Tocchetti, C. G., Ballin, J. D., Caceres, V., Zhou, L., Keceli, G., Rainer, P. P., Lee, D. I., Huke, S., Ziolo, M. T., Kranias, E. G., Toscano, J. P., Wilson, G. M., O'Rourke, B., Kass, D. A., Mahaney, J. E., and Paolocci, N. (2013) HNO enhances SERCA2a activity and cardiomyocyte function by promoting redox-dependent phospholamban oligomerization, *Antioxid. Redox Signaling*, in press.

39. Donzelli, S., Espey, M. G., Thomas, D. D., Mancardi, D., Tocchetti, C. G., Ridnour, L. A., Paolocci, N., King, S. B., Miranda, K. M., Lazzarino, G., Fukuto, J. M., and Wink, D. A. (2006) Discriminating formation of HNO from other reactive nitrogen oxide species, *Free Radical Biol. Med. 40*, 1056-1066.

40. Martin, G. E., and Hadden, C. E. (2000) Long-range ^{1}H-^{15}N heteronuclear shift correlation at natural abundance, *J. Nat. Prod. 63*, 543-585.

41. Lippmaa, E., Saluvere, T., and Laisaar, S. (1971) Spin-lattice relaxation of nitrogen-15 nuclei in organic compounds, *Chem. Phys. Lett. 11*, 120-123.

42. Farnell, L. F., Randall, E. W., and White, A. I. (1972) Effect of paramagnetic species on the nuclear magnetic resonance spectra of nitrogen-15, *J. Chem. Soc., Chem. Commun.*, 1159-1160.

43. Moriarty, R. M. (1965) The stereochemistry of sulfinamides. Magnetic nonequivalence of protons in the vicinity of the asymmetric sulfinamido group, *J. Org. Chem. 30*, 600-603.

44. (1990) The Chemistry of Sulphinic Acids, Esters and their Derivatives, (Patai, S., Ed.), pp 611-614, John Wiley & Sons Ltd, New York.

45. Bharatam, P. V., Amita, and Kaur, D. (2002) Theoretical studies on the S-N interaction in sulfinamides, *J. Phys. Org. Chem. 15*, 197-203.

46. Rawlings, N. D., and Barrett, A. J. (1994) Families of cysteine peptidases, *Methods Enzymol. 244*, 461-486.

47. Polgar, L. (2012) Catalytic Mechanisms of Cysteine Peptidases, In *Handbook of Proteolytic Enzymes (3rd Edition)* (Rawling, N. D., and Salvesen, G. S., Eds.), pp 1773-2491, Academic Press.

48. Storer, A. C., and Menard, R. (1994) Catalytic mechanism in papain family of cysteine peptidases, *Methods Enzymol. 244*, 486-500.

49. Frey, P. A., and Hegeman, A. D. (2007) Acyl Group Transfer: Proteases and Esterases, In *Enzymatic Reaction Mechanisms*, pp 314-317, Oxford University Press, New York.

50. Clarke, V., and Cole, E. R. (1989) Sulfenamides and sulfinamides. V. Conjugative affinity and pKa values of aryl sulfinamides, *Phosphorus, Sulfur Silicon Relat. Elem. 45*, 243-248.

51. Kossiakoff, A. A. (1988) Tertiary structure is a principal determinant to protein deamidation, *Science 240*, 191-194.

52. Chazin, W. J., and Kossiakoff, A. A. (1995) The role of secondary and tertiary structures in intramolecular deamidation of proteins, *Deamidation Isoaspartate Form. Pept. Proteins*, 193-206.

53. Xie, M., Shahrokh, Z., Kadkhodayan, M., Henzel, W. J., Powell, M. F., Borchardt, R. T., and Schowen, R. L. (2003) Asparagine deamidation in recombinant human lymphotoxin: Hindrance by three-dimensional structures, *J. Pharm. Sci. 92*, 869-880.

54. Mitchell, R. E. J., Chaiken, I. M., and Smith, E. L. (1970) Complete amino acid sequence of papain. Additions and corrections, *J. Biol. Chem. 245*, 3485-3492.

55. Wilson, M. A. (2011) The role of cysteine oxidation in DJ-1 function and dysfunction, *Antioxid. Redox Signaling 15*, 111-122.

56. Blackinton, J., Lakshminarasimhan, M., Thomas, K. J., Ahmad, R., Greggio, E., Raza, A. S., Cookson, M. R., and Wilson, M. A. (2009) Formation of a stabilized cysteine sulfinic acid is critical for the mitochondrial function of the Parkinsonism protein DJ-1, *J. Biol. Chem. 284*, 6476-6485.

57. Lin, J., Prahlad, J., and Wilson, M. A. (2012) Conservation of oxidative protein stabilization in an insect homologue of Parkinsonism-associated protein DJ-1, *Biochemistry 51*, 3799-3807.

58. Rhee, S. G., Chae, H. Z., and Kim, K. (2005) Peroxiredoxins: A historical overview and speculative preview of novel mechanisms and emerging concepts in cell signaling, *Free Radical Biol. Med. 38*, 1543-1552.

59. Joensson, T. J., Murray, M. S., Johnson, L. C., Poole, L. B., and Lowther, W. T. (2005) Structural basis for the retroreduction of inactivated peroxiredoxins by human sulfiredoxin, *Biochemistry 44*, 8634-8642.

60. Joensson, T. J., Murray, M. S., Johnson, L. C., and Lowther, W. T. (2008) Reduction of cysteine sulfinic acid in peroxiredoxin by sulfiredoxin proceeds directly through a sulfinic phosphoryl ester intermediate, *J. Biol. Chem. 283*, 23846-23851.

61. Hughes, M. N., and Cammack, R. (1999) Synthesis, chemistry, and applications of nitroxyl ion releasers sodium trioxodinitrate or Angeli's salt and Piloty's acid, *Methods Enzymol. 301*, 279-287.

62. Addison, C. C., Gamlen, G. A., and Thompson, R. (1952) The ultraviolet absorption spectra of sodium hyponitrite and sodium a-oxyhyponitrite: the analysis of mixtures with sodium nitrite and nitrate, *J. Chem. Soc.*, 338-345.

63. Drago, R. S., and Paulik, F. E. (1960) The reaction of nitrogen(II) oxide with diethylamine, *J. Am. Chem. Soc. FIELD Full Journal Title:Journal of the American Chemical Society 82*, 96-98.

64. Toscano, J. P., Brookfield, F. A., Cohen, A. D., Courtney, S. M., Frost, L. M., and Kalish, V. J. (2011) *N*-hydroxylsulfonamide derivatives as new physiologically useful nitroxyl donors, (Johns Hopkins University, USA). U.S. Patent 8,030,356.

65. Chan, W. C., White, P. D., and Editors (2000) *Fmoc Solid Phase Peptide Synthesis: A Practical Approach*.

66. Edelhoch, H. (1967) Spectroscopic determination of tryptophan and tyrosine in proteins, *Biochemistry 6*, 1948-1954.

67. Bonner, F. T., and Ravid, B. (1975) Thermal decomposition of oxyhyponitrite (sodium trioxodinitrate(II)) in aqueous solution, *Inorg. Chem. 14*, 558-563.

68. Afshar, R. K., Patra, A. K., and Mascharak, P. K. (2005) Light-induced inhibition of papain by a {Mn-NO}6 nitrosyl: Identification of papain-SNO adduct by mass spectrometry, *J. Inorg. Biochem. 99*, 1458-1464.

69. Qiang, Z., and Adams, C. (2004) Potentiometric determination of acid dissociation constants (pKa) for human and veterinary antibiotics, *Water Res 38*, 2874-2890.

70. Chaudhury, S., Lyskov, S., and Gray, J. J. (2010) PyRosetta: a script-based interface for implementing molecular modeling algorithms using Rosetta, *Bioinformatics 26*, 689-691.

71. Moriarty, R. M. (1964) Nuclear magnetic resonance spectrum of *N*-methyl sulfinamides. A model for the sulfinyl carbanion, *Tetrahedron Lett.*, 509-512.

72. Petrovic, A. G., and Polavarapu, P. L. (2007) Chiroptical spectroscopic determination of molecular structures of chiral sulfinamides: *t*-butanesulfinamide, *J. Phys. Chem. A 111*, 10938-10943.

73. Shapovalov, M. V., and Dunbrack, R. L., Jr. (2011) A smoothed backbone-dependent rotamer library for proteins derived from adaptive Kernel density estimates and regressions, *Structure 19*, 844-858.

74. Keceli, G., Moore, C. D., Labonte, J. W., and Toscano, J. P. (2013) NMR detection and study of hydrolysis of HNO-derived sulfinamides, *Biochemistry 52*, 7387-7396.

3.6 Supporting Information

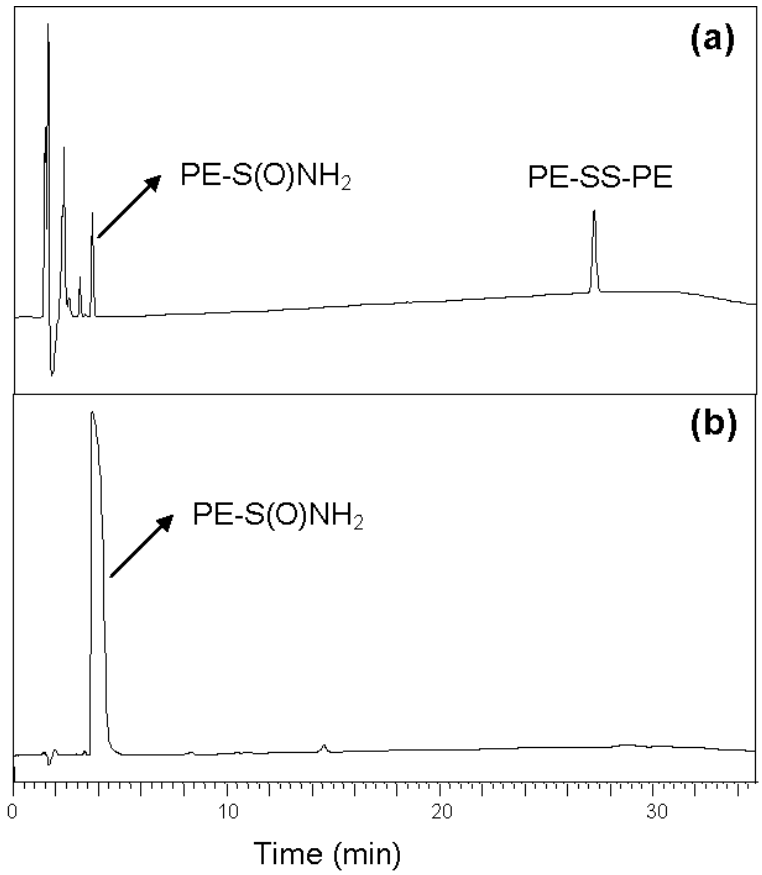

Figure 3-10. HPLC traces of (a) 2-phenylethanesulfinamide (PE-S(O)NH_2) formed via treatment of 2-phenylethanethiol (0.25 mM) with AS (1 mM) and (b) synthetic 2-phenylethanesulfinamide. The HNO-derived 2-phenylethanesulfinamide was confirmed by co-injection with the authentic sample as well as characterization by ESI-MS. PE-SS-PE indicates 2-phenylethane disulfide.

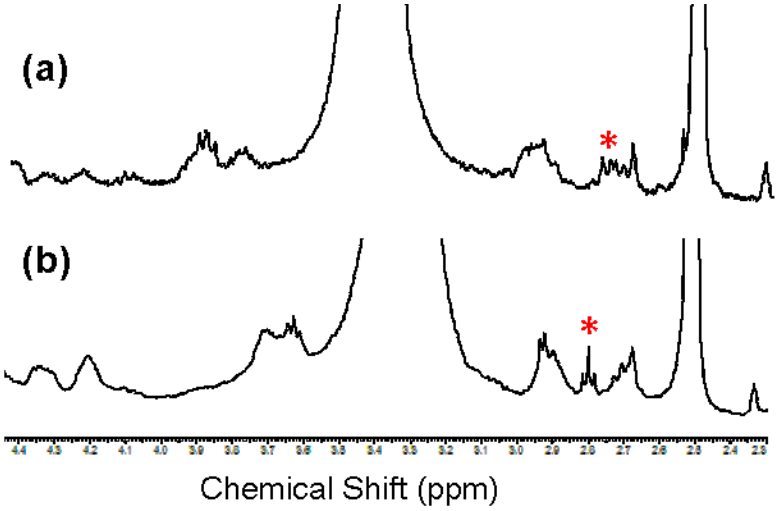

Figure 3-11. Selected region of ^{1}H NMR spectrum showing VYPCLA (0.1 mM) (a) untreated and (b) treated with 1 mM AS in 10 mM phosphate buffer with 50 μM DTPA (pH 7.4) at 37 ^{o}C for 30 min. The spectra were collected in DMSO-d_6 at 30 ^{o}C. The chemical shifts were assigned based on the COSY spectra of the unmodified and sulfinamide-modified sample. An asterisk (*) indicates the cysteine β-H's.

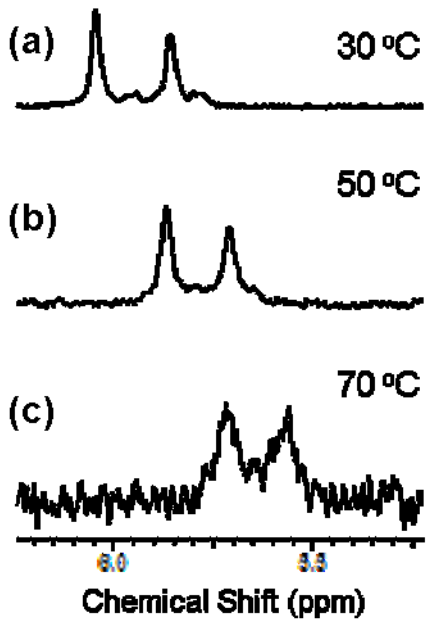

Figure 3-12. ^{15}N-edited ^{1}H 1D-NMR spectra of the VYPCLA sulfinamide at various temperatures. VYPCLA (0.1 mM) was treated with 1 mM ^{15}N-AS in 10 mM phosphate buffer with 50 μM DTPA (pH 7.4) at 37 °C for 30 min to form the corresponding sulfinamide. The sample was analyzed in DMSO-d_6 at (a) 30 °C, (b) 50 °C and (c) 70 °C.

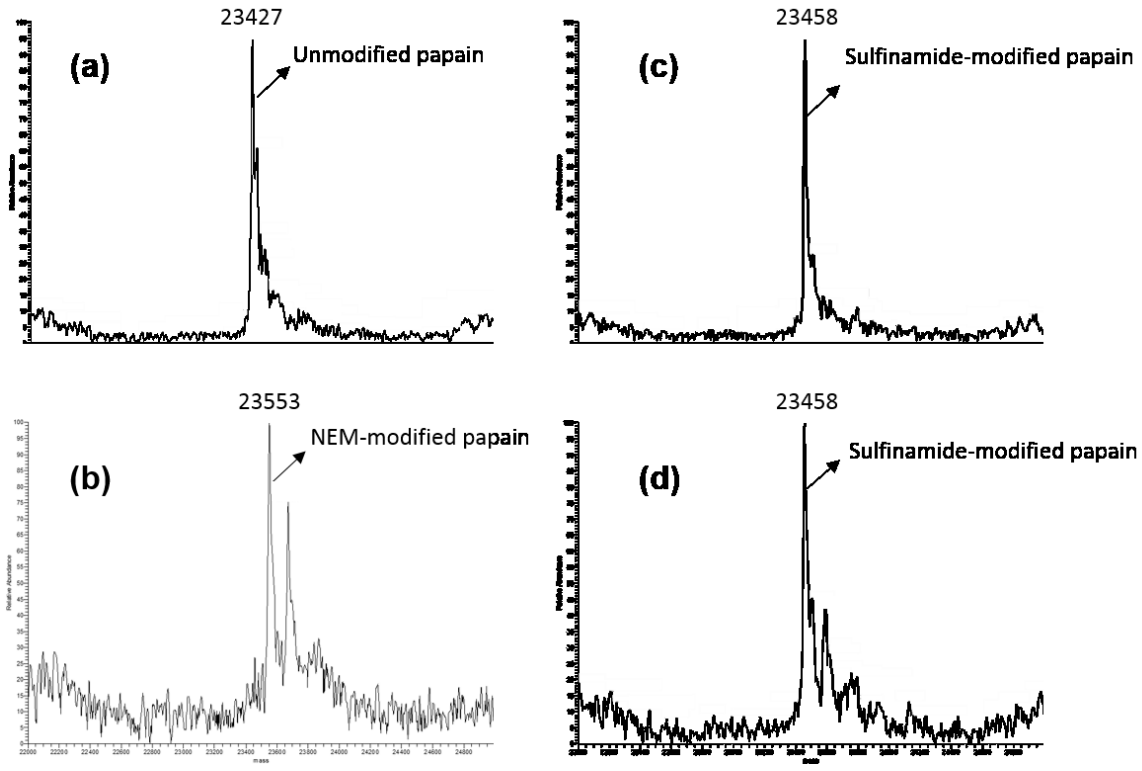

Figure 3-13. Deconvoluted ESI-MS spectra of papain (0.2 mM) (a) untreated or treated with (b) 2 mM NEM at 37 ºC for 1.5 h, (c) 1 mM AS at 37 ºC for 30 min, and (d) 1 mM AS at 37 ºC for 30 min followed by treatment with 2 mM NEM in 10 mM phosphate buffer with 50 μM DTPA. The samples were analyzed by ESI-MS following HPLC purification and concentration.

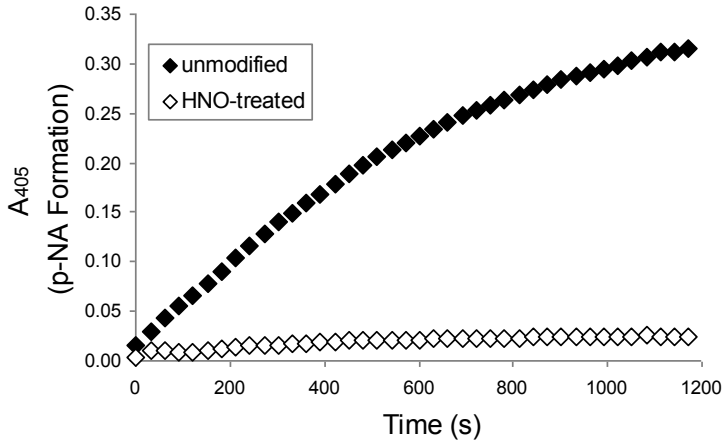

Figure 3-14. Previously activated papain (0.2 mM) was incubated in the absence (♦) or presence of 1 mM AS (◊) in 10 mM phosphate buffer with 50 μM DTPA (pH 7.4) at 37 ºC for 30 min. The samples were analyzed by following the absorbance at 405 nm corresponding to p-nitroaniline (p-NA) formation from L-BAPNA.

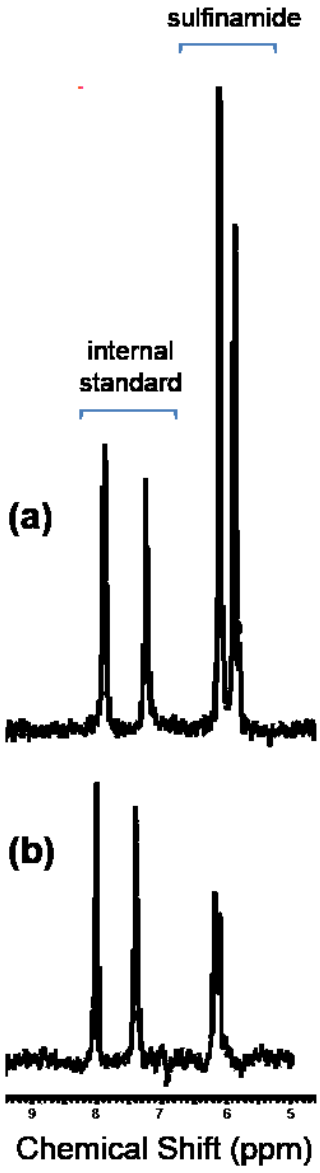

Figure 3-15. ^{15}N-edited ^{1}H NMR spectra of the reduction of HNO-derived VYPCLA sulfinamide. VYPCLA (0.1 mM) was treated with 1 mM ^{15}N-AS in 10 mM phosphate buffer with 50 μM DTPA (pH 7.4) at 37 ºC for 30 min to form the corresponding sulfinamide. The sulfinamide-containing sample was incubated in the presence of 50 mM BME at 37 ºC for 26 h in pH 7.4 buffer. VYPCLA sulfinamide (a) before and (b) after incubation with BME. The spectra were collected in DMSO-d_6 at 30 ºC. ^{15}N-labeled benzamide was added as an internal standard before NMR analysis.

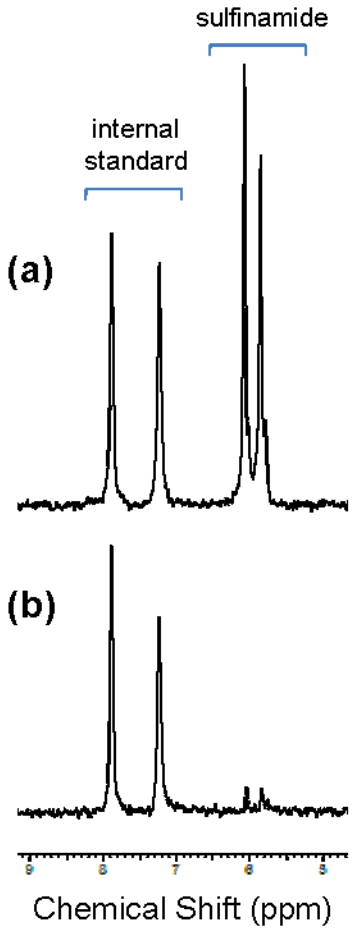

Figure 3-16. ^{15}N-edited ^{1}H NMR spectra of the hydrolysis of HNO-derived VYPCLA sulfinamide. VYPCLA (0.1 mM) was treated with 1 mM ^{15}N-AS in 10 mM phosphate buffer with 50 μM DTPA (pH 7.4) at 37 ºC for 30 min to form the corresponding sulfinamide. The sulfinamide-containing sample was boiled for one week in buffer. VYPCLA sulfinamide (a) before boiling and (b) after boiling. The spectra were collected in DMSO-d_6 at 30 ºC. ^{15}N-labeled benzamide was added as an internal standard before NMR analysis.

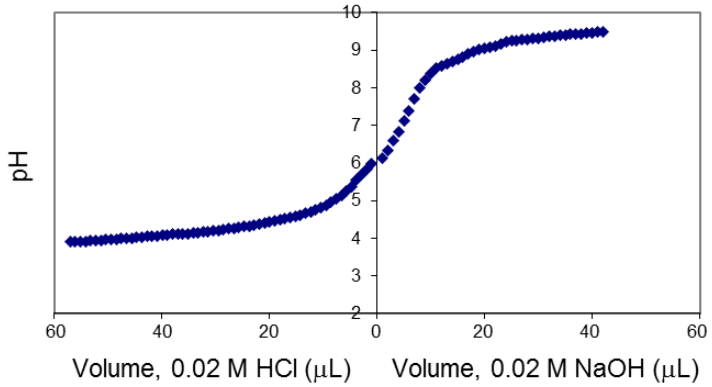

Figure 3-17. Titration curve for *t*-butanesulfinamide (2 mM) treated with 0.02 M HCl or 0.02 M NaOH in 0.05 M KCl at room temperature.

Chapter 4 – Reactivity of C-Terminal Cysteines with HNO

4.1 Introduction

Cysteine residues are known to form several oxidative modifications in the presence of reactive oxygen or nitrogen species.[1-4] These post-translational modifications, including disulfide bonds, sulfinamides, and sulfenic, sulfinic, and sulfonic acids, can affect protein structure and function with potential biological impacts.[1, 5, 6] Apart from the crucial roles of disulfide bonds, recent studies have emphasized the importance of sulfenic and sulfinic acids in redox catalysis and cell signaling.[3, 7-9] Nitroxyl (HNO), the protonated, one-electron reduced form of NO, is a potential therapeutic for several conditions including heart failure, alcoholism, vascular dysfunction, and cancer.[4, 10-12] Due to the highly thiophilic nature of HNO, the majority of its biological effects have been attributed to its reactivity with cysteines.[4, 12, 13] As shown in Scheme 4-1, HNO reacts with thiols to form an *N*-hydroxysulfenamide intermediate. This unstable species has been reported to form a sulfinamide or a disulfide depending on the concentration of thiol.[14, 15] At low thiol concentrations, the *N*-hydroxysulfenamide rearranges to produce a sulfinamide, presumably via a reaction pathway, which involves the dehydration of the protonated *N*-hydroxysulfenamide to form an alkyliminosulfonium intermediate (RS^{+}=N) followed by reaction with water as suggested by computational studies.[16] At high thiol concentrations, the formation of disulfide and hydroxylamine are favored.

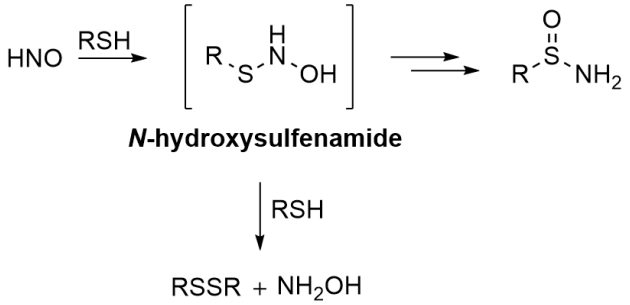

Scheme 4-1. The reaction of HNO with thiols

To gain insight into the pharmacological effects of HNO, we and others have investigated the production of HNO-derived thiol modifications and their consequences on protein function.[16-34] Previous studies on sulfinamide reactivity indicate that reduction to free thiols in the presence of excess thiol and hydrolysis to form sulfinic acids constitute the major reactions of sulfinamides at physiological pH and temperature.[21-23] We have also shown that sulfinamide hydrolysis can be facilitated in the active site of a cysteine protease, indicating that HNO-derived modifications can have different reactivities and consequently different biological impacts depending on their local environment.[22] In addition, recent reviews have highlighted the importance of microenvironment on the reaction of HNO with thiols.[35, 36]

With the aim of learning more about the factors that affect HNO-derived thiol modifications, we have further examined the reactivity of HNO with cysteine derivatives and cysteine-containing peptides. These efforts have led to the observation that, regardless of the conditions employed, sulfinamide formation does not occur on a C-terminal cysteine under physiological conditions. Mechanistic investigations have pointed to the intermediacy of a cyclic structure **1**, which can be hydrolyzed to form a sulfenic acid (Scheme 4-2).

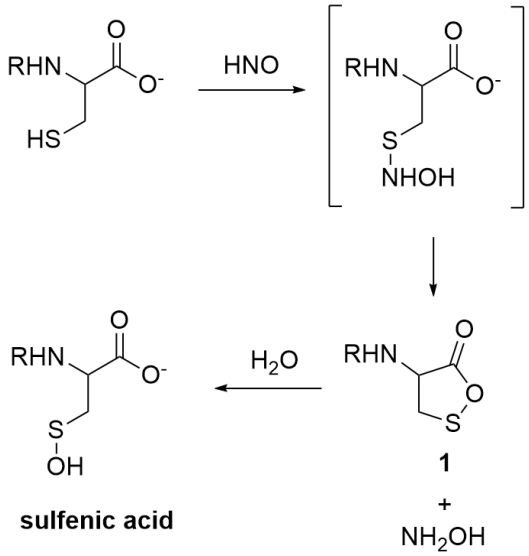

Scheme 4-2. The reaction of HNO with C-terminal cysteines

4.2 Results and Discussion

Thiols are considered to be one of the major targets of HNO in biological systems.[12, 13, 35, 37] Consistent with the complicated chemistry of sulfur, the nature and fate of HNO-derived modifications seem to be affected by factors including thiol concentration and the identity of nearby residues.[14, 15, 22, 23, 30, 35, 38] To gain more insight into the influence of local environment on HNO reactivity, we have explored how the position of the cysteine residue affects reactivity. For this purpose, we have investigated the formation of HNO-derived sulfinamides in cysteine, cysteine derivatives, and cysteine-containing peptides.

4.2.1 Effect of C-Terminus on HNO-Derived Sulfinamides in Cysteine Derivatives

Our previous studies have shown that several small organic molecule thiols and peptides containing internal cysteine residues can be modified to the corresponding sulfinamides by employing a thiol to HNO donor ratio of 1:5 or 1:10 under physiological conditions.[23] We treated *N*-acetyl-L-cysteine (NAC) with the H^{15}NO donor, ^{15}N-2-MSPA, under the same conditions and analyzed the resulting products with our ^{15}N-edited NMR sulfinamide detection method.[22] This method involves the application of an isotope filter for ^{15}N to achieve selective detection of protons attached to the ^{15}N nuclei, providing simplified NMR spectra.[22, 39] Surprisingly, no peaks were detected in the characteristic sulfinamide region (5.5 - 6.5 ppm) (Figure 4-1a), but a new peak was observed at 9.53 ppm. A similar spectrum was obtained upon treatment of NAC with ^{15}N-AS (Supporting Information). Although a previous study suggests the formation of *N*-acetylcysteinesulfinamide from the reaction of NAC and HNO, the product was reported to be unstable and could not be structurally characterized.[40]

To determine if the carboxylic acid of the C-terminus affects sulfinamide formation, we treated *N*-acetyl-L-cysteine methyl ester (NAC-E), in which the free carboxylic acid is replaced with an ester, with H^{15}NO. As shown in Figure 4-1b, the corresponding ^{15}N-labeled sulfinamide signals are now observed. Consistent with our previous studies, two characteristic sulfinamide peaks are detected at 5.89 and 5.94 ppm due to the formation of diastereomers.[22] Similar results were obtained when HABA was used as the HNO donor (Supporting Information). Control experiments carried out with NAC and NAC-E in the

presence of donor byproducts or hydroxylamine did not result in any ^{15}N-edited peaks (data not shown), indicating that these observations (Figure 4-1) are due to HNO reactivity.

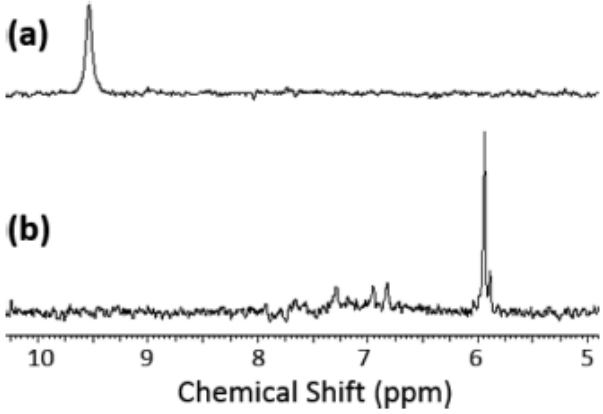

Figure 4-1. Selected region of ^{15}N-edited ^{1}H NMR spectrum (in DMSO-d_6 at 30 ^{o}C) showing ^{15}NH signals following the treatment of (a) NAC (0.1 mM) and (b) NAC-E (0.1 mM) with ^{15}N-2-MSPA (1 mM) in 10 mM phosphate buffer with 50 μM DTPA (pH 7.4) at 37 ^{o}C for 30 min.

4.2.2 Effect of N-Terminus on HNO-Derived Sulfinamides in Cysteine Derivatives

To determine if the free amino group of the N-terminus has a similar effect on the production of an HNO-derived sulfinamide, we conducted experiments with L-cysteine and L-cysteine ethyl ester, both possessing a free N-terminus. Consistent with the above results, sulfinamide signals (5.76 and 5.90 ppm) were detected with the L-cysteine ethyl ester, but not with L-cysteine, indicating that the presence of a free N-terminus does not affect formation of the HNO-derived sulfinamide (Figure 4-2a,b). Similarly, no sulfinamide was observed with D-penicillamine, which contains a free C-terminus, upon treatment with ^{15}N-2-MSPA (data not shown).

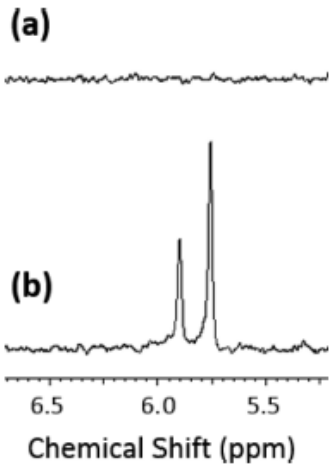

Figure 4-2. Selected region of ^{15}N-edited ^{1}H NMR spectrum (in DMSO-d_6 at 30 ºC) showing ^{15}NH signals following the treatment of (a) L-cysteine (0.1 mM) and (b) L-cysteine ethyl ester (0.1 mM) with ^{15}N-2-MSPA (1 mM) in 10 mM phosphate buffer with 50 μM DTPA (pH 7.4) at 37 ºC for 30 min.

4.2.3 Effect of C-Terminus on HNO-Derived Sulfinamides in Peptides

Given the above results, we next investigated the reactivity of HNO with cysteines in the dipeptide system, LC and CL. No sulfinamide peaks were observed upon analysis of H^{15}NO-treated LC by ^{15}N-edited NMR spectroscopy (Supporting Information). On the other hand, treatment of the N-terminal cysteine-containing peptide, CL, with ^{15}N-AS produced the corresponding sulfinamide (Supporting Information). Consistent with these observations, reaction of the hexapeptide AAAAAC with 2-MSPA also did not generate a sulfinamide (data not shown). These results suggest that cysteine derivatives and C-terminal cysteine-containing peptides react similarly with HNO, presumably due to the presence of a free carboxylate group.

4.2.4 HNO-Derived Modifications of C-Terminal Cysteines

Since sulfinamides are not observed with C-terminal cysteines, we explored the identity of HNO-induced modifications in these systems using the hexapeptide AFAAAC. To confirm the reactivity of HNO with this peptide and its methyl ester derivative, we initially applied our ^{15}N-edited NMR method (Figure 4-3a,b). As expected, characteristic sulfinamide signals at 5.90 and 5.95 ppm were detected only for the AFAAAC methyl ester (Figure 4-3b). Similar to our results with H^{15}NO-treated NAC (Figure 4-1a), a new peak at 9.65 ppm was observed in the ^{15}N-edited NMR spectrum of H^{15}NO-treated AFAAAC (Figure 4-3a). As indicated previously, the ^{15}N-edited NMR method detects only protons bonded to a ^{15}N nucleus.[22, 39] To test if the 9.65 ppm peak was due to residual ^{15}N-2-MSPA, we spiked the sample with the standard compound. As seen in Figure 4-3a, an NMR signal for this compound appears at 9.00 ppm. Additionally, no signal was detected upon exposure of ^{15}N-2-MSPA to the same incubation and sample preparation conditions in the absence of thiol (data not shown).

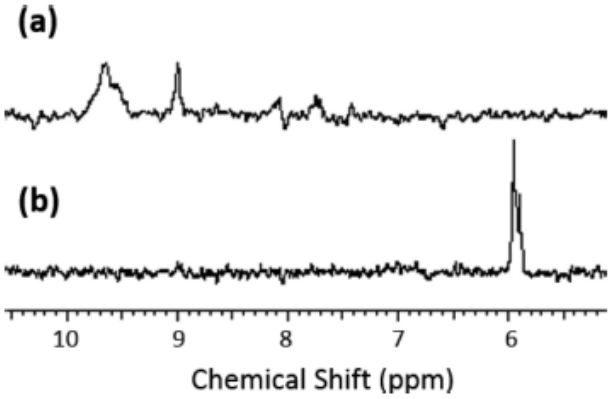

Figure 4-3. Selected region of ^{15}N-edited ^{1}H NMR spectrum (in DMSO-d_6 at 30 ºC) showing ^{15}NH signals following the treatment of (a) AFAAAC (0.1 mM) and (b) AFAAAC methyl ester (0.1 mM) with ^{15}N-2-MSPA (1 mM) in 10 mM phosphate buffer with 50 μM DTPA (pH 7.4) at 37 ºC for 30 min. In (a) the peak at 9.00 ppm corresponds to the ^{15}NH signal of ^{15}N-2-MSPA, which was spiked into the sample.

The reactivity of HNO with AFAAAC was further investigated by ESI-MS (Figure 4-4a-c). As shown in Figure 4b, a signal 32 Da heavier than the AFAAAC disulfide (*m/z* 1135 vs. 1103), which could correspond to the peptide thiosulfonate ($RS(O)_2SR$) (Scheme 4-3), is observed as well as less intense signals assigned to sulfinic acid (RSO_2H, *m/z* 585) and the AFAAAC disulfide (*m/z* 1103). We hypothesize that the thiosulfonate is formed from a sulfenic acid-derived thiosulfinate (see below). Moreover, another intense signal 63 Da heavier than the unmodified peptide (*m/z* 616 vs 553) is also detected (Figure 4-4b). Two possibilities for this latter signal are a peptide sulfohydroxamic acid **2** or hydroxamic acid derivative **3**, both of which have the same exact mass (Scheme 4-3). Since the formation of either **2** or **3** requires the addition of a nitrogen-containing species, we conducted an analogous experiment with the ^{15}N-labeled HNO donor, ^{15}N-2-MSPA. The +63 Da signal (*m/z* 616) is now replaced by a +64 Da signal (*m/z* 617) (Figure 4-4c). Notably, no other species were labeled with ^{15}N. Similar results were obtained with AS

(data not shown), further indicating that these observations are independent of the HNO donor used.

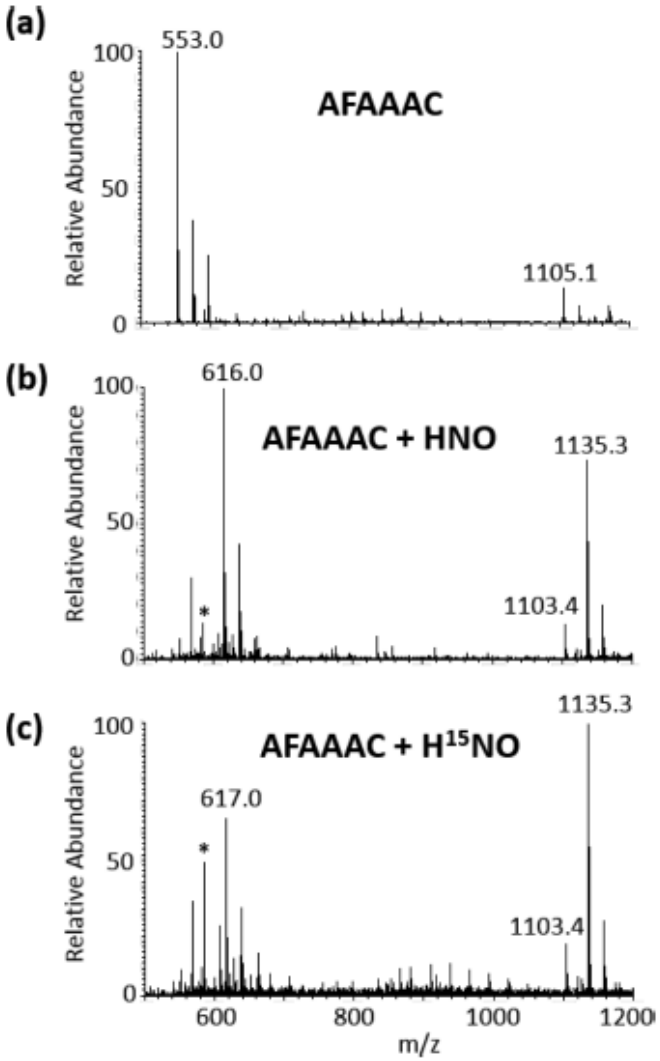

Figure 4-4. Selected region of ESI-MS spectrum showing AFAAAC (0.1 mM) (a) untreated or treated with (b) 2-MSPA (1 mM), and (c) ^{15}N-2-MSPA in 10 mM phosphate buffer with 50 μM DTPA (pH 7.4) at 37 ^{o}C for 30 min. Spectra show the peaks for unmodified peptide (*m/z* 553.0 ± 0.1), sulfinic acid (*m/z* 585.0 ± 0.1, indicated by an asterisk (*)), sulfohydroxamic acid **2** or hydroxamic acid derivative **3** (*m/z* 616.0 ± 0.1), disulfide (*m/z* 1103.3 ± 0.1), dimeric adduct (*m/z* 1105.1 ± 0.1) (commonly observed by mass spectrometry), and thiosulfonate (*m/z* 1135.3 ± 0.1).

Because the identity of the +63 Da peak could not be determined unambiguously from the ESI-MS data alone, we examined the AFAAAC peptide containing a hydroxamic

acid group at the C-terminal by ^{1}H NMR spectroscopy. In contrast to the HNO-treated AFAAAC sample, this peptide did not show any peaks at 9.65 ppm upon NMR analysis (data not shown), suggesting that the 9.65 ppm peak does not correspond to **3** and is likely due to sulfohydroxamic acid **2** (see Scheme 4-6 and text below for a detailed discussion).

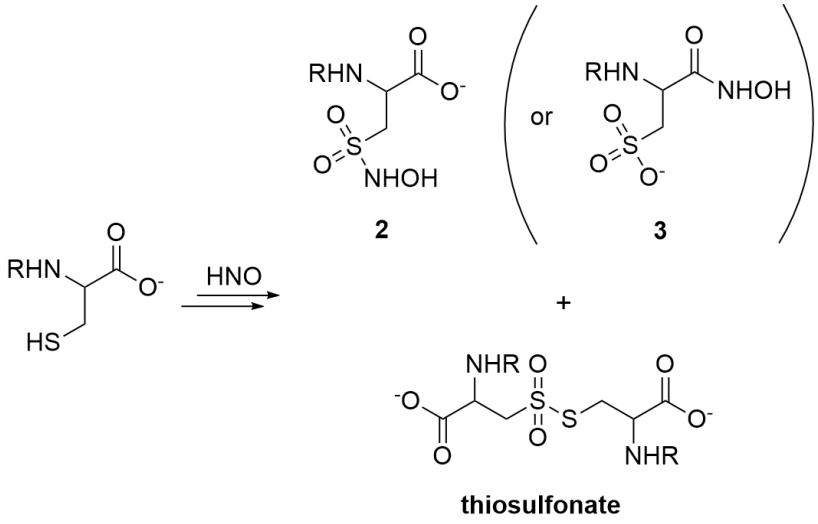

Scheme 4-3. Thiosulfonate and sulfohydroxamic/hydroxamic acid species

4.2.5 HNO-Derived Modifications of C-Terminal Cysteines under Anaerobic Conditions

HNO is known to react with molecular oxygen to form an as of yet unidentified HNO-O_2 adduct which can react as an oxidant.[41, 42] To understand whether the observed reactivity with C-terminal cysteines is due to HNO or the HNO-O_2 adduct, we incubated the AFAAAC peptide with 2-MSPA under argon-saturated conditions. As expected, control samples exposed to the same sample preparation procedures in the absence of 2-MSPA remained unchanged (Figure 4-5a). For HNO-treated samples, identical products were

obtained under air or argon-saturated conditions (Figures 4-4b and 4-5b), indicating that the observed modifications are independent of oxygen.

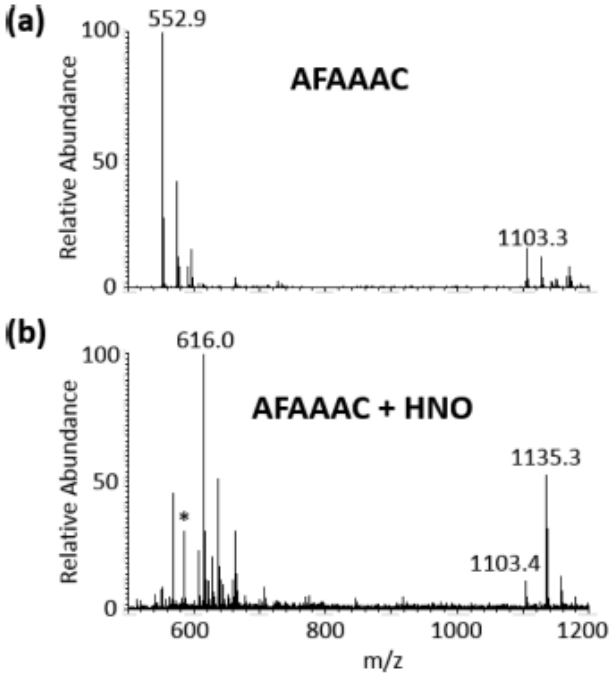

Figure 4-5. Selected region of ESI-MS spectrum showing AFAAAC (0.1 mM) (a) untreated, or treated with (b) 2-MSPA (1 mM) in 10 mM phosphate buffer with 50 μM DTPA (pH 7.4) at 37 ºC for 30 min under argon-saturated conditions. Spectra show the peaks for unmodified peptide (*m/z* 553.0 ± 0.1), sulfinic acid (*m/z* 585.0 ± 0.1, indicated by an asterisk (*)), sulfohydroxamic derivative **2** (*m/z* 616.0 ± 0.1), disulfide (*m/z* 1103.3 ± 0.1), dimeric adduct (*m/z* 1105.1 ± 0.1) (commonly observed by mass spectrometry), and thiosulfonate (*m/z* 1135.3 ± 0.1).

4.2.6 Formation of Thiosulfonate

To gain further evidence for the production of a thiosulfonate, we also examined the HNO-treated AFAAAC samples by a standard DTNB assay. As expected, no free thiol is detected following HNO treatment. Subsequent incubation with excess DTT results in the

recovery of ca. 65% of the total thiol content (data not shown), suggesting the presence of reducible (65%) and not-readily reducible (35%) species.

In addition, reaction of HNO-treated AFAAAC with thiophenol was examined by ESI-MS. Consistent with the known reactivity of thiosulfonate with thiols (Scheme 4-4),[43] the *m/z* 1135 signal completely disappeared following a short (20 min) incubation with thiol at room temperature. In addition to the peptide sulfinic acid and mixed disulfide (expected from thiol reduction of the thiosulfonate), the sulfohydroxamic acid **2** is still observed at *m/z* 616 under these conditions (Figure 4-6). No significant changes were detected in the ESI-MS spectrum following a similar, short incubation in the absence of thiol. Based on these results, the sulfohydroxamic acid **2** (and peptide sulfinic acid formed from the reduction of peptide thiosulfonate) may correspond to the non-reducible species observed in the above DTNB assay.

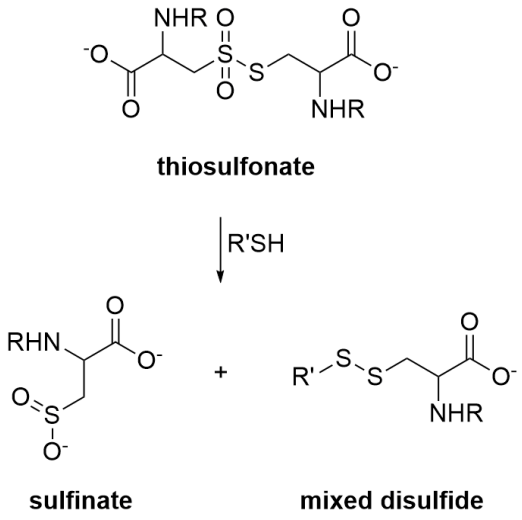

Scheme 4-4. Reduction of thiosulfonates

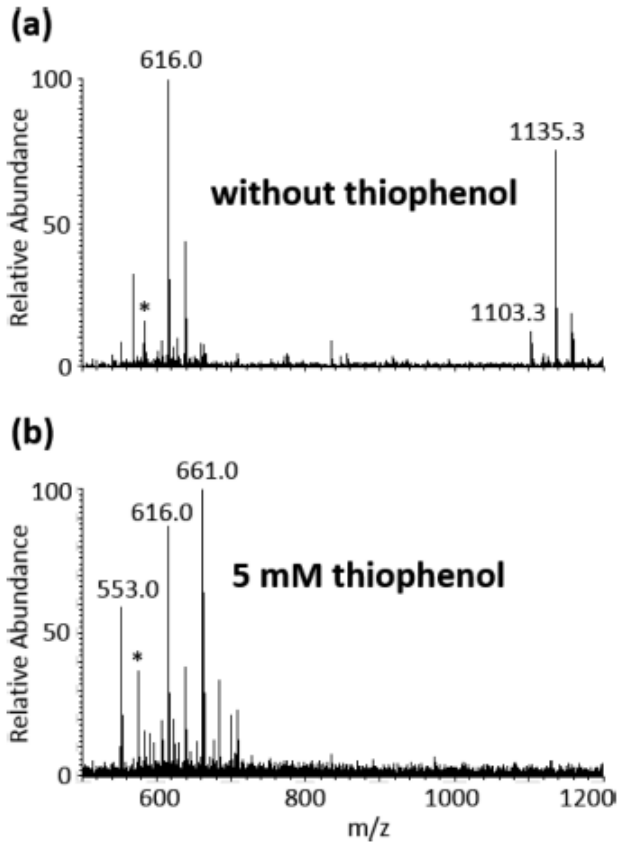

Figure 4-6. Selected region of ESI-MS spectrum showing AFAAAC (0.1 mM) treated with 2-MSPA (1 mM) in 10 mM phosphate buffer with 50 μM DTPA (pH 7.4) at 37 ºC for 30 min under argon-saturated conditions. The samples were incubated for an additional 20 min at RT (a) without or (b) with 5 mM thiophenol. Spectra show peaks for the unmodified peptide (*m/z* 553.0 ± 0.1), sulfinic acid (*m/z* 585.0 ± 0.1, indicated by an asterisk (*)), sulfohydroxamic derivative **2** (*m/z* 616.0 ± 0.1), disulfide (*m/z* 1103.3 ± 0.1), mixed disulfide (*m/z* 661.0 ± 0.1), and thiosulfonate (*m/z* 1135.3 ± 0.1).

Cysteine thiosulfonate is known to be hydrolyzed to form the corresponding sulfinic acid and disulfide (Scheme 5).[43] To test this reactivity, we incubated HNO-treated AFAAAC samples in buffer under physiological conditions for 22 h. The peptide thiosulfonate signal at *m/z* 1135 disappeared completely and the signals for sulfinic acid and disulfide are observed (Figure 7a,b), again consistent with thiosulfonate chemistry.

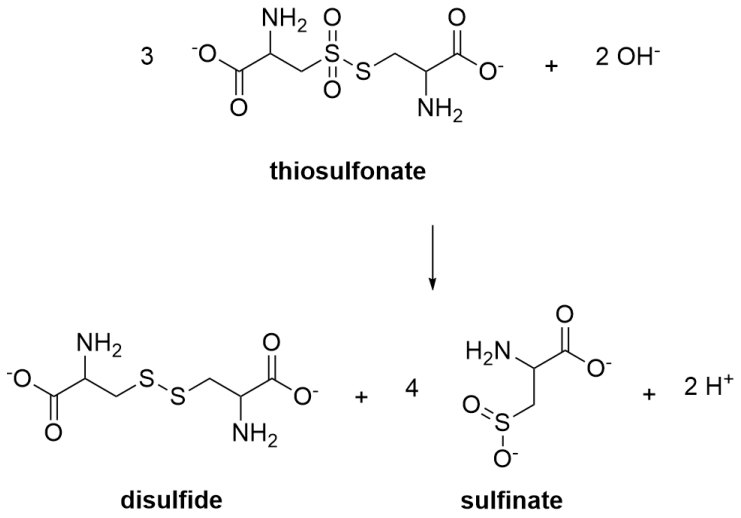

Scheme 4-5. Hydrolysis of cysteine thiosulfonate

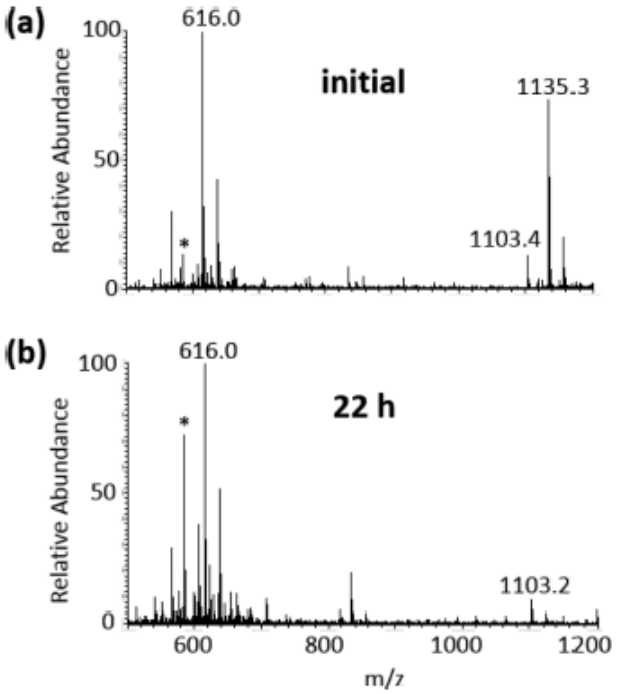

Figure 4-7. Selected region of ESI-MS spectrum showing AFAAAC (0.1 mM) treated with 2-MSPA (1 mM) in 10 mM phosphate buffer with 50 μM DTPA (pH 7.4) at 37 ºC for 30 min. The samples were incubated at physiological pH and temperature for 22 h. Spectra show the peaks for sulfinic acid (*m/z* 585.0 ± 0.1, indicated by an asterisk (*)), sulfohydroxamic derivative **2** (*m/z* 616.0 ± 0.1), disulfide (*m/z* 1103.3 ± 0.1), and thiosulfonate (*m/z* 1135.3 ± 0.1) at (a) initial time and (b) after 22 h.

4.2.7 Intermediacy of Sulfenic Acid

The formation of thiosulfonate from the reaction of HNO with C-terminal cysteines could be explained by the intermediacy of a sulfenic acid (RSOH) (Scheme 4-6). As mentioned previously, reaction of HNO with thiols results in the formation of an *N*-hydroxysulfenamide intermediate (Scheme 4-1). We hypothesize that in the case of a C-terminal cysteine, this unstable species can react with the carboxylic acid group to form a cyclic intermediate **1** (Schemes 4-2 and 4-6), whose generation has been proposed for the bromine-dependent oxidation of cystine to cysteic acid.[44] Subsequent hydrolysis of **1** would produce a sulfenic acid.[45] In the absence of excess thiol or stabilizing factors such as sterics, aromaticity, hydrogen bonding or protein environment, sulfenic acids are known to dimerize rapidly to form thiosulfinates (Scheme 4-6).[46-48] Recent studies indicate that at pH<10, the hydrolysis of cysteine thiosulfinates produces cysteine thiosulfonates.[43] Moreover, cysteine thiosulfonates ($RS(O)_2SR$) have been reported to be more stable at pH<7 and consequently become the predominant species at lower pH values.[43] Presumably, once the peptide sulfenic acid is formed, under our experimental conditions it is converted to the corresponding thiosulfinate (RS(O)SR), which is subsequently hydrolyzed to the thiosulfonate. The resulting peptide thiosulfonate ($RS(O)_2SR$) is expected to be stabilized by the acidic sample preparation conditions employed for ESI-MS, consistent with its observation.

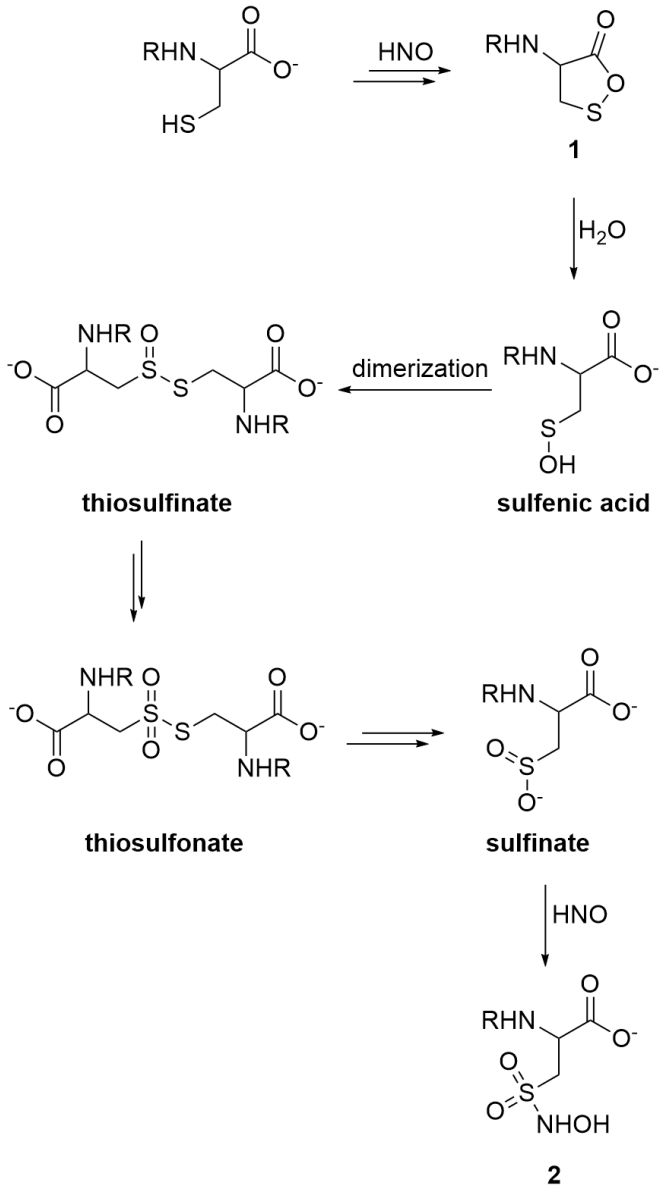

Scheme 4-6. Formation of the observed products

To explore other potential pathways for thiosulfonate formation, we conducted several control experiments involving oxidized derivatives of methanethiol or cysteine as model systems. Incubation of cysteinesulfinic acid, methanesulfinic acid, or dimethyl disulfide under physiologically-relevant conditions did not generate the corresponding thiosulfonates ($RS(O)_2SR$) (data not shown), indicating that simple oxidation is not the

origin of this species. Similarly, no reaction was observed upon incubation of dimethyl disulfide with methanesulfinic acid or L-cystine with L-cysteinesulfinic acid (data not shown). These results are consistent with the formation of thiosulfonate via the intermediacy of a sulfenic acid.

Due to the reactive nature of sulfenic acids, they are generally detected by employing dimedone-based traps.[49-52] Also, recent studies point to the use of benzoxaboroles as alternative sulfenic acid traps.[53] The use of either class of sulfenic acid trap, however, was not feasible due to the reactivity of dimedone-based traps with HNO, as determined by headspace GC and ^{15}N-edited NMR analyses, and the direct reactivity of benzoxaborole with HNO-donors (Supporting Information). Moreover, cysteinethiosulfinate and methyl methanethiosulfonate were observed to react with dimedone, consistent with recent reports (Supporting Information).[54]

4.2.8 Formation of Sulfohydroxamic Acid

As seen in Schemes 4-1 and 4-2, hydroxylamine (NH_2OH) is expected to be released upon reaction of HNO with excess thiol. Since hydroxylamine might play a role in the generation of sulfohydroxamic acid **2**, we looked into its reactivity in buffer with methanesulfinate ($CH_3SO_2^-$) and methyl methanethiosulfonate ($CH_3S(O)_2SCH_3$) by ^{1}H NMR. Although a reaction was observed between hydroxylamine and methyl methanethiosulfonate, the product does not correspond to methanesulfohydroxamic acid ($CH_3S(O)_2NHOH$) (Supporting Information), suggesting that the formation of **2** proceeds via a different pathway. No products were formed upon incubation of methanesulfinate with hydroxylamine (data not shown).

Previous kinetic studies indicate that sulfinates (RSO_2^-) can trap HNO, producing sulfohydroxamic acids.[55, 56] To test the feasibility of this reaction under the conditions of our experiments, we incubated methanesulfinate with the HNO-donors, 2-MSPA and AS (Figure 4-8a-b and Supporting Information, respectively). In both cases, the product was determined to be methanesulfohydroxamic acid ($CH_3S(O)_2NHOH$) via comparison with an independently prepared authentic standard. Moreover, the corresponding ^{15}NH peak, similar to the peak (ca. 9.6 ppm) detected with HNO-treated C-terminal cysteines (Figures 4-1 and 4-3), is observed upon treatment of methanesulfinate with ^{15}N-2-MSPA (Supporting Information). The downfield shift observed for the NAC (or peptide) sulfohydroxamic acid (ca. 9.6 ppm) compared with methanesulfohydroxamic acid (ca. 9 ppm) is presumably due to hydrogen-bonding between the sulfohydroxamic acid ^{15}NH and C-terminal carboxylate. Indeed, such an interaction is suggested by computational studies (Supporting Information).[57-59] Since sulfinates are formed upon reduction or hydrolysis of thiosulfonates (Schemes 4-4 and 4-5), these results represent a potential pathway to sulfohydroxamic acid **2** (Scheme 4-6). Consistent with these results, treatment of methyl methanethiosulfonate with either 2-MSPA or AS under the same conditions resulted in the formation of methanesulfohydroxamic acid as expected (data not shown).

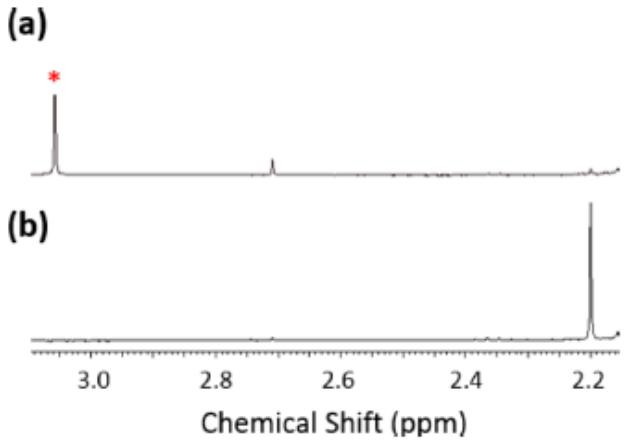

Figure 4-8. Selected region of ^{1}H NMR spectrum showing methanesulfinate (1 mM) incubated in 250 mM phosphate buffer with 50 μM DTPA (pH 7.4) at 37 ^{o}C for 30 min (a) with or (b) without 2-MSPA (10 mM). The peak at 2.18 ppm corresponds to methanesulfinate. An asterisk indicates the product (methanesulfohydroxamic acid, 3.06 ppm) formed due to the reaction of methanesulfinate and HNO. The small peak at 2.71 ppm corresponds to methanesulfonate (commonly observed due to oxidation of methanesulfinate). The spectra were collected in buffer/D_2O (90:10) at 25 ^{o}C.

4.3 Conclusions

We have demonstrated that the C-terminal carboxylate influences the nature of HNO-derived modifications of C-terminal cysteines. Unlike the standard end-products (sulfinamide and disulfide), the major products are now a thiosulfonate and a sulfohydroxamic acid derivative under the conditions of our experiments. Moreover, the formation of these new products takes place independent of oxygen, presumably via the intermediacy of a cyclic structure followed by formation of a sulfenic acid (Schemes 4-2 and 4-6). To the best of our knowledge, this is the first report of HNO-derived thiol modifications involving a sulfenic acid intermediate. Introduction of a C-terminal ester replaces this reactivity with the well-known sulfinamide generation, emphasizing the importance of local environment on HNO-induced modifications. Further investigations

are required to determine if similar effects are also produced by adjacent side chain carboxylates (e.g., aspartate or glutamate).

Proteomics studies conducted with cultured mammalian cells suggest that less than 10% of total protein cysteines are involved in disulfide bond formation, indicating the high availability of cysteine residues for modification.[60] Although the in vivo relevance of our results is yet to be determined, a simple database search reveals several important human proteins possessing C-terminal cysteine residues and unmodified carboxylates such as guanosine monophosphate reductase-2 (GMPR2), dihydropyrimidine dehydrogenase (DPD), elongin C, and sterol 27-hydroxylase (see Supporting Information for a more complete list). Considering the central role of sulfenic acids in cell signaling and redox regulation, which may modulate transcription factors, channel activity, and also affect phosphorylation, SUMOylation and ubiquitination levels in cells,[7, 61, 62] these findings may point to new biological and pharmacological properties of HNO.

4.4 Experimental Methods

Reagents. L-cysteine, *N*-acetyl-L-cysteine (NAC), *N*-acetylcysteine methyl ester (NAC-E), L-cysteine ethyl ester, D-penicillamine, L-cystine, L-cysteinesulfinic acid monohydrate, sodium methanesulfonate, *S*-methyl methanethiosulfonate, 5,5'-dithiobis(2-nitrobenzoic acid) (DTNB), dithiothreitol (DTT) were of the highest purity available and purchased from Sigma (St. Louis, MO). Dimethyl disulfide, sodium methanesulfinate and dimedone were purchased from Acros. 2-(Hydroxymethyl)benzeneboronic acid hemiester was purchased from Alfa Aesar (Ward Hill, MA). Peracetic acid (35%) was purchased from FMC Corporation (Philadelphia, PA). HPLC and MS grade acetonitrile (ACN) were purchased from Thermo Fisher Scientific (Rockford, IL). Dimethyl sulfoxide-d_6 (DMSO-

d$_6$), D_2O and ^{15}N-labeled hydroxylamine hydrochloride were purchased from Cambridge Isotope Laboratories (Andover, MA). The syntheses of HNO donors, Angeli's salt ($Na_2N_2O_3$, AS),[63] ^{15}N-labeled Angeli's salt (^{15}N-AS),[64] and 5-(*N*-hydroxylamine)-5-(acetyl-*O*-methoxyoxime)-*N,N*-dimethylbarbituric acid (HABA)[65] were carried out as previously described. The HNO donor, *N*-hydroxy-2-(methylsulfonyl)-benzenesulfonamide (2-MSPA),[66] the ^{15}N-labeled HNO donor, *^{15}N*-hydroxy-2-(methylsulfonyl)benzenesulfonamide (^{15}N-2-MSPA),[66] and the donor byproduct, 2-(methylsulfonyl)benzenesulfinic acid (2-MSSA) were a generous gift from Cardioxyl Pharmaceuticals. Methanesulfohydroxamic acid ($CH_3S(O)_2NHOH$) was synthesized following a literature procedure.[67, 68] The synthesis of cysteine thiosulfinate was carried out following a literature procedure and the purity of the product was confirmed by electrospray ionization mass spectrometry (ESI-MS).[69, 70] Milli Q water was used for all purifications and experiments.

Peptide Synthesis and Purification. Synthetic peptides AFAAAC, AAAAAC, CL and LC were synthesized on a Symphony Quartet peptide synthesizer (Protein Technologies Inc., Tucson, AZ) following Fmoc solid-phase peptide synthesis methods.[71] The crude product was dissolved in 0.1% trifluoroacetic acid (TFA) and purified by HPLC (Waters HPLC equipped with Delta 600 pump system and dual wavelength absorbance detector) on an Apollo C_{18} reverse-phase column using a linear gradient of 5-75% ACN with 0.1% TFA over 50 min at room temperature. Synthesis of AFAAAC hydroxamic acid was carried out by employing hydroxylamine Wang resin and the crude product was purified by HPLC in the absence of TFA. In all cases, peptide fractions were identified by ESI-MS. Pure fractions were pooled and lyophilized, and the purified product was

quantified based on the absorbance at 257 nm (ε_{257} = 195 M^{-1} cm^{-1}) or a DTNB assay.[72, 73] Peptides were stored at -80 °C in lyophilized form until use.

AFAAAC methyl ester was synthesized following literature procedures.[74] Briefly, AFAAAC was dissolved in 0.1 M acetyl chloride in methanol to have a final concentration of 2 mM and stirred at room temperature for 25 h. The solvent was then removed under vacuum at room temperature in a Savant Speedvac apparatus and the peptide was stored at -80 °C until use. The complete conversion of the peptide C-terminal carboxylic acid to the corresponding methyl ester was confirmed by ESI-MS.

Incubation of Thiols with HNO. The incubations were carried out as previously described.[22, 23] Cysteine derivatives or cysteine-containing peptides were dissolved in 10 mM sodium phosphate buffer with 50 μM of the metal chelator, diethylenetriamine pentaacetic acid (DTPA), at pH 7.4 to have a final concentration of 0.1 mM and used immediately. Stock solutions of AS or ^{15}N-AS were prepared in 0.01 M NaOH, kept on ice, and used within 15 min of preparation. Stock solutions of 2-MSPA, ^{15}N-2-MSPA, or HABA were prepared in ACN and used within 15 min of preparation. Stock solutions of the donor byproducts, NO_2^- and 2-MSSA were dissolved in 0.01 M NaOH and ACN/H_2O (1:1, v/v), respectively. The cysteine derivatives or cysteine-containing peptides were incubated with 1 mM AS, ^{15}N-AS, 2-MSPA, ^{15}N-2-MSPA, or HABA (as indicated) at 37 °C for 30 min in a block heater. In all cases, the final volume of ACN did not exceed 1% of the total. As controls, incubations were also carried out with donor byproducts NO_2^- and 2-MSSA under the same conditions. The samples were then prepared for either ESI-MS or NMR analysis.

For immediate ESI-MS analysis, the peptides were purified and desalted with C_{18} PepClean spin columns, and then diluted into 70% ACN with 0.1% TFA as described previously.[23] For NMR analysis, the samples were flash-frozen and lyophilized. Following lyophilization, the samples were re-dissolved in DMSO-d_6 for NMR analysis as described previously.[22]

Incubation of Thiols with HNO under Anaerobic Conditions. Cysteine-containing peptides were dissolved in pH 7.4 phosphate buffer as described above. The peptide solutions were purged with argon for 30 min prior to incubation with HNO-donors. A 0.1 M stock solution of 2-MSPA was prepared in ACN and purged with argon for 10 min. The argon-purged 2-MSPA solution was introduced via an air-tight syringe to have a final concentration of 1 mM and the samples were incubated at 37 ^{o}C for 30 min under continuous argon purging. Following incubation, the samples were purged for an additional 30 min at room temperature, opened to air and prepared for immediate ESI-MS analysis as described above. Also, control samples were prepared under the same conditions in the absence of 2-MSPA.

Incubation of Methyl Methanethiosulfonate with Hydroxylamine. Stock solutions of methanesulfinate ($CH_3SO_2^-$), methyl methanethiosulfonate ($CH_3S(O)_2SCH_3$), and hydroxylamine were prepared in pH 7.4 phosphate buffer and used within 15 min of preparation. Each oxidized sulfur compound was diluted into 250 mM phosphate buffer with 50 μM DTPA containing 10% D_2O to have a final concentration of 1 mM. The samples were incubated at 37 ^{o}C for 30 min in the presence or absence of 1 mM hydroxylamine (as indicated). The samples were then immediately analyzed by ^{1}H NMR spectroscopy.

Incubation of Methanesulfinate with HNO-Donors. Stock solutions of methanesulfinate, AS and 2-MSPA, and ^{15}N-2-MSPA were prepared as described above. Methanesulfinate was diluted into 250 mM phosphate buffer with 50 μM DTPA containing 10% D_2O to have a final concentration of 1 mM. The samples were incubated at 37 ^{o}C for 30 min in the presence or absence of 10 mM AS or 2-MSPA (as indicated). The samples were then immediately analyzed by ^{1}H NMR spectroscopy.

In some cases, methanesulfinate was diluted into 10 mM phosphate buffer with 50 μM DTPA to have a final concentration of 0.1 mM and the samples were incubated at 37 ^{o}C for 30 min in the presence of ^{15}N-2-MSPA (as indicated). The samples were then flash-frozen and lyophilized. Following lyophilization, the samples were re-dissolved in DMSO-d_6 for NMR analysis as described above.

Incubation of HNO-Donors with Dimedone and Benzoxaborole. Stock solution of ^{15}N-2-MSPA was prepared as described above. Stock solutions of dimedone were prepared in DMSO. Dimedone was diluted into 10 mM phosphate buffer with 50 μM DTPA at pH 7.4 to have a final concentration of 0.5 mM. The sample was then incubated with ^{15}N-2-MSPA (1 mM) at 37 ^{o}C for 30 min. Following lyophilization, the samples were analyzed by NMR spectroscopy.

Stock solution of AS and 2-MSPA were prepared as described above. HNO-donors (9 mM) were incubated with benzoxaborole (2-(hydroxymethyl)benzeneboronic acid hemiester) (9 mM) in 250 mM phosphate buffer with 50 μM DTPA at pH 7.4 containing 10% D_2O at 37 ^{o}C for 30 min. As a control, benzoxaborole (9 mM) was incubated in the absence of HNO-donors. The samples were immediately analyzed by ^{11}B NMR spectroscopy.

DTNB Assay for Quantification of Free Thiol. Stock solutions of DTT (1 M) were freshly prepared in water and used within 15 min of preparation. AFAAAC was incubated with the HNO-donor, 2-MSPA, or its byproduct as described above. The samples were then incubated with 10 mM DTT at 25 ^{o}C for 20 min. Aliquots were taken from each sample at various stages and the peptides were desalted with C_{18} PepClean spin columns to remove excess DTT. The solvent was then removed under vacuum at room temperature and the residue was re-dissolved in 10 mM phosphate buffer with 50 μM DTPA at pH 8. The free sulfhydryl content was immediately determined by DTNB titration.[73] The results were normalized with respect to the amount of free thiol in the initial sample. Control samples treated with donor byproduct were also analyzed under the same conditions.

NMR Analyses. All NMR analyses were conducted on a Bruker Avance-400 FT-NMR spectrometer operating at 400 and 128 MHz for ^{1}H and ^{11}B, respectively. ^{1}H NMR and ^{15}N-edited ^{1}H 1D-NMR analyses were carried out in DMSO-*d*$_6$ at 303 K. In some cases, ^{1}H NMR spectra were collected in pH 7.4 phosphate buffer with 10% D_2O at 298 K (as indicated). Solvent was suppressed by using 1 s pre-saturation pulse. ^{15}N-edited ^{1}H 1D-NMR spectra were acquired using the heteronuclear single quantum correlation (HSQC) pulse sequence for selection. Chemical shifts are reported in parts per million (ppm) relative to residual DMSO (2.49 ppm for ^{1}H) or residual H_2O (4.7 ppm for ^{1}H). All ^{11}B NMR experiments were carried out in pH 7.4 phosphate buffer with 10% D_2O at 295 K. Samples were analyzed in quartz NMR tubes and chemical shifts were referenced to $Et_2O{\bullet}BF_3$ (41.6 ppm for ^{11}B) in $CDCl_3$.

Computational Analyses. Calculations were performed using Spartan'14.[75] Following a conformation search on *N*-acetylcysteine sulfohydroxamic acid using

molecular mechanics, the geometry minimum in DMSO was determined by density functional theory (DFT) at the B3LYP/6-31G* level with the SM8 solvation model[76].

Mass Spectrometric Analyses. ESI-MS analysis was carried out on a Thermo Finnigan LCQ Deca Ion Trap Mass Spectrometer fitted with an electrospray ionization source, operating in the positive ion mode with an accuracy of ca. 0.1 m/z. In all experiments, samples were introduced to the instrument at a rate of 10 μL/min using a syringe pump via a silica capillary line. The heated capillary temperature was 250 °C and the spray voltage was 5 kV.

Nitrous Oxide Quantification by Headspace Gas Chromatography (GC). To determine the reactivity of dimedone with HNO, its dimerization product, nitrous oxide (N_2O), was analyzed by gas chromatography. Experiments were performed on a Varian CP-3800 instrument equipped with a 1041 manual injector, electron capture detector, and a Restek ShinCarbon ST 80/100 molecular sieve packed column. Grade 5.0 nitrogen was used as both the carrier (8 mL/min) and the make-up (22 mL/min) gas. The injector oven and the detector oven were kept at 200 °C and 300 °C, respectively. All N_2O analyses were performed with the column oven held constant at 150 °C. Stock solutions of AS, 2-MSPA, and dimedone were prepared as described above. HNO-donors were diluted into argon-saturated, pH 7.4 phosphate buffer with 50 μM DTPA to have a final concentration of 0.1 mM. The samples were incubated for 3 h at 37 ºC in the presence or absence of dimedone (0.5 mM) to ensure complete decomposition and equilibration of N_2O with the headspace. All gas injections were made using a 100 μL gastight syringe with a sample-lock.

4.5 References

1. Chung, H. S., Wang, S. B., Venkatraman, V., Murray, C. I., and Van Eyk, J. E. (2013) Cysteine oxidative posttranslational modifications: emerging regulation in the cardiovascular system, *Circ. Res. 112*, 382-392.
2. Ridnour, L. A., Thomas, D. D., Mancardi, D., Espey, M. G., Miranda, K. M., Paolocci, N., Feelisch, M., Fukuto, J., and Wink, D. A. (2004) The chemistry of nitrosative stress induced by nitric oxide and reactive nitrogen oxide species. Putting perspective on stressful biological situations, *Biol. Chem. 385*, 1-10.
3. Jacob, C., Battaglia, E., Burkholz, T., Peng, D., Bagrel, D., and Montenarh, M. (2012) Control of oxidative posttranslational cysteine modifications: from intricate chemistry to widespread biological and medical applications, *Chem. Res. Toxicol. 25*, 588-604.
4. Flores-Santana, W., Salmon, D. J., Donzelli, S., Switzer, C. H., Basudhar, D., Ridnour, L., Cheng, R., Glynn, S. A., Paolocci, N., Fukuto, J. M., Miranda, K. M., and Wink, D. A. (2011) The specificity of nitroxyl chemistry is unique among nitrogen oxides in biological systems, *Antioxid. Redox Signaling 14*, 1659-1674.
5. Go, Y. M., and Jones, D. P. (2013) The redox proteome, *J. Biol. Chem. 288*, 26512-26520.
6. Tocchetti, C. G., Stanley, B. A., Murray, C. I., Sivakumaran, V., Donzelli, S., Mancardi, D., Pagliaro, P., Gao, W. D., van Eyk, J., Kass, D. A., Wink, D. A., and Paolocci, N. (2011) Playing with cardiac "redox switches": The "HNO way" to modulate cardiac function, *Antioxid. Redox Signaling 14*, 1687-1698.

7. Lo Conte, M., and Carroll, K. S. (2013) The redox biochemistry of protein sulfenylation and sulfinylation, *J. Biol. Chem. 288*, 26480-26488.

8. Wilson, M. A. (2011) The role of cysteine oxidation in DJ-1 function and dysfunction, *Antioxid. Redox Signaling 15*, 111-122.

9. Klomsiri, C., Karplus, P. A., and Poole, L. B. (2011) Cysteine-based redox switches in enzymes, *Antioxid. Redox Signaling 14*, 1065-1077.

10. Paolocci, N., Katori, T., Champion, H. C., St John, M. E., Miranda, K. M., Fukuto, J. M., Wink, D. A., and Kass, D. A. (2003) Positive inotropic and lusitropic effects of HNO/NO^- in failing hearts: Independence from beta-adrenergic signaling, *Proc. Natl. Acad. Sci. U. S. A. 100*, 5537-5542.

11. Paolocci, N., Saavedra, W. F., Miranda, K. M., Martignani, C., Isoda, T., Hare, J. M., Espey, M. G., Fukuto, J. M., Feelisch, M., Wink, D. A., and Kass, D. A. (2001) Nitroxyl anion exerts redox-sensitive positive cardiac inotropy in vivo by calcitonin gene-related peptide signaling, *Proc. Natl. Acad. Sci. U. S. A. 98*, 10463-10468.

12. Kemp-Harper, B. K. (2011) Nitroxyl (HNO): A novel redox signaling molecule, *Antioxid. Redox Signaling 14*, 1609-1613.

13. Fukuto, J. M., Cisneros, C. J., and Kinkade, R. L. (2013) A comparison of the chemistry associated with the biological signaling and actions of nitroxyl (HNO) and nitric oxide (NO), *J. Inorg. Biochem. 118*, 201-208.

14. Doyle, M. P., Mahapatro, S. N., Broene, R. D., and Guy, J. K. (1988) Oxidation and reduction of hemoproteins by trioxodinitrate(II). The role of nitrosyl hydride and nitrite, *J. Am. Chem. Soc. 110*, 593-599.

15. Wong, P. S. Y., Hyun, J., Fukuto, J. M., Shirota, F. N., DeMaster, E. G., Shoeman, D. W., and Nagasawa, H. T. (1998) Reaction between *S*-nitrosothiols and thiols: Generation of nitroxyl (HNO) and subsequent chemistry, *Biochemistry 37*, 5362-5371.

16. Cheong, E., Tumbev, V., Abramson, J., Salama, G., and Stoyanovsky, D. A. (2005) Nitroxyl triggers Ca^{2+} release from skeletal and cardiac sarcoplasmic reticulum by oxidizing ryanodine receptors, *Cell Calcium 37*, 87-96.

17. Cook, N. M., Shinyashiki, M., Jackson, M. I., Leal, F. A., and Fukuto, J. M. (2003) Nitroxyl-mediated disruption of thiol proteins: inhibition of the yeast transcription factor Ace1, *Arch. Biochem. Biophys. 410*, 89-95.

18. Demaster, E. G., Redfern, B., and Nagasawa, H. T. (1998) Mechanisms of inhibition of aldehyde dehydrogenase by nitroxyl, the active metabolite of the alcohol deterrent agent cyanamide, *Biochem. Pharmacol. 55*, 2007-2015.

19. Froehlich, J. P., Mahaney, J. E., Keceli, G., Pavlos, C. M., Goldstein, R., Redwood, A. J., Sumbilla, C., Lee, D. I., Tocchetti, C. G., Kass, D. A., Paolocci, N., and Toscano, J. P. (2008) Phospholamban thiols play a central role in activation of the cardiac muscle sarcoplasmic reticulum calcium pump by nitroxyl, *Biochemistry 47*, 13150-13152.

20. Gao, W. D., Murray, C. I., Tian, Y., Zhong, X., DuMond, J. F., Shen, X., Stanley, B. A., Foster, D. B., Wink, D. A., King, S. B., Van Eyk, J. E., and Paolocci, N. (2012) Nitroxyl-mediated disulfide bond formation between cardiac myofilament cysteines enhances contractile function, *Circ. Res. 111*, 1002-1011.

21. Hoffman, M. D., Walsh, G. M., Rogalski, J. C., and Kast, J. (2009) Identification of nitroxyl-induced modifications in human platelet proteins using a novel mass spectrometric detection method, *Mol. Cell. Proteomics 8*, 887-903.

22. Keceli, G., Moore, C. D., Labonte, J. W., and Toscano, J. P. (2013) NMR detection and study of hydrolysis of HNO-derived sulfinamides, *Biochemistry 52*, 7387-7396.

23. Keceli, G., and Toscano, J. P. (2012) Reactivity of nitroxyl-derived sulfinamides, *Biochemistry 51*, 4206-4216.

24. Kim, W.-K., Choi, Y.-B., Rayudu, P. V., Das, P., Asaad, W., Arnelle, D. R., Stamler, J. S., and Lipton, S. A. (1999) Attenuation of NMDA receptor activity and neurotoxicity by nitroxyl anion, NO^-, *Neuron 24*, 461-469.

25. Landino, L. M., Koumas, M. T., Mason, C. E., and Alston, J. A. (2007) Modification of tubulin cysteines by nitric oxide and nitroxyl donors alters tubulin polymerization activity, *Chem. Res. Toxicol. 20*, 1693-1700.

26. Lopez, B. E., Rodriguez, C. E., Pribadi, M., Cook, N. M., Shinyashiki, M., and Fukuto, J. M. (2005) Inhibition of yeast glycolysis by nitroxyl (HNO): A mechanism of HNO toxicity and implications to HNO biology, *Arch. Biochem. Biophys. 442*, 140-148.

27. Lopez, B. E., Wink, D. A., and Fukuto, J. M. (2007) The inhibition of glyceraldehyde-3-phosphate dehydrogenase by nitroxyl (HNO), *Arch. Biochem. Biophys. 465*, 430-436.

28. Mitroka, S., Shoman, M. E., DuMond, J. F., Bellavia, L., Aly, O. M., Abdel-Aziz, M., Kim-Shapiro, D. B., and King, S. B. (2013) Direct and nitroxyl (HNO)-

mediated reactions of acyloxy nitroso compounds with the thiol-containing proteins glyceraldehyde 3-phosphate dehydrogenase and alkyl hydroperoxide reductase subunit C, *J. Med. Chem. 56*, 6583-6592.

29. Salie, M. J., Oram, D. S., Kuipers, D. P., Scripture, J. P., Chenge, J., MacDonald, G. J., and Louters, L. L. (2012) Nitroxyl (HNO) acutely activates the glucose uptake activity of GLUT1, *Biochimie 94*, 864-869.

30. Shen, B., and English, A. M. (2005) Mass spectrometric analysis of nitroxyl-mediated protein modification: Comparison of products formed with free and protein-based cysteines, *Biochemistry 44*, 14030-14044.

31. Sivakumaran, V., Stanley, B. A., Tocchetti, C. G., Ballin, J. D., Caceres, V., Zhou, L., Keceli, G., Rainer, P. P., Lee, D. I., Huke, S., Ziolo, M. T., Kranias, E. G., Toscano, J. P., Wilson, G. M., O'Rourke, B., Kass, D. A., Mahaney, J. E., and Paolocci, N. (2013) HNO enhances SERCA2a activity and cardiomyocyte function by promoting redox-dependent phospholamban oligomerization, *Antioxid. Redox Signaling 19*, 1185-1197.

32. Vaananen Antti, J., Kankuri, E., and Rauhala, P. (2005) Nitric oxide-related species-induced protein oxidation: reversible, irreversible, and protective effects on enzyme function of papain, *Free Radical Biol. Med. 38*, 1102-1111.

33. Vaananen Antti, J., Salmenpera, P., Hukkanen, M., Rauhala, P., and Kankuri, E. (2006) Cathepsin B is a differentiation-resistant target for nitroxyl (HNO) in THP-1 monocyte/macrophages, *Free Radical Biol. Med. 41*, 120-131.

34. Tocchetti, C. G., Wang, W., Froehlich, J. P., Huke, S., Aon, M. A., Wilson, G. M., Di Benedetto, G., O'Rourke, B., Gao, W. D., Wink, D. A., Toscano, J. P., Zaccolo,

M., Bers, D. M., Valdivia, H. H., Cheng, H., Kass, D. A., and Paolocci, N. (2007) Nitroxyl improves cellular heart function by directly enhancing cardiac sarcoplasmic reticulum Ca^{2+} cycling, *Circ. Res. 100*, 96-104.

35. Fukuto, J. M., and Carrington, S. J. (2011) HNO signaling mechanisms, *Antioxid. Redox Signaling 14*, 1649-1657.

36. Zhang, Y. (2013) Computational investigations of HNO in biology, *J. Inorg. Biochem. 118*, 191-200.

37. Choe, C. U., Lewerenz, J., Gerloff, C., Magnus, T., and Donzelli, S. (2011) Nitroxyl in the central nervous system, *Antioxid. Redox Signaling 14*, 1699-1711.

38. Sherman, M. P., Grither, W. R., and McCulla, R. D. (2010) Computational investigation of the reaction mechanisms of nitroxyl and thiols, *J. Org. Chem. 75*, 4014-4024.

39. Breeze, A. L. (2000) Isotope-filtered NMR methods for the study of biomolecular structure and interactions, *Prog. NMR Spectrosc. 36*, 323-372.

40. Shoeman, D. W., Shirota, F. N., DeMaster, E. G., and Nagasawa, H. T. (2000) Reaction of nitroxyl, an aldehyde dehydrogenase inhibitor, with *N*-acetyl-L-cysteine, *Alcohol 20*, 55-59.

41. Miranda, K. M., Dutton, A. S., Ridnour, L. A., Foreman, C. A., Ford, E., Paolocci, N., Katori, T., Tocchetti, C. G., Mancardi, D., Thomas, D. D., Espey, M. G., Houk, K. N., Fukuto, J. M., and Wink, D. A. (2005) Mechanism of aerobic decomposition of Angeli's salt (sodium trioxodinitrate) at physiological pH, *J. Am. Chem. Soc. 127*, 722-731.

42. Miranda, K. M. (2005) The chemistry of nitroxyl (HNO) and implications in biology, *Coordin. Chem. Rev. 249*, 433-455.

43. Nagy, P., and Ashby, M. T. (2007) Reactive sulfur species: Kinetics and mechanism of the hydrolysis of cysteine thiosulfinate ester, *Chem. Res. Toxicol. 20*, 1364-1372.

44. White, R. H. (1987) Oxidation of cystine to cysteic acid by bromine in ^{18}O-labelled water, evidence for cyclic carboxylic-sulfenic anhydride, *J. Labelled Cmpds. Radiopharm. 24*, 323-330.

45. Znamenskii, V. V., Efremov, A. D., Bystrova, V. M., and Kil'disheva, O. V. (1986) Synthesis and biological activity of carboxylic acid derivatives carrying sulfur-containing groups in the b-position *Khimiko-Farmatsevticheskii Zhurnal 20*, 843-847.

46. Block, E. (2013) Fifty years of smelling sulfur, *J. Sulfur Chem. 34*, 158-207.

47. Davis, F. A., Jenkins, L. A., and Billmers, R. L. (1986) Chemistry of sulfenic acids. 7. Reason for the high reactivity of sulfenic acids. Stabilization by intramolecular hydrogen bonding and electronegativity effects, *J. Org. Chem. 51*, 1033-1040.

48. Davis, F. A., Jenkins, R. A. J., Rizvi, S. Q. A., and Yocklovich, S. G. (1981) Chemistry of sulfenic acids. 3. Studies of sterically hindered sulfenic acids using flash vacuum pyrolysis, *J. Org. Chem. 46*, 3467-3474.

49. Klomsiri, C., Nelson, K. J., Bechtold, E., Soito, L., Johnson, L. C., Lowther, W. T., Ryu, S.-E., King, S. B., Furdui, C. M., and Poole, L. B. (2010) Use of dimedone-based chemical probes for sulfenic acid detection, *Methods Enzymol. 473*, 77-94.

50. Seo, Y. H., and Carroll, K. S. (2011) Quantification of protein sulfenic acid modifications using isotope-coded dimedone and iododimedone, *Angew Chem Int Ed Engl 50*, 1342-1345.

51. Gupta, V., and Carroll, K. S. (2014) Sulfenic acid chemistry, detection and cellular lifetime, *Biochim. Biophys. Acta 1840*, 847-875.

52. Furdui, C. M., and Poole, L. B. (2013) Chemical approaches to detect and analyze protein sulfenic acids, *Mass Spectrom. Rev.*

53. Liu, C. T., and Benkovic, S. J. (2013) Capturing a sulfenic acid with arylboronic acids and benzoxaborole, *J. Am. Chem. Soc. 135*, 14544-14547.

54. Reisz, J. A., Bechtold, E., King, S. B., Poole, L. B., and Furdui, C. M. (2013) Thiol-blocking electrophiles interfere with labeling and detection of protein sulfenic acids, *FEBS J 280*, 6150-6161.

55. Bonner, F. T., and Ko, Y. (1992) Kinetic, isotopic, and ^{15}N NMR study of *N*-hydroxybenzenesulfonamide decomposition: An HNO source reaction, *Inorg. Chem. 31*, 2514-2519.

56. Seel, F., and Bliefert, C. (1972) Der Mechanismus der Zersetzung des Natriumsalzes der Benzolsulfhydroxamsaure in wassriger Losung, *Z. anorg. allg. Chem. 394*, 187-196.

57. Becker, E. D. (1999) *High Resolution NMR: Theory and Chemical Applications*, Academic Press, San Diego.

58. Sternberg, U., and Brunner, E. (1994) The influence of short-range geometry on the chemical shift of protons in hydrogen bonds, *J. Magn. Reson., Ser. A 108*, 142-150.

59. Searle, M. S., Sharman, G. J., Groves, P., Benhamu, B., Beauregard, M. S., Westwell, M. S., Dancer, R. J., Maguire, A. J., Try, A. C., and Williams, D. H. (1996) Enthalpic (electrostatic) contribution to the chelate effect: a correlation between ligand binding constant and a specific hydrogen bond strength in complexes of glycopeptide antibiotics with cell wall analogues, *J. Chem. Soc., Perkin Trans. 1*, 2781-2786.

60. Hansen, R. E., Roth, D., and Winther, J. R. (2009) Quantifying the global cellular thiol-disulfide status, *Proc. Natl. Acad. Sci. U. S. A. 106*, 422-427.

61. Poole, L. B. (2003) Formation and functions of protein sulfenic acids, *Current Protocols in Toxicology 18*, 17.11.11-17.11.15.

62. Roos, G., and Messens, J. (2011) Protein sulfenic acid formation: from cellular damage to redox regulation, *Free Radical Biol. Med. 51*, 314-326.

63. Hughes, M. N., and Cammack, R. (1999) Synthesis, chemistry, and applications of nitroxyl ion releasers sodium trioxodinitrate or Angeli's salt and Piloty's acid, *Methods Enzymol. 301*, 279-287.

64. Bonner, F. T., and Ravid, B. (1975) Thermal decomposition of oxyhyponitrite (sodium trioxodinitrate(II)) in aqueous solution, *Inorg. Chem. 14*, 558-563.

65. Guthrie, D. A., Kim, N. Y., Siegler, M. A., Moore, C. D., and Toscano, J. P. (2012) Development of *N*-substituted hydroxylamines as efficient nitroxyl (HNO) donors, *J. Am. Chem. Soc. 134*, 1962-1965.

66. Toscano, J. P., Brookfield, F. A., Cohen, A. D., Courtney, S. M., Frost, L. M., and Kalish, V. J. (2011) *N*-hydroxylsulfonamide derivatives as new physiologically useful nitroxyl donors, (Johns Hopkins University, USA). U.S. Patent 8,030,356.

67. King, S. B., and Nagasawa, H. T. (1998) Chemical approaches towards generation of nitroxyl, *Methods Enzymol. 301*, 211-220.

68. Brink, K., Gombler, W., and Bliefert, C. (1977) Methylsulfonylhydroxylamin, *Z. anorg. allg. Chem. 429*, 255-260.

69. Nagy, P. A., M. T. (2005) Reactive sulfur species: Kinetics and mechanism of the oxidation of cystine by hypochlorous acid to give N,N'-Dichlorocystine, *Chem. Res. Toxicol. 18*, 919-923.

70. Walti, M., and Hope, D. B. (1971) Synthesis of the isomers of the mono- and di-hydroxy-analogues of cystine and comparison with metabolites excreted in the urine, *J. Chem. Soc., Perkin Trans. 1 12*, 2326-2328.

71. Chan, W. C., White, P. D., and Editors (2000) *Fmoc Solid Phase Peptide Synthesis: A Practical Approach*.

72. Dawson, R. M. C. E., D. C.; Elliott, W. H.; Jones, K. M. (1982) *Data for biochemical research*, 3rd ed., Oxford University Press, New York.

73. Ellman, G. L. (1959) Tissue sulfhydryl groups, *Arch. Biochem. Biophys. 82*, 70-77.

74. Lecchi, P., Olson, M., and Brancia, F. L. (2005) The role of esterification on detection of protonated and deprotonated peptide ions in matrix assisted laser desorption/ionization (MALDI) mass spectrometry (MS), *J. Am. Soc. Mass Spectrom. 16*, 1269-1274.

75. Spartan'14, Wavefunction Inc., Irvine, CA.

76. Marenich, A. V., Olson, R. M., Kelly, C. P., Cramer, C. J., and Truhlar, D. G. (2007) Self-consistent reaction field model for aqueous and nonaqueous solutions based on accurate polarized partial charges, *J. Chem. Theory Comput. 3*, 2011-2033.

4.6 Supporting Information

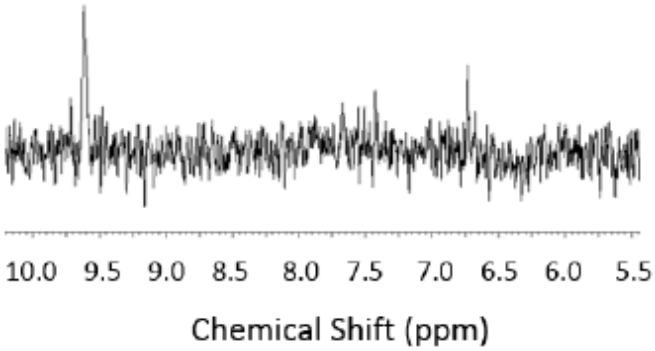

Figure 4-9. Selected region of ^{15}N-edited ^{1}H NMR spectrum (in DMSO-d_6 at 30 ^{o}C) showing ^{15}NH signals following the treatment of NAC (0.1 mM) with ^{15}N-AS (1 mM) in 10 mM phosphate buffer with 50 μM DTPA (pH 7.4) at 37 ^{o}C for 30 min.

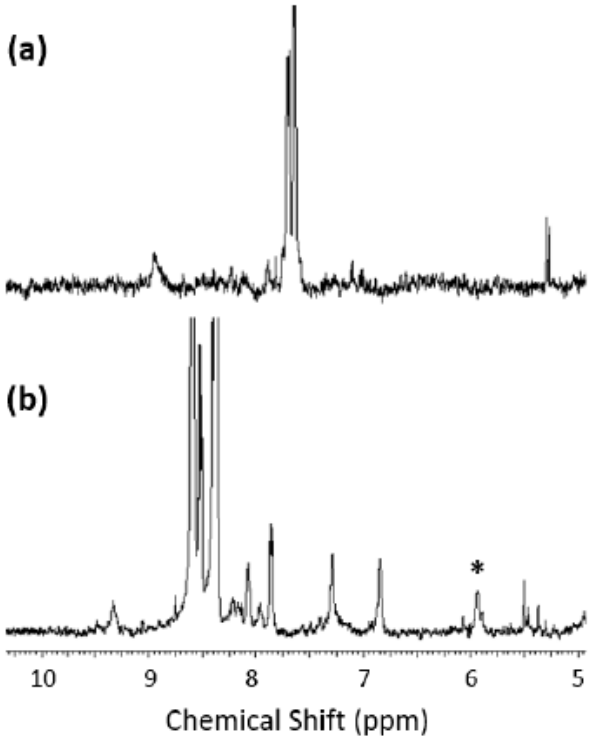

Figure 4-10. Selected region of ^{1}H NMR spectrum (in DMSO-d_6 at 30 ^{o}C) following the treatment of (a) NAC (0.1 mM) and (b) NAC-E (0.1 mM) with HABA (1 mM) in 10 mM phosphate buffer with 50 μM DTPA (pH 7.4) at 37 ^{o}C for 30 min. An asterisk indicates the sulfinamide NH signals.

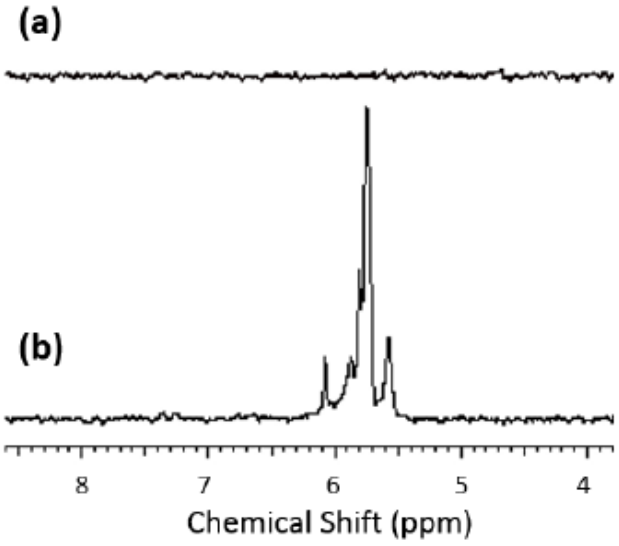

Figure 4-11. Selected region of ^{15}N-edited ^{1}H NMR spectrum (in DMSO-d_6 at 30 ^{o}C) showing ^{15}NH signals following the treatment of (a) LC (0.1 mM) and (b) CL (0.1 mM) with ^{15}N-AS (1 mM) in 10 mM phosphate buffer with 50 µM DTPA (pH 7.4) at 37 ^{o}C for 30 min. The additional sulfinamide peaks were formed due to the presence of a small amount of *N*-acetyl-CL impurity in the sample.

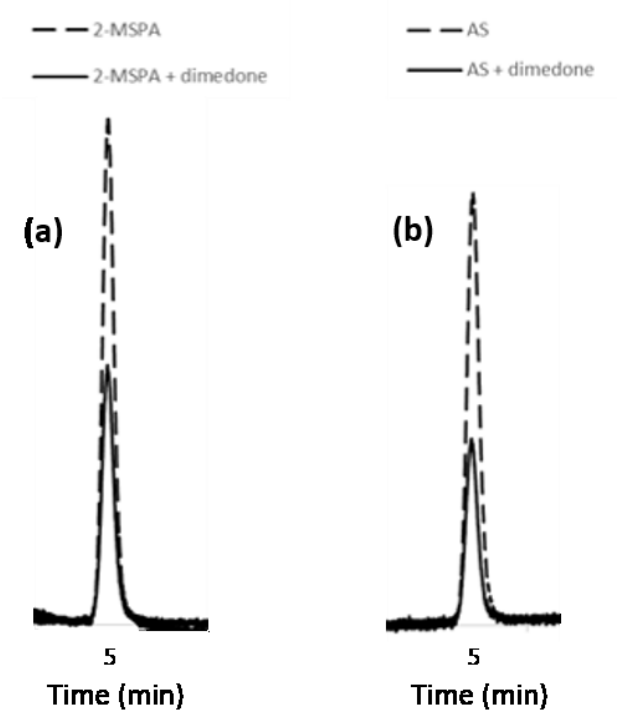

Figure 4-12. Selected region of headspace GC chromatogram showing nitrous oxide (the dimerization product of HNO) detected upon incubation of HNO-donors (a) 2-MSPA (0.1 mM) and (b) AS (0.1 mM) in the absence (dashed line) or in the presence of dimedone (0.5 mM) (solid line) in 10 mM phosphate buffer with 50 μM DTPA (pH 7.4) at 37 ºC for 30 min under argon-saturated conditions. The samples were analyzed 2.5 h after the incubation to ensure complete equilibration of nitrous oxide with the headspace.

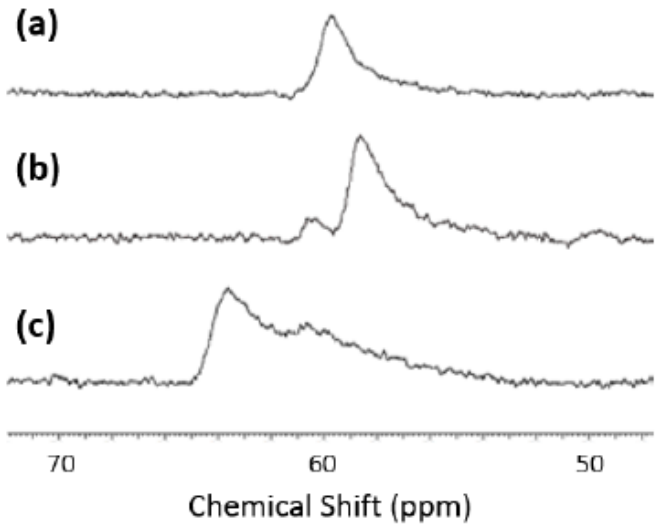

Figure 4-13. Selected region of ^{11}B NMR spectrum (buffer/D_2O (90:10) at 25 ^oC) showing ^{11}B signals of benzoxaborole (9 mM) (a) untreated or treated with (b) AS (9 mM), and (c) 2-MSPA (9 mM) in 10 mM phosphate buffer with 50 μM DTPA (pH 7.4) at 37 ^oC for 30 min.

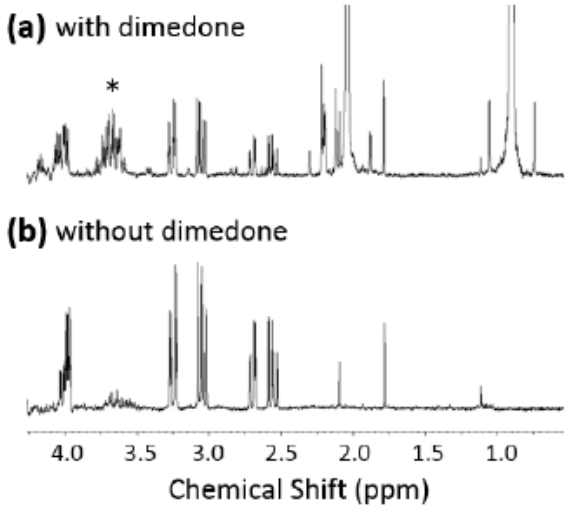

Figure 4-14. Selected region of ^1H NMR spectrum showing cysteine thiosulfinate (1 mM) incubated in 10 mM phosphate buffer with 50 μM DTPA (pH 7.4) at room temperature for 30 min (a) with or (b) without dimedone (5 mM). The peaks at 0.90 and 2.04 ppm correspond to dimedone. An asterisk indicates the product formed due to the reaction of cysteine thiosulfinate and dimedone. The spectra were collected in buffer/D_2O (90:10) at 25 ^oC.

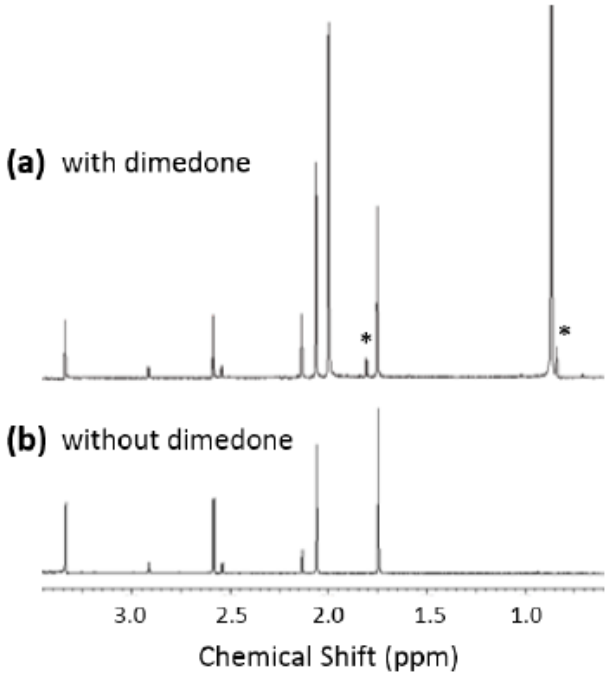

Figure 4-15. Selected region of ^{1}H NMR spectrum showing methyl methanethiosulfonate (1 mM) incubated in 10 mM phosphate buffer with 50 μM DTPA (pH 7.4) at room temperature for 30 min (a) with or (b) without dimedone (5 mM). The peaks at 0.90 and 2.04 ppm correspond to dimedone. An asterisk indicates the product formed due to the reaction of methyl methanethiosulfonate and dimedone. The spectra were collected in buffer/D_2O (90:10) at 25 ^{o}C.

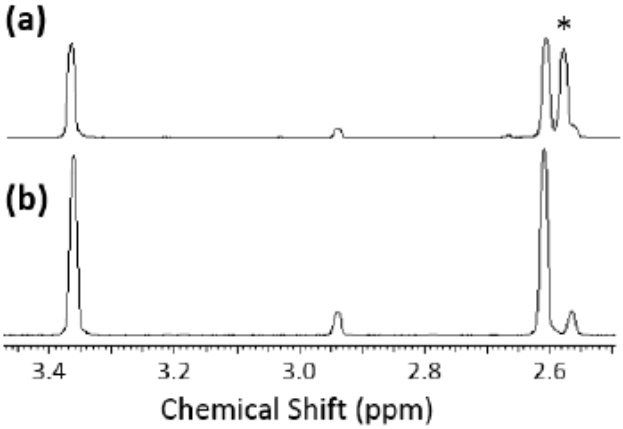

Figure 4-16. Selected region of ^{1}H NMR spectrum showing methyl methanethiosulfonate incubated in 250 mM phosphate buffer with 50 μM DTPA (pH 7.4) at room temperature for 30 min (a) with or (b) without hydroxylamine. The peaks at 3.36 and 2.61 ppm correspond to methyl methanethanethiosulfonate. An asterisk indicates the product formed due to the reaction of methyl methanethiosulfonate and hydroxylamine. The spectra were collected in buffer/D_2O (90:10) at 25 ^{o}C.

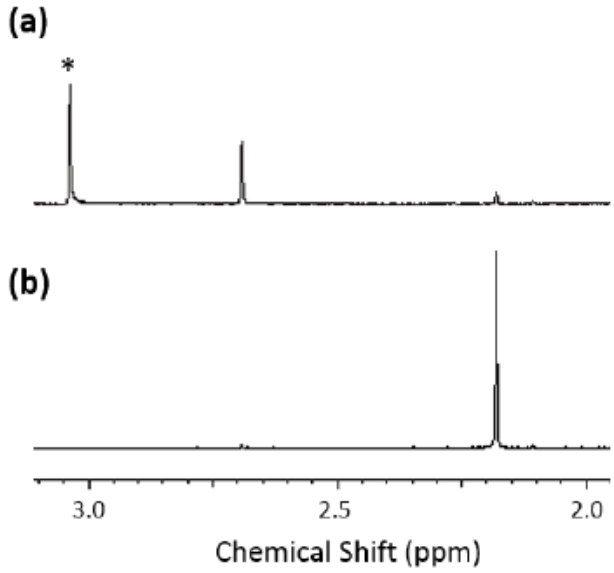

Figure 4-17. Selected region of ^{1}H NMR spectrum showing methanesulfinate incubated in 250 mM phosphate buffer with 50 μM DTPA (pH 7.4) at 37 ºC for 30 min (a) with or (b) without Angeli's salt (AS). The peaks at 2.18 ppm corresponds to methanesulfinate. An asterisk indicates the product formed due to the reaction of methanesulfinate and HNO. The small peak at 2.71 ppm corresponds to methanesulfonate (commonly observed due to oxidation of methanesulfinate). The spectra were collected in buffer/D_2O (90:10) at 25 ºC.

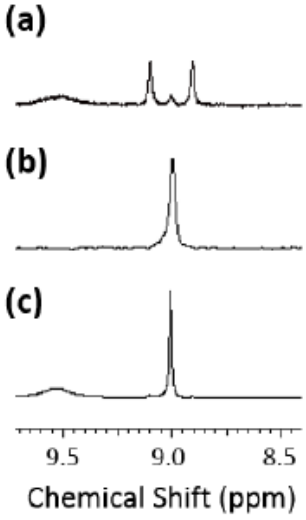

Figure 4-18. Selected region of (a) ^{1}H NMR and (b) ^{15}N-edited ^{1}H 1D-NMR spectrum showing ^{15}NH signals of methanesulfohydroxamic acid formed by treating methanesulfinate (0.1 mM) with ^{15}N-2-MSPA (1 mM) in 10 mM phosphate buffer with 50 μM DTPA (pH 7.4) at 37 ºC for 30 min. (c) ^{1}H NMR spectrum showing NH signal of standard methanesulfohydroxamic acid. The spectra were collected in DMSO-d_6 at 30 ºC.

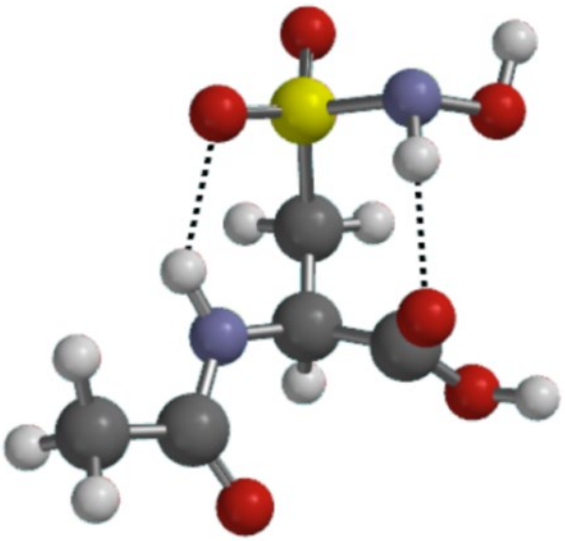

Figure 4-19. Minimized geometry of the NAC sulfohydroxamic acid (in DMSO) determined by DFT (B3LYP/6-31G* with the SM8 solvation model) calculations showing the expected hydrogen bonds.

Cartesian Coordinates (Angstroms)

	Atom		X	Y	Z
1	N	N	1.6410817	-0.1966512	-0.0476324
2	C	CA	0.6412091	0.4862651	-0.8368662
3	C	C	0.0821551	1.7128707	-0.1034166
4	O	O	-0.1435467	1.7740196	1.0929205
5	H	H	1.3709170	-1.0498755	0.4295358
6	H	HA	1.1052174	0.8639202	-1.7530937
7	C	CB	-0.4790085	-0.4635550	-1.3004796
8	S	SG	-1.3913631	-1.4019737	-0.0194647
9	H	1HB	-1.2340987	0.0733097	-1.8782897
10	H	2HB	-0.0562486	-1.2481264	-1.9364213
11	O	O1	-0.4265083	-2.0450127	0.8911381
12	O	O2	-2.4063607	-2.1935068	-0.7190537
13	N	N1	-2.2431244	-0.2917155	0.9863717
14	H	H1	-1.5580665	0.3484629	1.4050244
15	O	O3	-3.0640705	0.5553538	0.1724186
16	H	H2	-3.9280208	0.1091791	0.2041968
17	O	O4	-0.1846099	2.7204921	-0.9586481
18	H	H3	-0.5955974	3.4390132	-0.4399152
19	C	C1	2.8210567	0.4201349	0.2484061
20	O	O5	3.0769038	1.5522214	-0.1745440
21	C	C2	3.7899318	-0.3947576	1.0740018
22	H	H6	3.2841394	-1.0811049	1.7598057
23	H	H5	4.4251999	-0.9915765	0.4092132
24	H	H4	4.4346871	0.2772401	1.6435470

Table 4-1. Some C-terminal cysteine-containing proteins with free carboxylate

Proteins
Acid-sensing ion channel 2
Actin filament-binding protein frabin
Werner helicase-interacting protein 1
B-cell lymphoma 6 protein
Cbp/p300-interacting transactivator 1
Complement component C1q receptor
CST complex subunit CTC1
Dihydropyrimidine dehydrogenase
Glutathione S-transferase omega-2
GMP reductase 2
Interferon-induced, double-stranded RNA-activated protein kinase
L-xylulose reductase
Macrophage colony-stimulating factor 1 receptor
NADH-ubiquinone oxidoreductase 75 kDa subunit, mitochondrial
Nuclear receptor coactivator 3
Period circadian protein homolog 3
Protein lin-54 homolog
Differentiation-related gene 1 protein
Solute carrier organic anion transporter family member 1B1
Double-stranded RNA-binding protein Staufen homolog 1
Sterol 26-hydroxylase, mitochondrial
Structural maintenance of chromosomes protein 4
Syntaxin-5 (isoform 3)
Elongin-C
WD repeat-containing protein 5

Chapter 5 – Study of HNO Reactivity with Tryptophan

5.1 Introduction

HNO (nitroxyl) is the protonated, one-electron reduced form of NO, with its own important biological and pharmacological properties.[1-3] It has received significant attention due to its positive inotropic/lusitropic effects in normal and failing hearts, making it a potential heart failure therapeutic.[4, 5] Moreover, we and others have shown that HNO targets several proteins involved in Ca^{2+} cycling.[6-9] Recent reviews also highlight the possible benefits of HNO in conditions such as vascular dysfunction, cancer, and alcoholism.[2, 3] Thiols constitute one of the major biological targets of HNO.[3, 10, 11] Although HNO and NO are redox siblings, the thiol reactivity of HNO differs significantly from that of NO and normally results in the formation of a disulfide or a sulfinamide depending on the concentration of thiol (Scheme 5-1).[10, 11] Additionally, recent reports point to the nitrosative role of HNO in generating *N*-nitrosoindole species (Scheme 5-2).[12, 13] Although HNO-derived *N*-nitrosotryptophan (TrpNO) formation might be important in HNO pharmacology, information about this reactivity is scarce.

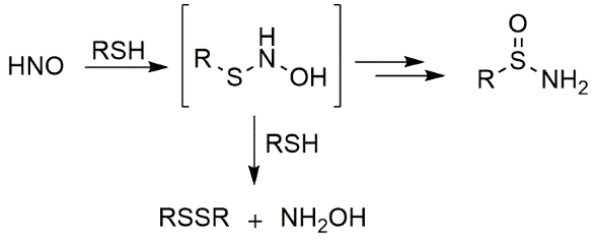

Scheme 5-1. Reaction of HNO with thiols

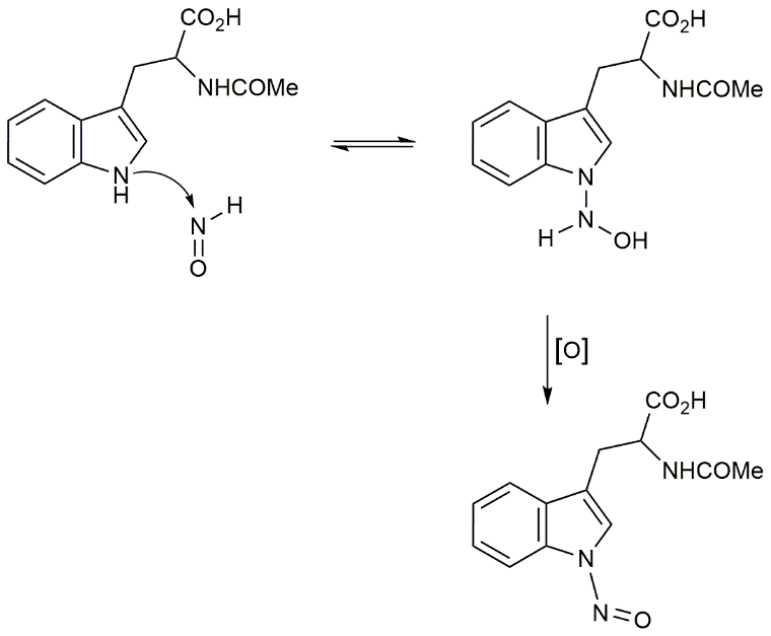

Scheme 5-2. Reaction of HNO with tryptophan[13]

5.2 Results and Discussion

To gain more insight into HNO reactivity, we have investigated TrpNO formation in the presence of a nearby cysteine residue. For this purpose, we used the synthetic peptide AGSCWA, which involves the active site sequence of the cysteine protease, papain, as well as several of its variants (CGSAWA, ACSAWA, AGCAWA, AGSAWC, GSAWCA, and AGSAWA). The small molecule *N*-acetyl-L-tryptophan was also employed for comparison.

As seen in Figure 5-1, treatment of the non-cysteine-containing peptide, AGSAWA, with different HNO-donors (Angeli's salt (AS) or *N*-hydroxy-2-(methylsulfonyl)benzenesulfonamide (2-MSPA)) at physiological pH and temperature results in the formation of the corresponding TrpNO-containing peptides (*m/z* 591) (Figure 5-1a-c). Due to the reported instability of TrpNO species to mass spectrometry

conditions,[14] electrospray ionization mass spectrometry (ESI-MS) data could be obtained only at relatively low temperatures (110 ºC). Upon treatment of the sample with the HNO-donor byproducts (nitrite or 2-(methylsulfonyl)benzenesulfinic acid (2-MSSA)) no TrpNO species are detected. Also, the use of a ^{15}N-labeled HNO-donor, ^{15}N-2-MSPA, provides the corresponding Trp^{15}NO-containing peptide (m/z 592) (Figure 5-1d). Similarly, the characteristic TrpNO peak was observed by UV-visible spectroscopy at 335 nm upon incubation of *N*-acetyl-L-tryptophan with the HNO donor, 2-bromo-*N*-hydroxybenzenesulfonamide (2-BrPA)[15] under the same conditions (data not shown). These results are consistent with previous reports suggesting the formation of HNO-derived TrpNO,[12, 13] and demonstrate that this modification is not specific to AS, but also takes place with other HNO-donors.

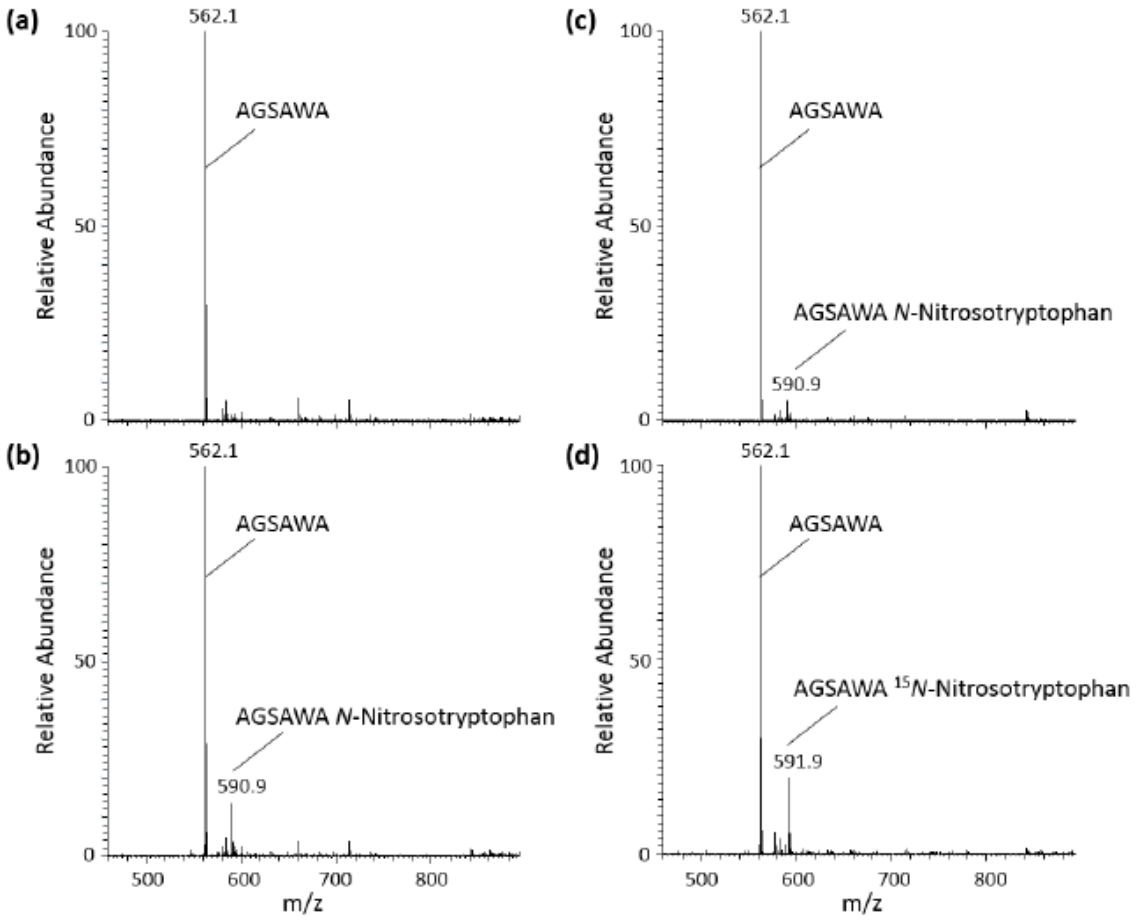

Figure 5-1. Selected region of ESI-MS spectra showing AGSAWA (0.3 mM) (a) untreated or treated with (b) 1 mM AS, (c) 1 mM 2-MSPA, and (d) 1 mM ^{15}N-2-MSPA in 10 mM phosphate buffer with 50 μM DTPA (pH 7.4) at 37 ^{o}C for 30 min.

To assess the feasibility of an HNO-derived tryptophan modification in the vicinity of a free thiol, we treated the peptides containing both a tryptophan and a cysteine residue with different ratios of HNO-donor in 10 mM phosphate buffer with 50 μM metal chelator at pH 7.4 (Figure 5-2). The amount of thiol in the unmodified peptide samples was found to be similar based on a standard 5,5'-dithiobis(2-nitrobenzoic acid) (DTNB) assay (data not shown).[16] Following a 30 min-incubation with AS at physiological pH and temperature, the presence of TrpNO was analyzed by UV-visible spectroscopy (ε_{335} = 6100 $M^{-1}cm^{-1}$).[17]

TrpNO is observed in all peptides upon treatment of 10-fold excess or equimolar amount of HNO-donor. As expected, the percent yield of TrpNO is significantly higher in the presence of excess HNO-donor (ca. 24% vs ca. 3%) (Figure 5-2 and Supporting Information). Side-by-side control experiments conducted with the AS byproduct, nitrite, did not produce any TrpNO peaks in either case (data not shown). Comparisons with *N*-acetyl-L-tryptophan and AGSAWA indicate that although similar TrpNO yields are obtained for the samples in the presence of excess AS, the TrpNO yields are lower in cysteine-containing peptides upon treatment with an equimolar amount of AS (Figure 5-2). These results suggest that the reaction of HNO with tryptophan is approximately 1-2 orders of magnitude slower than the corresponding reaction with cysteine. It should also be noted that no significant TrpNO modification was observed under anaerobic conditions, consistent with previous reports (data not shown).[13]

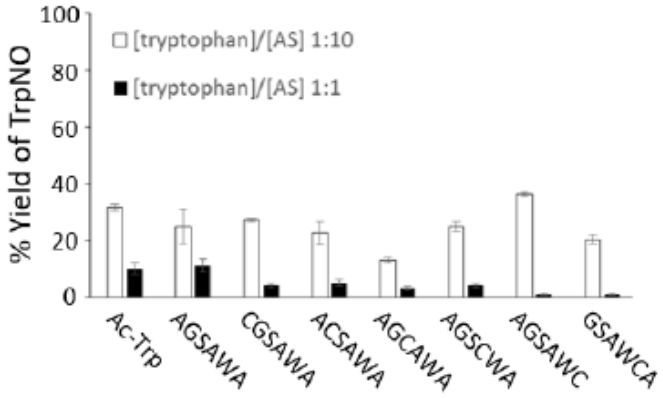

Figure 5-2. Percent yield of *N*-nitrosotryptophan (TrpNO) observed upon incubation of *N*-acetyl-L-tryptophan (Ac-Trp) or synthetic peptides with 10-fold excess ((□), [tryptophan]=0.1 mM, [AS]=1 mM) or equimolar ((■), [tryptophan]=0.3 mM, [AS]=0.3 mM) amounts of HNO-donor in 10 mM phosphate buffer with 50 μM DTPA (pH 7.4) at 37 ºC for 30 min. The percent yield of TrpNO was determined by UV-visible spectroscopy with respect to the amount of tryptophan in the control samples (SEM ± 6%, n≥2).

Since HNO is known to be very thiophilic (Scheme 5-1), the extent of HNO-derived cysteine modifications in the above samples was determined by a DTNB assay. As seen in Figure 5-3, treatment of the cysteine and tryptophan-containing peptides with equimolar amounts of AS results in the complete depletion of thiols, indicating that all cysteine residues are modified to the corresponding sulfinamide or disulfide species. Consistent with these results, no free thiol is detected following incubation of the peptides with excess HNO-donor (data not shown). Importantly, comparable quantities of free thiol are observed in the untreated and nitrite-treated samples, suggesting that the depletion in thiol is due to HNO treatment (Figure 5-3). Overall, these results reveal that cysteine is more reactive towards HNO than tryptophan.

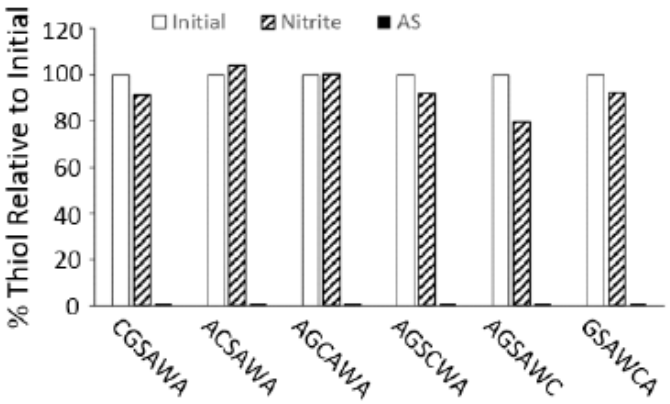

Figure 5-3. Standard DTNB analyses of peptides (0.3 mM) initially (□), or following treatment with nitrite ((▨), 0.3 mM) and AS ((■), 0.3 mM) in 10 mM phosphate buffer with 50 μM DTPA (pH 7.4) at 37 ^{o}C for 30 min. The amounts of free thiol were normalized with respect to that detected in the initial peptide samples.

Since cysteines were found to be completely modified upon HNO treatment, all the TrpNO-containing peptides are also expected to carry an HNO-derived cysteine modification. To gain more insight about the products formed, we first analyzed the

peptide samples with our ^{15}N-edited nuclear magnetic resonance (NMR) method for sulfinamide detection.[18] In this method, application of an isotope filter for ^{15}N allows the selective detection of protons attached to the ^{15}N nuclei and provides simplified NMR spectra.[18, 19] Consistent with the expected reactivity of HNO, the corresponding sulfinamides are observed for all cysteine-containing peptides upon treatment with 10-fold excess H^{15}NO-donor (Supporting Information),[10, 11, 20] except for AGSAWC, which has a C-terminal cysteine and possesses an atypical reactivity, which we have recently examined in detail.[21] With the use of an internal standard, ^{15}N-labeled benzamide, the approximate relative yields of sulfinamides were estimated; they follow the order AGSCWA≈GSAWCA>ACSAWA>AGCAWA>CGSAWA.

To investigate the presence of doubly modified-peptides, we examined HNO-treated AGSCWA and CGSAWA by ESI-MS. These results indicate that HNO-induced TrpNO modification is observed on both sulfinamide and disulfide-containing peptides (Figure 5-4 and Supporting Information). Further studies are required to determine if TrpNO formation has a preference for either one of these thiol modifications. Treatment with nitrite did not produce any modifications under these conditions.

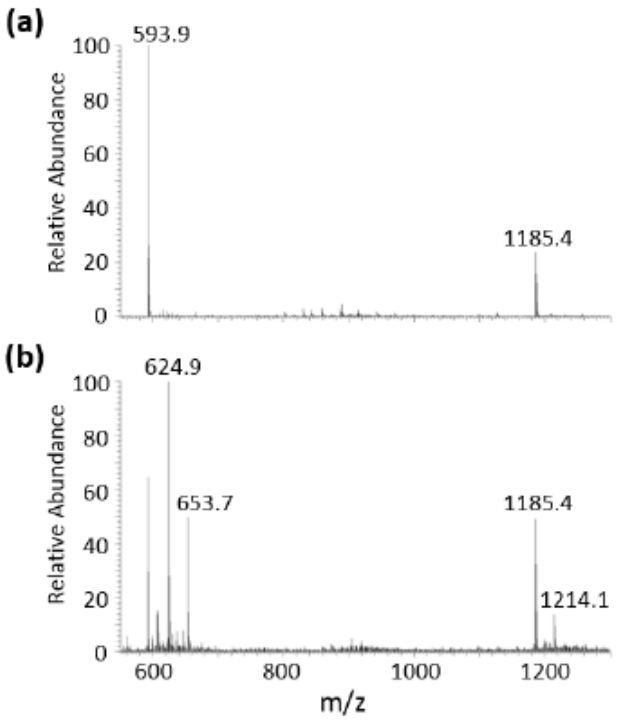

Figure 5-4. Selected region of ESI-MS spectra showing CGSAWA (0.1 mM) treated with (a) nitrite (1 mM) and (b) AS (1 mM) in 10 mM phosphate buffer with 50 μM DTPA (pH 7.4) at 37 °C for 30 min. The peaks were assigned to the unmodified peptide (*m/z* 593.9 ± 0.1), peptide sulfinamide (*m/z* 624.9 ± 0.1), peptide sulfinamide carrying a TrpNO modification (*m/z* 653.7 ± 0.1), peptide disulfide (*m/z* 1185.4 ± 0.1), and peptide disulfide carrying a TrpNO modification (*m/z* 1214.1 ± 0.1).

Since TrpNO is known to undergo denitrosation upon incubation with thiols,[22-24] we have also examined the aerobic denitrosation of TrpNO-containing peptides in the presence of excess L-cysteine (5 mM). The observed rates for TrpNO disappearance under pseudo-first-order conditions were determined by UV-visible spectroscopy. Similar results ($k_{obs} \approx 8.4 \times 10^{-4}$ s^{-1}) were obtained for all TrpNO-containing peptides, indicating the presence of a nearby HNO-derived cysteine modification does not have a significant effect on denitrosation under these conditions (Table 5-1 and Supporting Information). Comparison with k_{obs} for *N*-acetyl-*N*-nitroso-tryptophan (ca. 1.2×10^{-3} s^{-1}), which is in agreement with the reported values for glutathione and other nucleophiles,[23, 25]

demonstrates that the observed rates of denitrosation are slightly slower for peptide samples examined (Table 5-1), potentially due to steric hindrance.[23] Under aerobic conditions, the kinetic behavior of HNO-derived *N*-acetyl-*N*-nitrosotryptophan is the same as the synthetic standard (data not shown), with the observed rates reaching a limiting value in the presence of ca. 1 mM L-cysteine, consistent with the literature.[22, 23, 25, 26]

Table 5-1. Observed rates for denitrosation of HNO-derived *N*-nitrosotryptophan species in the presence of 5mM L-cysteine[a]

N-Nitrosotryptophan species	k_{obs} x 10^4 (s^{-1})[b]	k_{obs} x 10^4 (s^{-1})[c]
Ac-Trp	12 ± 0.1	5.3
AGSAWA	7.9 ± 0.1	4.8
CGSAWA	9.2 ± 0.1	6.7
ACSAWA	9.3 ± 0.2	N/A
AGCAWA	8.0 ± 0.4	N/A
AGSCWA	8.1 ± 0.5	5.0
AGSAWC	8.9 ± 0.6	4.8
GSAWCA	7.7 ± 0.3	4.5

[a]The HNO-derived *N*-nitrosotryptophan samples were treated with excess L-cysteine (5 mM) at physiological pH and temperature. The observed rates are reported as mean ± SEM (n = 2).
[b]Data were collected under aerobic conditions.
[c]Data were collected under argon-saturated conditions. The observed rates are reported as single values.

Consistent with the suggested role of oxygen,[23] the observed rates for denitrosation of all TrpNO-containing peptides were slower (ca. 5.2 x 10^{-4} s^{-1}) upon treatment with 5 mM cysteine under anaerobic conditions (Table 5-1). It should also be noted that, the observed rates for denitrosation in the absence of L-cysteine were increased slightly under

argon-saturated conditions (ca. 3.3 x 10^{-4} s^{-1} vs. ca. 1.7 x 10^{-4} s^{-1}). By monitoring the observed rates of denitrosation of HNO-derived *N*-acetyl-*N*-nitrosotryptophan as a function of L-cysteine concentration (0-10 mM), the second-order rate constant for the reaction of *N*-acetyl-*N*-nitrosotryptophan with L-cysteine (k_{cys}) can be estimated from the pseudo-first-order equation $k_{obs} = k_o + k_{cys}$[cysteine], where k_o is the rate of *N*-acetyl-*N*-nitrosotryptophan decay in the absence of L-cysteine. This analysis (Figure 5-5) gives k_{cys}=5.8 x 10^{-2} M^{-1} s^{-1} under argon-saturated conditions.

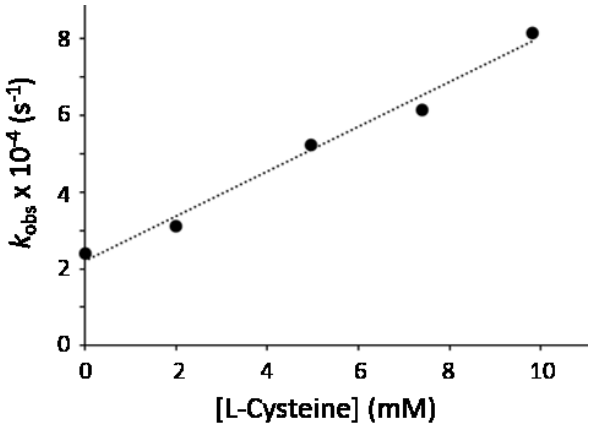

Figure 5-5. Observed rates of denitrosation of HNO-derived *N*-acetyl-*N*-nitrosotryptophan as a function of L-cysteine concentration in 10 mM phosphate buffer with 50 μM DTPA (pH 7.4) at 37 ºC. The values represent the mean of two independent experiments.

5.3 Conclusions

In summary, the observation of TrpNO formation with different HNO-donors confirms that this modification of tryptophan is due to HNO reactivity. We have examined HNO reactivity with tryptophan in peptides in the presence or absence of a nearby cysteine residue. Our results confirm the highly reactive nature of cysteine towards HNO compared

with that of tryptophan. Consequently, in the presence of cysteine, excess HNO is required for significant amounts of TrpNO formation.

5.4 Experimental Methods

Reagents. *N*-acetyltryptophan was of the highest purity available and purchased from Advanced Chemtech. L-cysteine and 5,5'-dithiobis(2-nitrobenzoic acid) (DTNB) were of the highest purity available and purchased from Sigma (St. Louis, MO). HPLC grade acetonitrile (ACN) was purchased from Thermo Fisher Scientific (Rockford, IL). Dimethyl sulfoxide-d_6 (DMSO-d_6) and ^{15}N-labeled hydroxylamine hydrochloride were purchased from Cambridge Isotope Laboratories (Andover, MA). The syntheses of HNO donors, Angeli's salt ($Na_2N_2O_3$, AS),[27] ^{15}N-labeled Angeli's salt (^{15}N-AS),[28] and 2-bromo-*N*-hydroxybenzenesulfonamide (2-BrPA),[15] were carried out as previously described. The HNO donor, *N*-hydroxy-2-(methylsulfonyl)benzenesulfonamide (2-MSPA), the ^{15}N-labeled HNO donor, *^{15}N*-hydroxy-2-(methylsulfonyl)benzenesulfonamide (^{15}N-2-MSPA), and the donor byproduct, 2-(methylsulfonyl)benzenesulfinic acid (2-MSSA), were generous gifts from Cardioxyl Pharmaceuticals. As a standard, *N*-acetyl-*N*-nitrosotryptophan was independently synthesized and characterized following a literature procedure.[22] Milli Q water was used for all purifications and experiments.

Peptide Synthesis and Purification. Synthetic peptides AGSAWA, CGSAWC, ACSAWA, AGCAWA, AGSCWA, AGSAWC and GSAWCA were synthesized on a Symphony Quartet peptide synthesizer (Protein Technologies Inc., Tucson, AZ) following Fmoc solid-phase peptide synthesis methods.[29] The crude product was dissolved in 0.1% trifluoroacetic acid (TFA) and purified by HPLC (Waters HPLC equipped with Delta 600 pump system and dual wavelength absorbance detector) on an Apollo C_{18} reverse-phase

column using a linear gradient of 5-75% ACN with 0.1% TFA over 50 min at room temperature. Peptide fractions were identified by electrospray ionization mass spectrometry (ESI-MS). Pure fractions were pooled and lyophilized, and the purified product was quantified based on the absorbance at 280 nm (ε_{280}= 5500 M^{-1} cm^{-1}).[30] In all cases, peptides were stored at -80 °C in lyophilized form until use.

Incubation of Indoles with HNO. *N*-acetyl-tryptophan and tryptophan-containing peptides were dissolved in 10 mM sodium phosphate buffer with 50 μM of the metal chelator, diethylenetriamine pentaacetic acid (DTPA), at pH 7.4 to have a final concentration of 0.1 or 0.3 mM (as indicated) and used immediately. Stock solutions of AS or ^{15}N-AS were prepared in 0.01 M NaOH, kept on ice, and used within 15 min of preparation. Stock solutions of 2-MSPA or ^{15}N-2-MSPA were prepared in ACN and used within 15 min of preparation. Stock solutions of the donor byproducts, NO_2^- and 2-MSSA were dissolved in 0.01 M NaOH and ACN/H_2O (1:1, v/v), respectively. *N*-acetyl-tryptophan or tryptophan-containing peptides were incubated with 0.3 or 1 mM AS, ^{15}N-AS, 2-MSPA, or ^{15}N-2-MSPA (as indicated) at 37 °C for 30 min in a block heater. In all cases, the final volume of ACN did not exceed 1% of the total volume. As controls, incubations were also carried out with donor byproducts NO_2^- and 2-MSSA under the same conditions. The samples were then analyzed based on the absorbance at 335 (ε_{335} = 6100 M^{-1} cm^{-1})[17] or prepared for ESI-MS analysis. For immediate ESI-MS analysis, the peptides were purified and desalted with C_{18} PepClean spin columns, and then diluted into 70% ACN with 0.1% TFA as described previously.[20]

In some cases, the samples were purged with argon for 30 min prior to incubation with HNO-donors. A 0.1 M stock solution of AS was purged with argon for 5 min. The

argon-purged AS solution was introduced via an air-tight syringe to have a final concentration of 1 mM and the samples were incubated at 37 ºC for 30 min under continuous argon purging. Following incubation, the samples were opened to air and analyzed by UV-visible spectroscopy. Also, control samples were prepared with NO_2^- under the same conditions.

DTNB Assay for Quantification of Free Thiol. Tryptophan-containing peptides were dissolved in 10 mM sodium phosphate buffer with 50 μM DTPA at pH 7.4 to have a final concentration of 0.3 mM and incubated with 0.3 mM AS as described above. Aliquots were taken at various time intervals and the free sulfhydryl content was immediately determined by DTNB titration.[16] The results were corrected for the amount of free thiol in the initial sample and normalized with respect to the initial. As a control, the samples were also incubated with NO_2^- under the same conditions and analyzed.

Incubation of *N*-Nitrosotryptophan-Containing Samples with L-Cysteine. *N*-acetyl-tryptophan and tryptophan-containing peptides (0.1 mM) were incubated with AS (1 mM) to form the corresponding TrpNO-containing species as described above. The samples were then incubated in the presence or absence of L-cysteine (5 mM) in pH 7.4 phosphate buffer at 37 ºC and the reaction was followed by UV-visible spectroscopy at 335 nm in kinetics mode for 1 h. In all cases, spectra were recorded at 180 s intervals.

In some cases, following the generation of TrpNO-containing species with HNO, the samples were purged with argon for 5 min, and the spectrophotometric analyses were carried out under argon upon addition of excess L-cysteine (as indicated). To determine the second-order rate constant, HNO-derived *N*-acetyl-*N*-nitrosotryptophan was incubated with varying concentrations (0-10 mM) of L-cysteine under argon-saturated conditions. In

all cases, the kinetic traces fit to a single-exponential decay. The second-order rate constant was determined by plotting the observed rates against the concentration of excess L-cysteine.

Mass Spectrometric Analyses. ESI-MS analysis was carried out on a Thermo Finnigan LCQ Deca Ion Trap Mass Spectrometer fitted with an electrospray ionization source, operating in the positive ion mode with an accuracy of ca. 0.1 m/z. In all experiments, samples were introduced to the instrument at a rate of 10 μL/min using a syringe pump via a silica capillary line. The heated capillary temperature was 110 °C and the spray voltage was 5 kV.

NMR Analyses. All ^{1}H-NMR and ^{15}N-edited ^{1}H 1D-NMR analyses were carried out on a Bruker Avance 400 MHz FT-NMR spectrometer. ^{1}H NMR and ^{15}N-edited ^{1}H 1D-NMR analyses were carried out in DMSO-d_6 at 303 K. ^{15}N-edited ^{1}H 1D-NMR spectra were acquired using the HSQC pulse sequence for selection. Chemical shifts are reported in parts per million (ppm) relative to residual DMSO (2.49 ppm for ^{1}H).

5.5 References

1. Tocchetti, C. G., Stanley, B. A., Murray, C. I., Sivakumaran, V., Donzelli, S., Mancardi, D., Pagliaro, P., Gao, W. D., van Eyk, J., Kass, D. A., Wink, D. A., and Paolocci, N. (2011) Playing with cardiac "redox switches": The "HNO way" to modulate cardiac function, *Antioxid. Redox Signaling 14*, 1687-1698.
2. Kemp-Harper, B. K. (2011) Nitroxyl (HNO): A novel redox signaling molecule, *Antioxid. Redox Signaling 14*, 1609-1613.
3. Flores-Santana, W., Salmon, D. J., Donzelli, S., Switzer, C. H., Basudhar, D., Ridnour, L., Cheng, R., Glynn, S. A., Paolocci, N., Fukuto, J. M., Miranda, K. M.,

and Wink, D. A. (2011) The specificity of nitroxyl chemistry is unique among nitrogen oxides in biological systems, *Antioxid. Redox Signaling 14*, 1659-1674.

4. Paolocci, N., Katori, T., Champion, H. C., St John, M. E., Miranda, K. M., Fukuto, J. M., Wink, D. A., and Kass, D. A. (2003) Positive inotropic and lusitropic effects of HNO/NO^- in failing hearts: Independence from beta-adrenergic signaling, *Proc. Natl. Acad. Sci. U. S. A. 100*, 5537-5542.

5. Paolocci, N., Saavedra, W. F., Miranda, K. M., Martignani, C., Isoda, T., Hare, J. M., Espey, M. G., Fukuto, J. M., Feelisch, M., Wink, D. A., and Kass, D. A. (2001) Nitroxyl anion exerts redox-sensitive positive cardiac inotropy in vivo by calcitonin gene-related peptide signaling, *Proc. Natl. Acad. Sci. U. S. A. 98*, 10463-10468.

6. Froehlich, J. P., Mahaney, J. E., Keceli, G., Pavlos, C. M., Goldstein, R., Redwood, A. J., Sumbilla, C., Lee, D. I., Tocchetti, C. G., Kass, D. A., Paolocci, N., and Toscano, J. P. (2008) Phospholamban thiols play a central role in activation of the cardiac muscle sarcoplasmic reticulum calcium pump by nitroxyl, *Biochemistry 47*, 13150-13152.

7. Sivakumaran, V., Stanley, B. A., Tocchetti, C. G., Ballin, J. D., Caceres, V., Zhou, L., Keceli, G., Rainer, P. P., Lee, D. I., Huke, S., Ziolo, M. T., Kranias, E. G., Toscano, J. P., Wilson, G. M., O'Rourke, B., Kass, D. A., Mahaney, J. E., and Paolocci, N. (2013) HNO enhances SERCA2a activity and cardiomyocyte function by promoting redox-dependent phospholamban oligomerization, *Antioxid. Redox Signaling 19*, 1185-1197.

8. Tocchetti, C. G., Wang, W., Froehlich, J. P., Huke, S., Aon, M. A., Wilson, G. M., Di Benedetto, G., O'Rourke, B., Gao, W. D., Wink, D. A., Toscano, J. P., Zaccolo,

M., Bers, D. M., Valdivia, H. H., Cheng, H., Kass, D. A., and Paolocci, N. (2007) Nitroxyl improves cellular heart function by directly enhancing cardiac sarcoplasmic reticulum Ca^{2+} cycling, *Circ. Res. 100*, 96-104.

9. Gao, W. D., Murray, C. I., Tian, Y., Zhong, X., DuMond, J. F., Shen, X., Stanley, B. A., Foster, D. B., Wink, D. A., King, S. B., Van Eyk, J. E., and Paolocci, N. (2012) Nitroxyl-mediated disulfide bond formation between cardiac myofilament cysteines enhances contractile function, *Circ. Res. 111*, 1002-1011.

10. Wong, P. S. Y., Hyun, J., Fukuto, J. M., Shirota, F. N., DeMaster, E. G., Shoeman, D. W., and Nagasawa, H. T. (1998) Reaction between *S*-nitrosothiols and thiols: Generation of nitroxyl (HNO) and subsequent chemistry, *Biochemistry 37*, 5362-5371.

11. Doyle, M. P., Mahapatro, S. N., Broene, R. D., and Guy, J. K. (1988) Oxidation and reduction of hemoproteins by trioxodinitrate(II). The role of nitrosyl hydride and nitrite, *J. Am. Chem. Soc. 110*, 593-599.

12. Suzuki, T., Mower, H. F., Friesen, M. D., Gilibert, I., Sawa, T., and Ohshima, H. (2004) Nitration and nitrosation of *N*-acetyl-L-tryptophan and tryptophan residues in proteins by various reactive nitrogen species, *Free Radical Biol. Med. 37*, 671-681.

13. Peyrot, F., Fernandez, B. O., Bryan, N. S., Feelisch, M., and Ducrocq, C. (2006) *N*-Nitroso products from the reduction of indoles with Angeli's salt, *Chem. Res. Toxicol. 19*, 58-67.

14. Hao, G., and Gross, S. S. (2006) Electrospray tandem mass spectrometry analysis of S- and N-nitrosopeptides: facile loss of NO and radical-induced fragmentation, *J. Am. Soc. Mass Spectrom. 17*, 1725-1730.

15. Toscano, J. P., Brookfield, F. A., Cohen, A. D., Courtney, S. M., Frost, L. M., and Kalish, V. J. (2011) *N*-hydroxylsulfonamide derivatives as new physiologically useful nitroxyl donors, (Johns Hopkins University, USA). U.S. Patent 8,030,356.

16. Ellman, G. L. (1959) Tissue sulfhydryl groups, *Arch. Biochem. Biophys. 82*, 70-77.

17. Bonnett, R., and Holleyhead, R. (1974) Reaction of tryptophan derivatives with nitrite, *J. Chem. Soc., Perkin Trans. 1*, 962-964.

18. Keceli, G., Moore, C. D., Labonte, J. W., and Toscano, J. P. (2013) NMR detection and study of hydrolysis of HNO-derived sulfinamides, *Biochemistry 52*, 7387-7396.

19. Breeze, A. L. (2000) Isotope-filtered NMR methods for the study of biomolecular structure and interactions, *Prog. NMR Spectrosc. 36*, 323-372.

20. Keceli, G., and Toscano, J. P. (2012) Reactivity of nitroxyl-derived sulfinamides, *Biochemistry 51*, 4206-4216.

21. Keceli, G., and Toscano, J. P. Reactivity of C-terminal cysteines with HNO, submitted to *Biochemistry*.

22. Sonnenschein, K., de Groot, H., and Kirsch, M. (2004) Formation of *S*-nitrosothiols from regiospecific reaction of thiols with N-nitrosotryptophan derivatives, *J. Biol. Chem. 279*, 45433-45440.

23. Jourd'heuil, F. L., Lowery, A. M., Melton, E. M., Mnaimneh, S., Bryan, N. S., Fernandez, B. O., Park, J.-H., Ha, C.-E., Bhagavan, N. V., Feelisch, M., and

Jourd'heuil, D. (2010) Redox-sensitivity and site-specificity of S- and N-denitrosation in proteins, *PLoS ONE 5*, e14400.

24. Kirsch, M., and Korth, H. G. (2007) Generation, basic chemistry, and detection of N-nitrosotryptophan derivatives, *Org. Biomol. Chem. 5*, 3889-3894.

25. Meyer, T. A., and Williams, D. L. H. (1982) Denitrosation of *N*-acetyl-N^1-nitrosotryptophan in acid solution, *J. Chem. Soc. Perkin Trans. 2*, 1383-1387.

26. De Biase, P. M., Turjanski, A. G., Estrin, D. A., and Doctorevich, F. (2005) Mechanisms of NO release by N^1-nitrosomelatonin: Nucleophilic attack versus reducing pathways, *J. Org. Chem. 70*, 5790-5798.

27. Hughes, M. N., and Cammack, R. (1999) Synthesis, chemistry, and applications of nitroxyl ion releasers sodium trioxodinitrate or Angeli's salt and Piloty's acid, *Methods Enzymol. 301*, 279-287.

28. Bonner, F. T., and Ravid, B. (1975) Thermal decomposition of oxyhyponitrite (sodium trioxodinitrate(II)) in aqueous solution, *Inorg. Chem. 14*, 558-563.

29. Chan, W. C., White, P. D., and Editors (2000) *Fmoc Solid Phase Peptide Synthesis: A Practical Approach*.

30. Edelhoch, H. (1967) Spectroscopic determination of tryptophan and tyrosine in proteins, *Biochemistry 6*, 1948-1954.

5.6 Supporting Information

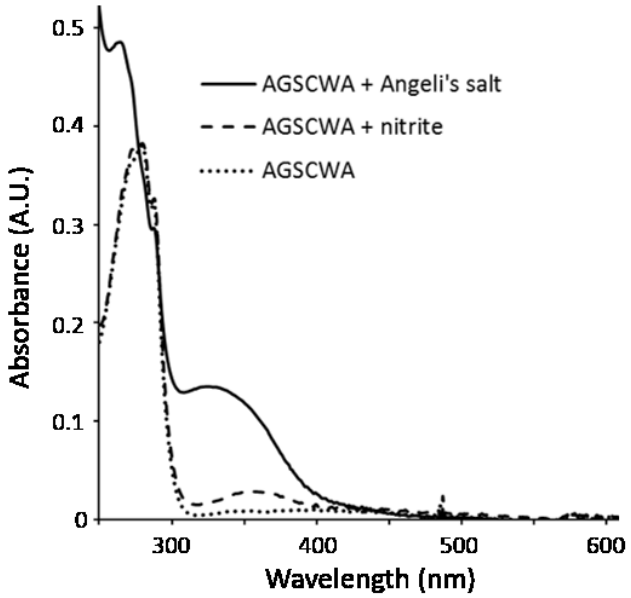

Figure 5-6. Selected region of UV-visible spectra showing AGSCWA (0.1 mM) treated with AS (1 mM) (-) and nitrite (1 mM) (--) in 10 mM phosphate buffer with 50 μM DTPA (pH 7.4) at 37 ^{o}C for 30 min. The spectra were collected in buffer at 25 ^{o}C (λ_{max} = 335 nm).

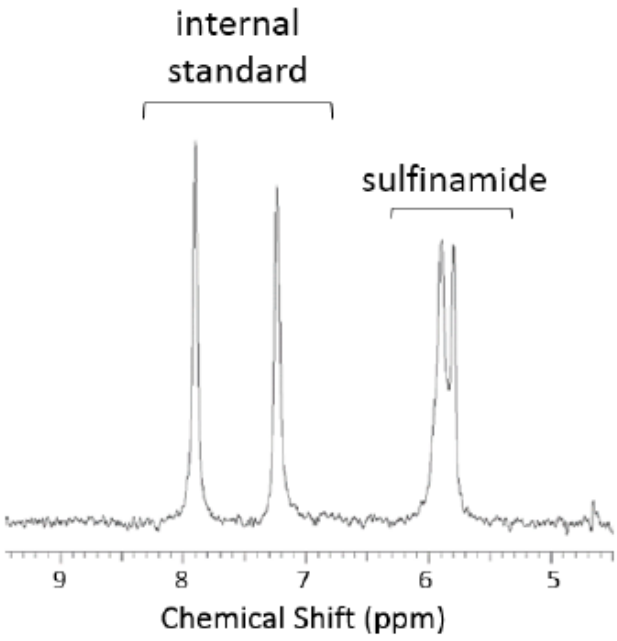

Figure 5-7. Selected region of ^{15}N-edited NMR spectrum showing AGSCWA (0.1 mM) treated with AS (1 mM) in 10 mM phosphate buffer with 50 μM DTPA (pH 7.4) at 37 ºC for 30 min. ^{15}N-labeled benzamide was added as an internal standard before NMR analysis.

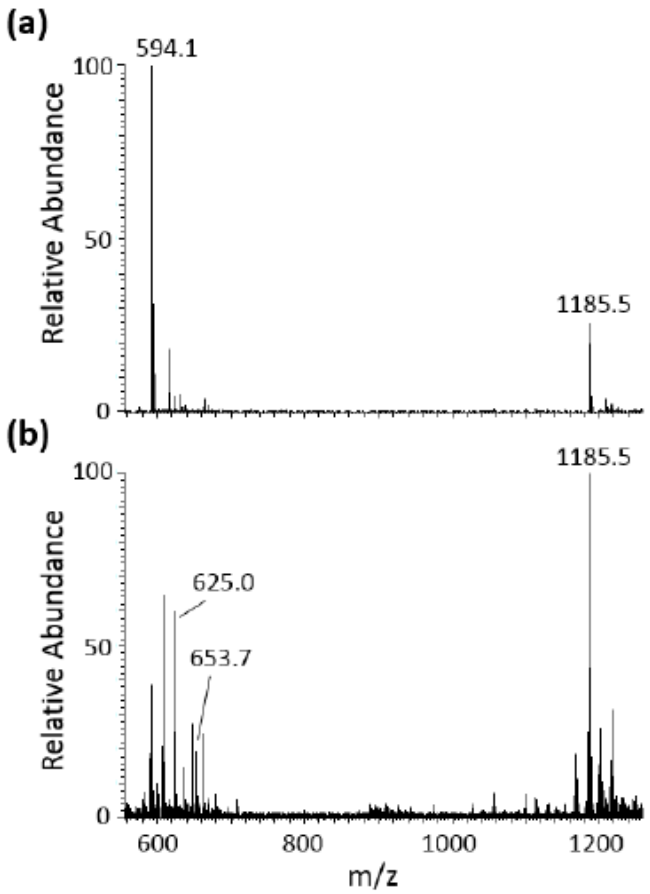

Figure 5-8. Selected region of ESI-MS spectra showing AGSCWA (0.1 mM) treated with (a) nitrite (1 mM) and (b) AS (1 mM) in 10 mM phosphate buffer with 50 μM DTPA (pH 7.4) at 37 ºC for 30 min. The peaks were assigned to the unmodified peptide (*m/z* 594.1 ± 0.1), peptide sulfinamide (*m/z* 625.0 ± 0.1), and peptide disulfide (*m/z* 1185.5 ± 0.1). The peak labeled with asterisk (*) was assigned to the peptide sulfinamide carrying a TrpNO modification (*m/z* 653.7 ± 0.1).

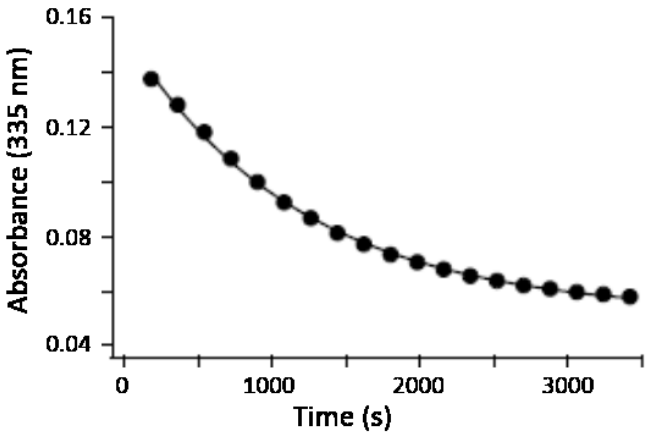

Figure 5-9. Representative kinetic trace at 335 nm showing the denitrosation of HNO-derived AGSCWA *N*-nitrosotryptophan in the presence of excess L-cysteine (5 mM) in 10 mM phosphate buffer with 50 μM DTPA (pH 7.4) at 37 ^{o}C.

Chapter 6 – Effects of HNO on Phospholamban and Its Interaction with Sarco(endo)plasmic Reticulum Ca^{2+}-ATPase

6.1 Introduction

Congestive heart failure is an abnormality, which frequently involves reduced cardiac contractility and slowed muscle relaxation.[1, 2] A common component of treatment of heart failure often involves the use of vasodilators such as NO donors which serve mainly to enhance relaxation.[3] Recently, HNO donors have been shown to augment contractility and accelerate relaxation in both normal and failing hearts.[4-7]

Several studies have suggested that the biological effects and reactivity of HNO are distinct from those of NO.[5, 6, 8, 9] In the case of cardiac function, NO acts via a cGMP signal transduction pathway by means of activating soluble guanylate cyclase, which results in increased cGMP levels.[10] On the other hand, it has been determined that HNO acts independent of both cGMP and cAMP pathways.[6, 11]

Cardiac function is regulated by varying the cytosolic calcium ion concentration in heart muscle cells (Figure 6-1). The trigger for cardiac muscle contraction is a large (ca. 1 μM) cytosolic concentration of Ca^{2+} and the signal for contraction is a roughly 90% drop in the Ca^{2+} concentration. These concentration fluctuations are achieved in part by the release and capture of Ca^{2+} ions by the sarco(endo)plasmic reticulum (SR). In humans, greater than 70% of cytosolic Ca^{2+} is pumped into the SR by SR Ca^{2+}-ATPase (SERCA2a).

The lumenal Ca^{2+} is released back into the cytosol by Ca^{2+}-release channels (Ryanodine Receptors; RyRs).[12]

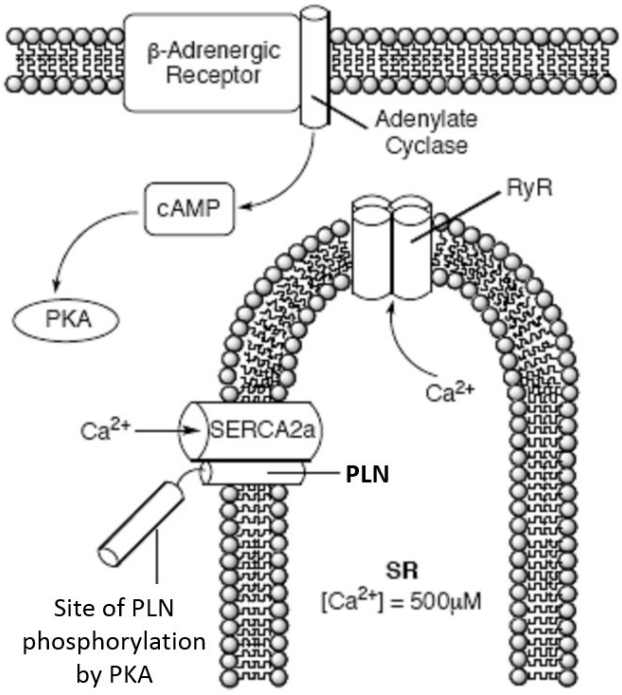

Figure 6-1. Cardiac Signaling Pathways. Adapted from MacLennan, D. H., and Kranias, E. G. (2003) Phospholamban: A crucial regulator of cardiac contractility, *Nature Rev. Mol. Cell Biol. 4*, 566-577.

The SERCA pump is located in the SR within muscle cells and has three major isoforms, SERCA1-3.[13] It plays a key role in smooth, cardiac, and skeletal muscle relaxation.[13] SERCA2a is the predominant isoform found in cardiac muscle.[12] It is a 110 kDa integral membrane protein with three cytoplasmic domains (N, A and P) and one transmembrane domain (M).[14] SERCA2a pumps two Ca^{2+} into the SR per ATP hydrolyzed.[13]

Phospholamban (PLN) is a 52 amino acid transmembrane protein that is located in the SR. PLN is associated with SERCA2a, and depending on its phosphorylation state, regulates the activity of SERCA2a.[12, 15, 16] In the dephosphorylated state, PLN functionally

couples with SERCA2a resulting in the inhibition of SERCA2a activity and the reduction of both cardiac relaxation rates and contractility.[17] This inhibition is relieved by phosphorylation of PLN.[12]

PLN is phosphorylated by protein kinase A (PKA), which is part of the β-adrenergic pathway (Figure 6-1). The signal-transduction is initiated by the release of adrenaline and other β-agonists into the blood.[12] The binding of a β-agonist to the β-adrenergic receptor results in the stimulation of cyclic adenosine monophosphate (cAMP) formation by adenylate cyclase. The increase in the cytosolic levels of cAMP affects the activity of PKA, which carries out the phosphorylation of PLN.[17]

Sequence analysis of PLN has shown that the 6.1 kDa protein is organized in three domains: cytosolic domain Ia (residues 1-20), cytosolic domain Ib (21-30) and domain II (31-52), which traverses the membrane.[18] Domain Ia is a cytosolic helical region containing Ser 16, the site of phosphorylation by PKA.[19] Despite this cytosolic phosphorylation, studies have shown that the inhibition of SERCA2a is due to the interaction of the transmembrane region of PLN and SERCA2a.[20] Thus, it is suggested that the interaction between PLN cytosolic domain Ia and SERCA2a is not inhibitory, but phosphorylation in this domain results in a conformational change that disrupts the inhibitory transmembrane interaction.

In the SR membrane or in sodium dodecyl sulfate (SDS) gels, PLN exists as an equilibrium mixture of a homopentamer and a monomer.[21, 22] Based on site-directed mutagenesis studies, it has been concluded that PLN-PLN and PLN-SERCA2a interactions are on opposite faces of the PLN transmembrane helix and that the PLN homopentamer is stabilized by hydrophobic interactions. Since mutations favoring PLN monomer result in

superinhibition of SERCA2a, it is suggested that the PLN monomer is the inhibitory species.[23]

Previous work by Paolocci et al. has demonstrated that HNO enhances cardiac sarcoplasmic reticulum Ca^{2+} cycling without affecting the overall Ca^{2+} reserve in the system.[11] Based on their Ca^{2+} uptake experiments, the authors conclude that HNO stimulates Ca^{2+} uptake by a mechanism that could involve direct targeting of SERCA2a or the relief of phospholamban inhibition by HNO. Furthermore, they have shown that HNO improves Ca^{2+} release by stimulating RyR2 in isolated rodent myocytes and reconstituted in lipid bilayers.[11]

To gain more insight into the mechanisms underlying the improvement of Ca^{2+} cycling by HNO, we have investigated the effects of HNO on the PLN/SERCA2a system in collaboration with Dr. Nazareno Paolocci (Division of Cardiology, Johns Hopkins Medical Institutions, and Department of Clinical Medicine, University of Perugia), Dr. James E. Mahaney (Department of Biochemistry, Virginia Polytechnic Institute and State University, and Edward Via Virginia College of Osteopathic Medicine), and the late Dr. Jeffrey P. Froehlich (Division of Cardiology, Johns Hopkins Medical Institutions, and Department of Biochemistry and Molecular Biology, University of Maryland School of Medicine).

6.2 Effects of HNO on Phospholamban

Previous work has demonstrated that HNO activates SERCA2a in isolated murine cardiomyocytes.[11] Moreover, this effect was also observed in isolated murine heart SR vesicles, indicating that it is independent of β-adrenergic pathway.[4, 11] Activity studies were conducted with SERCA2a expressed in the presence or absence of PLN in High Five (HF) insect cell microsomes to study SERCA2a stimulation by HNO.

Recent work with expressed Ca^{2+} pump proteins suggests that activation of the cardiac SR Ca^{2+} pump following the relief of PLN inhibition involves changes in the kinetic behavior of the Ca^{2+}-ATPase consistent with SERCA2a oligomerization.[24] These changes include stabilization of the ADP-sensitive phosphoenzyme, E1P, and allosteric activation of dephosphorylation by ATP, resulting in increased turnover of the ADP-insensitive phosphoenzyme, E2P. Expression of SERCA2a without PLN in HF insect cells activates E2P turnover.[24]

Treatment of co-expressed SERCA2a and PLN with 0.25 mM of the HNO donor, Angeli's salt (AS), resulted in acceleration of SERCA2a dephosphorylation. Moreover, this activation of SERCA2a was observed only in the presence of PLN, indicating that HNO-induced effects are PLN-dependent. Similarly, HNO stimulated SERCA2a activity in intact wild-type, but not in PLN knock-out SR vesicles. Consistent with these observations, inotropic action of HNO was significantly diminished in PLN knock-out myocytes and whole hearts. These findings point to the importance of PLN in HNO-induced effects on myocardial contractility and relaxation.

6.2.1 Formation of HNO-Derived PLN Dimer

Based on the known reactivity of HNO, the observed effect of HNO on Ca^{2+} uptake may be due to the modification of PLN thiol residues. PLN has three cysteine residues (36, 41 and 46) all in its transmembrane region.[23] According to the proposed helical wheel model of PLN pentamer, C36 and C41 are in close proximity in adjacent PLN helices (Figure 6-2).[25]

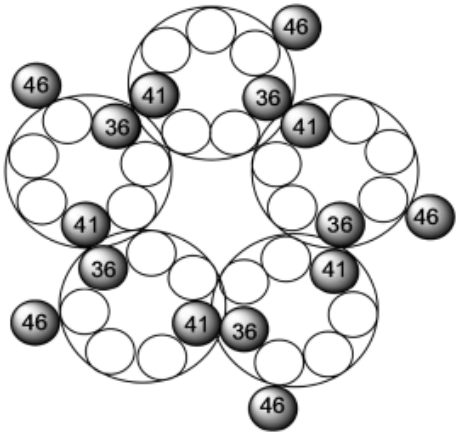

Figure 6-2. Helical wheel model of PLN pentamer. Adapted from Karim, C. B., Stamm, J. D., Jones, L. R., and Thomas, D. D. (1998) Cysteine reactivity and oligomeric structures of phospholamban and its mutants, *Biochemistry 37*, 12074-12081.

Previous research in the Toscano group had produced promising results,[26] which encouraged us to investigate the effects of HNO on PLN further. First of all, the aqueous (pH 7.4) reactions of HNO (generated via AS) with cysteine, serine, tyrosine, and lysine were examined and only cysteine was found to be consumed. Also SDS-PAGE experiments combined with western blotting and immunodetection techniques were utilized to observe the effects of HNO on PLN-PLN interactions.

Treatment of PLN microsomes with 5 mM and above concentrations of AS resulted in the formation of a new band, which is attributed to the PLN dimer. As can be seen in

Figure 6-3, the amount of PLN dimer increases with increasing AS concentration. Moreover, boiling the AS-treated samples to convert the pentamer into monomer resulted in an increase in the amount of observed dimer, which may point to the generation of dimer within the PLN pentamer. Analogous experiments with the 0-10 mM of the NO donor, DEA/NO,[27] did not result in the formation of any dimer.

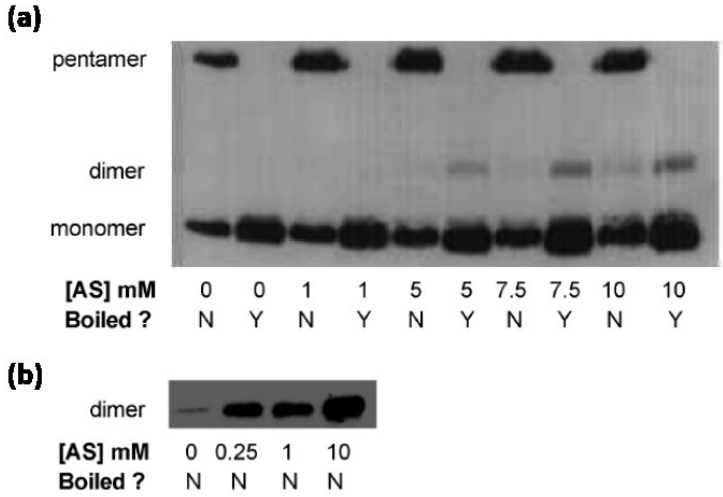

Figure 6-3. (a) Effect of HNO generated from AS on PLN dimer formation in HF insect cell microsomes with a short (30 s) exposure time. (b) Visualization of the PLN dimer with a prolonged (30 min) exposure time.

To understand if PLN dimer formation can be correlated to the HNO-induced activation of SERCA2a in the presence of PLN, we have also employed lower concentrations of AS, which were used in the activity studies. As expected, PLN dimer was detected following 0-1 mM AS treatment under the same conditions (Figure 6-3). Notably, formation of PLN dimers and tetramers were also observed in intact cardiomyocytes and hearts extracts upon treatment with AS.

We have also investigated PLN dimer formation using a different HNO-donor, *N*-hydroxy-2-bromobenzenesulfonamide (2-BrPA). Treatment of PLN microsomes with 0-10 mM AS, resulted in the expected dimer formation (Figure 6-4), suggesting that these findings are not specific to AS and can be observed with other HNO-donors. It should be also noted that, in some cases, a small amount of dimer was present in the PLN samples before any treatment.

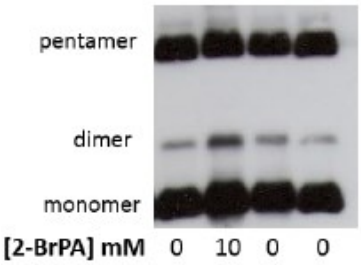

Figure 6-4. Effect of HNO generated from 2-BrPA on PLN dimer formation in HF insect cell microsomes with a short (30 s) exposure time. Lanes (from right) correspond to treatments with 10% DMSO, 2-BrPA, decomposed 2-BrPA, and the sulfinic acid, decomposition byproduct of 2-BrPA, respectively.

As mentioned previously, HNO is known to react with O_2 to produce an uncharacterized HNO-O_2 adduct, which has oxidative properties.[28, 29] To understand if O_2 plays a role in PLN dimer formation, we treated PLN microsomes with AS or 2-BrPA under argon. These results demonstrate that PLN dimer is formed due to HNO reactivity, independent of O_2 (Figure 6-5). Moreover, similar yields of the PLN dimer were obtained upon treatment with AS under air or argon. Comparison of the corresponding yields for 2-BrPA-treated samples have shown that the yields of the PLN dimer were higher in argon-saturated samples (Figure 6-6), presumably due to slight oxidation of 2-BrPA in the

absence of metal chelator, which results in its decomposition via a non-HNO-producing pathway, consequently lowering the yield of HNO.[30]

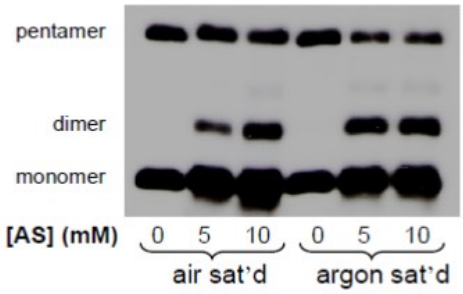

Figure 6-5. Microsomes containing expressed PLN were diluted to 1 mg/ml (in 0.1 M PBS containing 100 μM EDTA) and then purged either with argon or compressed air in septum-sealed vials. Aliquots of AS stock solution were added via syringe to the samples such that the final concentration of AS was 0, 5 or 10 mM. After incubating at 37 ºC for 30 min, the samples were again purged with argon or compressed air to remove any gaseous reactive nitrogen oxide species that may have formed. Loading buffer was then added and the samples were subjected to SDS-PAGE analysis.

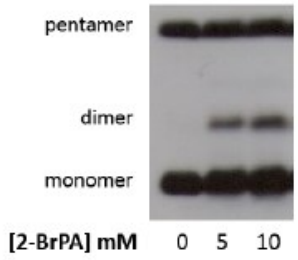

Figure 6-6. Microsomes containing expressed PLN were diluted to 1 mg/ml (in 0.1 M PBS containing 100 μM EDTA) and then purged with argon in septum-sealed vials. Aliquots of 2-BrPA stock solution were added via syringe to the samples such that the final concentration of 2-BrPA was 0, 5 or 10 mM. After incubating at 37 ºC for 30 min, the samples were again purged with argon or compressed air to remove any gaseous reactive nitrogen oxide species that may have formed. Loading buffer was then added and the samples were subjected to SDS-PAGE analysis.

To test the involvement of cysteine residues in the formation of the HNO-derived PLN dimer, we have employed the null-cysteine mutant of PLN (C36,41,46A-PLN). Administration of 0, 1, 5 and 10 mM AS did not result in any dimer formation (Figure 6-7). However, these results are difficult to interpret due to the absence of pentamers in these species. Notably, no SERCA2a stimulation was observed upon treatment of microsomes containing co-expressed SERCA2a and null-cysteine PLN. Moreover, cysteine blocking experiments using N-ethylmaleimide (NEM)[31] has provided further support for the involvement of thiol residues in the HNO-induced PLN dimer formation. When PLN was pre-treated with NEM prior to incubation with AS under argon, no PLN dimer was observed (Figure 6-8). These findings are consistent with previous experiments in the Toscano group conducted under aerobic conditions.[26] Although NEM can scavenge HNO to some extent, significant quenching of HNO is not expected under these conditions (see Chapter 7.1.1). Overall, our results indicate the importance of cysteine residues in HNO-derived modification of PLN.

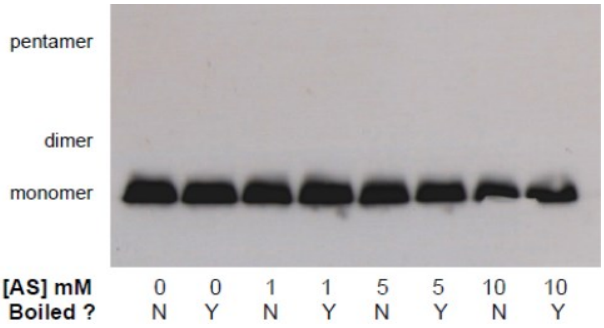

Figure 6-7. Insect cell microsomes containing expressed null-cysteine PLN were diluted to 1 mg/ml (in 0.05 M PBS at pH 7.4) and incubated with varying concentrations of AS for 30 min at 37 ^{o}C. After the addition of loading buffer, the samples in the indicated lanes were boiled for 5 min prior to loading and SDS-PAGE analysis.

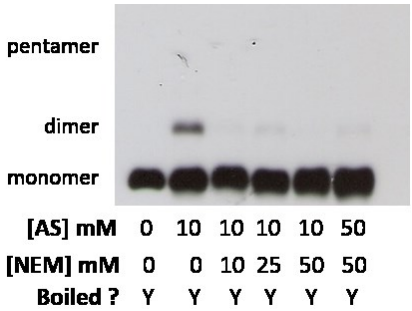

Figure 6-8. Insect cell microsomes containing expressed PLN were diluted to 1 mg/ml (in 0.1 M PBS containing 100 μM EDTA at pH 7.4) and treated with varying concentrations of NEM at room temperature for 1 h. The samples were then purged with argon in septum-sealed vials. Aliquots of AS stock solution were added via syringe to the samples such that the final concentration of AS was 0, 10 or 50 mM. After incubating at 37 ^{o}C for 30 min, the samples were again purged with argon to remove any gaseous reactive nitrogen oxide species that may have formed. Loading buffer was then added and the samples were boiled for 10 min prior to SDS-PAGE analysis.

As mentioned previously, HNO generally reacts with thiols to form a disulfide or a sulfinamide (Scheme 2-1). To gain more insight into the nature of HNO-induced effects on PLN, we have investigated its reversibility. Prior studies in the Toscano group have revealed that the HNO-induced PLN dimer can be completely reduced by tris(2-carboxyethyl)phosphine (TCEP).[26] Moreover, we have shown that the dimer is reduced upon treatment with the thiol-based reducing agent, dithiothreitol (DTT), in a concentration-dependent manner (Figure 6-9). Although less efficient, reduction of the dimer by β-mercaptoethanol (BME) was also observed. Our results indicate that PLN monomer can be recovered following 30 min incubation with reducing agents. Remarkably, these results were reproduced in cardiomyocytes and heart extracts. Similarly, exposure of HNO-treated SERCA2a and PLN-containing microsomes to DTT restored the kinetic parameters to baseline levels.

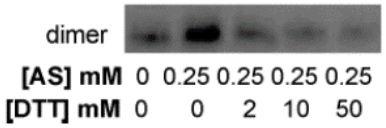

Figure 6-9. Insect cell microsomes containing expressed PLN were diluted to 1 mg/ml (in 0.05 M PBS at pH 7.4) and treated with 0.25 mM AS at 37 ºC for 30 min. The samples were then incubated in the presence or absence of indicated amount of DTT at room temperature for 1 h. Following the incubation, loading buffer was added and the samples were subjected to SDS-PAGE analysis.

Despite the lack of reactivity observed following treatment of *t*-butanesulfinamide with DTT or TCEP at room temperature for 12 h, presumably due to steric reasons, our detailed studies on the reduction of sulfinamides at physiological pH and temperature have revealed that small organic molecule, peptide, and protein sulfinamides can be reduced back to free thiols in the presence of excess thiol (Chapter 2). Similar experiments conducted with a model sulfinamide, 2-phenylethanesulfinamide, have demonstrated the reduction of the corresponding sulfinamide with TCEP. Although the time frames of sulfinamide and disulfide reductions are significantly different (Chapter 2), our studies have also shown that the reactivity of HNO-derived modifications are dependent on protein environment (Chapter 3). Moreover, mutation of key leucine and isoleucine residues in PLN transmembrane domain have been shown to destabilize the PLN pentameric structure, thus reducing the PLN pentamer/monomer ratio and increasing inhibition of SERCA2a.[32-34] Therefore, the presence of a potential sulfinamide modification, which could either disturb the functional coupling between PLN and SERCA2a directly, or by stabilizing PLN dimer, could not be eliminated.

Based on these findings, the potential modifications on PLN are an intermolecular disulfide, an intramolecular disulfide, and/or a sulfinamide (Figure 6-10). Although the cysteine residues in PLN do not seem to be positioned to facilitate an intramolecular

disulfide linkage, recent reports highlight the existence of forbidden disulfide bonds between *i* and *i+5* residues in α-helices of various proteins.[35] Consequently, an HNO-derived intramolecular disulfide modification involving PLN Cys36-Cys41 or Cys41-Cys46 might be a plausible option. Moreover, formation of an intramolecular disulfide bond could distort the conformation of PLN, thus perturbing its functional coupling with SERCA2a and relieving the inhibition.

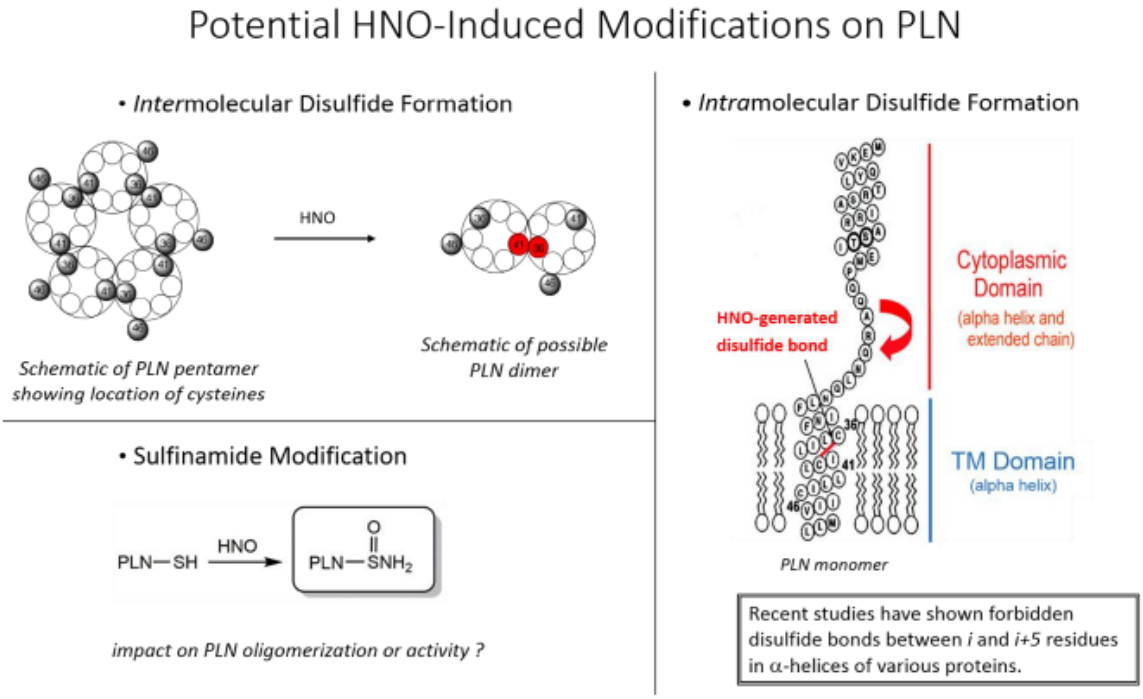

Figure 6-10. Potential HNO-induced modifications on PLN: inter- or intramolecular disulfide, and/or sulfinamide formation.

Our current data seem to indicate that HNO promotes intermolecular disulfide bond formation between PLN monomers, presumably formed within the PLN pentamer. The presence of an intermolecular disulfide linkage would result in the formation of PLN

oligomers at the expense of PLN monomers, decreasing the amount of inhibitory PLN species. Moreover, recent studies have shown that a missense mutation (R9C) in PLN's cytoplasmic region increases the stability of the PLN pentamer, precluding its interaction with SERCA2a.[36]

6.2.2 Synthesis and Reconstitution of wt-PLN and Its Single Cysteine Variants

To obtain high purity PLN samples in large quantities, we synthesized wild-type PLN and its single cysteine variants (C36,41A-PLN, C36,41A-PLN, and C41,46A-PLN) using our department's automated peptide synthesis system following a reported literature procedure,[37, 38] which involves a modified Fmoc-based solid-phase method (Figure 6-11). In this procedure, the major challenges in PLN synthesis (hydrophobicity and length) were overcome by employing coupling reactions extended to 6 h as well as using a pseudoproline dipeptide (Leu7-Thr8) and a polyethylene glycol-polystyrene resin. The synthesis takes approximately 11 days if it proceeds uninterrupted.

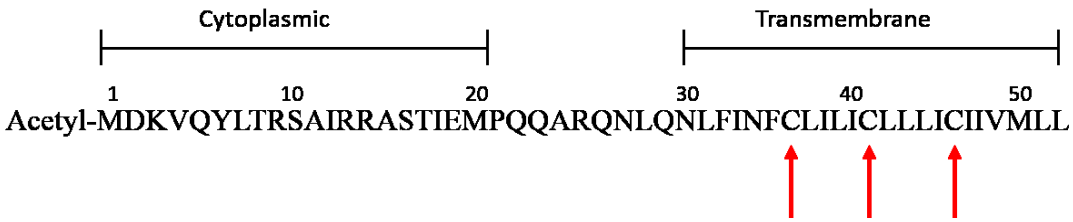

Figure 6-11. Sequence of wild-type PLN. Red arrows indicate the positions of cysteine residues.

The synthesized protein was purified by HPLC, lyophilized, characterized by MALDI-TOF MS (Figure 6-12) and reconstituted into phospholipids (DOPC/DOPE 4:1) according to a published procedure (Figure 6-13).[37, 39] PLN was determined to be α-helical in the non-ionic detergent $C_{12}E_8$, and in phospholipids by circular dichroism spectroscopy (Figure 6-13). The reconstituted PLN was identical to the native PLN on SDS-PAGE, forming both monomer and pentamer (Figure 6-13).

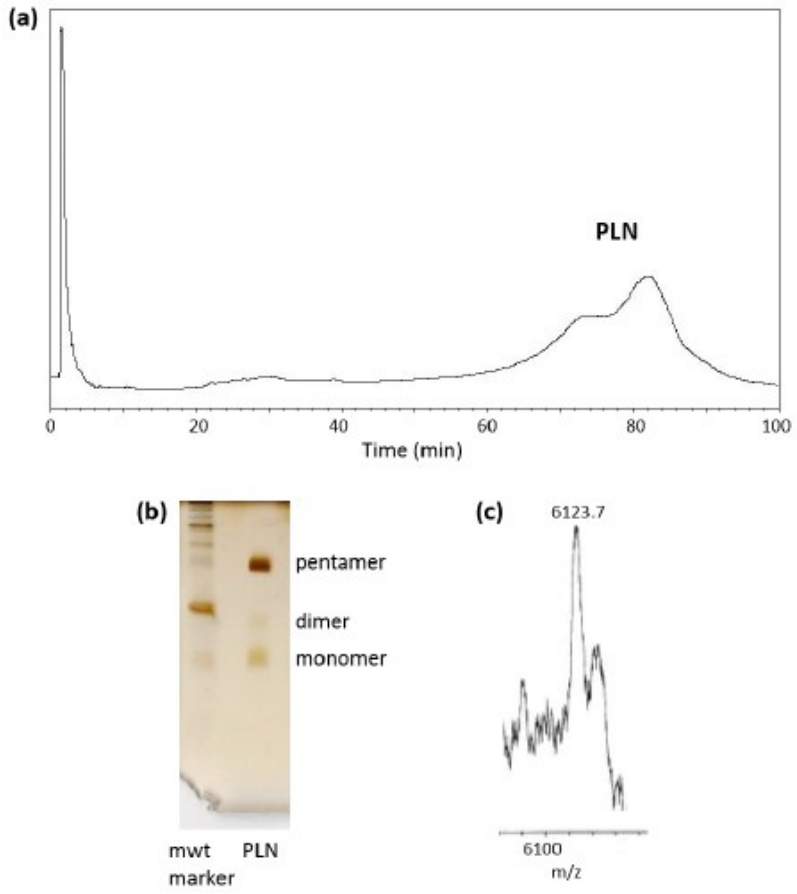

Figure 6-12. (a) HPLC spectrum of synthetic PLN (crude). (b) Silver stained gel showing synthetic PLN. (c) Selected region of MALDI-MS spectrum showing synthetic PLN (*m/z* 6123.7 ± 1).

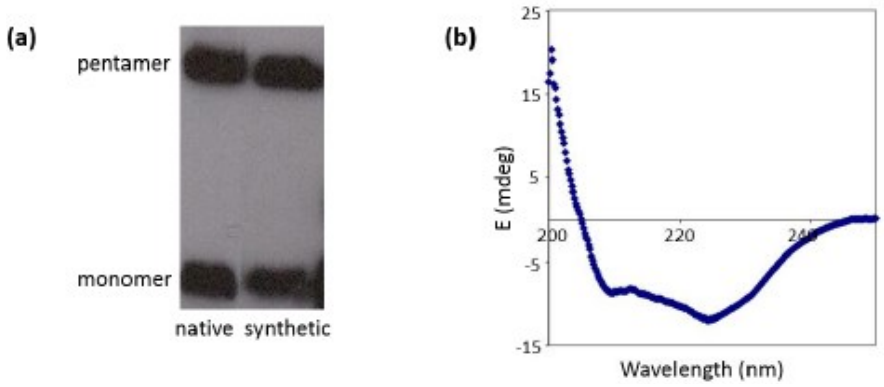

Figure 6-13. (a) Western blot showing the monomer and pentamer bands for PLN reconstituted in phospholipids (DOPC/DOPE 4:1). Native PLN corresponds to PLN expressed in insect cell microsomes. (b) CD spectrum of PLN reconstituted in phospholipids.

6.2.3 Studies to Purify HNO-Treated PLN Monomer and Dimer

We have conducted preliminary studies to purify HNO-treated PLN species for spectroscopic characterization. Previous research in the Toscano group as well as our initial studies were focused on purifying the PLN monomer and dimer from microsomal samples following HNO-treatment. The strategy involved immunoprecipitation of PLN samples with anti-PLN monoclonal antibody (2D12), and isolation of samples by SDS-PAGE followed by electroelution. Although we were able to immunoprecipitate both monomeric and dimeric PLN species, this method was not convenient due to extremely low yields.

To increase the yield of purified PLN, we decided to eliminate immunoprecipitation and employ synthetic PLN as described above. Following separation on SDS-PAGE, the protein was extracted from the gel by electroelution. It should be noted that size and hydrophobicity precluded the passive elution of either intact PLN (6.1 kDa) or the peptide containing its transmembrane region (3 kDa) upon in-gel digestion. Moreover,

electroelution of PLN could only be achieved upon addition of 0.02% SDS to electroelution and soaking buffers.

Since characterization techniques such as mass spectrometry (MS) require the removal of detergents prior to analysis, we explored feasible methods to remove SDS from the PLN sample. Due to the hydrophobicity of PLN, precipitation of the sample by acetone was not feasible. Moreover, washing the lyophilized PLN sample with water or employment of dialysis methods were not sufficient to remove protein-bound SDS as determined by a methylene blue assay.[40] Approximately 10-fold decrease in SDS was achieved by two consecutive applications of a modified chloroform/methanol/water extraction[41], but unfortunately, this was accompanied by ca. 50% loss in PLN.

6.2.4 Preliminary Studies to Investigate PLN by Mass Spectrometry

Mass spectrometry of PLN is extremely challenging due to the very low ion yields stemming from its hydrophobic nature. We have attempted to solve this issue via several different approaches and conditions. Since intact PLN is more soluble and easier to handle compared with its transmembrane region, initially we followed a top-down strategy. Briefly, we employed matrix-assisted laser desorption ionization mass spectrometry (MALDI-MS) either in linear or reflectron modes, and used several matrices and spotting techniques. Moreover, we prepared various concentrations of PLN (0.005-5 mg/ml) in methanol or methanol/chloroform solutions containing trifluoroacetic acid (0.025-1%) or formic acid (1-20%). Best results were obtained with 0.5 mg/ml PLN (in methanol containing 0.025% TFA), α-cyanohydroxycinnamic acid and the dried-droplet method in linear mode. Although we were able to detect pure, intact, full-length PLN by MALDI-

MS, the signal to noise was not sufficient to study modifications (Figure 6-12). It should be also noted that preliminary efforts to analyze PLN with reflectron in-source decay MALDI-MS resulted in random fragmentation of the protein rather than providing any useful sequence information.

Since we obtained promising spectra with the PLN peptide, Gln22-Leu52, we explored digestion of PLN using the serine proteases, Staphylococcus aureus protease V8 (Glu-C) and trypsin. Glu-C selectively cleaves peptide bonds C-terminal to Glu and remains active even in the presence of 20% methanol. Also, it is known to cleave at Asp at a rate approximately 100-300 times slower than at Glu. PLN has only one cleavage site (Glu19) for Glu-C, producing peptides with molecular weights 2284.6 and 3859.8 g/mol. Preliminary studies to digest PLN with various concentrations of Glu-C in the presence or absence of an MS-compatible detergent were not successful, presumably due to PLN aggregation during the long incubation (19 h) in 20 mM ammonium acetate buffer containing 20% methanol. Similar results were obtained with trypsin.

Although there might be other strategies and conditions to be explored, these studies indicate that utilization of mass spectrometry techniques for studying PLN are very challenging and inconvenient due to the extremely hydrophobic nature of this protein. Not surprisingly, to the best of our knowledge, there are no detailed mass spectrometry studies of PLN.

6.3 Effects of HNO on the Interaction of Phospholamban and SERCA2a

As mentioned previously, HNO-induced of SERCA2a activation as well as the enhanced myocardial contractility and relaxation are PLN-dependent. To elucidate the effect of HNO on SERCA2a-PLN interaction, we have employed co-immunoprecipitation and SDS-PAGE experiments.

Initially we treated co-expressed SERCA2a and PLN with HNO, and analyzed the samples by SDS-PAGE and western blotting. Visualization of the bands by an anti-PLN antibody revealed that the HNO-derived PLN dimer can be observed in the presence of SERCA2a. Moreover, no bands corresponding to a SERCA-PLN heterodimer were detected in the presence or absence of HNO treatment, suggesting the lack of a covalent interaction between SERCA2a and PLN under either condition. It should be noted that reported literature demonstrates the detection of this heterodimer by the anti-PLN antibody upon treatment of the proteins with cross-linking agents.[42]

We employed co-immunoprecipitation experiments to determine if HNO physically dissociates PLN from SERCA2a, and consequently removes the PLN inhibition on SERCA2a by decreasing the amount of PLN-bound SERCA2a. As seen in Figure 6-14 this procedure involves precipitation of co-expressed SERCA2a and PLN microsomes with anti-SERCA2a antibody, which pulls down both PLN-bound and unbound SERCA2a. Following SDS-PAGE and western blotting, the samples are visualized with anti-PLN antibody (Figure 6-14). Thus, any PLN band detected by this procedure originates from PLN-bound SERCA2a.

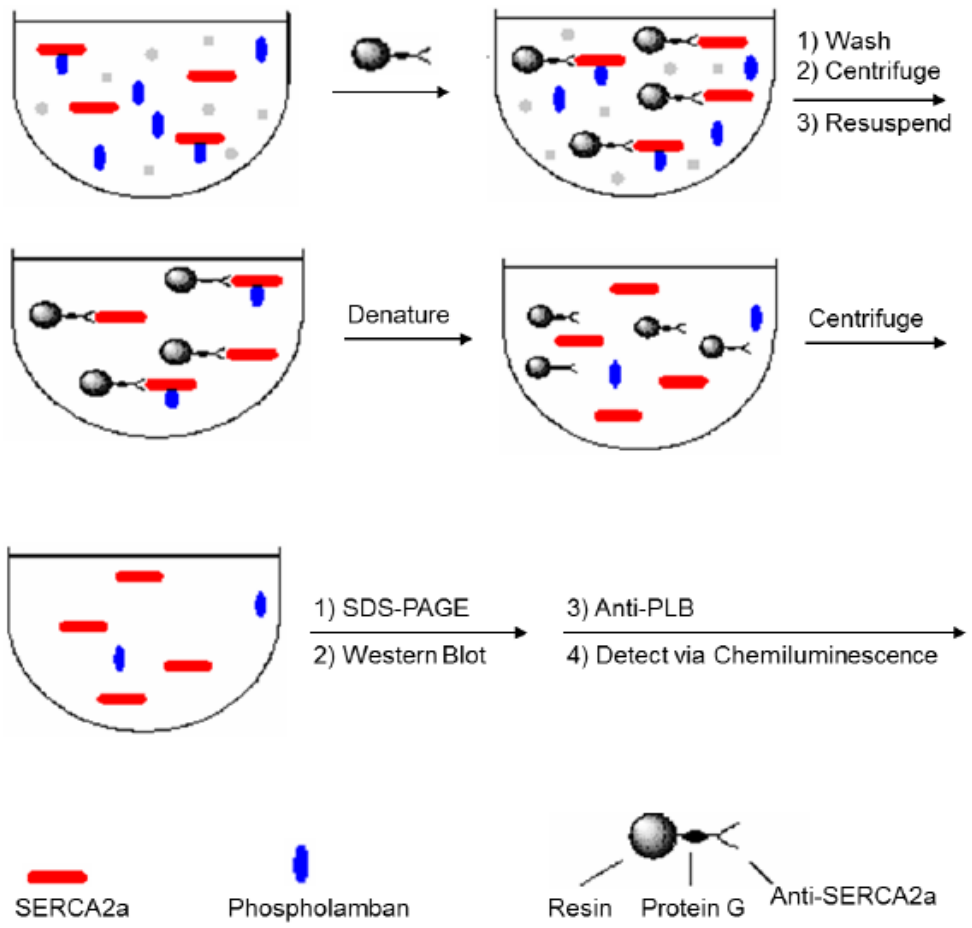

Figure 6-14. Co-immunoprecipitation procedure for co-expressed SERCA2a and PLN.

Co-immunoprecipitation of samples in the presence or absence of prior HNO treatment revealed that the relative fraction of PLN associated with SERCA2a is effectively unchanged (Figure 6-15). These results indicate that PLN remains physically associated with SERCA2a upon exposure to HNO, in accordance with literature suggesting that PLN remains bound to SERCA even though inhibition is relieved.[16, 43, 44] Moreover, analysis of the co-immunoprecipitated samples without boiling prior to SDS-PAGE led to the observation of PLN oligomers independent of HNO treatment (Figure 6-15). Consistent

with a recent co-crystallization study,[43] these observations point to a potential physical interaction between PLN oligomers and SERCA2a. It should be noted that although we have also attempted to perform the co-immunoprecipitation in the reverse order (i.e., precipitation with anti-PLN antibody (2D12) and visualization with anti-SERCA2a), these efforts were unsuccessful due to the disruption of SERCA2a/PLN complex in the presence of anti-PLN antibody, as reported in the literature.[45]

Figure 6-15. Microsomes containing co-expressed SERCA2a and PLN were treated with 0, 2.5, or 5 mM AS. Samples were co-immunoprecipitated with monoclonal anti-SERCA2a antibody. The immunoprecipitates were eluted by incubating the samples at (a) 37 oC, (b) by boiling. The proteins were detected by monoclonal anti-PLN antibody (2D12). (c) The bar graph showing the total amount of PLN associated with SERCA2a, is the average of triplicate experiments.

The influence of HNO on the SERCA2a/PLN interaction was explored further using fluorescence spectroscopy in collaboration with the Mahaney group. These studies have shown that HNO alleviates PLN inhibition of SERCA2a [Ca^{2+}]-dependent conformational flexibility, with a concomitant increase in SERCA2a activity.[46] Moreover, these effects were observed only in the presence of PLN. Similarly, electron paramagnetic resonance (EPR) spectroscopy analyses demonstrated an increase in SERCA2a rotational mobility upon HNO treatment only in the presence of PLN.[46] These findings are attributed

to the changes in the size of the rotating unit, stemming from relief of PLN inhibition on SERCA2a by HNO, and consequent oligomerization of the pump. This behavior is also consistent with functional uncoupling of PLN from SERCA2a via PKA-induced PLN phosphorylation.[15]

Overall, our results indicate that HNO functionally uncouples PLN from SERCA2a, although the physical association remains. Moreover, the lack of PKA in the microsomal systems confirms that this effect is independent of PKA-induced phosphorylation of PLN.

6.4 Conclusions

Collaborative studies have shown that HNO activates Ca^{2+} uptake by SERCA2a in a PLN-dependent manner. The lack of HNO effect in the absence or blockage of PLN cysteine residues, and the reversible nature of this modification by thiol-based reducing agents or TCEP suggest that PLN cysteine residues are targets of HNO. Our SDS-PAGE experiments indicate the formation of HNO-induced PLN oligomers in microsomal samples, isolated cardiomyocytes, and heart extracts.

Based on the known chemisty of HNO,[47-49] the potential modifications of PLN are an intermolecular disulfide, an intramolecular disulfide, and/or a sulfinamide (Figure 6-10). Our current data imply the formation of an intermolecular disulfide bond between PLN monomers, presumably formed within the PLN pentamer, resulting in a decrease in the amount of inhibitory PLN monomer. However, further studies are required to determine the exact nature and location of HNO-derived modification(s) on PLN.

Our co-immunoprecipitation studies indicate that PLN remains physically associated with SERCA2a upon HNO treatment. Combined with kinetic and spectroscopic

studies investigating the effects of HNO on the SERCA2a/PLN interaction, we conclude that HNO functionally uncouples PLN from SERCA2a, presumably by affecting PLN oligomerization. The studies conducted in isolated cardiomytes and whole hearts confirm the central role of PLN in HNO-induced effects on myocardial contractility and relaxation.[46] Moreover, this effect is independent of PKA-induced phosphorylation of PLN, as shown by the lack of change in PLN phosphorylation status,[46] and suggest that PLN function can be modified in a redox-dependent manner that augments cardiac contraction and relaxation.

6.5 Future Directions

Considering the role of HNO as a potential heart failure therapeutic, it will be important to understand fully the mechanism responsible for HNO-induced effects on the SERCA2a/PLN system. To achieve this, unambiguous characterization of HNO-derived modifications on PLN are needed.

Several studies have employed solution and solid-state NMR techniques to investigate the structural topology and dynamics of monomeric and pentameric PLN, its interaction with lipids, its regulation of SERCA, and the effect of phosphorylation on PLN in lipid bilayer, detergent micelles and organic solvents.[38, 50-56] One of the major approaches is to utilize ^{15}N uniformly- or selectively-labeled PLN.

As mentioned previously, the ^{15}N-edited NMR method proved to be a powerful technique for the detection of HNO-derived sulfinamides. Following reconstitution of synthetic PLN and its single cysteine variants into dodecylphosphocholine (DPC) micelles, which have been typically employed in the solution NMR studies of PLN,[52, 54, 55] samples can be treated with an ^{15}N-labeled HNO donor and analyzed using the ^{15}N-edited NMR

method. These studies would allow the detection of potential HNO-derived sulfinamides on PLN. Moreover, ^{15}N-edited ^{1}H-^{1}H NOESY experiments may be employed to determine the location of H^{15}NO-induced sulfinamide(s) formed in PLN. Since ^{1}H NMR data are available for Cys36 and Cys46 of PLN in the literature,[50] we expect the corresponding signals to be distinguishable. Additionally, single cysteine PLN variants can serve as standards.

To gain more insight into the sites of HNO reactivity, formation of the HNO-induced PLN dimer can be explored in single cysteine PLN variants by SDS-PAGE analysis. Reports indicate the destabilization of the PLN pentamer upon mutation of Cys41 to Ala.[57] Considering the results pointing to the generation of HNO-derived PLN dimer within the pentamer, the formation of this species might be affected in C36,41A-PLN and C41,46A-PLN.

The presence of a potential disulfide bond can be determined by alkylation of the H^{15}NO-modified PLN sample with isotopically-labeled, cysteine-specific alkylating agents (e.g., iodoacetamide) with or without prior reduction. In each case, the amount of alkylation can be quantified with an internal standard and compared to the amount of alkylation in the absence of prior H^{15}NO treatment. We expect all three cysteines to be fully alkylated in the untreated sample.

As demonstrated in Chapter 2, in lower dielectric constant environments sulfinamide reduction by thiols is more facile in a peptide structure compared with a non-peptide organic molecule. Moreover, the time-frame for sulfinamide reduction is significantly longer than that for disulfide reduction under the same conditions. The single cysteine variants of PLN reconstituted in DPC micelles can also be utilized to study the

reactivity of any potentially formed HNO-induced sulfinamide modifications in the presence of α-helical structure and hydrophobic environment. For this purpose, ^{15}N-edited NMR experiments can be conducted in the presence or absence of reducing agents analogous to our recent ESI-MS and NMR studies involving short peptides.[58, 59]

6.6 Other Reactivity Studies with Phospholamban and Sarco(endo)plasmic Reticulum Ca^{2+}-ATPase

6.6.1 Preliminary Studies with PLN and *C*-Nitroso Compounds

Thiol groups are known to react with *C*-nitroso compounds.[60, 61] Moreover, studies indicate that *C*-nitroso compounds, nitrosobenzene (NB), 1-nitrosoadamantane (NA), 2-methyl-2-nitrosopropane (MNP) can mimic and act as a more stable version of HNO in inhibiting aldehyde dehydrogenase (AlDH) and glyceraldehyde-3-phosphate dehydrogenase (GAPDH).[62, 63] AlDH was shown to be inhibited by NB, NA, and 2-MNP with IC_{50} values of 2.5, 8.6, and 150 μM, respectively.[63] The IC_{50} value for AS was determined to be 1.3 μM under anaerobic conditions.[63] The inhibition of GAPDH was less efficient with NB compared with AS ($IC_{50} \approx 1$ mM vs. complete inhibition with 0.1 mM AS).[62] Although highly toxic, administration of NB has shown in vivo activity towards AlDH in rats.

We have shown that HNO reacts with PLN to form the corresponding dimeric species. To determine if PLN behaves similarly with the *C*-nitroso compounds, we have employed the commercially available NB and MNP. In solution, both compounds turned blue, consistent with the presence of monomeric *C*-nitroso species.[64] Treatment of PLN-containing microsomes with 5 and 10 mM AS or NB provided similar results, indicating

PLN thiols are accessible to NB (Figure 6-16). Moreover, the extent of PLN oligomer formation was the same following 30 min or 2 h incubation at 37 ºC (Figure 6-16). It should be also noted that incubation with NB corresponds to a bolus addition of HNO, rather than its slow release from AS, precluding direct comparisons.

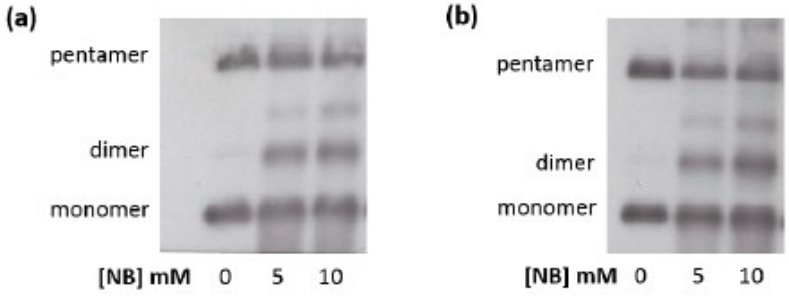

Figure 6-16. Insect cell microsomes containing expressed PLN were diluted to 1 mg/ml (in 0.05 M PBS at pH 7.4) and incubated with varying concentrations of nitrosobenzene (NB) for (a) 30 min or (b) 2 h at 37 ºC. Loading buffer was then added and the samples were subjected to SDS-PAGE analysis.

To gain more insight into the efficiency of NB, we treated PLN with lower concentrations of NB (from 0.1 μM to 1 mM). As shown in Figure 6-17 among the NB concentrations tested, the PLN dimer was only detected upon incubation with 1 mM NB.

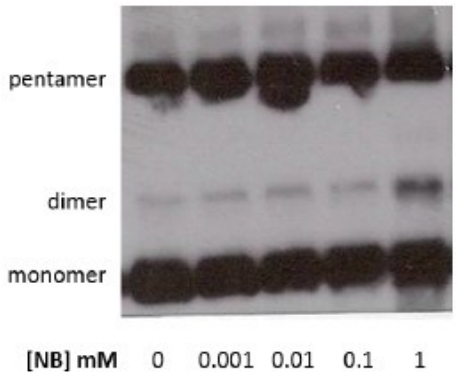

Figure 6-17. Insect cell microsomes containing expressed PLN were diluted to 1 mg/ml (in 0.05 M PBS at pH 7.4) and incubated with 0-1 mM nitrosobenzene (NB) for 30 min at 37 ºC. Loading buffer was then added and the samples were subjected to SDS-PAGE analysis.

To avoid the highly toxic nature of aromatic *C*-nitroso compounds, we decided to test 1-chloro-1-nitrosocyclohexane (CNCH) and MNP. Attempts to employ CNCH were unsuccessful due to the extremely low solubility of this compound in several solvents. Following equilibration of MNP for 1 h under argon-saturated conditions to establish the monomer/dimer ratio, PLN was incubated with various concentrations of MNP for 30 min or 2 h at 37 ºC. Although no MNP-derived PLN dimer was observed upon 30 min incubation, a faint dimer band was detected following 2 h incubation with 10 mM MNP (Figure 6-18).

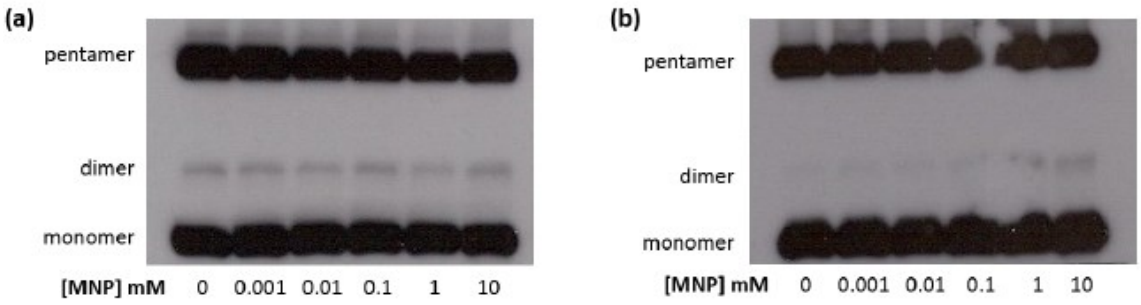

Figure 6-18. Insect cell microsomes containing expressed PLN were diluted to 1 mg/ml (in 0.05 M PBS at pH 7.4) and incubated with varying concentrations of 2-methyl-2-nitrosopropane (MNP) for (a) 30 min or (b) 2 h at 37 ^{o}C. Loading buffer was then added and the samples were subjected to SDS-PAGE analysis.

Since only monomeric MNP would be reactive towards thiols, we confirmed the monomer/dimer ratio of MNP by UV-visible spectroscopy. Analyses in buffer and diethyl ether showed the percentage of monomeric species to be ca. 77 and 90, respectively. Moreover, longer incubation of samples resulted in a decrease in monomeric species. Consistent with these observations, MNP (10 mM) with PLN following an overnight equilibration did not lead to the formation of PLN dimer. In accordance with previous studies with AlDH,[65] our results point to the relatively unreactive nature of MNP towards PLN thiols, presumably due to steric hindrance.

6.6.2 Reactivity of PLN with Peroxynitrite

Peroxynitrite ($ONOO^-$) is generated from the diffusion-controlled reaction of nitric oxide (NO) and superoxide ($O_2^{\bullet -}$).[66, 67] It has a pK_a of 6.8 and studies report that ca. 80% of $ONOO^-$ is in anionic form under physiological conditions.[68] Moreover, $ONOO^-$ has been shown to cross biological membranes via an anion channel, and as ONOOH via passive diffusion.[69] Major biological targets of $ONOO^-$ include metal centers, DNA, lipids,

cysteine, tryptophan, tyrosine and methionine residues.[68, 70-75] It is also known to result in protein fragmentation and formation of protein carbonyls.[75]

We have conducted preliminary studies to assess the effect of $ONOO^-$ on PLN. For these experiments, we utilized both 5-amino-3-(4-morpholinyl)-1,2,3-oxadiazolium chloride (SIN-1) (Scheme 6-1), an NO and $O_2^{\bullet-}$ donor, and authentic $ONOO^-$.[76] SIN-1 has a half-life of ca. 40 min under physiological conditions.[77, 78]

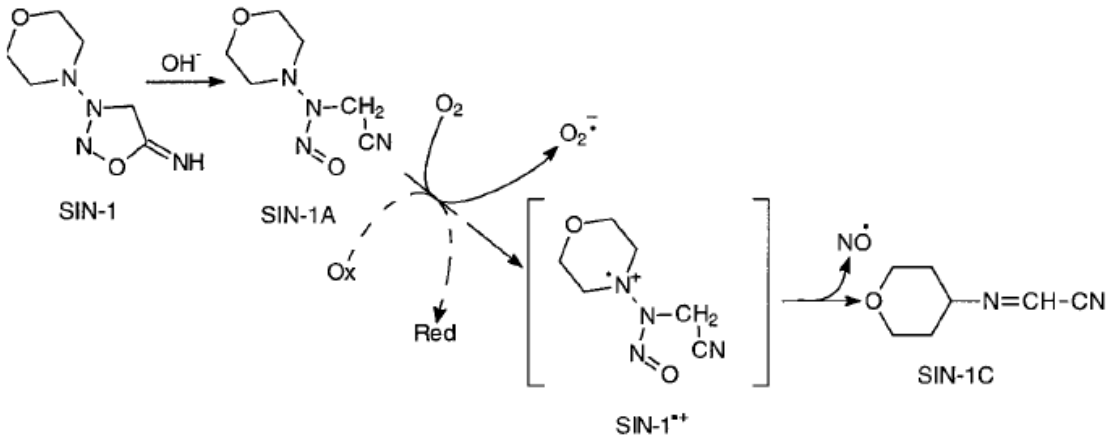

Scheme 6-1. Decomposition of 5-amino-3-(4-morpholinyl)-1,2,3-oxadiazolium chloride (SIN-1) under physiological conditions to generate nitric oxide (NO) and superoxide ($O_2^{\bullet-}$), which react with a diffusion-controlled rate to form peroxynitrite ($ONOO^-$). Singh, R. J., Hogg, N., Joseph, J., Konorev, E., and Kalyanaraman, B. (1999) The peroxynitrite generator, SIN-1, becomes a nitric oxide donor in the presence of electron acceptors, *Arch. Biochem. Biophys. 361*, 331-339.

Treatment of microsomes containing expressed PLN with 5 or 10 mM SIN-1, resulted in the formation of PLN dimer (Figure 6-19). However, it was accompanied by significant protein fragmentation (Figure 6-19). Moreover, the band corresponding to the PLN pentamer appeared at a slightly higher molecular weight in the SIN-1-treated samples compared with the untreated samples. Considering the highly reactive nature of ONOO-

with several amino acids,[70-72, 75] the increase in the molecular weight of the pentamer could be attributed to the modification of different PLN residues (Figure 6-19). It should be also noted that no PLN modifications were observed in the absence of SIN-1 decomposition, indicating that these effects are due to $ONOO^-$ and not SIN-1 or its organic byproduct.[26] As expected, bolus addition of authentic $ONOO^-$ produced the same results (Figure 6-20).

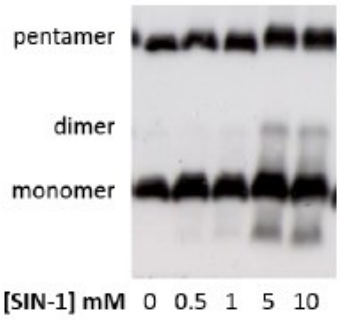

Figure 6-19. Insect cell microsomes containing expressed PLN were diluted to 1 mg/ml (in 0.1 M PBS containing 100 μM EDTA at pH 7.4) and incubated with varying concentrations of 5-amino-3-(4-morpholinyl)-1,2,3-oxadiazolium chloride (SIN-1) for 3 h at 37 °C. Loading buffer was then added and the samples were subjected to SDS-PAGE analysis.

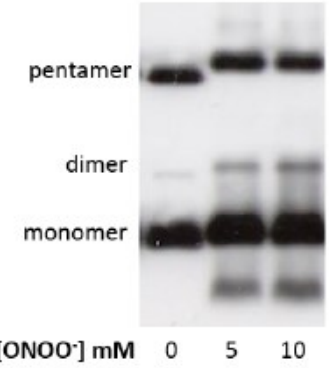

Figure 6-20. Insect cell microsomes containing expressed PLN were diluted to 1 mg/ml (in 0.1 M PBS containing 100 μM EDTA at pH 7.4) and incubated with varying concentrations of authentic peroxynitrite ($ONOO^-$) for 30 min at 37 °C. Loading buffer was then added and the samples were subjected to SDS-PAGE analysis.

$ONOO^-$ is known to react with tyrosine residues to form a dityrosine or a 3-nitrotyrosine. Moreover, this reactivity becomes more prominent in the presence of carbon dioxide (CO_2). Since $ONOO^-$-derived dityrosine formation could be responsible for the generation of PLN dimer, we tested this possibility by blocking PLN cysteines with NEM. The lack of PLN dimer reveals that this modification is due to modification of PLN cysteine residues rather than tyrosine (Figure 6-21). Consistent with the involvement of non-cysteine residues, $ONOO^-$-derived increase in the molecular weight of PLN pentamer was still observed (Figure 6-21). Interestingly, increasing concentrations of $ONOO^-$ resulted in destabilization of PLN pentamer especially in the presence of NEM. Importantly, significant amounts of protein fragmentation were observed in all $ONOO^-$-treated PLN samples.

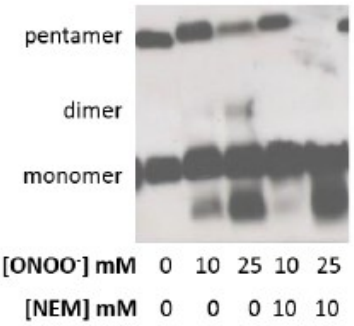

Figure 6-21. Insect cell microsomes containing expressed PLN were diluted to 1 mg/ml (in 0.1 M PBS containing 100 μM EDTA at pH 7.4) and pretreated with 0 or 10 mM NEM for 1 h at room temperature. The samples were then incubated with varying concentrations of authentic peroxynitrite ($ONOO^-$) for 30 min at 37 ºC. After the incubation, loading buffer was added and the samples were subjected to SDS-PAGE analysis.

These initial findings indicate that although $ONOO^-$ results in the formation of PLN dimer, possibly via its reactivity towards cysteines, the overall impact of $ONOO^-$ on PLN is significantly different from HNO.

6.6.3 Preliminary Studies on the Effects of HNO on Sarco(endo)plasmic Reticulum Ca^{2+}-ATPase

Recent studies have suggested that HNO may directly stimulate SERCA2a activity by promoting reversible *S*-glutathiolation on SERCA2a at Cys674.[79] However, the impact of this modification on myocyte and heart function, or the simultaneous changes in PLN were not explored.[79] As mentioned previously, our activity studies indicate the vital role of PLN and its cysteine residues in HNO-induced SERCA2a stimulation.

We have conducted preliminary studies to explore the effects of HNO on SERCA2a. For this purpose, we utilized microsomes expressing SERCA2a. On SDS-PAGE gel, wild-type SERCA2a primarily migrates as a monomer. Previous investigations in Toscano group have shown that treatment of SERCA2a with HNO results in a substantial decrease in SERCA2a monomer, presumably due to the formation of SERCA2a higher oligomers.[26] The reactivity of SERCA2a with HNO was also seen in the presence of co-expressed SERCA2a and PLN samples. Moreover, this effect was not observed upon incubation of SERCA2a with the nitric oxide donor, DEA/NO.[26] We have probed the decrease in SERCA2a as a function of AS concentration. As shown in Figure 6-22 the amount of SERCA2a monomer diminished upon treatment with AS in a concentration-dependent manner. At relatively higher concentrations of AS, presumably, the loss of HNO due to dimerization became more prominent.

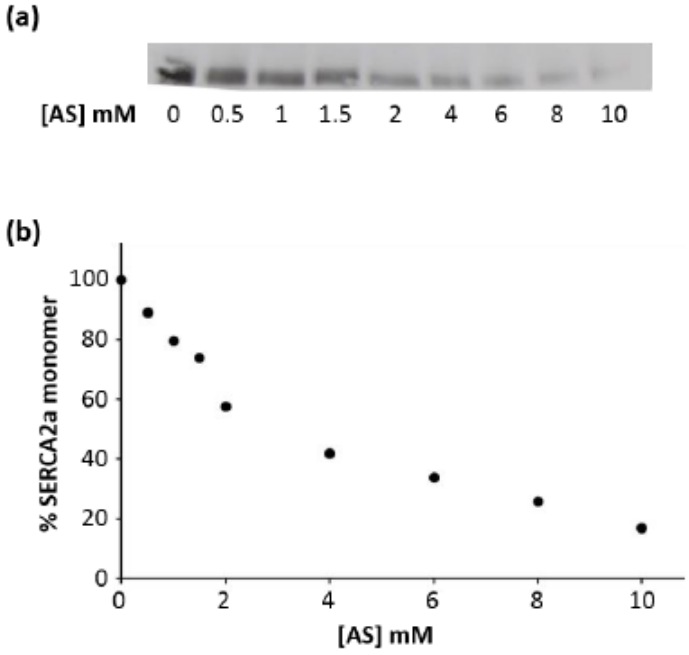

Figure 6-22. Insect cell microsomes containing expressed SERCA2a were diluted to 1.5 mg/ml (in immunoprecipitation buffer at pH 7.5) and centrifuged at 12 000 for 5 min. The samples were then incubated with varying concentrations of AS for 30 min at 37 ºC. After the incubation, loading buffer was added and the samples were subjected to SDS-PAGE analysis. (a) Selected region of western blot showing SERCA2a monomer incubated in the presence or absence of AS. (b) Graph showing the percentage of SERCA2a monomer observed upon HNO treatment.

Treatment of SERCA2a with $ONOO^-$ (produced from SIN-1) also resulted in the disappearance of the monomer, likely, attributable to the generation of SERCA2a oligomers. Moreover, this behavior was not observed in the absence of SIN-1 decomposition, supporting the involvement of $ONOO^-$ (Figure 6-23).

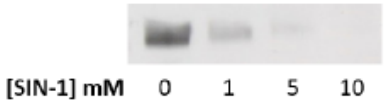

Figure 6-23. Insect cell microsomes containing expressed SERCA2a were diluted to 1.5 mg/ml (in immunoprecipitation buffer at pH 7.5) and centrifuged at 12 000 for 5 min. The samples were then incubated with varying concentrations of 5-amino-3-(4-morpholinyl)-1,2,3-oxadiazolium chloride (SIN-1) for 3 h at 37 ºC. After the incubation, loading buffer was added and the samples were subjected to SDS-PAGE analysis.

To examine the role of SERCA2a cysteines in the HNO-derived modification of SERCA2a, we blocked the cysteine residues with *N*-ethylmaleimide (NEM). Following incubation with HNO, no decrease in the amount of SERCA2a monomer was detected in NEM-treated samples, indicating the importance of SERCA2a cysteine residues in this process (Figure 6-24).

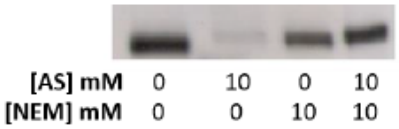

Figure 6-24. Insect cell microsomes containing expressed SERCA2a were diluted to 1.5 mg/ml (in immunoprecipitation buffer at pH 7.5) and centrifuged at 12 000 for 5 min. The samples were pretreated with 0 or 10 mM NEM for 1 h at room temperature. The samples were then incubated in the presence or absence of 10 mM AS for 30 min at 37 ºC. After the incubation, loading buffer was added and the samples were subjected to SDS-PAGE analysis.

The reversibility of the HNO-derived modifications on SERCA2a were investigated by employing dithiothreitol (DTT) and tris(2-carboxyethyl)phosphine (TCEP). The incubation of the HNO-treated SERCA2a samples with high concentrations of DTT or TCEP resulted in the partial recovery of the SERCA2a monomer, consistent with the involvement of cysteine residues (Figure 6-25). It should be also noted that

increasing the concentration of reducing agents from 50 to 250 mM did not provide complete recovery of the SERCA2a monomer.

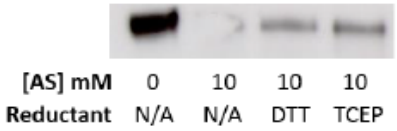

Figure 6-25. Insect cell microsomes containing expressed SERCA2a were diluted to 1.5 mg/ml (in immunoprecipitation buffer at pH 7.5) and centrifuged at 12 000 for 5 min. The samples were then incubated in the presence or absence of AS for 30 min at 37 ºC. Following the incubation, the samples were treated with 50 mM DTT or TCEP. Loading buffer was then added and the samples were subjected to SDS-PAGE analysis.

In summary, these findings point to a potential modification(s) of SERCA2a by HNO. However, the impact of these modification(s) on SERCA2a/PLN system as well as their physiological relevance requires further investigation. It should be also noted that a major hurdle in studying SERCA2a oligomerization by electrophoresis is the smearing observed on the gel, a condition commonly seen with very hydrophobic, high molecular weight, membrane/transmembrane proteins. Although we have been able to observe the SERCA2a monomer band clearly, it has not been possible to identify the oligomers due to extreme smearing. Despite our attempts to obtain better resolution by the addition of 8 M urea to SDS sample buffer, use of gradient gels, exclusion of heating, or centrifugation of samples to remove insoluble materials, we were not able to solve this issue. To obtain more information on SERCA2a oligomerization via electrophoresis techniques, better resolution is required.

6.7 Experimental Methods

Reagents. N-ethylmaleimide (NEM), sodium dodecyl sulfate (SDS), octaethylene glycol monododecyl ether ($C_{12}E_8$), *t*-butanesulfinamide, nitrosobenzene (NB), 2-methyl-2-nitrosopropane (MNP) dimer, tris(2-carboxyethyl)phosphine (TCEP), and dithiothreitol (DTT) were of the highest purity available and purchased from Sigma (St. Louis, MO). Bicinchoninic acid (BCA) assay kit, urea, HPLC-grade acetonitrile (ACN), HPLC-grade isopropanol (IPA), and trifluoroacetic acid (TFA) were of the highest purity available and purchased from Thermo Fisher Scientific (Rockford, IL). HPLC-grade IPA was further purified via distillation. Anti-PLN monoclonal antibody (2D12) and anti-SERCA2a monoclonal antibody were obtained from Affinity Bioreagents (Golden, CO). Horseradish peroxidase-conjugated anti-mouse IgG secondary antibody were purchased from Upstate Cell Signaling Solutions (Lake Placid, NY). Molecular weight marker and polyvinylidene fluoride (PVDF) membranes were obtained from Bio-Rad. Enhanced chemiluminescence reagents (ECL Western Blotting Substrate) was purchased from Pierce (Rockford, IL). The pseudoproline dipeptide of Fmoc-Leu-Thr ($\Psi^{Me,Me}$ Pro)-OH was purchased from Novabiochem (San Diego, CA). The phospholipids, dioleoylphosphatidylethanolamine (DOPE) and dioleoylphosphatidylcholine (DOPC), were obtained from Avanti Polar Lipids. The peroxynitrite-donor, 5-amino-3-(4-morpholinyl)-1,2,3-oxadiazolium chloride (SIN-1), was obtained from Calbiochem (San Diego, CA). The syntheses of HNO-donors, Angeli's salt ($Na_2N_2O_3$, AS)[73] and 2-bromo-*N*-hydroxybenzenesulfonamide (2-BrPA),[80] and NO-donor (DEA/NO) were carried out as previously described. Authentic peroxynitrite ($ONOO^-$) was synthesized and characterized following a literature procedure.[81] High Five insect cell ER microsomes expressing wild-type PLN, null-cysteine

PLN (C36,41,46A-PLN), SERCA2a, or co-expressing SERCA2a and PLN were kindly provided by Dr. James E. Mahaney (Edward Via Virginia College of Osteopathic Medicine).

Treatment of PLN with HNO-Donors. High Five insect cell ER microsomes expressing wild-type PLN and null-cysteine PLN (C36,41,46A-PLN) were diluted to 0.25, 0.5 or 1 mg/ml in 0.05 M phosphate-buffered saline (PBS) at pH 7.4 unless otherwise indicated. Stock solutions of AS were prepared in 10 mM NaOH and used within 15 minutes. Stock solutions of 2-BrPA were prepared in dimethyl sulfoxide (DMSO) and used within 15 minutes. The samples were incubated with varying concentrations of HNO-donor at 37 ºC for 30 min unless otherwise indicated. The samples were then diluted with SDS sample buffer and analyzed by electrophoresis, western blotting and immunodetection. For experiments involving prolonged exposures for visualization via chemiluminescence, 8 M urea was added to SDS sample buffer.

Treatment of PLN with HNO-Donors under Anaerobic Conditions. Stock solutions of AS and 2-BrPA were prepared as described above and purged with argon. High Five insect cell ER microsomes expressing wild-type PLN were diluted to 1 mg/ml in 0.1 M phosphate-buffered saline (PBS) with 100 μM EDTA at pH 7.4. The samples were placed in glass vials sealed with rubber septa and purged with argon or compressed air for 4 min. Following the introduction of various concentrations of HNO-donor, the samples were incubated at 37 ºC for 30 min. After the incubation, the samples were purged with argon for an additional 3 min to remove any nitrogen oxide species. The samples were then diluted with SDS sample buffer, and analyzed by electrophoresis, western blotting and immunodetection.

In some cases, PLN was labeled with NEM prior to purging with argon as described

below. Following treatment with HNO-donors under anaerobic conditions, the samples were analyzed.

Treatment of SERCA2a or Co-expressed SERCA2a and PLN with HNO-Donors. High Five insect cell ER microsomes expressing wild-type SERCA2a or co-expressed SERCA2a and PLN were diluted to 1.5 mg/ml in 0.05 M PBS at pH 7.4 or in immunoprecipitation buffer ([in mM]: 110 sucrose, 5 Tris-HCl, 75 KCl, 20 HEPES; 150 NaCl, 1 EDTA, 2 PMSF, 0.5% Tween 20) at pH 7.5. In some cases, the samples were centrifuged at 12000 rpm at room temperature for 5 min to remove insoluble material. Stock solutions of AS were prepared in 10 mM NaOH and used within 15 minutes. The samples were then incubated with varying concentrations of AS at 37 ^{o}C for 30 min unless otherwise indicated. The samples were then diluted with SDS sample buffer and analyzed by electrophoresis, western blotting and immunodetection.

Treatment of PLN and SERCA2a with Reducing Agents. High Five insect cell ER microsomes expressing wild-type PLN or SERCA2a were incubated with AS as described above. Stock solutions of DTT and TCEP were freshly prepared in sterilized, deionized water. The samples were incubated with various concentrations of the reducing agents for 30 min at room temperature or 37 ^{o}C (as indicated). The samples were then diluted with SDS sample buffer and analyzed by electrophoresis, western blotting and immunodetection.

Labeling of PLN and SERCA2a with NEM. Stock solutions of NEM were prepared in sterilized, deionized water. High Five insect cell ER microsomes expressing wild-type PLN or SERCA2a diluted in 0.05 M PBS at pH 7.4 to have a final concentration of 0.25, 0.5, 1, or 1.5 mg/ml. The samples were then incubated with various concentrations

of NEM at room temperature prior to treatment with HNO.

Treatment of PLN or SERCA2a with DEA/NO, SIN-1, Synthetic $ONOO^-$, and *C*-Nitroso Compounds. High Five insect cell ER microsomes expressing wild-type PLN or SERCA2a diluted in 0.05 M PBS at pH 7.4 or in immunoprecipitation buffer ([in mM]: 110 sucrose, 5 Tris-HCl, 75 KCl, 20 HEPES; 150 NaCl, 1 EDTA, 2 PMSF, 0.5% Tween 20) at pH 7.5 to have a final concentration of 0.25, 0.5, 1, or 1.5 mg/ml. Stock solutions of DEA/NO, SIN-1, and NB were dissolved in 0.01 M NaOH, 0.002 M HCl, and DMSO, respectively and used within 15 min of preparation. Stock solutions of MNP were prepared in argon-saturated DMSO, and stirred at room temperature for 1 h or overnight (as indicated) to establish monomer/dimer equilibrium. Solutions of $ONOO^-$ in ca. 1 M NaOH were used immediately following quantification by UV-visible spectroscopy. PLN or SERCA2a samples were then incubated with various concentrations of DEA/NO, SIN-1, synthetic $ONOO^-$, or *C*-nitroso compounds at room temperature or 37 ^oC for various time intervals (as indicated). To avoid potential photolysis, the incubations with *C*-nitroso compounds were carried out strictly in the dark. The samples were then diluted with SDS sample buffer and analyzed by electrophoresis, western blotting and immunodetection.

Electrophoresis, Western Blotting and Immunodetection. SDS-PAGE using 15% polyacrylamide was performed using standard procedures.[82] Samples were either loaded directly or boiled for 5 min prior to loading. Upon separation by gel electrophoresis, the proteins were transferred via western blotting onto PVDF membrane. After blocking the membrane with 1% non-fat dry milk for 1 h, it was incubated overnight at 4 ^oC with anti-PLN monoclonal antibody (2D12). The membrane was washed and incubated for 1 h with horseradish peroxidase-conjugated anti-mouse IgG secondary antibody.

After washing, the chemiluminescent signals were generated by treating the membrane with enhanced chemiluminescence reagents and captured on film following either normal (30 s) or prolonged (30 min) exposure. PLN bands (monomer, dimer, pentamer) were assigned based on a standard molecular weight marker. For experiments with prolonged exposure, a very weak PLN dimer bands is observed (along with the monomer and dimer bands) prior to exposure to AS; the dimer band intensity increases substantially upon exposure to AS. All gels and western blots were run using a Bio-Rad Mini-Protean II electrophoresis and western blotting system. The results were quantified by a Bio-Rad GS-670 imaging densitometer.

Synthesis and Purification of PLN. Full-length phospholamban (PLB) in the presence or absence of the N-terminal acetyl cap was synthesized according to a literature procedure, which involves a modified Fmoc-based solid-phase method.[37, 38] Starting with Fmoc-L-Leu-PEG-PS resin (initial loading 0.19 mmol/g), the 52 residue protein was assembled in 11 days. Acidolyzable side-chain protecting groups were 2,2,4,6,7-pentamethyldihydrobenzofuran-5-sulfonyl (Pbf) for Arg; trityl (Trt) for Asn, Gln, His and Cys; tert-butyl ester (OtBu) for Glu and Asp; tert-butyloxycarbonyl (tBoc) for Lys; tert-butyl ether for Ser, Thr and Tyr. A double coupling protocol was used with a capping step following the recoupling as a part of the protocol. Fmoc removal was achieved with 20% piperidine in NMP. Couplings were performed using 10-fold excess of Fmoc-amino acids activated by HBTU/DIEA. In some cases, the difficulty of the coupling of Leu7 to Thr8 was overcome by using the pseudoproline dipeptide of Fmoc-Leu-Thr ($\Psi^{Me,Me}$ Pro)-OH. Also some couplings were achieved by extending the reaction time to 6 h. The synthesis was carried out on a Symphony Quartet peptide synthesizer.

Crude PLN was cleaved off the resin using a cleavage cocktail containing TFA/thioanisole/phenol/water/1,2-ethanedithiol 82.5:5:5:5:2.5, and precipitated using methyl *t*-butyl ether.[83] Synthetic PLN was dissolved in neat TFA, and purified by HPLC (Waters HPLC equipped with Delta 600 pump system and dual wavelength absorbance detector) on a Vydac C_4 reverse-phase column using a linear gradient from water/ACN/IPA/TFA 95:2:3:0.1 to 5:38:57:0.1 over 100 min at 40 ^oC.[83] PLN fractions were identified via electrophoresis and immunodetection. Pure fractions were pooled and lyophilized, and the purified product was quantified by a standard BCA assay.[84]

Reconstitution of PLN into Phospholipids. The phospholipids DOPC and DOPE were mixed in 4:1 ratio in chloroform ($CHCl_3$). Synthetic PLN was added onto the phospholipids to have a final ratio of lipid/PLN 200:1. The final concentrations of PLN, DOPC, and DOPE were approximately 0.01, 2, and 0.5 mM, respectively. Following vortexing (5 min), the solvent was evaporated with N_2. The samples were then lyophilized for ca. 2-4 h. The lyophilized samples were re-dissolved in either 0.05 M PBS or 10 mM phosphate buffer at pH 7.4 by several cycles of vortexing, and sonication to ensure liposome formation. Reconstitution was completed following a freeze (-20 ^oC, ca. 2 d)-thaw cycle.

Analysis of PLN by Circular Dichroism. PLN reconstituted into phospholipids, diluted into 10 mM phosphate buffer at pH 7.4, and exposed to a freeze-thaw cycle was passed through an extruder containing polycarbonate membrane with 100 nm pore size to form unilamellar liposomal suspensions. As a standard, PLN was also dissolved in a 0.3% solution of the nonionic detergent, $C_{12}E_8$, which is known to promote the α-helical conformation of PLN,[85] and analyzed following a freeze (-20 ^oC, ca. 2 d)-thaw cycle. The presence of α-helical structure was determined by circular dichroism at 20 ^oC in 0.2 or 1.0

mm pathlength, quartz cuvettes. All the data were collected over the 190-260 nm region with the following settings: 50 nm/s scan rate, 4 s response time, and two accumulations (scans). As controls, lipid and buffer solutions were analyzed in the absence of reconstituted PLN.

Co-immunoprecipitation of SERCA2a and PLN (with different concentrations of AS). Microsomes co-expressed with SERCA2a and PLN (11 mg/ml in 250 mM sucrose, 10 mM histidine, pH 7.2) were diluted to 0.25 mg/ml in immunoprecipitation buffer ([in mM]: 110 sucrose, 5 Tris-HCl, 75 KCl, 20 HEPES; 150 NaCl, 1 EDTA, 2 PMSF, 0.5% Tween 20). The microsomes were centrifuged for 15 min at 16,000 g to remove large microsomal debris. Recombinant protein G sepharose was added to the cleared solution and the sample was rocked at 4 °C overnight to collect all proteins bound non-specifically to protein G sepharose. The supernatant was obtained by centrifugation (1 min at 4000 g). Then the solution was divided into equal aliquots and incubated with 0 and 5 mM AS/HNO for 30 min at 37 °C. The samples were rocked overnight at 4°C with protein G sepharose which has been pretreated with monoclonal anti-SERCA2a antibody. Immunoprecipitates were then collected by centrifugation (1 min at 4000 g) and washed three times with ice cold wash buffer (pH = 7.5, (in mM): 20 HEPES, 150 NaCl, 1 EDTA, 1.5 BME, 1% Tween 20). Non-reducing sample loading buffer was added after re-suspending the protein-bound beads in 0.05 M PBS (pH = 7.4). Proteins were eluted from the beads by incubating the samples at 37 °C for 15 min or by boiling for 10 min. Beads were collected by centrifugation (1 min at 4000 g). Aliquots of the supernatant (containing the immunoprecipitates) were then loaded onto 15% polyacrylamide gels and the proteins were separated by using standard SDS-PAGE protocols. Upon separation, proteins were

transferred onto PVDF membranes via western blotting. After blocking open membrane sites in skim milk suspension for 1 h at room temperature, the membranes were incubated overnight at 4°C with anti-PLN monoclonal antibody (2D12) specific for the epitope between 2 and 25 of wt-PLN. The membranes were washed three times for 10 min each with cold Tris-HCl (pH 7.5, 150 mM NaCl; Tris- buffered saline [TBS]), with 0.1% Tween 20. The membranes were then incubated for 1 h at room temperature with horseradish peroxidase-conjugated anti-mouse IgG secondary antibody and washed three times with cold TBS/0.1% Tween 20. Chemiluminescent signals were generated by treating the membranes with enhanced chemiluminescence reagents and captured on film. The results were quantified by a Bio-Rad GS-670 imaging densitometer.

Mass Spectrometry of PLN. For MALDI-MS analysis, synthetic PLN (0.5 mg/ml, 0.75 μl) in methanol was spotted with α-cyanohydroxycinnamic acid (10 mg/ml in ACN/water/TFA 50:50:0.05 (v/v), 0.75 μL). A total of 5000 shots were accumulated with a frequency of 100 Hz. All MALDI-MS analyses were conducted in linear mode using a Bruker Autoflex III MALDI-TOF/TOF instrument equipped with a 355 nm pulsed UV laser.

The ESI-MS spectrum of PLN peptide, Gln22-Leu52, was obtained by dissolving the crude peptide in ACN with 1% TFA. ESI-MS analysis was carried out on a Thermo Finnigan LCQ Deca Ion Trap Mass Spectrometer fitted with an electrospray ionization source, operating in the positive ion mode with an accuracy of ca. 0.1 m/z. In all experiments, the samples were introduced to the instrument at a rate of 10 μL/min using a syringe pump via a silica capillary line. The heated capillary temperature was 250 °C and the spray voltage was 5 kV.

Electroelution of PLN. SDS-PAGE was run using 15% polyacrylamide as described above. Following electrophoresis, one lane was excised and stained with silver staining to locate the PLN band. The regions of the gel corresponding to PLN bands were estimated and excised based on the stained gel piece. The excised gel pieces were soaked in soaking buffer (25 mM Tris and 192 mM glycine containing 0.2% SDS at pH 8.3). The electroelution was carried out in electroelution buffer (25 mM Tris and 192 mM glycine containing 0.02% SDS at pH 8.3). The eluates were collected following 6 h electroelution at 200 V and an additional 12 h electroelution at 96 V. All the experiments were carried out using Whatman Elutrap electroelution system, and BT1 and BT2 membranes recommended by the manufacturer.

The complete electroelution of the samples was confirmed by silver staining of the excised gel pieces. Also the presence of PLN in the eluate was determined electrophoresis, western blotting and immunodetection as described above.

Recovery of PLN from SDS Solutions. A modified chloroform/methanol/water (1:4:3 v/v) extraction procedure[41] was employed to remove SDS from the eluates following the electroelution of PLN. Briefly, SDS was removed by using two consecutive chloroform/methanol/water extractions, in which the final addition of MeOH to precipitate PLN from the chloroform solution was replaced with evaporation of chloroform.

The efficiency of the method was determined by quantification of the amount of remaining SDS after each step by a colorimetric assay employing methylene blue (ε_{651}=80000 $M^{-1}cm^{-1}$).[40, 41]

Treatment of *t*-Butanesulfinamide with Reducing Agents. A 0.12 M solution of t-butanesulfinamide was prepared in 0.05 M PBS (pH 7.4). The solution was divided into

two equal aliquots and DTT or TCEP was added to one of the aliquots such that the final concentration of DTT or TCEP were 0.5 M. The solutions were incubated at room temperature overnight. Each solution was then acidified, extracted with a total volume of 15 mL ether, and analyzed by gas chromatography-mass spectrometry (GC-MS). This analysis indicated no reaction between *t*-butanesulfinamide and DTT or TCEP.

Analysis of MNP by UV-Visible Spectroscopy. The stock solutions of MNP were prepared in DMSO. The amount of MNP dimer in 0.05 M PBS at pH 7.4 or in diethyl ether was calculated based on the absorbances at 287 and 295 nm, respectively. (ε_{287}= 8000 $M^{-1}cm^{-1}$, ε_{295}=8000 $M^{-1}cm^{-1}$).[86]

SERCA2a Activity Studies. All the kinetic assays and analyses were conducted by late Dr. Jeffrey P. Froehlich (Division of Cardiology, Johns Hopkins Medical Institutions). Briefly, activation of the cardiac SR Ca^{2+} pump by HNO in the presence or absence of wild-type or null-cysteine PLN (C36,41,46A-PLN) was investigated by measuring the kinetics of spontaneous dephosphorylation of SERCA2a revealed by chasing the phosphorylated enzyme with EGTA.[87, 88] In some cases, the effects of DTT on HNO-treated microsomes were also analyzed.

In some cases, effect of HNO on SERCA2a ATPase activity in the presence or absence of PLN were examined by Mahaney group (Department of Biochemistry, Edward Via Virginia College of Osteopathic Medicine) using the malachite green-ammonium molybdate assay.[46, 89]

Fluorescence Spectroscopy and EPR Analyses. All fluroscence and EPR spectroscopic analyses investigating the effects of HNO on SERCA2a in the presence or

absence of PLN were conducted by Mahaney group (Department of Biochemistry, Edward Via Virginia College of Osteopathic Medicine).

Isolated Myocyte, Whole Heart, and Animal Studies. All the in vivo and in vitro studies investigating the effects of HNO on isolated myocytes, heart extracts, regular or $PLN^{-/-}$ mice were conducted by Paolocci group (Division of Cardiology, Johns Hopkins Medical Institutions).

6.8 References

1. Hasenfuss, G., and Teerlink, J. R. (2011) Cardiac inotropes: Current agents and future directions, *Eur. Heart J. 32*, 1838-1845.
2. Houser, S. R., and Margulies, K. B. (2003) Is depressed myocyte contractility centrally involved in heart failure?, *Circ. Res. 92*, 350-358.
3. Balligand, J. L., Feron, O., and Kelly, R. A. (2000) Role of Nitric Oxide in Myocardial Function, In *Nitric Oxide: Biology and Pathobiology* (Ignarro, L. J., Ed.), pp 585-632, Academic Press, San Diego.
4. Paolocci, N., Katori, T., Champion, H. C., St John, M. E., Miranda, K. M., Fukuto, J. M., Wink, D. A., and Kass, D. A. (2003) Positive inotropic and lusitropic effects of HNO/NO^- in failing hearts: Independence from beta-adrenergic signaling, *Proc. Natl. Acad. Sci. U. S. A. 100*, 5537-5542.
5. Tocchetti, C. G., Stanley, B. A., Murray, C. I., Sivakumaran, V., Donzelli, S., Mancardi, D., Pagliaro, P., Gao, W. D., van Eyk, J., Kass, D. A., Wink, D. A., and Paolocci, N. (2011) Playing with cardiac "redox switches": The "HNO way" to modulate cardiac function, *Antioxid. Redox Signaling 14*, 1687-1698.

6. Paolocci, N., Jackson, M. I., Lopez, B. E., Miranda, K. M., Tocchetti, C. G., Wink, D. A., Hobbs, A. J., and Fukuto, J. M. (2007) The pharmacology of nitroxyl (HNO) and its therapeutic potential: Not just the janus face of NO, *Pharmacol. Ther. 113*, 442-458.

7. Paolocci, N., Saavedra, W. F., Miranda, K. M., Martignani, C., Isoda, T., Hare, J. M., Espey, M. G., Fukuto, J. M., Feelisch, M., Wink, D. A., and Kass, D. A. (2001) Nitroxyl anion exerts redox-sensitive positive cardiac inotropy in vivo by calcitonin gene-related peptide signaling, *Proc. Natl. Acad. Sci. U. S. A. 98*, 10463-10468.

8. Fukuto, J. M., Cisneros, C. J., and Kinkade, R. L. (2013) A comparison of the chemistry associated with the biological signaling and actions of nitroxyl (HNO) and nitric oxide (NO), *J. Inorg. Biochem. 118*, 201-208.

9. Doctorevich, F., Bikiel, D., Pellegrino, J., Suarez, S. A., Larsen, A., and Marti, M. A. (2011) Nitroxyl (azanone) trapping by metalloporphyrins, *Coordin. Chem. Rev. 255*, 2764-2784.

10. Balligand, J. L., Feron, O., and Kelly, R. A. (2000) Role of Nitric Oxide in Myocardial Function, In *Nitric Oxide: Biology and Pathobiology* (Ignarro, L. J., Ed.), Academic Press, San Diego.

11. Tocchetti, C. G., Wang, W., Froehlich, J. P., Huke, S., Aon, M. A., Wilson, G. M., Di Benedetto, G., O'Rourke, B., Gao, W. D., Wink, D. A., Toscano, J. P., Zaccolo, M., Bers, D. M., Valdivia, H. H., Cheng, H., Kass, D. A., and Paolocci, N. (2007) Nitroxyl improves cellular heart function by directly enhancing cardiac sarcoplasmic reticulum Ca^{2+} cycling, *Circ. Res. 100*, 96-104.

12. MacLennan, D. H., and Kranias, E. G. (2003) Phospholamban: A crucial regulator of cardiac contractility, *Nature Rev. Mol. Cell Biol. 4*, 566-577.

13. Frank, K. F., Bolck, B., Erdmann, E., and Schwinger, R. H. G. (2003) Sarcoplasmic reticulum Ca^{2+}-ATPase modulates cardiac contraction and relaxation, *Cardiovasc. Res. 57*, 20-27.

14. Toyoshima, C., Nakasako, M., Nomura, H., and Ogawa, H. (2000) Crystal structure of the calcium pump of sarcoplasmic reticulum at 2.6 Å resolution, *Nature 405*, 647-655.

15. James, Z. M., McCaffrey, J. E., Torgersen, K. D., Karim, C. B., and Thomas, D. D. (2012) Protein-protein interactions in calcium transport regulation probed by saturation transfer electron paramagnetic resonance, *Biophys. J. 103*, 1370-1378.

16. Li, J., Bigelow, D., and Squier, T. C. (2003) Phosphorylation by cAMP-dependent protein kinase modulates the structural coupling between the transmembrane and cytosolic domains of phospholamban, *Biochemistry 42*, 10674-10682.

17. Hagemann, D., and Xiao, R.-P. (2002) Dual site phospholamban phosphorylation and its physiological relevance in the heart, *Trends Cardiovascul. Med. 12*, 51-56.

18. Simmerman, H. K. B., and Jones, L. R. (1998) Phospholamban: Protein structure, mechanism of action and role in cardiac function, *Physiol. Rev. 78*, 921-947.

19. James, P., Inui, M., Tada, M., Chiesi, M., and Carafoli, E. (1989) Nature and site of phospholamban regulation of the Ca^{2+} pump of sarcoplasmic reticulum, *Nature 342*, 90-92.

20. Kimura, Y., Kurzydlowski, K., Tada, M., and MacLennan, D. H. (1996) Phospholamban regulates the Ca^{2+}-ATPase through intramembrane interactions, *J. Biol. Chem. 271*, 21726-21731.

21. Jones, L. R., Simmerman, H. K. B., Wilson, W. W., Gurd, F. R. N., and Wegener, A. D. (1985) Purification and characterization of phospholamban from canine cardiac sarcoplasmic reticulum, *J. Biol. Chem. 260*, 7721-7730.

22. Wegener, A. D., and Jones, L. R. (1984) Phosphorylation-induced mobility shift in phospholamban in sodium dodecyl sulfate-polyacrylamide gels, *J. Biol. Chem. 259*, 1834-1841.

23. Kimura, Y., Kurzydlowski, K., Tada, M., and MacLennan, D. H. (1997) Phospholamban inhibitory function is activated by depolymerization, *J. Biol. Chem. 272*, 15061-15064.

24. Mahaney, J. E., Albers, R. W., Waggoner, J. R., Kutchai, H. C., and Froehlich, J. P. (2005) Intermolecular conformational coupling and free energy exchange enhance the catalytic efficiency of cardiac muscle SERCA2a following the relief of phospholamban inhibition, *Biochemistry 44*, 7713-7724.

25. Karim, C. B., Stamm, J. D., Jones, L. R., and Thomas, D. D. (1998) Cysteine reactivity and oligomeric structures of phospholamban and its mutants, *Biochemistry 37*, 12074-12081.

26. Pavlos, C. M. (2006) Diazeniumdiolates: Photochemistry, thermal chemistry, and their use as potential heart failure therapeutics, p 135, Johns Hopkins University.

27. Hrabie, J. A., and Keefer, L. K. (2002) Chemistry of the nitric oxide-releasing diazeniumdiolate ("nitrosohydroxylamine") functional group and its oxygen-substituted derivatives, *Chem. Rev. 102*, 1135-1154.

28. Miranda, K. M., Dutton, A. S., Ridnour, L. A., Foreman, C. A., Ford, E., Paolocci, N., Katori, T., Tocchetti, C. G., Mancardi, D., Thomas, D. D., Espey, M. G., Houk, K. N., Fukuto, J. M., and Wink, D. A. (2005) Mechanism of aerobic decomposition of Angeli's salt (sodium trioxodinitrate) at physiological pH, *J. Am. Chem. Soc. 127*, 722-731.

29. Miranda, K. M. (2005) The chemistry of nitroxyl (HNO) and implications in biology, *Coordin. Chem. Rev. 249*, 433-455.

30. Cohen, A. D. (2007) The time-resolved infrared spectroscopic study of an iminooxirane, a nitronic anhydride, and acylnitroso species: The development of novel *N*-hydroxysulfonamides as physiological nitroxyl donors, p 144, Johns Hopkins University.

31. Anderton, B. H. (1970) Reaction of N-ethyl maleimide with malate dehydrogenase, *FEBS Lett. 12*, 65-68.

32. Autry, J. M., and Jones, L. R. (1997) Functional co-expression of the canine cardiac Ca2+ pump and phospholamban in Spodoptera frugiperda (Sf21) cells reveals new insights on ATPase regulation, *J. Biol. Chem. 272*, 15872-15880.

33. Freeman, K., Lerman, I., Kranias, E. G., Bohlmeyer, T., Bristow, M. R., Lefkowitz, R. J., Iaccarino, G., Koch, W. J., and Leinwand, L. A. (2001) Alterations in cardiac adrenergic signaling and calcium cycling differentially affect the progression of cardiomyopathy, *J. Clin. Invest. 107*, 967-974.

34. Haghighi, K., Schmidt, A. G., Hoit, B. D., Brittsan, A. G., Yatani, A., Lester, J. W., Zhai, J., Kimura, Y., Dorn, G. W., MacLennan, D. H., and Kranias, E. G. (2001) Superinhibition of sarcoplasmic reticulum function by phospholamban induces cardiac contractile failure, *J. Biol. Chem. 276*, 24145-24152.

35. Wouters, M. A., George, R. A., and Haworth, N. L. (2007) "Forbidden" disulfides: Their role as redox switches, *Current Protein and Peptide Science 8*, 484-495.

36. Ha, K. N., Masterson, L. R., Hou, Z., Verardi, R., Walsh, N., Veglia, G., and Robia, S. L. (2011) Lethal Arg9Cys phospholamban mutation hinders Ca^{2+}-ATPase regulation and phosphorylation by protein kinase A, *Proc. Natl. Acad. Sci. U. S. A. 108*, 2735-2740.

37. Karim, C. B., Marquardt, C. G., Stamm, J. D., Barany, G., and Thomas, D. D. (2000) Synthetic null-cysteine phospholamban analogue and the corresponding transmembrane domain inhibit the Ca-ATPase, *Biochemistry 39*, 10892-10897.

38. Abu-Baker, S., and Lorigan, G. A. (2006) Phospholamban and its phosphorylated form interact differently with lipid bilayers: A ^{31}P, ^{2}H, and ^{13}C Solid-State NMR Spectroscopic Study, *Biochemistry 45*, 13312-13322.

39. Karim, C. B., Zhang, Z., and Thomas, D. D. (2007) Synthesis of TOAC spin-labeled proteins and reconstitution in lipid membranes, *Nat. Protoc. 2*, 42-49.

40. Arand, M., Friedberg, T., and Oesch, F. (1992) Colorimetric quantitation of trace amounts of sodium lauryl sulfate in the presence of nucleic acids and proteins, *Anal. Biochem. 207*, 73-75.

41. Puchades, M., Westman, A., Blennow, K., and Davidsson, P. (1999) Removal of sodium dodecyl sulfate from protein samples prior to matrix-assisted laser

desorption/ionization mass spectrometry, *Rapid Commun. Mass Spectrom. 13*, 344-349.

42. Jones, L. R., Cornea, R. L., and Chen, Z. (2002) Close proximity between residue 30 of phospholamban and cysteine 318 of the cardiac Ca^{2+} pump revealed by intermolecular thiol cross-linking, *J. Biol. Chem. 277*, 28319-28329.

43. Glaves, J. P., Trieber, C. A., Ceholski, D. A., Stokes, D. L., and Young, H. S. (2011) Phosphorylation and mutation of phospholamban alter physical interactions with the sarcoplasmic reticulum calcium pump, *J. Mol. Biol. 405*, 707-723.

44. Mueller, B., Karim, C. B., Negroshov, I. V., Kutchai, H. C., and Thomas, D. D. (2004) Direct detection of phospholamban and sarcoplasmic reticulum Ca-ATPase interaction in membranes using fluorescence resonance energy transfer, *Biochemistry 43*, 8754-8765.

45. Chen, Z., Akin, B. L., and Jones, L. R. (2007) Mechanism of reversal of phospholamban inhibition of the cardiac Ca^{2+}-ATPase by protein kinase A and by anti-phospholamban monoclonal antibody 2D12, *J. Biol. Chem. 282*, 20968-20976.

46. Sivakumaran, V., Stanley, B. A., Tocchetti, C. G., Ballin, J. D., Caceres, V., Zhou, L., Keceli, G., Rainer, P. P., Lee, D. I., Huke, S., Ziolo, M. T., Kranias, E. G., Toscano, J. P., Wilson, G. M., O'Rourke, B., Kass, D. A., Mahaney, J. E., and Paolocci, N. (2013) HNO enhances SERCA2a activity and cardiomyocyte function by promoting redox-dependent phospholamban oligomerization, *Antioxid. Redox Signaling 19*, 1185-1197.

47. Wong, P. S. Y., Hyun, J., Fukuto, J. M., Shirota, F. N., DeMaster, E. G., Shoeman, D. W., and Nagasawa, H. T. (1998) Reaction between *S*-nitrosothiols and thiols:

Generation of nitroxyl (HNO) and subsequent chemistry, *Biochemistry 37*, 5362-5371.

48. Doyle, M. P., Mahapatro, S. N., Broene, R. D., and Guy, J. K. (1988) Oxidation and reduction of hemoproteins by trioxodinitrate(II). The role of nitrosyl hydride and nitrite, *J. Am. Chem. Soc. 110*, 593-599.

49. Keceli, G., and Toscano, J. P. Reactivity of C-terminal cysteines with HNO, submitted to *Biochemistry*.

50. Lamberth, S., Schmid, H., Muenchbach, M., Vorherr, T., Krebs, J., Carafoli, E., and Griesinger, C. (2000) NMR solution structure of phospholamban, *Helv. Chim. Acta 83*, 2141-2152.

51. Zamoon, J., Mascioni, A., Thomas, D. D., and Veglia, G. (2003) NMR solution structure and topological orientation of monomeric phospholamban in dodecylphosphocholine micelle, *Biophys. J. 85*, 2589-2598.

52. Oxenoid, K., and Chou, J. J. (2005) The structure of phospholamban pentamer reveals a channel-like architecture in membranes, *Proc. Natl. Acad. Sci. U. S. A. 102*, 10870-10875.

53. Traaseth, N. J., Shi, L., Verardi, R., Mullen, D. G., Barany, G., and Veglia, G. (2009) Structure and topology of monomeric phospholamban in lipid membranes determined by a hybrid solution and solid-state NMR approach, *Proc. Natl. Acad. Sci. U. S. A. 106*, 10165-10170.

54. Traaseth, N. J., Ha, K. N., Verardi, R., Shi, L., Buffy, J. J., Masterson, L. R., and Veglia, G. (2008) Structural and dynamic basis of phospholamban and sarcolipin inhibition of Ca^{2+}-ATPase, *Biochemistry 47*, 3-13.

55. Veglia, G., Ha, K. N., Shi, L., Verardi, R., and Traaseth, N. J. (2010) What can we learn from a small regulatory membrane protein?, *Methods Mol. Biol. 654*, 303-319.

56. Verardi, R., Shi, L., Traaseth, N. J., Walsh, N., and Veglia, G. (2011) Structural topology of phospholamban pentamer in lipid bilayers by a hybrid solution and solid-state NMR method, *Proc. Natl. Acad. Sci. U. S. A. 108*, 9101-9106.

57. Karim, C. B., Stamm, J. D., Karim, J., Jones, L. R., and Thomas, D. D. (1998) Cysteine reactivity and oligomeric structures of phospholamban and its mutants, *Biochemistry 37*, 12074-12081.

58. Keceli, G., and Toscano, J. P. (2012) Reactivity of nitroxyl-derived sulfinamides, *Biochemistry 51*, 4206-4216.

59. Keceli, G., Moore, C. D., Labonte, J. W., and Toscano, J. P. (2013) NMR detection and study of hydrolysis of HNO-derived sulfinamides, *Biochemistry 52*, 7387-7396.

60. Ellis, M. K., Hill, S., and Foster, P. M. D. (1992) Reactions of nitrosobenzenes with biological thiols: Identification and reactivity of glutathion-*S*-yl conjugates, *Chem.-Biol. Interactions 82*, 151-163.

61. Eyer, P. (1979) Reactions of nitrosobenzene with reduced glutathione, *Chem.-Biol. Interactions 24*, 227-239.

62. Conway, T. T., DeMaster, E. G., Lee, M. J. C., and Nagasawa, H. T. (1998) Prodrugs of nitroxyl and nitrosobenzene as cascade latentiated inhibitors of aldehyde dehydrogenase, *J. Med. Chem. 41*, 2903-2909.

63. Nagasawa, H. T., Yost, Y., Elberling, J. A., Shirota, F. N., and DeMaster, E. G. (1993) Nitroxyl analogs as inhibitors of aldehyde dehydrogenase: C-Nitroso compounds, *Biochem. Pharmacol. 45*, 2129-2134.

64. Gowenlock, B. G., and Richter-Addo, G. B. (2004) Preparations of *C*-nitroso compounds, *Chem. Rev. 104*, 3315-3340.

65. Demaster, E. G., Redfern, B., and Nagasawa, H. T. (1998) Mechanisms of inhibition of aldehyde dehydrogenase by nitroxyl, the active metabolite of the alcohol deterrent agent cyanamide, *Biochem. Pharmacol. 55*, 2007-2015.

66. Huie, R. E., and Padmaja, S. (1993) The reaction of NO with superoxide, *Free Radical Research Communications 18*, 195-199.

67. Goldstein, S., and Czapski, G. (1995) The reaction of $NO^{\bullet}$ with $O2^{\bullet-}$ and $HO_2^{\bullet}$: A pulse radiolysis study, *Free Radical Biol. Med. 19*, 505-510.

68. Radi, R., Cassina, A., Hodara, R., Quijano, C., and Castro, L. (2002) Peroxynitrite reactions and formation in mitochondria, *Free Radical Biol. Med. 33*, 1451-1464.

69. Denicola, A., Souza, J. M., and Radi, R. (1998) Diffusion of peroxynitrite across erythrocyte membranes, *Proc. Natl. Acad. Sci. U. S. A. 95*, 3566-3571.

70. Ji, Y., and Bennett, B. M. (2003) Activation of microsomal glutathione *S*-transferase by peroxynitrite, *Mol. Pharmacol. 63*, 136-146.

71. Pryor, W. A., Jin, X., and Squadrito, G. L. (1994) One- and two-electron oxidations of methionine by peroxynitrite, *Proc. Natl. Acad. Sci. U. S. A. 91*, 11173-11177.

72. Radi, R., Beckman, J. S., Bush, K. M., and Freeman, B. A. (1991) Peroxynitrite oxidation of sulfhydryls, *J. Biol. Chem. 266*, 4244-4250.

73. Hughes, M. N., Nicklin, H. G., and Sackrule, W. A. C. (1971) The chemistry of peroxonitrites. Part III. The reaction of peroxonitrite with nucleophiles in alkali, and other nitrite producing reactions, *J. Chem. Soc. A*, 3722-3725.

74. Kato, Y., Kawakishi, S., Aoki, T., Itakura, K., and Osawa, T. (1997) Oxidative modification of tryptophan residues exposed to peroxynitrite, *Biochem. Biophys. Res. Commun. 234*, 82-84.

75. Ischiropoulos, H., and Al-Mehdi, A. (1995) Peroxynitrite-mediated oxidative protein modifications, *FEBS Lett. 364*, 279-282.

76. Singh, R. J., Hogg, N., Joseph, J., Konorev, E., and Kalyanaraman, B. (1999) The peroxynitrite generator, SIN-1, becomes a nitric oxide donor in the presence of electron acceptors, *Arch. Biochem. Biophys. 361*, 331-339.

77. Christen, S., Woodall, A. A., Shigenaga, M. K., Southwell-Keely, P. T., Duncan, M. W., and Ames, B. N. (1997) g-Tocopherol traps mutagenic electrophiles such as NOx and complements a-tocopherol: Physiological implications, *Proc. Natl. Acad. Sci. U. S. A. 94*, 3217-3222.

78. Hodges, G. R., Marwaha, J., Paul, T., and Ingold, K. U. (2000) A novel procedure for generating both nitric oxide and superoxide in situ from chemical sources at any chosen mole ratio. First application: Tyrosine oxidation and a comparison with preformed peroxynitrite, *Chem. Res. Toxicol. 13*, 1287-1293.

79. Lancel, S., Zhang, J., Evangelista, A., Trucillo, M. P., Tong, X. Y., Siwik, D. A., Cohen, R. A., and Colucci, W. S. (2009) Nitroxyl activates SERCA in cardiac myocytes via glutathiolation of cysteine 674, *Circ. Res. 104*, 720-723.

80. Toscano, J. P., Brookfield, F. A., Cohen, A. D., Courtney, S. M., Frost, L. M., and Kalish, V. J. (2011) *N*-hydroxylsulfonamide derivatives as new physiologically useful nitroxyl donors, (Johns Hopkins University, USA). U.S. Patent 8,030,356.

81. Beckman, J. S., Beckman, T. W., Chen, J., Marshall, P. A., and Freeman, B. A. (1990) Apparent hydroxyl radical production by peroxynitrite: Implications for endothelial injury from nitric oxide and superoxide, *Proc. Natl. Acad. Sci. U. S. A. 87*, 1620-1624.

82. Laemmli, U. K. (1970) Cleavage of structural proteins during the assembly of the head of bacteriophage T4, *Nature 227*, 680-685.

83. Lockwood, N. A., Tu, R. S., Zhang, Z., Tirrell, M. V., Thomas, D. D., and Karim, C. B. (2003) Structure and function of integral membrane protein domains resolved by peptide-amphiphiles: Application to phospholamban, *Biopolymers 69*, 283-292.

84. Smith, P. K., Krohn, R. I., Hermanson, G. T., Mallia, A. K., Gartner, F. H., Provenzano, M. D., Fujimoto, E. K., Goeke, N. M., Olson, B. J., and Klenk, D. C. (1985) Measurement of protein using bicinchoninic acid, *Anal. Biochem. 150*, 76-85.

85. Mayer, E. J., McKenna, E., Garsky, V. M., Burke, C. J., Mach, H., Middaugh, C. R., Sardana, M., Smith, J. S., and Johnson, R. G., Jr. (1996) Biochemical and biophysical comparison of native and chemically synthesized phospholamban and a monomeric phospholamban analog, *J. Biol. Chem. 271*, 1669-1677.

86. Makino, K., Suzuki, N., Moriya, F., Rokushika, S., and Hatano, H. (1981) A fundamental study on aqueous solutions of 2-methyl-2-nitrosopropane as a spin trap, *Radiat. Res. 86*, 294-310.

87. Froehlich, J. P., Mahaney, J. E., Keceli, G., Pavlos, C. M., Goldstein, R., Redwood, A. J., Sumbilla, C., Lee, D. I., Tocchetti, C. G., Kass, D. A., Paolocci, N., and Toscano, J. P. (2008) Phospholamban thiols play a central role in activation of the cardiac muscle sarcoplasmic reticulum calcium pump by nitroxyl, *Biochemistry 47*, 13150-13152.

88. Sumida, M., Wang, T., Schwartz, A., Younkin, C., and Froehlich, J. P. (1980) The calcium ion-dependent ATPase partial reactions in cardiac and skeletal sarcoplasmic reticulum. A comparison of transient state kinetic data, *J. Biol. Chem. 255*, 1497-1503.

89. Lanzetta, P. A., Alvarez, L. J., Reinach, P. S., and Candia, O. A. (1979) An improved assay for nanomole amounts of inorganic phosphate, *Anal. Biochem. 100*, 95-97.

Chapter 7 – Miscellaneous Reactivity Studies

7.1 HNO Partitioning Preference between Aqueous and Hydrophobic Phases

Studies have shown that, in biological systems, HNO can reach and modify several protein thiols without being trapped by cellular glutathione (GSH).[1, 2] Although the mechanisms involved have not been established, partitioning of HNO into cellular membranes has been suggested as a potential pathway.[3] Lancaster and co-workers have demonstrated that NO partitions into biological membranes by comparing the rates of NO autooxidation in the presence of detergent micelles and in aqueous solution.[4] Unlike NO, HNO undergoes a rapid dimerization reaction, which results in the formation of nitrous oxide (N_2O) and H_2O (Scheme 7-1).[5-7] To learn more about HNO and its properties, we have investigated the HNO partitioning preference between aqueous and hydrophobic phases.

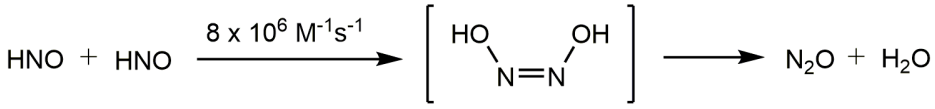

Scheme 7-1. Dimerization of HNO

7.1.1 HNO Partitioning into Bovine Serum Albumin (BSA) via Headspace Gas Chromatography Analyses

N_2O headspace analysis via gas chromatography (GC) is a generally used method for the indirect detection of HNO.[8-12] We intended to determine the HNO partitioning preference for hydrophobic versus aqueous phases by utilizing this technique. Albumin is the major protein in blood plasma and known to have hydrophobic pockets. In fact, albumin binds and holds numerous ligands including noble gases.[13] Moreover, studies have suggested the partitioning of NO and O_2 into the hydrophobic compartments of albumin, which consequently acts an N_2O_3 reserve in plasma.[14] We wished to employ bovine serum albumin (BSA) as the hydrophobic phase and test its potential as a carrier for HNO.

The reaction of BSA with HNO was investigated by analyzing the amount of N_2O in the headspace upon incubation of 0.05 mM unmodified BSA with 0.1 mM HNO-donors, AS or 2-BrPA. These results indicate that 35 and 22% decrease in total N_2O with respect to the amount of N_2O obtained in the absence of traps, pointing to the scavenging of HNO by BSA, consistent with a reported mass spectrometry study.[15] Moreover, the use of 0.5 mM BSA results in all almost complete (91%) quenching of HNO generated from 0.1 mM AS. Although the above results indicate quenching of HNO by BSA, the extent of quenching is lower than expected. Since the single free thiol (Cys34) of BSA might partially exist in a mixed disulfide with cysteine or GSH, we reduced BSA samples with DTT. Following incubation with AS, an approximately 87% decrease was observed in total N_2O with respect to the amount of N_2O obtained in the absence of traps. Table 7-1 shows the percent yields of N_2O obtained from headspace GC analyses.

Table 7-1. Percent yields of N_2O obtained following decomposition of AS under different conditions

Samples[a]	% N_2O Yield[b]
AS	76
AS + GSH	6
AS + BSA	7
AS + NEM-Treated BSA	56
AS + BSA + GSH	5
AS + NEM-Treated BSA + GSH	5

[a] AS (0.1 mM) was incubated in the presence or absence of different traps in 0.1 M PBS containing 100 μM DTPA (pH 7.4) at 37 °C for 30 min under argon. The concentrations of GSH, BSA, and NEM-treated BSA were 0.1, 0.05 and 0.05 mM, respectively.
[b] Percent yields were calculated based on the theoretical maximum of N_2O.

To distinguish between the reactivity of HNO with BSA Cys34 and the potential partitioning of HNO/N_2O into BSA hydrophobic pockets, we intended to block the BSA free thiol with *N*-ethylmaleimide (NEM). Initial control experiments conducted with AS (0.1 mM) and various concentrations of NEM (0-5 mM) indicated that the absolute yield of N_2O is decreased in the presence of NEM under these conditions (Figure 7-1). To avoid complications, the samples were dialyzed against PBS following NEM treatment. No decrease in N_2O was detected upon incubation of dialyzed control samples with AS in the absence of BSA.

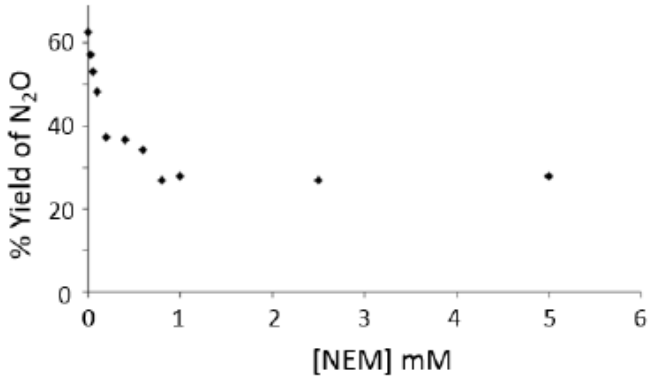

Figure 7-1. Percent yield of N_2O upon treatment of NEM (0-5 mM) with AS (0.1 mM). Yields were calculated based on the theoretical maximum yield of N_2O.

As shown in Table 7-1, incubation of NEM-treated BSA (0.05 or 0.1 mM) with AS (0.1 mM) resulted in a decrease in the percent N_2O yield compared with the percent N_2O yield obtained from AS in the absence of traps. Moreover, the decrease in percent N_2O yield is less in the presence of NEM-treated BSA compared with unmodified BSA. Although HNO is known to react with Trp, making Trp134 and Trp213 of BSA potential targets, the presence of oxygen is required for product formation.[16, 17] Overall, these results potentially suggest the partitioning of HNO/N_2O into BSA hydrophobic pockets.

To be able to distinguish between HNO and N_2O partitioning, we have examined the partitioning of standard N_2O between buffer and headspace. Our initial results did not show any significant changes in the partitioning coefficient of N_2O due to the addition of 0.9 mM BSA or 2.5 mM NEM to buffer, indicating the partitioning preference of HNO rather than N_2O into BSA hydrophobic pockets. However, further experiments are needed to confirm these findings.

We have also conducted preliminary experiments to investigate the potential protective effect of BSA on HNO against trapping by GSH. Since GSH is an aqueous thiol, it will quench only the HNO that has partitioned to the aqueous phase. The effect of

GSH on percent N_2O yield was first determined by incubating GSH (0-0.5 mM) with AS (0.1 mM). As shown in Figure 7-2, almost complete trapping was observed with 0.1 mM GSH. No significant difference was observed in percent N_2O yield upon treatment of AS with GSH in the presence or absence of NEM-treated BSA, indicating the lack of a protective effect of BSA on HNO (Table 7-1).

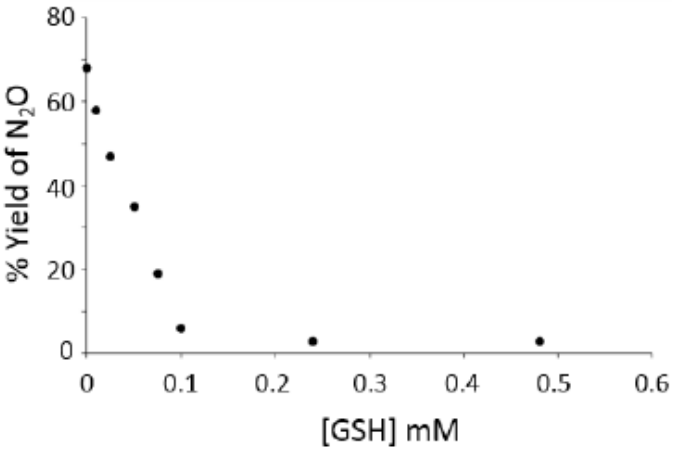

Figure 7-2. Percent yield of N_2O upon treatment of GSH (0-0.5 mM) with AS (0.1 mM). Yields were calculated based on the theoretical maximum yield of N_2O.

7.1.2 HNO Partitioning into Detergent Micelles via High Pressure Liquid Chromatography Analyses

The partitioning preference of HNO into hydrophobic versus aqueous phases was also investigated by employing detergent micelles as the hydrophobic phase. For this purpose, we investigated the trapping of HNO by GSH in the presence of sodium dodecyl sulfate (SDS) or Tween 20 micelles and analyzed the HNO-derived GSH modifications by high pressure liquid chromatography (HPLC). As mentioned previously, HNO generally reacts with thiols to form a disulfide or a sulfinamide depending on the concentration of

thiol.[18, 19] If HNO has a partitioning preference for hydrophobic phases, then the presence of detergent micelles would provide protection against the scavenging of HNO by GSH, resulting in a decrease in HNO-derived modifications.

We confirmed the formation of detergent micelles by the change in λ_{max} of Coomassie Brilliant Blue R.[20] Treatment of SDS in 0.1 M PBS containing 100 μM EDTA (pH 7.4) with Coomassie Brilliant Blue R at room temperature and 37 ^{o}C resulted in λ_{max} to shift from 560 to 591 nm at 0.14 and 6.4 mM SDS, respectively. Similar experiments conducted with Tween 20 in buffer at room temperature demonstrated micelle generation at 0.08 mM Tween 20. These results are comparable to the reported critical micelle concentration (cmc) values for SDS (8.9 mM at 37 ^{o}C)[21] and Tween 20 (0.06 mM at room temperature)[22].

The trapping of HNO by GSH was investigated by incubating GSH (0.5-2 mM) with AS (1 or 5 mM) at physiological pH and temperature in the presence or absence of SDS (10 or 700 mM) or Tween 20 (81 mM) to ensure micelle formation. Under these conditions the HNO-derived modifications mainly consisted of glutathione disulfide (GSSG) as expected.[23] In all cases, similar GSSG yields were obtained in the presence or absence of detergent micelles, suggesting the lack of a protective effect on HNO towards GSH scavenging at least at these GSH/micelle concentrations (Figure 7-3). Incubations carried out under anaerobic conditions also produced similar results, confirming that GSSG formation is due to HNO treatment. Consistent with these, no significant trend was observed in GSSG yields upon employment of varied concentrations of SDS (0-300 mM) or Tween 20 (0-81 mM) (Figure 7-4). As a control, the solubility of GSH in Tween 20 was tested and GSH was found to be insoluble at concentrations as low as 0.06 mM.

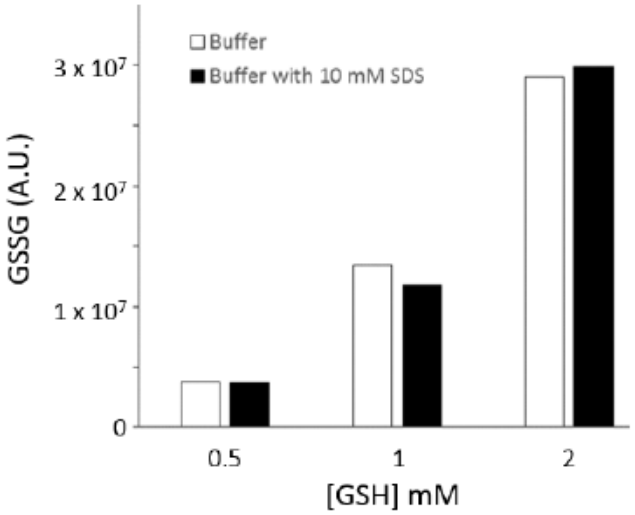

Figure 7-3. Area of glutathione disulfide (GSSG) peak detected by HPLC upon treatment of glutathione (GSH) (0.5-2 mM) with 1 mM AS in pH 7.4 PBS in the absence (□) or presence of 10 mM SDS (■) at 37 ºC for 30 min under argon.

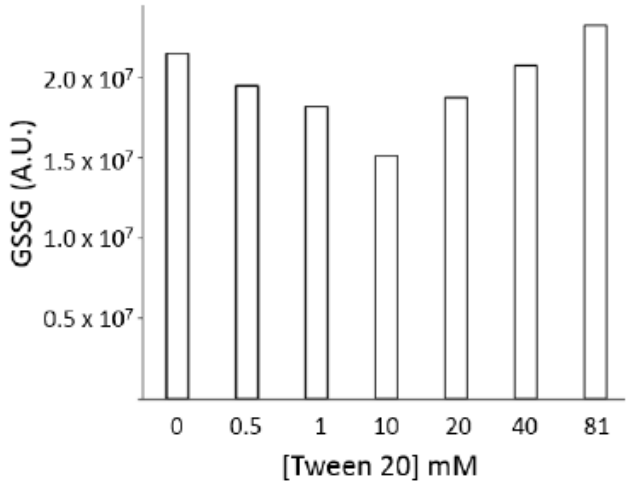

Figure 7-4. Area of glutathione disulfide (GSSG) peak detected by HPLC upon treatment of glutathione (GSH) (2 mM) with 5 mM AS in pH 7.4 PBS in the presence of Tween 20 (0-81 mM) at room temperature for 2 h at room temperature.

Since thermal decomposition of AS to form HNO has a half-life of approximately 2.4 min under physiological conditions, we conducted preliminary studies to investigate the effects of rapid HNO introduction on partitioning. Upon photolysis at 254 nm, the

complete decomposition of 5 mM AS was achieved in 7 min as detected by UV-visible spectroscopy. No significant difference was observed in GSSG yields upon photolysis of AS in the presence or absence of 700 mM SDS.

Although the partitioning preference of HNO into hydrophobic or aqueous phases could not be determined unambiguously, our overall results indicate that neither BSA nor detergent micelles are able to protect HNO from trapping by GSH under the conditions examined. However, further experiments are required to distinguish between the lack of HNO partitioning into hydrophobic phases and the presence of slow partitioning, which is outcompeted by thiol reactivity.

7.1.3 Experimental Methods

Reagents. Bovine serum albumin (BSA), glutathione (GSH), *N*-ethylmaleimide (NEM), 5,5'-dithiobis-(2-nitrobenzoic acid) (DTNB), sodium dodecyl sulfate (SDS), and dithiothreitol (DTT) were of the highest purity available and purchased from Sigma (St. Louis, MO). Coomassie Brilliant Blue R was obtained from Biorad. Nitrous oxide (45 ppm) balanced with nitrogen was obtained from Airgas. Bicinchoninic acid (BCA) assay kit, dialysis tubing, HPLC grade acetonitrile (ACN) and Tween 20 were purchased from Thermo Fisher Scientific (Rockford, IL). The syntheses of HNO-donors, Angeli's salt ($Na_2N_2O_3$, AS)[24] and 2-bromo-*N*-hydroxybenzenesulfonamide (2-BrPA)[25] were carried out as previously described.

Preparation of BSA Samples. BSA was dissolved in 0.1 M phosphate-buffered saline (PBS) containing 100 μM EDTA at pH 7.4 to have a final concentration of 0.05, 0.1 mM. The samples were incubated with 0.5 or 1 mM NEM (as indicated) for 1 h at room temperature to block BSA free thiol (Cys 34) and dialyzed overnight against 0.1 M PBS

containing 100 μM EDTA (pH 7.4) with three solution changes to remove excess NEM. Control experiments were also conducted in the absence of BSA or NEM. In some cases, BSA samples were reduced with 2 mM DTT and dialyzed against 0.1 M PBS for 18 h prior to NEM treatment. The total protein concentrations were determined at various stages of sample preparation by using a standard BCA assay.[26]

Incubations with HNO-Donors. Stock solutions of AS and 2-BrPA were prepared in 0.01 M NaOH and ACN, respectively, and used within 15 min of preparation. For headspace GC analysis, the samples (5 ml) containing BSA (0.05, 0.1 or 0.5 mM), GSH (0-0.5 mM), or NEM (0-5 mM) in 0.1 M PBS containing 100 μM EDTA at pH 7.4 were placed in 15 ml vials sealed with rubber septa and purged with argon as reported previously[27]. Following the introduction of AS (0.1 mM) or 2-BrPA (0.1 mM) via a gastight syringe, the samples were then incubated at 37 ºC and 1 atm for 1.5 h to ensure complete decomposition of HNO-donor and equilibration of N_2O with the headspace. The samples were then analyzed for N_2O by headspace GC analyses. In all cases, the final concentration of ACN was less than or equal to 1% (v/v). To determine if NEM-treated BSA could protect HNO from GSH scavenging, for some experiments BSA samples were incubated with AS in the presence of 0.05 or 0.1 mM GSH (as indicated). Side-by-side control experiments were also conducted in the absence of any HNO scavengers to detect the maximum amount of N_2O that could be obtained.

For HPLC analysis, GSH was dissolved in 0.1 M PBS containing 100 μM EDTA in the presence of 0-700 mM SDS or 0-81 mM Tween 20 to have a final concentration of 0.5-2 mM. The samples were then incubated with 1 or 5 mM AS for 30 min at 37 ºC or 2 h at room temperature (as indicated). Samples containing Tween 20 were incubated and

stored in the dark due to the light sensitivity of this detergent. In some cases, incubations with AS were carried out under argon saturated conditions as described above. The samples were then filtered through 0.45 μm filters and analyzed by HPLC.

Incubations with N_2O. To determine whether the presence of NEM or BSA affects the partitioning coefficient of N_2O between the solution and the headspace, empty vials were purged with N_2O (45 ppm). Following the addition 89 μM NEM-treated BSA in buffer in the presence of a ventilation needle to keep the pressure constant, the samples were incubated at 37 ^oC for 1.5 h. Then the amount of N_2O in the headspace was determined by GC analysis.

Headspace GC Analyses. All headspace GC analyses were conducted on a Varian CP-3800 instrument equipped with 1041 manual injector, electron capture detector (ECD), and a 25 m 5Å molecular sieve capillary column. The injector, column oven, and ECD were operated at 200, 200 and 300 ^oC, respectively, and ultrahigh purity nitrogen was used as the carrier gas. The column flow was set to 8 ml/min. All injections were conducted by using a 100 μL gastight syringe equipped with a sample-lock. Calibration curves were prepared by using an N_2O tank and the absolute amount of N_2O in the samples were determined by employing ideal gas law and Henry's law constant as described previously.[27] The percent yields of N_2O were calculated based on the theoretical maximum of N_2O. In some cases the relative percent yields were determined by normalizing the amount of N_2O with respect to the total amount of N_2O obtained from AS in the absence of HNO scavengers.

Quantification of Free Thiol by DTNB Assay. The amount of free thiol in various BSA or GSH samples in 0.1 M PBS with 100 μM EDTA at pH 7.4 were quantified by

using DTNB titration.[28] The concentration of free thiol was determined by utilizing the literature extinction coefficient (λ_{412}=13600 m^{-1} cm^{-1}).[28]

Photolysis of AS. GSH (2 mM) was dissolved in 0.1 M PBS containing 100 μM EDTA at pH 7.4 in the presence or absence of 700 mM SDS. Upon the addition of 5 mM AS, the samples were photolyzed at 254 nm for 7 min. The samples were then analyzed by UV-visible spectroscopy. Following storage of samples in the fridge overnight, the samples were also analyzed by HPLC. Control samples prepared in the absence of AS were photolyzed and analyzed under the same conditions.

HPLC Analyses. All analyses were performed on a Waters HPLC equipped with Delta 600 pump system, dual wavelength absorbance detector, and manual injector. The samples were analyzed on an Apollo C_{18} reverse-phase column using a literature method.[23] The peaks were assigned by co-injection with standards. The peaks were integrated by using Waters Millenium software.

7.2 Studies with Glutathione Reductase and Glutaredoxin System

As mentioned previously, treatment of papain, a cysteine protease, with HNO results in the inhibition of enzyme activity due to the formation of a sulfinamide at its active site thiol.[29, 30] In the presence of excess thiol, the sulfinamide modification of papain can be reduced back to free thiol, accompanied by a recovery of papain activity (Chapter 2).[31] We investigated the effect of glutathione reductase and glutaredoxin system (Scheme 7-2)[32] on sulfinamide reduction.

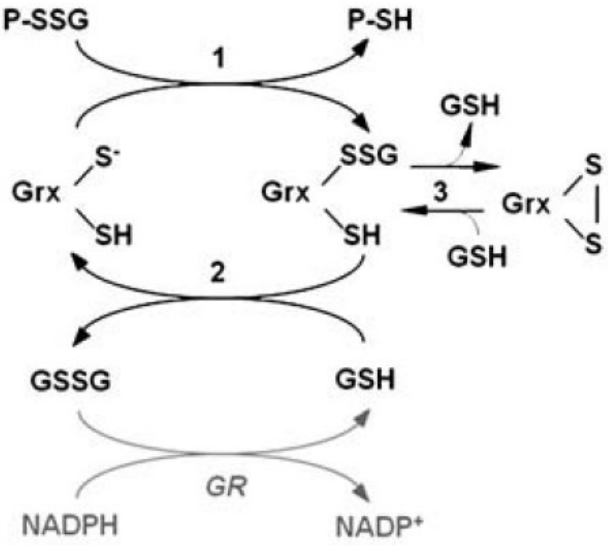

Scheme 7-2. Traditional model of glutaredoxin (Grx) catalysis. The mechanism involves the reduction of S-glutathionylated proteins (P) by Grx in the presence of glutathione reductase (GR), GSH, and NADPH. Gallogly, M. M., Starke, D. W., and Mieyal, J. J. (2009) Mechanistic and kinetic details of catalysis of thiol-disulfide exchange by glutaredoxins and potential mechanisms of regulation, *Antioxid. Redox Signaling 11*, 1059-1081.

7.2.1 Reactivity of HNO-Treated Papain with Glutathione Reductase and Glutaredoxin System

Glutathione reductase (GR) is a homodimeric enzyme (ca. 100 kDa), which reduces glutathione disulfide (GSSG) to two molecules of glutathione (GSH) in an NADPH-dependent process.[33]

Since sulfinamide modification on papain can be reduced by GSH,[31] we tested if the reduction could be facilitated in the presence of GR and NADPH. Incubation of sulfinamide-modified papain with 1 or 5 mM GSH in the presence of catalytic amount of GR and 0.2 mM NADPH at physiological pH and temperature did not increase the observed gain of activity compared with the previous results (Figure 7-5). However, this

ineffectiveness of GR could be due to its inhibition by physiological levels of GSH.[34] Although a slight recovery in papain activity is observed upon treatment with GR and NADPH in the absence of GSH, it was not significant (Figure 7-5). Similarly no significant change in activity was detected upon incubation of HNO-treated papain with GR or NADPH in the absence of GSH.

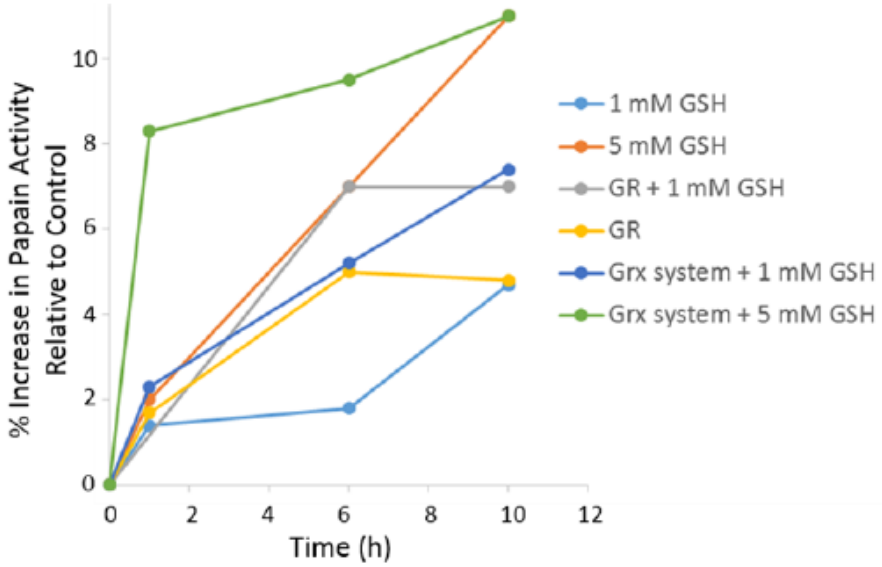

Figure 7-5. Reduction of HNO-derived sulfinamide in papain under different conditions. Previously activated papain (0.2 mg/ml) was treated with 0.1 mM AS. The samples were incubated with 1 or 5 mM GSH in the presence or absence of glutathione reductase (GR, 6 μg/ml) and NADPH (0.2 mM), or glutaredoxin (Grx) system (0.026 units/ml Grx, 6 μg/ml GR, 0.2 mM NADPH) in phosphate buffer at 37 ºC.

Glutaredoxins (Grx) are 11-13 kDa enzymes, which are members of the thioredoxin superfamily and are involved in the deglutathionylation of glutathionylated substrates or protein disulfide substrates.[32, 33] Studies have reported the slow deglutathionylation of papain mixed disulfide (papain-SSG) by Grx in the presence of GSH.[35] Since the reduction of the sulfinamide on the papain active site cysteine back to free thiol presumably involves a papain-SSG intermediate (Chapter 2),[31] we have conducted preliminary experiments to

investigate the effect of Grx system on the reduction of sulfinamide-modified papain by GSH.

The presence of 0.2 mM NADPH and catalytic amounts of Grx and GR did not result in a significant increase in gain of activity upon treatment of sulfinamide-modified papain with 1 or 5 mM GSH (Figure 7-5). It should be also noted that possible inhibition of GR caused by higher concentration of GSH might have affected the overall efficiency of the Grx system. Although our results indicate the lack of a significant impact of GR or Grx system on sulfinamide reduction in papain under these conditions, further studies at low GSH levels and shorter incubation times are needed to determine the exact effects of both enzymes.

7.2.2 Experimental Methods

Reagents. Glutathione (GSH), papain, N_{α}-Benzoyl-L-arginine 4-nitroanilide hydrochloride (L-BAPNA), glutathione reductase (GR), β-Nicotinamide adenine dinucleotide 2′-phosphate reduced tetrasodium salt hydrate (NADPH), bovine serum albumin (BSA), and dithiothreitol (DTT) were of the highest purity available and purchased from Sigma (St. Louis, MO). Glutaredoxin-1 (Grx) was purchased from ATGen. 2-Hydroxyethyl disulfide (HED) was purchased from Thermo Fisher Scientific (Rockford, IL). The synthesis of HNO-donor, Angeli's salt ($Na_2N_2O_3$, AS) was carried out as previously described.[24] Milli Q water was used for all purifications and experiments.

Activation of Papain. A 0.5 mg/ml papain solution was prepared by dissolving the lyophilized enzyme in 82 mM sodium phosphate buffer with 410 μM DTPA at pH 7.4. The papain sample was activated by treating it with 2 mM DTT for 1.5 h at room temperature to reconvert its single free cysteine to the sulfhydryl form. The activated

enzyme was stored at -20 °C. Before analysis, it was thawed and desalted with Zeba spin desalting columns to remove excess DTT. The papain solution was then diluted to 0.2 mg/ml with sodium phosphate buffer. To overcome batch to batch variation in the actual activity of the reduced papain preparation, all activity results are expressed as a percentage of the indicated control.

Determination of Grx Activity. Grx activity was determined by following a slightly modified literature procedure.[36-38] Briefly, a solution of 1 mM GSH, 0.7 mM HED, 0.01 mg/ml BSA, 0.2 mM NADPH, 6 μg/ml GR, and 2 mM EDTA in 0.1 M Tris-HCl at pH 7.4 was incubated at 30 ^{o}C for 3 min. The kinetic analysis was started by the addition of Grx in 20 mM Tris-HCl with 10% glycerol at pH 8 to have a final concentration of 0.5 μg/ml. The reaction was followed at 340 nm for 5 min by UV-visible spectroscopy (ε_{340}=6200 $M^{-1}cm^{-1}$).[39] 1 unit corresponds to 1 μmole of NADPH oxidized per minute at 30 °C per ml of Grx.

Incubation of Papain Solutions and Activity Assay. A solution of 0.2 mg/ml activated papain in 82 mM sodium phosphate buffer with 410 μM DTPA at pH 7.4 was divided into two and the aliquots were incubated with 0 or 0.1 mM AS at 37 °C for 30 min. Following the addition of 1 or 5 mM GSH, 0.2 mM NADPH, 6 μg/ml GR, and 0.026 units/ml Grx were then added to both solutions to have the required concentration and the samples were incubated at 37 °C. Aliquots were taken from each sample at certain time intervals, and immediately analyzed by a 20 min kinetic assay using L-BAPNA as the substrate.[29] For some experiments, the samples were incubated with NADPH (0.2 mM) and GR (6 or 27 μg/ml) GR in the presence or absence of GSH (1 or 5 mM) to investigate the reduction of sulfinamide-modified papain by GR. Also HNO-treated samples were

separately incubated with 0.2 mM NADPH or 27 μg/ml GR to test their effects. In all cases, the sample incubated without AS served as the control sample to correct for the decrease in papain activity due to long incubations. All the spectrophotometric analyses were conducted on a Hewlett-Packard 8453 Diode Array Spectrophotometer.

7.3 Studies with Nitrite

One of the most common HNO-donors is Angeli's salt, which produces nitrite (NO_2^-) as the byproduct. Nitrite is known to produce nitrosating species, especially under acidic conditions (Scheme 7-3).[40] Also, recent reviews highlight the role of nitrite in NO production.[40-42] To understand potential side reactions due to AS-produced nitrite, we investigated NO_2^- reactivity.

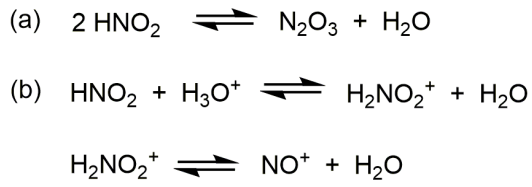

Scheme 7-3. Formation of nitrosating species from nitrite under acidic conditions.

7.3.1 Nitrite-Induced Complications in Sulfinamide Formation

Thiols react with nitrosating species to form S-nitrosothiols (RSNO), which can react further with excess thiol to release HNO.[19] To determine if NO_2^- acts as a nitrosating agent under physiological conditions, we tested S-nitrosation of β-mercaptoethanol (BME) in the presence of metal chelator, DTPA, by ^{15}N NMR. Incubation of 0.1 M $^{15}NO_2^-$ with equimolar amount of BME at physiological pH and temperature did not result in the detection of the corresponding nitrosothiol species (BME-S^{15}NO). Similarly, *S*-

nitrosoglutathione (GSNO) was not observed by UV-visible spectroscopy upon treatment of GSH with NO_2^-. These results are consistent with previously reported kinetic studies.[43]

Studies indicate that freezing nitrite-containing samples in sodium phosphate buffers at neutral pH results in the S-nitrosation of cysteine residues.[44] Moreover, this process has been attributed to the formation of nitrosating species from nitrite due to the pH shift (from pH 7.4 to ca. 4-5) in sodium phosphate buffers during freezing.[44, 45] Consistent with these reports, we observed ^{15}N-labeled S-nitrosoglutathione ($GS^{15}NO$, 769 ppm) by ^{15}N NMR upon freezing 10 mM ^{15}N-labeled nitrite ($^{15}NO_2^-$) with equimolar amounts of GSH in pH 7.4 and 8.5, but not in pH 11, sodium phosphate buffer (Figure 7-6). In all cases, no $GS^{15}NO$ could be detected prior to freezing.

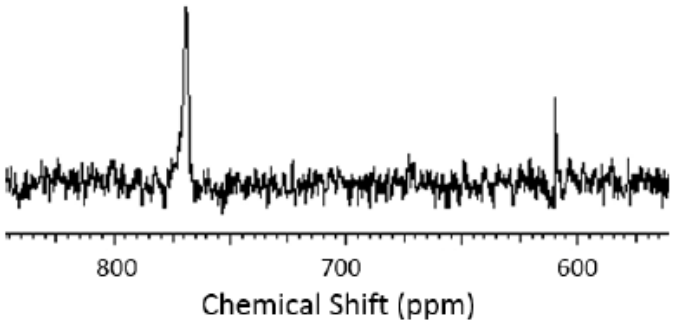

Figure 7-6. Selected region of ^{15}N NMR spectrum of $^{15}NO_2^-$ (10 mM) frozen with GSH (10 mM) in 0.25 M sodium phosphate buffer containing 50 μM DTPA at pH 7.4. Peaks at 609 and 769 ppm were assigned to $^{15}NO_2^-$ and $GS^{15}NO$, respectively.

To learn more about this effect and understand the potential complications in HNO-derived modifications, we examined thiol samples in the presence of NO_2^- by NMR spectroscopy. Surprisingly, freezing of equimolar amounts of NO_2^- and BME in pH 7.4 sodium phosphate buffer at -75 ^oC resulted in the detection of a small peak at 5.68 ppm (Figure 7-7), which corresponds to BME sulfinamide.[30] Larger amounts of the BME

sulfinamide were detected in the presence of 1 mM NO_2^- and 50 mM BME. Moreover, upon conducting the experiment with $^{15}NO_2^-$ (Figure 7-7), the sulfinamide peak was observed by our ^{15}N-edited NMR method for sulfinamide detection (Chapter 3).[30] Similarly, freezing of $^{15}NO_2^-$ with a cysteine-containing peptide, VYPCLA, produced small amount of the corresponding sulfinamide. It should also be noted that this effect is not observed upon freezing of samples that had been previously incubated with equimolar or excess amounts of AS due to the complete modification of thiols by HNO. As shown in Chapter 3, no unlabeled sulfinamide is observed upon prior treatment of BME with 10-fold excess ^{15}N-AS, which decomposes to produce ^{15}N-labeled HNO ($H^{15}NO$) and unlabeled NO_2^-. Freezing of 1 mM nitrate (NO_3^-) and 50 mM BME under the same conditions did not result in any sulfinamide formation.

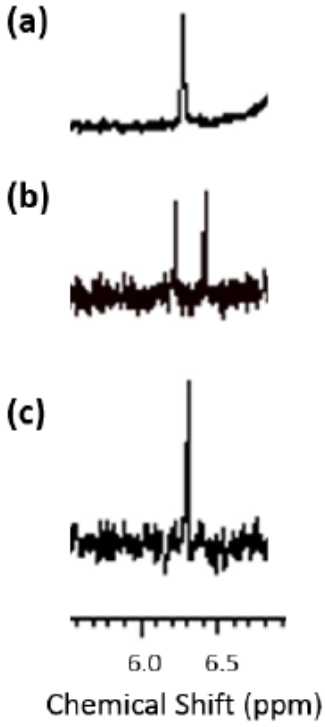

Figure 7-7. Selected region of ^{1}H NMR spectrum of (a) NO_2^- (1 mM), (b) $^{15}NO_2^-$ (10 mM), and (c) ^{15}N-edited NMR spectrum of $^{15}NO_2^-$ (10 mM) frozen with BME (10 mM) in 10 mM sodium phosphate buffer containing 50 μM DTPA at pH 7.4 showing NH and ^{15}NH peaks of BME sulfinamide.

Since sulfinamide formation is considered to be unique to HNO among reactive nitrogen species, these observations could be explained by the formation of nitrosating species from NO_2^- during the freezing process in sodium phosphate buffer, and consequent formation of S-nitrosothiol. As mentioned above, reaction of S-nitrosothiols with excess thiol would result in the formation of HNO,[19] followed by sulfinamide generation, which is expected to be promoted under acidic conditions.

We have also investigated this process with sodium phosphate buffers at different pH values. The BME sulfinamide was observed at pH 8.5; however, no sulfinamide formation was detected upon the freezing of NO_2^- with BME in pH 5 or pH 11 buffer.

Despite the low yields of sulfinamides obtained, these results demonstrate a potential nitrite-induced complication in studying sulfinamide formation and emphasize the need for control experiments when working with AS.

7.3.2 Experimental Methods

Reagents. Glutathione (GSH) and β-mercaptoethanol (BME), sodium nitrite ($NaNO_2$), and sodium nitrate ($NaNO_3$) were of the highest purity available and purchased from Sigma (St. Louis, MO). ^{15}N-labeled sodium nitrite ($Na^{15}NO_2$) and deuterated dimethyl sulfoxide (DMSO-d_6) were obtained from Cambridge Isotope Labs (Andover, MA). Synthesis and purification of VYPCLA was carried out as described in Chapters 2 and 3. Milli Q water was used for all purifications and experiments.

Treatment of Thiols with Nitrite. $NaNO_2$ or $Na^{15}NO_2$ were dissolved in 10 mM phosphate buffer with 50 μM DTPA at various pH values to have a final concentration of 1 mM. β-Mercaptoethanol (BME) or VYPCLA were added to the nitrite solution in buffer to have a final concentration of 1 or 50 mM. The samples were frozen at -75 ^oC. Following lyophilization, the samples were dissolved in DMSO-d_6 and analyzed by ^1H NMR or ^{15}N-edited ^1H NMR.

For direct ^{15}N NMR experiments, $Na^{15}NO_2$ was dissolved in 0.25 M sodium phosphate buffer with 50 μM DTPA at various pH values to have a final concentration of 10 mM. Following the addition of 10 mM GSH, the samples were frozen at -75 ^oC and lyophilized. The samples were then dissolved in 10% D_2O and analyzed by ^{15}N NMR. In some cases, BME (0.1 M) was incubated with 0.1 M $^{15}NO_2^-$ in 0.25 M sodium phosphate buffer with 50 μM DTPA (pH 7.4) at 37 ^oC and followed by ^{15}N NMR for 45 min.

Treatment of Thiols with Nitrate. $NaNO_3$ was dissolved in 10 mM phosphate buffer with 50 μM DTPA at various pH values to have a final concentration of 1 mM. BME was added to the nitrate solution in buffer to have a final concentration of 1 mM. The samples were frozen at -75 ºC. Following lyophilization, the samples were dissolved in DMSO-d_6 and analyzed by ^{1}H NMR.

NMR Analyses. All ^{1}H-NMR and ^{15}N-edited ^{1}H 1D-NMR analyses were carried out on a Bruker Avance 400 MHz FT-NMR spectrometer. ^{1}H NMR and ^{15}N-edited ^{1}H 1D-NMR analyses were carried out in DMSO-d_6 at 303 K. ^{15}N-edited ^{1}H 1D-NMR spectra were acquired using the HSQC pulse sequence for selection. Chemical shifts are reported in parts per million (ppm) relative to residual DMSO (2.49 ppm for ^{1}H) or residual H_2O (4.7 ppm for ^{1}H).

UV-Visible Spectroscopy Analyses. $NaNO_2$ (10 mM) was dissolved in 0.25 M sodium phosphate buffer with 50 μM DTPA (pH 7.4) and incubated at 37 ºC for 45 min. Following the addition of GSH to have a final concentration of 10 mM, the sample was analyzed before and after freezing (-75 ºC) by UV-visible spectroscopy at 25 ºC. All the spectrophotometric analyses were conducted on a Hewlett-Packard 8453 Diode Array Spectrophotometer.

7.4 Studies on the Reactivity of HNO with Bovine Serum Albumin

As mentioned in section 7.1.1, bovine serum albumin (BSA) has a single free thiol (Cys34) which has been shown to react with HNO in a recent study.[13, 15] Moreover, the formation of a cyclic sulfinamide involving Cys34 and a nearby Lys or Arg upon treatment of BSA with HNO has been proposed (Scheme 7-4).[15] However, bottom-up mass

spectrometric approaches to identify the modification were unsuccessful.[15] We have conducted preliminary experiments to learn more about the nature of this modification.

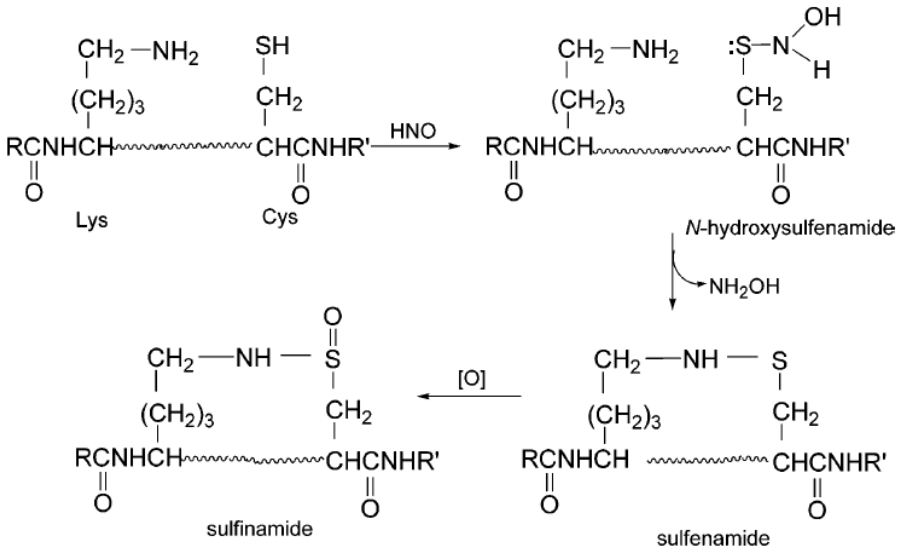

Scheme 7-4. Proposed reaction of HNO with BSA. Shen, B., and English, A. M. (2005) Mass spectrometric analysis of nitroxyl-mediated protein modification: Comparison of products formed with free and protein-based cysteines, *Biochemistry 44*, 14030-14044.

7.4.1 Detection of BSA by Reflector In-Source Decay MALDI Mass Spectrometry

We wished to investigate the HNO-derived cysteine modification on BSA by utilizing mass spectrometry (MS). Although BSA was observed by MALDI-MS and ESI-MS techniques, the resolution was not high enough to investigate this modification. Since HNO-derived modifications might not be completely stable to tryptic digestion conditions,[46] we decided to employ a top-down mass spectrometric approach.

Reflector in-source decay (ISD) is a MALDI-MS method used to obtain sequence information from pure, intact proteins.[47, 48] This technique depends on the spontaneous

fragmentation of molecular ions within the ion source to produce mainly c-type ions from the N-terminus and y- or z-type of ions from the C-terminus (Scheme 7-5).[47, 48] The reflector ISD-MALDI-MS technique is useful for m/z range of 1000-4000 (from approximately the 10th to the 40th residue from each terminal). However, ion yields are typically poor and generally 5-20 pmol of analyte is required on the MALDI plate.[47, 48]

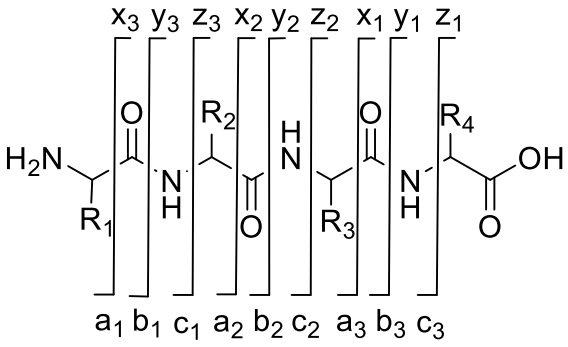

Scheme 7-5. Fragment ions produced by CID from protonated peptides. Biemann, K. (1992) Mass spectrometry of peptides and proteins, *Annu. Rev. Biochem. 61*, 977-1010.

Initial studies with different matrices and various protein concentrations revealed that "super-DHB" (a mixture of 2,5-dihydroxybenzoic acid and 2-hydroxy-5-methoxybenzoic acid) and a theoretical amount of 150 pmol of BSA gave the best results. BSA N-terminal amino acids up to Glu63 could be detected. Moreover, increasing the number of scans allowed us to get sequence information up to Ala78 (Figure 7-8). It should also be noted that the Cys34 b-ion was observed rather than the c-ion due to the cyclic structure of the following Pro35.[49]

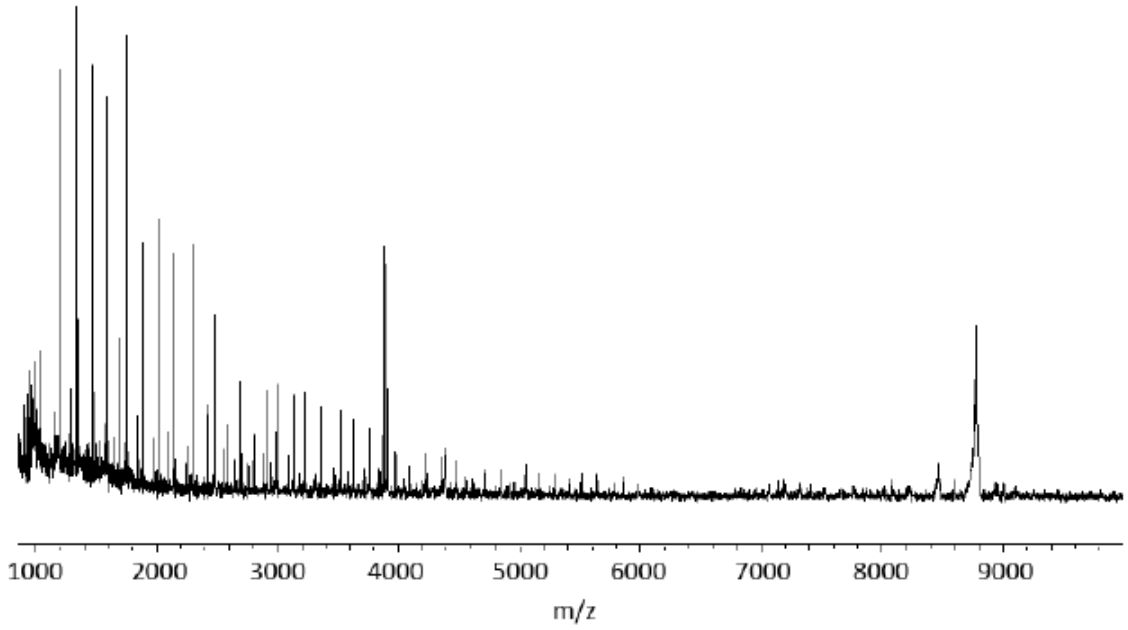

Figure 7-8. Selected region of reflector ISD-MALDI-MS spectrum.

7.4.2 Studies to Determine HNO-Derived Cysteine Modification on BSA

Recent mass spectrometry studies indicate a mass increase of +14 Da on BSA following incubation with AS, which could correspond either to the formation of an intramolecular, cyclic sulfinamide with a nearby Lys or Arg residue (Scheme 7-4), or the RS^{+}=NH intermediate shown in Scheme 7-6.[15, 18, 19, 50]

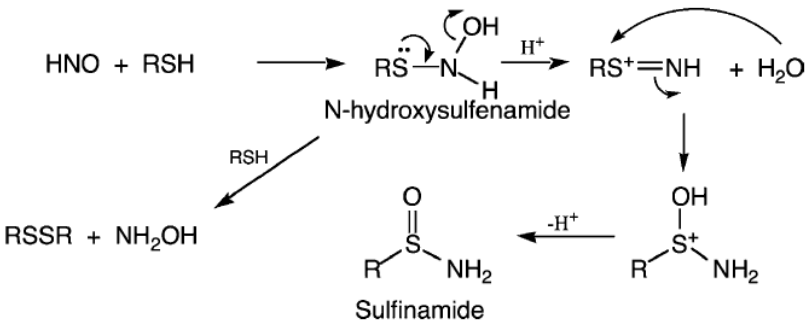

Scheme 7-6. Reaction of HNO with thiols showing the proposed intermediates. Lopez, B. E., Rodriguez, C. E., Pribadi, M., Cook, N. M., Shinyashiki, M., and Fukuto, J. M. (2005) Inhibition of yeast glycolysis by nitroxyl (HNO): A mechanism of HNO toxicity and implications to HNO biology, *Arch. Biochem. Biophys. 442*, 140-148.

To gain more insight into the nature of HNO-derived cysteine modification, we analyzed BSA in the presence or absence of HNO treatment. Reflector ISD-MALDI-MS studies demonstrated a gap in sequence readout (starting from Cys34) upon treatment of BSA with HNO, consistent with the presence of a cyclic structure (Figure 7-9). Although some peaks with m/z values >4500 were detected in some HNO-treated BSA samples, unambiguous assignments were not possible due to the low resolution observed in these regions. However, in some cases, a- or c-ions, which could be assigned to Val77 or Ala78 were detected. These observations might suggest that the cyclic structure is located within the Cys34-Ala78 region. Surprisingly, the reported +14 Da increase in mass was not observed. It should also be noted that a peak which could be assigned to a regular sulfinamide or sulfinic acid was detected in some cases, however the lack of enough resolution or intensity precluded unambiguous assignment.

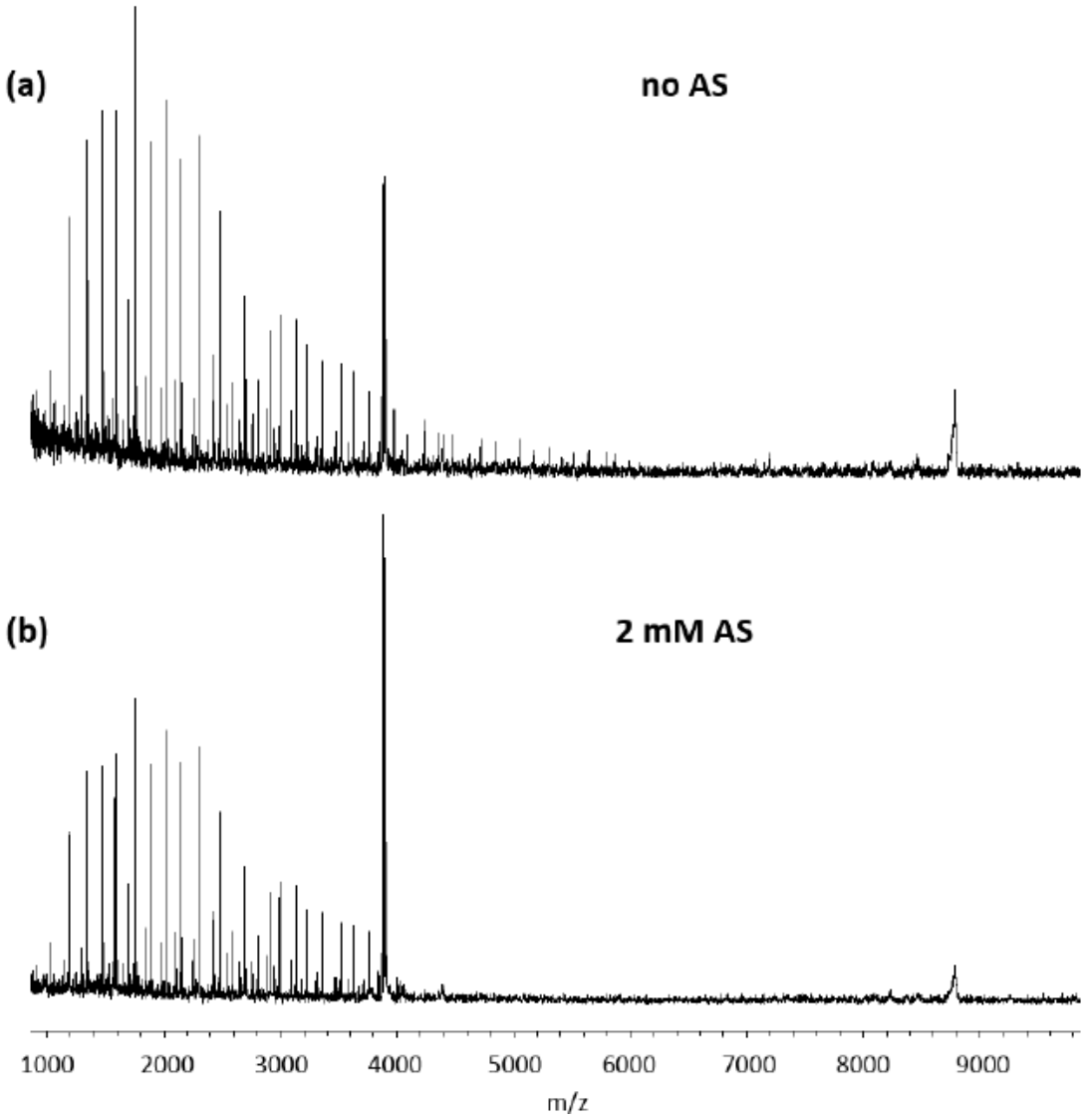

Figure 7-9. Selected region of reflector ISD-MALDI-MS spectrum showing BSA incubated (a) in the absence or (b) in the presence of 2 mM AS.

We also analyzed H^{15}NO-treated BSA with our ^{15}N-edited NMR method for sulfinamide detection.[30] As mentioned previously, this method detects the protons bonded to ^{15}N nuclei.[51] In the presence of a regular sulfinamide formed with H^{15}NO, the incorporation of ^{15}N is observed and consequently sulfinamide ^{15}NH peaks are detected.[30] However, in the case of an intramolecular, cyclic sulfinamide formed with a nearby Lys or Arg, no ^{15}N incorporation is expected. No significant ^{15}NH peaks were detected upon

treatment of BSA with excess ^{15}N-labeled AS (^{15}N-AS), indicating the lack of detectable amounts of regular sulfinamide.

As shown in Scheme 7-6, exposure to HNO could also result in disulfide formation. Although not likely, the presence of an HNO-derived BSA dimer was investigated by SDS-PAGE experiments. As expected, no HNO-derived BSA dimer was observed upon incubation of BSA with AS. Following treatment with dithiothreitol (DTT), the intensity of BSA monomer band remained the same, confirming the lack of HNO-derived BSA higher oligomers. Notably, BSA bands appeared at a slightly higher molecular weight upon DTT treatment with or without prior exposure of BSA samples to HNO, presumably due to the formation of BSA-DTT adducts. Overall, our results support the formation of a cyclic structure as the major product.

We have also conducted preliminary reactivity studies to examine the cyclic modification. Since the +14 Da increase on BSA upon HNO treatment is attributed to the oxidation of HNO-derived cyclic sulfenamide to the corresponding cyclic sulfinamide (Scheme 7-4),[15] we analyzed the samples following 2 h or overnight incubation at room temperature. The ISD-MALDI-MS spectra were essentially the same before and after the incubation, and no mass increase was observed in any peaks with m/z values >4500. Similar results were obtained in the absence of chelator. To assess the potential effect of buffer salts on oxidation, samples were also incubated with AS in Milli Q water containing 0.1 mM DTPA at pH 7.4.[15] As expected, only partial modification of BSA was obtained under these conditions, presumably due to the incomplete decomposition of AS. These results indicate the lack of further oxidation in this region under our conditions.

Sulfenamides are known to generate sulfonic acids (-SO_3H) upon exposure to hydrogen peroxide (H_2O_2).[52] We tested this reactivity by incubating HNO-treated BSA samples with NEM to block any residual free thiols, and then treating them with H_2O_2. Reflector ISD-MALDI-MS analysis showed new peaks, which could be assigned to sulfonic acid-modified residues in the Cys34-Ala78 region. Notably, no sulfonic acid modification was observed in the absence of HNO-treatment prior to incubation with NEM followed by H_2O_2. Although these results are consistent with the reactivity of sulfenamides, better resolution as well as control experiments with sulfinamides are needed.

The hydrolysis of the cyclic structure was examined by reflector ISD-MALDI-MS. Hydrolysis of this structure is expected to result in ring opening, consequently removing the gap in sequence readout. We initially attempted to hydrolyze HNO-treated BSA under acidic conditions (10 min at pH 1-2). Although a peak assigned to the Pro35 a-ion was detected, no other peaks with higher m/z values were observed. Upon boiling HNO-treated BSA at pH 7.4 for 30 min, new peaks appeared. Despite the low intensities observed, these results might suggest at least a partial hydrolysis of the cyclic structure; further studies are required.

We also attempted to exploit the ring opening strategy to distinguish between a cyclic sulfenamide and a cyclic sulfinamide. Compounds with amine functionality including N_α-acetyl-L-lysine methyl ester, aniline, *O*-methylhydroxylamine and *O*-benzylhydroxylamine were incubated with HNO-treated BSA under several conditions. However, no change in the spectra was observed in the presence or absence of amines, presumably due to lack of reactivity with the cyclic structure.

To learn more about the cyclic modification in HNO-treated BSA, we explored its reversibility in the presence of reducing agents. Following a short (15 min) incubation at 37 ^{o}C in the presence of excess DTT, peaks were detected in the Cys34-Ala78 region, indicating significant reduction of cyclic structure (Figure 7-10). Interestingly, the peak that had been assigned to a regular sulfinamide or sulfinic acid was still observed (Figure 7-10). This peak disappeared following 26 h incubation with excess DTT. Moreover, the peak intensities increased and more peaks became apparent in the Cys34-Ala78 region (Figure 7-10). It should be noted that the spectrum of unmodified BSA also improved upon incubation with DTT, presumable due to the reduction of BSA disulfide linkages. These observations demonstrate that HNO-derived cysteine modifications on BSA can be reduced in the presence of excess thiol, and might point to the more readily reducible nature of the cyclic structure compared to a regular sulfinamide or sulfinic acid.

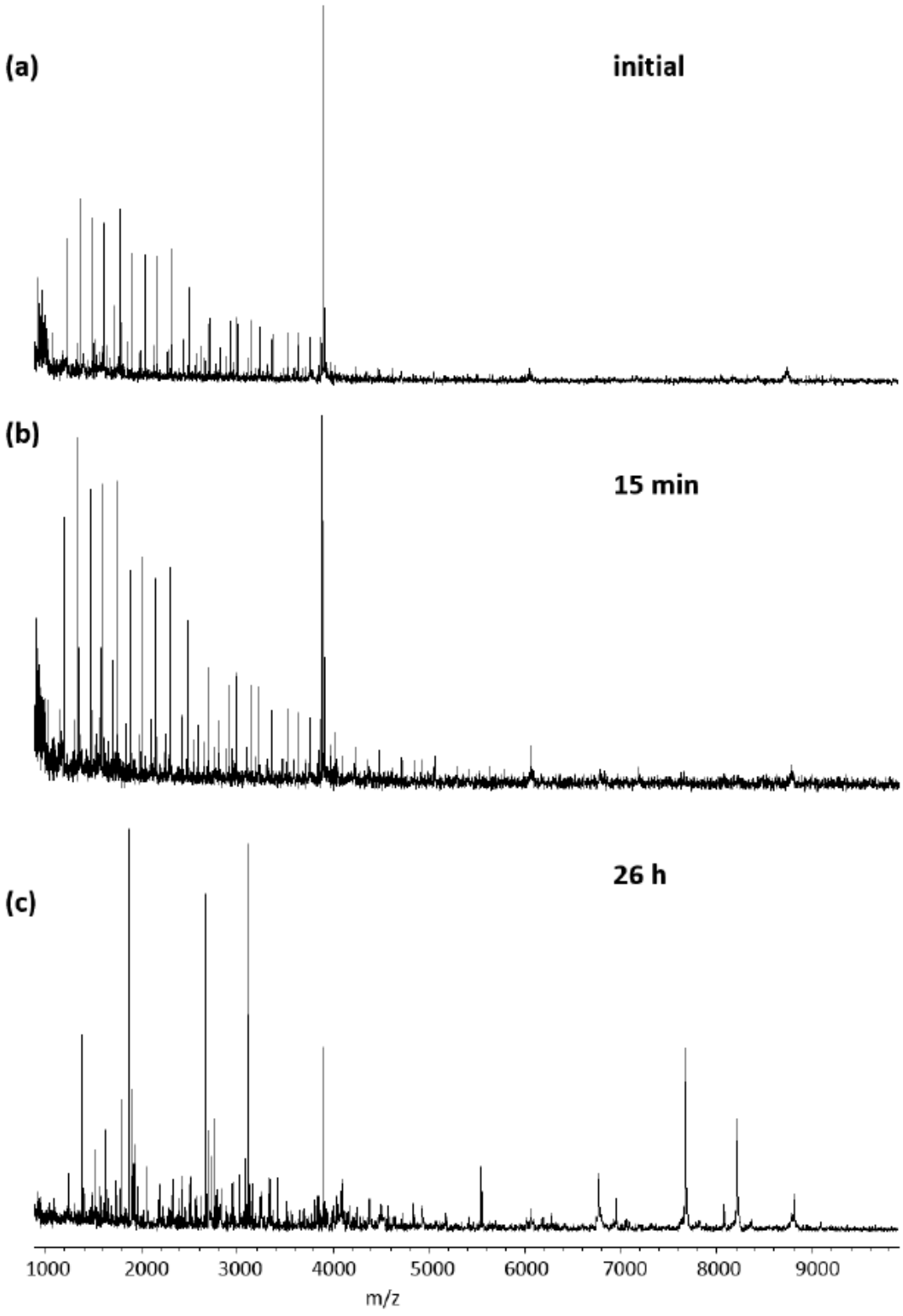

Figure 7-10. Selected region of reflector ISD-MALDI-MS spectrum showing BSA incubated with 2 mM AS followed by treatment with DTT at 37 ^{o}C. The spectra correspond to (a) initial, (b) 15 min, and (c) 26 h after the addition of DTT.

7.4.3 Labeling Studies with BSA

Labeling approaches are commonly used to investigate protein modifications.[53, 54] We conducted preliminary studies utilizing several labeling agents to explore BSA residues involved in the formation of the HNO-derived cyclic structure.

Consistent with previous studies,[15] blocking cysteine with *N*-ethylmaleimide (NEM) prevented the formation of the cyclic structure. Moreover, the putative sulfinamide or sulfinic acid peak was not observed, supporting our assignment. Similarly, incubation of HNO-treated BSA with NEM did not show any NEM-modified peaks. These results confirm the involvement of cysteine in the generation of the cyclic structure.

To investigate the potential role of Lys residues, we attempted to employ 3-sulfosuccinimid-1-yl acetate (Sulfo-NHS-Acetate) (Scheme 7-7).[55] However, control experiments conducted with the VYPCGA model peptide in the presence of N_{α}-acetyl-L-lysine methyl ester revealed the labeling of Cys with Sulfo-NHS-Acetate. To avoid complications due to the lack of labeling agent specificity, we treated the samples with AS prior to the addition of Sulfo-NHS-Acetate. In the case of a Lys modification by HNO, no labeling is expected to occur provided that the cyclic structure remains intact. Reflector ISD-MALDI-MS analysis indicated the presence of Lys labeling upon incubation of HNO-treated samples with Sulfo-NHS-Acetate. Although these results might point to the inertness of Lys to HNO-induced modification, the possibility of ring opening during Sulfo-NHS-Acetate incubation could not be eliminated. Efforts to probe the potential involvement of Arg by utilizing *p*-hydroxyphenylglyoxal (HPG) (Scheme 7-8)[56] were unsuccessful due to inefficient labeling with this reagent as determined by reflector ISD-MALDI-MS and UV-visible spectroscopy.

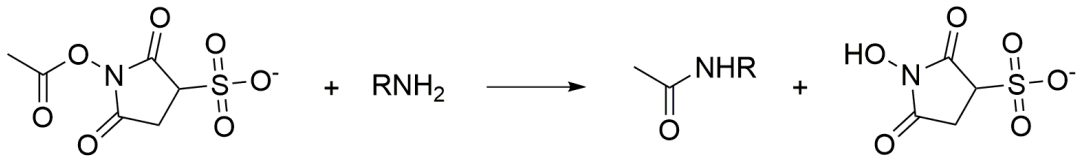

Scheme 7-7. Reaction of 3-sulfosuccinimid-1-yl acetate (Sulfo-NHS-Acetate) with amines. Hermanson, G. T. (2013) *Bioconjugate Techniques*, 3 ed., Academic Press, San Diego.

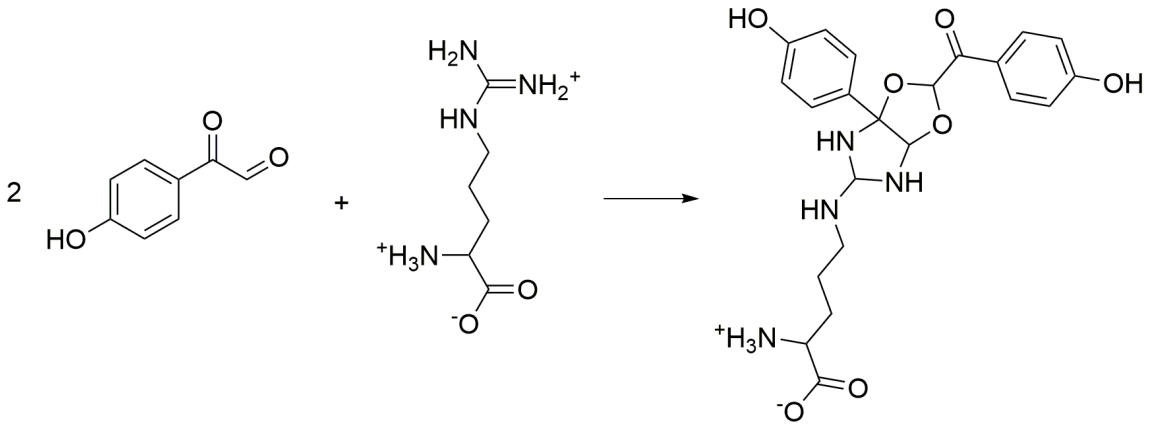

Scheme 7-8. Reaction of *p*-hydroxyphenylglyoxal (HPG) with amines. Lundblad, R. L. (2006) *The Evolution from Protein Chemistry to Proteomics: Basic Science to Clinical Application*, 2 ed., CRC Press, Boca Raton.

In summary, we have conducted preliminary studies to explore the HNO-derived cysteine modification on BSA. Although our results agree with the formation of a cyclic structure as the major product, and likely point to the structure being a cyclic sulfenamide located in Cys34-Ala78 region, further investigations employing more efficient and specific labeling agents, or BSA mutants as well as more efficient detection methods are needed to identify the exact nature of this modification.

7.4.4 Experimental Methods

Reagents. Mass spectrometry-grade bovine serum albumin (BSA) was obtained from Protea Biosciences (Morgantown, WV). BSA (electrophoresis-grade), N_{α}-acetyl-L-lysine methyl ester, super-DHB (2,5-dihydroxybenzoic acid and 2-hydroxy-5-methoxybenzoic acid 10:1 v/v), and *N*-ethylmaleimide (NEM) were of the highest purity available and purchased from Sigma (St. Louis, MO). Dithiothreitol (DTT), 3-sulfosuccinimid-1-yl acetate (Sulfo-NHS-Acetate), p-hydroxyphenylglyoxal (HPG) were obtained from Pierce (Rockford, IL). Deuterated dimethyl sulfoxide (DMSO-d_6) was obtained from Cambridge Isotope Labs (Andover, MA). Aniline, *O*-methylhydroxylamine, *O*-benzylhydroxylamine, hydrogen peroxide (H_2O_2), and MS-grade acetonitrile (ACN) were purchased from Thermo Fisher Scientific (Rockford, IL). Synthesis of Angeli's salt (AS)[24] and ^{15}N-labeled AS (^{15}N-AS)[57] were carried out as described previously. Synthesis and purification of VYPCGA was carried out as described in Chapter 2. Milli Q water was used for all purifications and experiments.

Preparation of BSA. MS-grade BSA was employed for all ISD-MALDI-MS experiments. Electrophoresis-grade BSA was dissolved in 10 mM phosphate buffer with 50 μM DTPA at pH 7.4 to have a final concentration of 0.2 mM. The samples were then pre-incubated with 2 mM DTT for 3 h at room temperature to generate its single free thiol and desalted with Zeba spin columns to remove excess DTT.

Incubation of BSA with HNO-Donor. Stock solutions of AS were prepared in 0.01 M NaOH and used within 15 min of preparation. BSA (MS-grade or electrophoresis grade) was dissolved in 10 mM phosphate buffer with 50 μM DTPA at pH 7.4 to have a final concentration of 0.2 mM. BSA samples were incubated in the presence or absence of

1 or 2 mM AS or ^{15}N-AS at 37 ºC for 30 min. As a control, the samples were also incubated with AS byproduct, NO_2^- (2 mM). In some cases, BSA samples were prepared in 0.1 mM DTPA at pH 7.4 and incubated with AS (1 mM) at room temperature for 1 h.

To investigate the oxidation of HNO-treated BSA, the samples were incubated in the presence of absence of metal chelator at room temperature for 2 or 18 h. In some cases, samples exposed to HNO followed by NEM treatment (see below) were further incubated with 1 mM H_2O_2 at room temperature for 1 h.

For reflector ISD-MALDI-MS analyses, the samples were desalted using C_4 ziptips and spotted on the MALDI plate using dried-droplet method. Super-DHB was employed as the matrix for all reflector ISD-MALDI-MS analyses. ^{15}N-edited NMR analyses were carried out in DMSO-*d*$_6$ as described in Chapter 3.

Hydrolysis of HNO-Treated BSA. BSA samples (0.2 mM) were incubated with AS (2 mM) as described above. The samples were then boiled for 30 min in pH 7.4 buffer. In some cases, the HNO-treated samples were adjusted to pH 1-2 with TFA and incubated at 37 ºC for 10 min. Following incubation, the samples were neutralized with NaOH and prepared for ISD-MALDI-MS analysis as described above.

Reduction of HNO-Treated BSA. BSA samples (0.2 mM) were incubated with AS (2 mM) as described above. The samples were then treated with 50 mM DTT for 15 min or 26 h at 37 ºC and prepared for ISD-MALDI-MS analysis as described above.

Incubations of BSA with Labeling Agents. Stock solutions of NEM (0.1 M), Sulfo-NHS-Acetate (0.2 M), and HPG (0.1 M) were prepared in Milli Q water. Unmodified or HNO-treated BSA samples were treated with NEM (2 mM, 1 h, room temperature), Sulfo-NHS-Acetate (30 mM, 2.5 h, room temperature), or HPG (20 or 100

mM, 3-40 h, 37 ºC) in 10 mM phosphate buffer with 50 μM DTPA at pH 7.4 prior or following HNO-treatment. To avoid pH changes during Sulfo-NHS-Acetate incubation, the samples were monitored by pH paper and re-adjusted to pH 7.4 when needed.

Samples labeled with NEM or Sulfo-NHS-Acetate were desalted using C_4 ziptips. Samples labeled with HPG were precipitated with acetone to remove the bulk of HPG prior to desalting with C_4 ziptips.

Incubations of BSA with Amines. BSA samples (0.2 mM) were incubated with AS (2 mM) as described above. The samples were then treated with N_α-acetyl-L-lysine methyl ester (2 or 10 mM) in 10 mM phosphate buffer with 50 μM DTPA (pH 7.4) at 37 or 55 ºC for 3-14 h. Incubations with aniline (10 mM), *O*-methylhydroxylamine (10 mM), and *O*-benzylhydroxylamine (10 mM) were conducted in pH 5 or 7.4 phosphate buffer at 37, 55 or 65 ºC for 3-26 h. Following incubation, the samples were prepared for ISD-MALDI-MS analysis as described above.

Mass Spectrometry Analyses. All ISD-MALDI-MS analyses were conducted in reflectron mode using a Bruker Autoflex III MALDI-TOF/TOF instrument equipped with a 355 nm pulsed UV laser. A total of 60000 shots were accumulated for each ISD-MALDI-MS spectrum. The spectra were externally calibrated with unmodified BSA. All spectra were analyzed by using Biotools 3.2 software.

NMR Analyses. All ^{1}H-NMR and ^{15}N-edited ^{1}H 1D-NMR analyses were carried out on a Bruker Avance 400 MHz FT-NMR spectrometer. ^{1}H NMR and ^{15}N-edited ^{1}H 1D-NMR analyses were carried out in DMSO-d_6 at 303 K. ^{15}N-edited ^{1}H 1D-NMR spectra were acquired using the HSQC pulse sequence for selection. Chemical shifts are reported in parts per million (ppm) relative to residual DMSO (2.49 ppm for ^{1}H).

Electrophoresis. BSA samples (0.2 mM) were incubated with AS (2 mM) as described above. The samples were then incubated in the presence or absence of 50 mM DTT for 1 h at room temperature. Following 1:53 dilution into a mixture of SDS sample buffer and pH 7.4 phosphate buffer, the samples were loaded onto gel. SDS-PAGE using 10% polyacrylamide was performed employing standard procedures.[58] Following electrophoresis, the bands were visualized by Ag staining.

UV-Visible Spectroscopy Analyses. HPG-labeled BSA samples were diluted into 82 mM phosphate buffer with 450 μM DTPA at pH 9 and analyzed at 340 nm (ε_{340} = 1.83 x 10^4 M^{-1} cm^{-1}).[59] All the spectrophotometric analyses were conducted on a Hewlett-Packard 8453 Diode Array Spectrophotometer.

7.5 Preliminary Studies on the Reactivity of VYPCLA with Acyloxy Nitroso Compounds

Recent studies have employed acyloxy nitroso compounds as a new class of HNO-donors.[60, 61] These compounds exist as blue, monomeric C-nitroso compounds, which release HNO upon hydrolysis.[60, 61] We have conducted preliminary studies to investigate the reactivity of VYPCLA with the acyloxy nitroso compounds, 1-nitrosocyclohexyl trifluoroacetate (NCTFA) and 1-nitrosocyclohexyl pivalate (NCP), in collaboration with the King group (Wake Forest University).

NCP NCTFA

Figure 7-11. Chemical structures of the acyloxy nitroso compounds

7.5.1 Reactivity of VYPCLA with NCTFA and NCP

Studies have shown that the hydrolysis rate of acyloxy nitroso compounds to produce HNO depends on pH and the structure of the ester portion of the molecule.[60, 61] In MeOH/pH 7.4 buffer 50:50 (v/v) at room temperature, NCTFA was reported to decompose immediately, whereas NCP has a half-life of 37.8 h.[61] Although these compounds release HNO in the absence of traps, their reactivity with thiols is more complicated due to the possibility of a direct reaction between the thiol and acyloxy nitroso precursor.[61] Moreover, the competing pathways (hydrolysis vs. direct reaction) would ultimately produce the same products, a disulfide, a carboxylic acid, and cyclohexanone oxime (Scheme 7-9).[61]

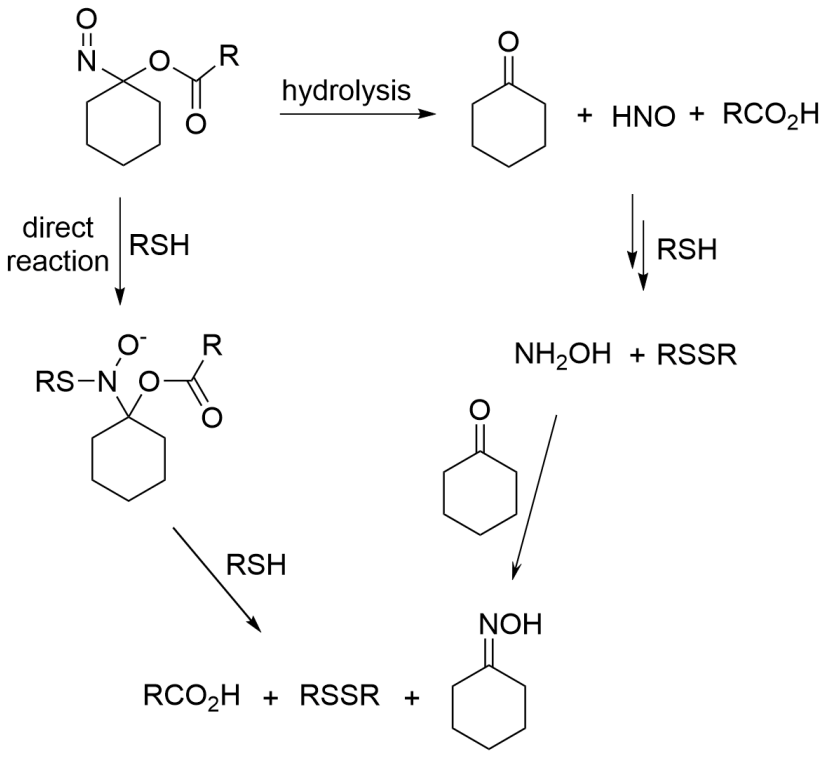

Scheme 7-9. Hydrolysis and direct reaction pathways for the reaction of acyloxy nitroso compounds with thiols. Shoman, M. E.; DuMond, J. F.; Isbell, T. S.; Crawford, J. H.; Brandon, A.; Honovar, J.; Vitturi, D. A.; White, C. R.; Patel, R. P.; King, S. B. (2011) *J. Med. Chem.* ***54***, 1059-1070.

To gain more insight about the reactivity of acyloxy nitroso compounds with thiols, we treated the hexapeptide, VYPCLA, with NCTFA or NCP. As shown in Chapter 2, high sulfinamide yields are obtained upon incubation of VYPCLA (0.1 mM) with various concentrations of Angeli's salt (AS). Since sulfinamide formation is unique to HNO, detection of sulfinamide would point to the intermediacy of HNO via the hydrolysis pathway. Due to solubility issues, these reactivity studies were carried out in MeOH/pH 7.4 buffer 50:50 (v/v). Treatment of VYPCLA (0.1 mM) with 0.1, 0.3, 1 and 5 mM NCTFA resulted in the detection of 0, 10, 7 and 3% sulfinamide, respectively. Similarly the amount of disulfide formation (ca. 33%) stayed the same from 0.3 to 5 mM. Assuming the MeOH/buffer system has no effect on the reaction, the trend for sulfinamide formation seems to be different than that of the other HNO-donors we have investigated. For comparison, as shown in Figure 2-1, the corresponding sulfinamide yields were 73, 81, 86, 97 and 95% upon employment of AS in pH 7.4 buffer.

The samples were analyzed with NCP following two different incubation times (2 h and 6 days). Upon 2 h incubation with NCP, both the unmodified peptide and the disulfide were detected. Approximately 40, 38, and 48% of the peptide (0.1 mM) was modified to the corresponding disulfide in the presence of 0.1, 0.3, and 5 mM NCP. Considering the half-life of the compound, the disulfide seems to have originated from the direct reaction of NCP with the peptide (rather than from HNO formation).

Incubation of VYPCLA (0.1 mM) in the presence or absence of NCP (0.1 or 0.3 mM) for 6 days resulted in the formation of disulfide. Several other peaks were observed upon incubating the peptide with 5 mM NCP for 6 days (not observed upon 2 h incubation). Importantly, no sulfinamide was detected following 2 h- or 6 day-incubation of VYPCLA

with NCP. Overall, these results point to the involvement of a non-HNO producing pathway under these conditions.

7.5.2 Experimental Methods

Reagents. The acyloxy nitroso compounds, 1-nitrosocyclohexyl trifluoroacetate (NCTFA) and 1-nitrosocyclohexyl pivalate (NCP) were a generous gift from Dr. S. Bruce King. MS-grade acetonitrile (ACN) was purchased from Thermo Fisher Scientific (Rockford, IL). Synthesis and purification of VYPCLA was carried out as described in Chapters 2 and 3. Milli Q water was used for all purifications and experiments.

Incubation of acyloxy nitroso compounds with VYPCLA. VYPCLA was dissolved in MeOH/pH 7.4 phosphate buffer 50:50 (v/v) to have a final concentration of 0.1 mM. In all cases, 10 mM phosphate buffer with 50 μM DTPA at pH 7.4 was employed. Stock solutions of NCTFA (0.5 M) and NCP (0.5 M) were prepared in ACN. Samples were incubated with 0-5 mM NCTFA at room temperature for 2 h. Incubations of VYPCLA (0.1 mM) with 0-5 mM NCP were carried out at room temperature for 2 h or 6 days. The samples were then frozen and lyophilized. Following lyophilization, the samples were dissolved in Milli Q water and desalted with C_{18} PepClean spin columns. The samples were then diluted into 70% ACN with 0.1% TFA for immediate ESI-MS analysis.

Mass Spectrometric Analyses. ESI-MS analysis was carried out on a Thermo Finnigan LCQ Deca Ion Trap Mass Spectrometer fitted with an electrospray ionization source, operating in the positive ion mode with an accuracy of ca. 0.1 m/z. In all experiments, the samples were introduced to the instrument at a rate of 10 μL/min using a

syringe pump via a silica capillary line. The heated capillary temperature was 250 °C and the spray voltage was 5 kV.

Analysis of the Data. For ESI-MS experiments, the quantification was done by calculating the percentage of sulfinamide in the total thiol-containing peptide species (mainly free thiol, disulfide, and sulfinamide) based on their relative peak intensities in the averaged spectrum.

7.6 References

1. Lopez, B. E., Rodriguez, C. E., Pribadi, M., Cook, N. M., Shinyashiki, M., and Fukuto, J. M. (2005) Inhibition of yeast glycolysis by nitroxyl (HNO): A mechanism of HNO toxicity and implications to HNO biology, *Arch. Biochem. Biophys. 442*, 140-148.
2. Sivakumaran, V., Stanley, B. A., Tocchetti, C. G., Ballin, J. D., Caceres, V., Zhou, L., Keceli, G., Rainer, P. P., Lee, D. I., Huke, S., Ziolo, M. T., Kranias, E. G., Toscano, J. P., Wilson, G. M., O'Rourke, B., Kass, D. A., Mahaney, J. E., and Paolocci, N. (2013) HNO enhances SERCA2a activity and cardiomyocyte function by promoting redox-dependent phospholamban oligomerization, *Antioxid. Redox Signaling 19*, 1185-1197.
3. Espey, M. G., Miranda, K. M., Thomas, D. D., and Wink, D. A. (2002) Ingress and reactive chemistry of nitroxyl-derived species within human cells, *Free Radical Biol. Med. 33*, 827-834.
4. Liu, X., Miller, M. J. S., Joshi, M. S., Thomas, D. D., and Lancaster, J. R., Jr. (1998) Accelerated reaction of nitric oxide with O_2 within the hydrophobic interior of biological membranes, *Proc. Natl. Acad. Sci. U. S. A. 95*, 2175-2179.

5. Fukuto, J. M., and Carrington, S. J. (2011) HNO signaling mechanisms, *Antioxid. Redox Signaling 14*, 1649-1657.

6. Hoffmann, R., Gleiter, R., and Mallory, F. B. (1970) Non-least-motion potential surfaces. The dimerization of methylenes and nitroso compounds, *J. Am. Chem. Soc. 92*, 1460-1466.

7. Bazylinski, D. A., and Hollocher, T. C. (1985) Evidence from the reaction between trioxodinitrate (II) and ^{15}NO that trioxodinitrate(II) decomposes into nitrosyl hydride and nitrite in neutral aqueous solution, *Inorg. Chem. 24*, 4285-4288.

8. Shoeman, D. W., Shirota, F. N., DeMaster, E. G., and Nagasawa, H. T. (2000) Reaction of nitroxyl, an aldehyde dehydrogenase inhibitor, with *N*-acetyl-L-cysteine, *Alcohol 20*, 55-59.

9. Lee, M. J. C., Nagasawa, H. T., Elberling, J. A., and DeMaster, E. G. (1992) Prodrugs of nitroxyl as inhibitors of aldehyde dehydrogenase, *J. Med. Chem. 35*, 3648-3652.

10. Ware, R. W., Jr., and King, S. B. (2000) *P*-Nitrophosphate compounds: New *N*-*O* heterodienophiles and nitroxyl delivery agents *J. Org. Chem. 65*, 8725-8729.

11. Sutton, A. D., Williamson, M., Weismiller, H., and Toscano, J. P. (2012) Optimization of HNO production from *N,O*-bis-acylated hydroxylamine derivatives, *Org. Lett. 14*, 472-475.

12. Guthrie, D. A., Kim, N. Y., Siegler, M. A., Moore, C. D., and Toscano, J. P. (2012) Development of *N*-substituted hydroxylamines as efficient nitroxyl (HNO) donors, *J. Am. Chem. Soc. 134*, 1962-1965.

13. Peters, T., Jr. (1995) *All About Albumin: Biochemistry, Genetics, and Medical Applications*, 1 ed., Academic Press, New York.

14. Rafikova, O., Rafikov, R., and Nudler, E. (2002) Catalysis of *S*-nitrosothiols formation by serum albumin: The mechanism and implication in vascular control, *Proc. Natl. Acad. Sci. U. S. A. 99*, 5913-5918.

15. Shen, B., and English, A. M. (2005) Mass spectrometric analysis of nitroxyl-mediated protein modification: Comparison of products formed with free and protein-based cysteines, *Biochemistry 44*, 14030-14044.

16. Suzuki, T., Mower, H. F., Friesen, M. D., Gilibert, I., Sawa, T., and Ohshima, H. (2004) Nitration and nitrosation of *N*-acetyl-L-tryptophan and tryptophan residues in proteins by various reactive nitrogen species, *Free Radical Biol. Med. 37*, 671-681.

17. Peyrot, F., Fernandez, B. O., Bryan, N. S., Feelisch, M., and Ducrocq, C. (2006) *N*-Nitroso products from the reduction of indoles with Angeli's salt, *Chem. Res. Toxicol. 19*, 58-67.

18. Doyle, M. P., Mahapatro, S. N., Broene, R. D., and Guy, J. K. (1988) Oxidation and reduction of hemoproteins by trioxodinitrate(II). The role of nitrosyl hydride and nitrite, *J. Am. Chem. Soc. 110*, 593-599.

19. Wong, P. S. Y., Hyun, J., Fukuto, J. M., Shirota, F. N., DeMaster, E. G., Shoeman, D. W., and Nagasawa, H. T. (1998) Reaction between *S*-nitrosothiols and thiols: Generation of nitroxyl (HNO) and subsequent chemistry, *Biochemistry 37*, 5362-5371.

20. Kato, M., Ozawa, S., and Hayashi, R. (1997) Effects of high pressure and temperature on micelle formation of sodium deoxycholate and sodium dodecylsulfate, *Lipids 32*, 1229-1230.

21. Chatterjee, A., Moulik, S. P., Sanyal, S. K., Mishra, B. K., and Puri, P. M. (2001) Thermodynamics of micelle formation of ionic surfactants: A critical assessment for sodium dodecyl sulfate, cetyl pyridinium chloride and dioctyl sulfosuccinate (Na salt) by microcalorimetric, conductometric, and tensiometric measurements, *J. Phys. Chem. B 105*, 12823-12831.

22. Helenius, A., McCaslin, D. R., Fries, E., and Tanford, C. (1979) Properties of detergents, *Methods Enzymol. 56*, 734-749.

23. Donzelli, S., Espey, M. G., Thomas, D. D., Mancardi, D., Tocchetti, C. G., Ridnour, L. A., Paolocci, N., King, S. B., Miranda, K. M., Lazzarino, G., Fukuto, J. M., and Wink, D. A. (2006) Discriminating formation of HNO from other reactive nitrogen oxide species, *Free Radical Biol. Med. 40*, 1056-1066.

24. Hughes, M. N., and Cammack, R. (1999) Synthesis, chemistry, and applications of nitroxyl ion releasers sodium trioxodinitrate or Angeli's salt and Piloty's acid, *Methods Enzymol. 301*, 279-287.

25. Toscano, J. P., Brookfield, F. A., Cohen, A. D., Courtney, S. M., Frost, L. M., and Kalish, V. J. (2011) *N*-hydroxylsulfonamide derivatives as new physiologically useful nitroxyl donors, (Johns Hopkins University, USA). U.S. Patent 8,030,356.

26. Smith, P. K., Krohn, R. I., Hermanson, G. T., Mallia, A. K., Gartner, F. H., Provenzano, M. D., Fujimoto, E. K., Goeke, N. M., Olson, B. J., and Klenk, D. C.

(1985) Measurement of protein using bicinchoninic acid, *Anal. Biochem. 150*, 76-85.

27. Cohen, A. D. (2007) The time-resolved infrared spectroscopic study of an iminooxirane, a nitronic anhydride, and acylnitroso species: The development of novel *N*-hydroxysulfonamides as physiological nitroxyl donors, p 144, Johns Hopkins University.

28. Ellman, G. L. (1959) Tissue sulfhydryl groups, *Arch. Biochem. Biophys. 82*, 70-77.

29. Vaananen Antti, J., Kankuri, E., and Rauhala, P. (2005) Nitric oxide-related species-induced protein oxidation: reversible, irreversible, and protective effects on enzyme function of papain, *Free Radical Biol. Med. 38*, 1102-1111.

30. Keceli, G., Moore, C. D., Labonte, J. W., and Toscano, J. P. (2013) NMR detection and study of hydrolysis of HNO-derived sulfinamides, *Biochemistry 52*, 7387-7396.

31. Keceli, G., and Toscano, J. P. (2012) Reactivity of nitroxyl-derived sulfinamides, *Biochemistry 51*, 4206-4216.

32. Gallogly, M. M., Starke, D. W., and Mieyal, J. J. (2009) Mechanistic and kinetic details of catalysis of thiol-disulfide exchange by glutaredoxins and potential mechanisms of regulation, *Antioxid. Redox Signaling 11*, 1059-1081.

33. Deponte, M. (2013) Glutathione catalysis and the reaction mechanisms of glutathione-dependent enzymes, *Biochim. Biophys. Acta 1830*, 3217-3266.

34. Chung, P. M., Cappel, R. E., and Gilbert, H. F. (1991) Inhibition of glutathione disulfide reductase by glutathione, *Arch. Biochem. Biophys. 288*, 48-53.

35. Gravina, S. A., and Mieyal, J. J. (1993) Thioltransferase is a specific glutathionyl mixed-disulfide oxidoreductase, *Biochemistry 32*, 3368-3376.

36. Johansson, C., Lillig, C. H., and Holmgren, A. (2004) Human mitochondrial glutaredoxin reduces *S*-glutathionylated proteins with high affinity accepting electrons from either glutathione or thioredoxin reductase, *J. Biol. Chem. 279*, 7537-7543.

37. Zaffagnini, M., Michelet, L., Massot, V., Trost, P., and Lemaire, S. D. (2008) Biochemical characterization of glutaredoxins from chlamydomonas reinhardtii reveals the unique properties of a chloroplastic CGFS-type glutaredoxin, *J. Biol. Chem. 283*, 8868-8876.

38. Li, M., Yang, Q., Gao, Y., and Wu, Q. (2007) N-Terminus deletion affecting the preparation of soluble cyanobacterial glutaredoxin in Escherichia coli, *Biochemistry (Moscow) 72*, 313-319.

39. Bergmeyer, H. U. (1974) *Methods of Enzymatic Analysis*, Vol. 1, Academic Press, New York.

40. Williams, D. L. H. (2004) *Nitrosation Reactions and the Chemistry of Nitric Oxide*, 1 ed., Elsevier, San Diego.

41. Pereira, C., Ferreira, N. R., Rocha, B. S., Barbosa, R. M., and Laranjinha, J. (2013) The redox interplay between nitrite and nitric oxide: From the gut to the brain, *Redox Biology 1*, 276-284.

42. Zweier, J. L., Samouilov, A., and Kuppusamy, P. (1999) Non-enzymatic nitric oxide synthesis in biological systems, *Biochim. Biophys. Acta 1411*, 250-262.

43. Grossi, L., and Montevecchi, P. C. (2002) *S*-Nitrosocysteine and cystine from reaction of cysteine with nitrous acid. A kinetic investigation, *J. Org. Chem. 67*, 8625.

44. Daiber, A., Bachschmid, M., Kavakli, C., Frein, D., Wendt, M., Ullrich, V., and Munzel, T. (2003) A new pitfall in detecting biological end products of nitric oxide-nitration, nitros(yl)ation and nitrite/nitrate artefacts during freezing, *Nitric Oxide 9*, 44-52.

45. Gomez, G., Pikal, M. J., and Rodriguez-Hornedo, N. (2001) Effect of initial buffer composition on pH changes during far-from-equilibrium freezing of sodium phaosphate buffer solutions, *Pharm. Res. 18*, 90-97.

46. Hoffman, M. D., Walsh, G. M., Rogalski, J. C., and Kast, J. (2009) Identification of nitroxyl-induced modifications in human platelet proteins using a novel mass spectrometric detection method, *Mol. Cell. Proteomics 8*, 887-903.

47. Hanisch, F.-G. (2011) Top-down sequencing of O-glycoproteins by in-source decay matrix-assisted laser desorption ionization mass spectrometry for glycosylation site analysis, *Anal. Chem. 83*, 4829-4837.

48. Brown, R. S., and Lennon, J. J. (1995) Sequence-specific fragmentation of matrix-assisted laser-desorbed protein/peptide ions, *Anal. Chem. 67*, 3990-3999.

49. Reiber, D. C., Grover, T. A., and Brown, R. S. (1998) Identifying proteins using matrix-assisted laser desorption/ionization in-source fragmentation data combined with database searching, *Anal. Chem. 70*, 673-683.

50. Sherman, M. P., Grither, W. R., and McCulla, R. D. (2010) Computational investigation of the reaction mechanisms of nitroxyl and thiols, *J. Org. Chem. 75*, 4014-4024.

51. Breeze, A. L. (2000) Isotope-filtered NMR methods for the study of biomolecular structure and interactions, *Prog. NMR Spectrosc. 36*, 323-372.

52. Salmeen, A., Andersen, J. N., Myers, M. P., Meng, T.-C., Hinks, J. A., Tonks, N. K., and Barford, D. (2003) Redox regulation of protein tyrosine phosphatase 1B involves a sulphenyl-amide intermediate, *Nature 423*, 769-773.

53. Chalker, J. M., Bernardes, G. J. L., and Davis, B. G. (2011) A "tag-and-modify" approach to site-selective protein modification, *Acc. Chem. Res. 44*, 730-741.

54. Leonard, S. E., and Carroll, K. S. (2011) Chemical omics' approaches for understanding protein cysteine oxidation in biology, *Curr. Opin. Chem. Biol. 15*, 88-102.

55. Hermanson, G. T. (2013) *Bioconjugate Techniques*, 3 ed., Academic Press, San Diego.

56. Lundblad, R. L. (2006) *The Evolution from Protein Chemistry to Proteomics: Basic Science to Clinical Application*, 2 ed., CRC Press, Boca Raton.

57. Bonner, F. T., and Ravid, B. (1975) Thermal decomposition of oxyhyponitrite (sodium trioxodinitrate(II)) in aqueous solution, *Inorg. Chem. 14*, 558-563.

58. Laemmli, U. K. (1970) Cleavage of structural proteins during the assembly of the head of bacteriophage T4, *Nature 227*, 680-685.

59. Yamasaki, R. B., Vega, A., and Feeney, R. E. (1980) Modification of available arginine residues in proteins by p-hydroxyphenylglyoxal, *Anal. Biochem. 109*, 32-40.

60. Sha, X., Isbell, T. S., Patel, R. P., Day, C. S., and King, S. B. (2006) Hydrolysis of acyloxy nitroso compounds yields nitroxyl (HNO), *J. Am. Chem. Soc. 128*, 9687-9692.

61. Shoman, M. E., DuMond, J. F., Isbell, T. S., Crawford, J. H., Brandon, A., Honovar, J., Vitturi, D. A., White, C. R., Patel, R. P., and King, S. B. (2011) Acyloxy nitroso compounds as nitroxyl (HNO) donors: Kinetics, reactions with thiols, and vasodilation properties, *J. Med. Chem. 54*, 1059-1070.

Chapter 8 – Post-Study Caffeine Administration Enhances Memory Consolidation in Humans

8.1 Introduction

Studies indicate caffeine is one of the most frequently used psychoactive stimulants.[1] The effects of caffeine are increased arousal, vigilance, attention, and processing speed. Despite the known cognitive enhancing properties of caffeine,[2] its effects on long-term memory have not been investigated in detail. Previous studies have involved the administration of caffeine before learning.[2] Since caffeine was present at the time of the learning or memory task, it was not possible to distinguish the effect of caffeine on memory from its other effects such as increased alertness and attention.

In a post-study design, the subjects, who were randomly assigned to an experimental or control group, are tested following a treatment (e.g., caffeine administration after the subjects had a chance to study the material).[3] Animal studies conducted following these procedures have reported enhancement of memory consolidation.[4-6] In a collaborative project, we assisted the studies of the Yassa group (Department of Psychological and Brain Sciences, Johns Hopkins University) in investigating the effect of caffeine administered post-training on the consolidation or storage of memories for later recall. This double-blind study involved a memory test and an HPLC assay to quantify caffeine and paraxanthine levels in the samples collected from participants.

8.2 Results and Discussion

8.2.1 Detection of Caffeine Metabolites by HPLC

High pressure liquid chromatography (HPLC) is a commonly used technique to analyze drug and metabolite concentrations in biological samples.[7-9] Moreover, several HPLC assays have been reported to quantify caffeine and its major metabolite, paraxanthine, (Figure 8-1) in plasma, saliva or urine samples.[10-14] Due to its easily obtainable and non-invasive nature, we decided to employ saliva as the matrix. Notably, recent literature indicates the consistent and reproducible correlations obtained between saliva and plasma paraxanthine/caffeine ratios as well as plasma caffeine clearance.[11, 13, 15, 16]

To detect caffeine and paraxanthine levels in saliva, we employed a modified literature procedure.[14] The sample extraction and HPLC conditions were optimized using paraxanthine and caffeine standards prepared in Milli Q water or caffeine-free saliva. Elimination of a centrifugation step and increasing the organic content of the mobile phase from 10 to 12% acetonitrile allowed us to shorten the overall analysis time significantly (ca. 60 min versus ca. 40 min for each sample). As seen in Figure 8-1, the retention times of paraxanthine, caffeine, and the internal standard (benzotriazole) were ca. 5.1, 9.5 and 12.0 min, respectively.

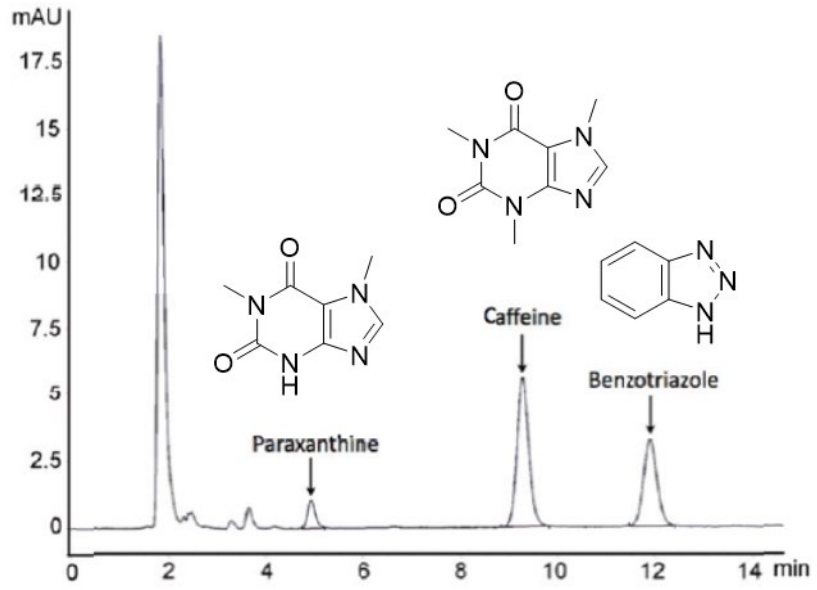

Figure 8-1. Representative HPLC trace collected at 280 nm showing distinct peaks for paraxanthine (5.1 min), caffeine (9.5 min) and the internal standard, benzotriazole (12.0 min). The compounds were extracted from salivary samples following caffeine administration.

Using standard caffeine or paraxanthine samples under our conditions, the sensitivity limits in Milli Q water and saliva were determined to be ca. 0.03 mg/ml (0.15 μM) and ca. 0.05 mg/ml (ca. 0.26 μM), respectively (Figure 8-2 and 8-3). The extraction efficiencies of caffeine, paraxanthine, and benzotriazole from saliva were also found to be similar (ca. 72, 63 and 73%, respectively). Moreover, the assay was highly reproducible under our conditions.

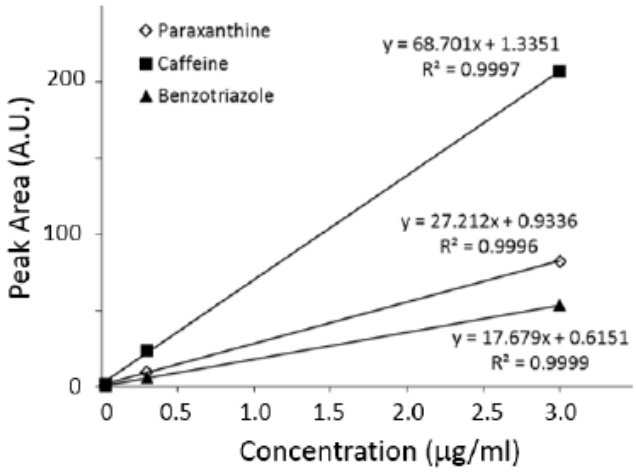

Figure 8-2. Linearity and sensitivity of HPLC detection for caffeine, paraxanthine, and the benzotriazole dissolved in Milli Q water.

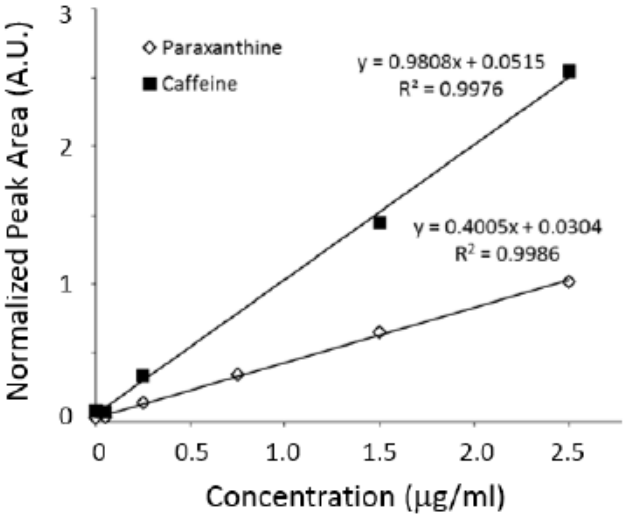

Figure 8-3. Linearity and sensitivity of HPLC detection for caffeine and paraxanthine standards dissolved in caffeine-free saliva. The peak areas were normalized with respect to the peak area of the internal standard, benzotriazole.

8.2.2 Memory Tests and Analyses of Caffeine Metabolites from Subjects

Memory consolidation is a neurological process involving the transfer of information from short-term memory to long-term memory.[17, 18] To investigate the effect of caffeine on memory consolidation, a randomized, double-blind, placebo-controlled trial was conducted in caffeine-naive participants. In these investigations, the participants incidentally studied images of objects, then received either 200 mg caffeine or placebo. Twenty-four hours after the study session, the participants were subjected to a memory test, in which they were shown some items they saw the previous day (targets), some new items (foils), and some items that were similar, but not identical, to the ones they saw before (lures) (Figure 8-4). The participants were asked to identify these items as "old", "new", or "similar". Salivary samples were also collected at baseline and 1 h, 3 h and 24 h after the administration of caffeine or placebo to quantify caffeine metabolites (Figure 8-4). These studies have shown that the participants who received caffeine were more likely to distinguish between "lure" and "target" items compared to participants who received placebo.

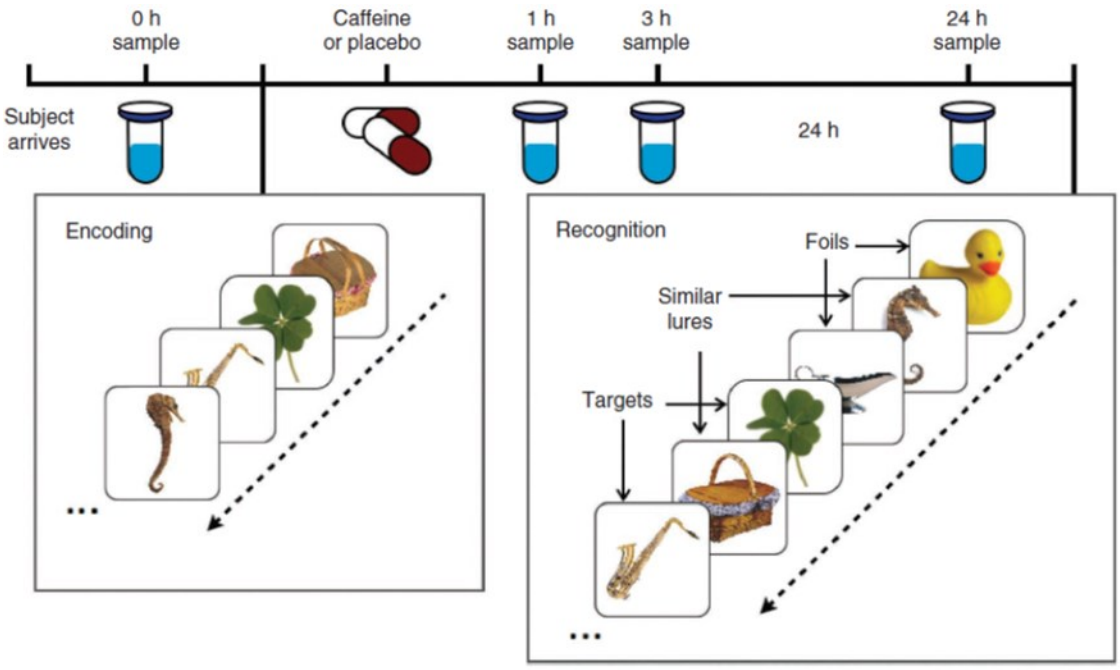

Figure 8-4. Outline of study design.

The caffeine absorption and metabolism of participants through the twenty-four hour time period were determined by HPLC analysis of the collected salivary samples. As shown in Figure 8-5, we observed a significant increase in the sum of caffeine and paraxanthine levels after 1 and 3 h of caffeine administration, followed by a return to the baseline level after 24 h. These observations are consistent with the caffeine metabolism in humans.[19] As expected, the sum of caffeine and paraxanthine levels remained unchanged in participants who received the placebo (Figure 8-5).

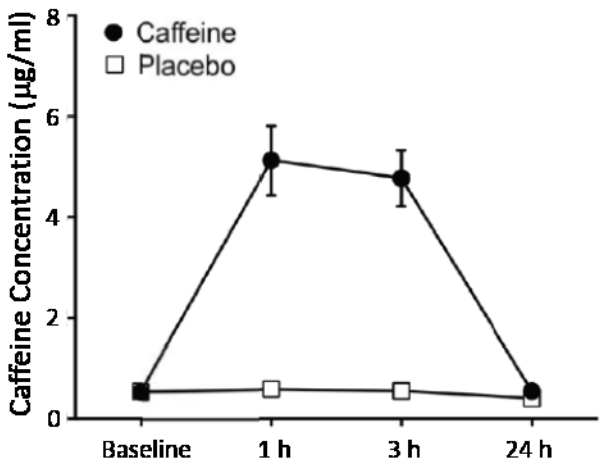

Figure 8-5. Group averages of the sum of caffeine and paraxanthine concentrations (μg/ml) detected by HPLC analysis. Both the caffeine and placebo group had negligible amounts of caffeine and paraxanthine in saliva at baseline. The caffeine group had a significant increase in caffeine and paraxanthine concentrations at 1 h and 3 h, then declined to baseline at 24 hours (SEM ± 1). The placebo group had no such increase in caffeine or paraxanthine.

Since caffeine might also affect retrieval (the process of obtaining memory information from wherever it has been stored)[20], a delayed manipulation experiment, in which caffeine was administered 1 h before the memory test (24 h after the initial study session) was conducted. No significant improvement in memory was observed compared with placebo, indicating that caffeine does not affect retrieval. To follow the sum of caffeine and paraxanthine levels, we tested the salivary samples collected prior to the initial study session and at the time of the memory test. Similar to the above results, the increase in caffeine and paraxanthine levels were observed only in participants who received caffeine.

The effect of different caffeine doses was also explored by administration of 100, 200 and 300 mg of caffeine. In all cases, HPLC analysis of the salivary samples obtained at baseline, 1 h and 24 h after caffeine administration was consistent with the administered

dose of caffeine. Participants who received 200 or 300 mg caffeine had similar performances on the memory test. This was significantly higher compared to participants who received 100 mg caffeine or placebo. These results suggest that a dose of at least 200 mg is required to observe the enhancing effect of caffeine on consolidation of memory.

8.3 Conclusions

A post-study design was employed to examine the effects of caffeine consumption on human long-term memory. Moreover, the levels of caffeine and its primary metabolite, paraxanthine, in salivary samples were quantified at various time intervals by using an HPLC assay. Overall, these studies demonstrate that caffeine enhances consolidation of long-term memory in humans. Further investigations are required to understand the mechanisms by which caffeine can potentiate memory.

8.4 Experimental Methods

Reagents. Caffeine, paraxanthine and benzotriazole were of the highest purity available and purchased from Sigma (St. Louis, MO). HPLC grade acetonitrile (ACN) was obtained from Thermo Fisher Scientific (Rockford, IL). Milli Q water was used for all purifications and experiments.

Subjects. 160 healthy, caffeine-naïve subjects between the ages of 18 and 30 participated in the study. Participants were excluded because of compromised saliva samples (5 participants), caffeine content in baseline salivary samples (18 participants) or in 1 h sample (1 participant) or in 24 h sample (9 participants), at chance discrimination performance (8 participants) and mini mental state examination scores below 26 (2 participants).

Saliva Collection. Subjects provided 1 ml samples of saliva following a standardized saliva collection protocol (Salimetrics kit) in 2 ml cryovial test tubes, which were refrigerated at -80 ^{o}C within 24 h of collection.

Determination of Caffeine and Paraxanthine Levels in Saliva. Saliva samples collected from the subjects at various time intervals were analyzed based on a modified literature procedure.[14] Briefly, benzotriazole (50 μL of 5.0 μg/mL solution) was added to 100 μL of each saliva sample as an internal standard. The samples were then extracted with 4 mL ethyl acetate. The organic layer which contained caffeine, paraxanthine, and benzotriazole was transferred to a separate test tube and the solvent was evaporated with condensed air at 55 ^{o}C. The dried samples were stored at -20 ^{o}C until HPLC analysis. On the day of the analysis, the samples were re-dissolved in 200 μL Milli Q water, filtered (0.2 μm pore size), and analyzed by HPLC. All the analyses were performed on an Apollo C_{18} reverse-phase column connected to an Agilent 1200 HPLC system equipped with a quaternary pump, diode array detector and a standard autosampler. The mobile phase consisted of 12% acetonitrile with 0.1% trifluoroacetic acid at room temperature and the compounds were followed at 280 nm for 15 minutes. The amounts of caffeine and paraxanthine were normalized with respect to the internal standard and quantified based on calibration curves constructed from standards that were prepared in Milli Q water and exposed to the same sample preparation procedures.

Memory Test and Statistical Analysis. All memory tests and statistical analyses were performed by Yassa group. Briefly, a hippocampal memory-dependent task particularly taxing pattern separation was employed.[21] Group comparisons were conducted using unpaired *t*-tests, one-way and two-way ANOVAs.

8.5 References

1. Nawrot, P., Jordan, S., Eastwood, J., Rotstein, J., Hugenholtz, A., and Feeley, M. (2003) Effects of caffeine on human health, *Food Addit. Contam. 20*.
2. Nehlig, A. (2010) Is caffeine a cognitive enhancer?, *J. Alzheimers Dis. 20 (suppl. 1)*, S85-S94.
3. Campbell, D. T., and Stanley, J. C. (1966) *Experimental and Quasi-Experimental Designs for Research*, 1 ed., Houghton Mifflin Company, Boston.
4. Castellano, C. (1976) Effects of caffeine on discrimination learning, consolidation, and learned behavior in mice *Psychopharmacology 48*, 255-260.
5. Botton, P. H., Costa, M. S., Ardais, A. P., Mioranzza, S., Souza, D. O., Rocha, J., and Porciuncula, L. O. (2010) Caffeine prevents disruption of memory consolidation in the inhibitory avoidance and novel object recognition tasks by scopolamine in adult mice, *Behavioral Brain Research 214*, 254-259.
6. Angelucci, M., Cesario, C., Rosalen, P., and Cunha, C. (2002) Effects of caffeine on learning and memory in rats tested in the Morris water maze, *Braz. J. Med. Biol. Res. 35*, 1201-1208.
7. Goncalves, D., Alves, G., Soares-da-Silva, P., and Falcao, A. (2012) Bioanalytical chromatographic methods for the determination of catechol-*O*-methyltransferase inhibitors in rodents and human samples: A review, *Anal. Chim. Acta 710*, 17-32.
8. DiFrancesco, R., Maduke, G., Patel, R., Taylor, C. R., and Morse, G. D. (2013) Antiretroviral bioanalysis methods of tissues and body biofluids, *Bioanalysis 5*, 351-368.

9. Kortz, L., Helmschrodt, C., and Ceglarek, U. (2011) Fast liquid chromatography combined with mass spectrometry for the analysis of metabolites and proteins in human body fluids, *Analytical and Bioanalytical Chemistry 399*, 2635-2644.

10. O'Connell, S. E., and Zurzola, F. J. (1984) Rapid quantitative liquid chromatographic determination of caffeine levels in plasma after oral dosing, *J. Pharm. Sci. 73*, 1009-1011.

11. Alkaysi, H. N., Salem, M. S., and el-Sayed, Y. M. (1988) High performance liquid chromatographic analysis of caffeine concentrations in plasma and saliva, *J. Clin. Pharm. Ther. 13*, 109-115.

12. Butler, M. A., Lang, N. P., Young, J. F., Caporaso, N. E., Vienis, P., Hayes, R. B., Teitel, C. H., Massengill, J. P., Lawsen, M. F., and Kadlubar, F. F. (1992) Determination of CYP1A2 and NAT2 phenotypes in human populations by analysis of caffeine urinary metabolites, *Pharmacogenetics 2*, 116-127.

13. Carrillo, J. A., Christensen, M., Ramos, S. I., Alm, C., Dahl, M. L., Benitez, J., and Bertilsson, L. (2000) Evaluation of caffeine as an in vivo probe for CYP1A2 using measurements in plasma, saliva, and urine, *Ther. Drug Monit. 22*, 409-417.

14. Perera, V., Gross, A. S., and McLachlan, A. J. (2010) Caffeine and paraxanthine HPLC assay for CYP1A2 phenotype assessment using saliva and plasma, *Biomed. Chromatogr. 24*, 1136-1144.

15. Fuhr, U., and Rost, K. L. (1994) Simple and reliable CYP1A2 phenotyping by the paraxanthine/caffeine ratio in plasma and in saliva, *Pharmacogenetics 4*, 109-116.

16. Spigset, O., Hagg, S., Soderstrom, E., and Dahlqvist, R. (1999) The paraxanthine : caffeine ratio in serum or in saliva as a measure of CYP1A2 activity: When should the sample be obtained?, *Pharmacogenetics 9*, 409-412.

17. Dudai, Y. (2004) The neurobiology of consolidations, or, how stable is the engram?, *Annu. Rev. Psychol. 55*, 51-86.

18. McGaugh, J. L. (2000) Memory - a century of consolidation, *Science 287*, 248-251.

19. Fredholm, B. B., Battig, K., Holmen, J., Nehlig, A., and Zvartau, E. E. (1999) Actions of caffeine in the brain with special reference to factors that contribute to its widespread use, *Pharmacological Reviews 51*, 83-133.

20. O'Toole, M. (2005) In *Miller-Keane Encyclopedia and Dictionary of Medicine, Nursing, and Allied Health* 7th ed., W. B. Saunders Co.

21. Yassa, M. A., and Stark, C. E. L. (2011) Pattern separation in the hippocampus, *Trends Neurosci. 34*, 515-525.

Curriculum Vita

Gizem Keceli was born on August 13, 1981 in Adana, Turkey. She was raised in Adana and attended Ozel Tarsus Amerikan Koleji. In 1999, she began undergraduate studies at Bogazici University, Istanbul, Turkey. She did her undergraduate research in the laboratories of Professor Guniz Buyuktur and Professor Ilknur Dogan, where she assisted the kinetic studies of oxazolidinedione derivatives and the synthesis of thiobarbituric acid derivatives. Also throughout her undergraduate studies, she was involved in summer internships at SASA DUPONT Sabanci Polyester and Kromsan Chromium Chemicals. She received a Bachelor of Science degree with Honors and Salutatorian Award in Chemistry from Bogazici University in May of 2003.

Gizem joined the laboratory of Professor John P. Toscano at Johns Hopkins University in March of 2006. Her research focused on the nature and reactivity of HNO-derived cysteine and tryptophan modifications in several systems including small organic molecules, peptides, and proteins. She received her Doctorate of Philosophy in Chemistry from Johns Hopkins University in May of 2014.

During her graduate studies at Johns Hopkins University, Gizem received Society for Free Radical Biology and Medicine Young Investigator Award and JHU Alexander Kossiakoff Award given in recognition of outstanding research accomplishment in chemistry.